DEVELOPMENTAL PROGRAMING OF VERTEBRATE HEALTH AND DISEASE

EDITED BY: Gina Galli, Sonnet Jonker and Dane Alan Crossley II
PUBLISHED IN: Frontiers in Physiology

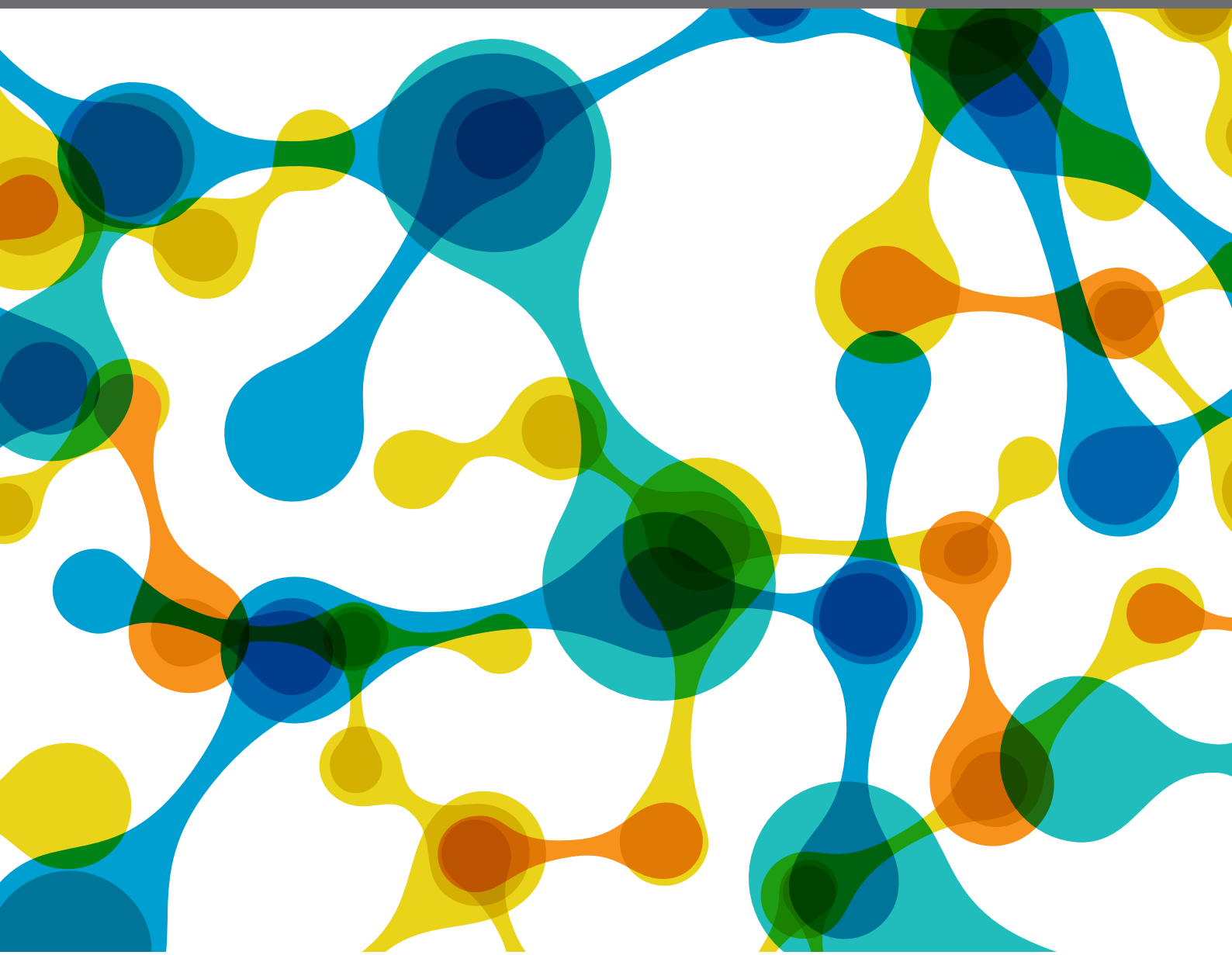

frontiers Research Topics

frontiers

Frontiers eBook Copyright Statement

The copyright in the text of individual articles in this eBook is the property of their respective authors or their respective institutions or funders. The copyright in graphics and images within each article may be subject to copyright of other parties. In both cases this is subject to a license granted to Frontiers.

The compilation of articles constituting this eBook is the property of Frontiers.

Each article within this eBook, and the eBook itself, are published under the most recent version of the Creative Commons CC-BY licence. The version current at the date of publication of this eBook is CC-BY 4.0. If the CC-BY licence is updated, the licence granted by Frontiers is automatically updated to the new version.

When exercising any right under the CC-BY licence, Frontiers must be attributed as the original publisher of the article or eBook, as applicable.

Authors have the responsibility of ensuring that any graphics or other materials which are the property of others may be included in the CC-BY licence, but this should be checked before relying on the CC-BY licence to reproduce those materials. Any copyright notices relating to those materials must be complied with.

Copyright and source acknowledgement notices may not be removed and must be displayed in any copy, derivative work or partial copy which includes the elements in question.

All copyright, and all rights therein, are protected by national and international copyright laws. The above represents a summary only. For further information please read Frontiers' Conditions for Website Use and Copyright Statement, and the applicable CC-BY licence.

ISSN 1664-8714
ISBN 978-2-88966-802-1
DOI 10.3389/978-2-88966-802-1

About Frontiers

Frontiers is more than just an open-access publisher of scholarly articles: it is a pioneering approach to the world of academia, radically improving the way scholarly research is managed. The grand vision of Frontiers is a world where all people have an equal opportunity to seek, share and generate knowledge. Frontiers provides immediate and permanent online open access to all its publications, but this alone is not enough to realize our grand goals.

Frontiers Journal Series

The Frontiers Journal Series is a multi-tier and interdisciplinary set of open-access, online journals, promising a paradigm shift from the current review, selection and dissemination processes in academic publishing. All Frontiers journals are driven by researchers for researchers; therefore, they constitute a service to the scholarly community. At the same time, the Frontiers Journal Series operates on a revolutionary invention, the tiered publishing system, initially addressing specific communities of scholars, and gradually climbing up to broader public understanding, thus serving the interests of the lay society, too.

Dedication to Quality

Each Frontiers article is a landmark of the highest quality, thanks to genuinely collaborative interactions between authors and review editors, who include some of the world's best academicians. Research must be certified by peers before entering a stream of knowledge that may eventually reach the public - and shape society; therefore, Frontiers only applies the most rigorous and unbiased reviews.
Frontiers revolutionizes research publishing by freely delivering the most outstanding research, evaluated with no bias from both the academic and social point of view. By applying the most advanced information technologies, Frontiers is catapulting scholarly publishing into a new generation.

What are Frontiers Research Topics?

Frontiers Research Topics are very popular trademarks of the Frontiers Journals Series: they are collections of at least ten articles, all centered on a particular subject. With their unique mix of varied contributions from Original Research to Review Articles, Frontiers Research Topics unify the most influential researchers, the latest key findings and historical advances in a hot research area! Find out more on how to host your own Frontiers Research Topic or contribute to one as an author by contacting the Frontiers Editorial Office: frontiersin.org/about/contact

DEVELOPMENTAL PROGRAMING OF VERTEBRATE HEALTH AND DISEASE

Topic Editors:
Gina Galli, The University of Manchester, United Kingdom
Sonnet Jonker, Oregon Health and Science University, United States
Dane Alan Crossley II, University of North Texas System, United States

Citation: Galli, G., Jonker, S., Crossley II, D. A., eds. (2021). Developmental Programing of Vertebrate Health and Disease. Lausanne: Frontiers Media SA. doi: 10.3389/978-2-88966-802-1

Table of Contents

frontiers in Physiology

ORIGINAL RESEARCH
published: 01 May 2019
doi: 10.3389/fphys.2019.00515

Maternal Restricted- and Over-Feeding During Gestation Result in Distinct Lipid and Amino Acid Metabolite Profiles in the Longissimus Muscle of the Offspring

*Dominique E. Martin[1,2], Amanda K. Jones[1,3], Sambhu M. Pillai[1,4], Maria L. Hoffman[1,5], Katelyn K. McFadden[1,6], Steven A. Zinn[1], Kristen E. Govoni[1] and Sarah A. Reed[1]**

[1] Department of Animal Science, University of Connecticut, Storrs, CT, United States, [2] Department of Psychology, Providence College, Providence, RI, United States, [3] Department of Pediatrics, School of Medicine, University of Colorado, Aurora, Aurora, CO, United States, [4] School of Medicine, Georgetown University, Washington, DC, United States, [5] Department of Fisheries, Animal and Veterinary Sciences, The University of Rhode Island, Kingston, RI, United States, [6] Cummings School of Veterinary Medicine, Tufts University, North Grafton, MA, United States

OPEN ACCESS

Edited by:
Sonnet Jonker,
Oregon Health & Science University,
United States

Reviewed by:
Sarah L. Alderman,
University of Guelph, Canada
Dean A. Myers,
The University of Oklahoma Health Sciences Center, United States

***Correspondence:**
Sarah A. Reed
sarah.reed@uconn.edu

Specialty section:
This article was submitted to Embryonic and Developmental Physiology, a section of the journal Frontiers in Physiology

Received: 14 January 2019
Accepted: 11 April 2019
Published: 01 May 2019

Citation:
Martin DE, Jones AK, Pillai SM, Hoffman ML, McFadden KK, Zinn SA, Govoni KE and Reed SA (2019) Maternal Restricted- and Over-Feeding During Gestation Result in Distinct Lipid and Amino Acid Metabolite Profiles in the Longissimus Muscle of the Offspring. Front. Physiol. 10:515. doi: 10.3389/fphys.2019.00515

Maternal over- and restricted-feeding during gestation have similar negative consequences for the offspring, including decreased muscularity, increased adiposity, and altered metabolism. Our objective was to determine the effects of poor maternal nutrition during gestation (over- and restricted-feeding) on the offspring muscle metabolite profile. Pregnant ewes (n = 47) were fed 60% (RES), 100% (CON), or 140% (OVER) of NRC requirements starting at day 30.2 ± 0.2 of gestation. Offspring sample collection occurred at days 90 and 135 of gestation, and within 24 h of birth. C2C12 myoblasts were cultured in serum collected from offspring at birth (n = 18; 6 offspring per treatment) for analysis of oxidative and glycolytic capacity. Unbiased metabolite analysis of longissimus muscle samples (n = 72; 8 fetuses per treatment per time point) was performed using mass spectrometry. Data were analyzed by ANOVA for main effects of treatment, time point, and their interaction. Cells cultured in serum from RES offspring exhibited increased proton leak 49% (p = 0.01) compared with CON, but no other variables of mitochondrial respiration or glycolytic function were altered. Mass spectrometry identified 612 metabolites. Principle component analysis identified day of gestation as the primary driver of metabolic change; however, maternal diet also altered the lipid and amino acid profiles in offspring. The abundance of 53 amino acid metabolites and 89 lipid metabolites was altered in RES compared with CON ($p \leq 0.05$), including phospholipids, sphingolipids, and ceramides within the lipid metabolism pathway and metabolites involved in glutamate, histidine, and glutathione metabolism. Similarly, abundance of 63 amino acid metabolites and 70 lipid metabolites was altered in OVER compared with CON ($p \leq 0.05$). These include metabolites involved in glutamate, histidine, lysine, and tryptophan metabolism and phosphatidylethanolamine, lysophospholipids, and fatty acids involved in lipid metabolism. Further, the amino acid and lipid profiles diverged between RES and OVER, with 69 amino acid and 118

lipid metabolites differing ($p \leq 0.05$) between groups. Therefore, maternal diet affects metabolite abundance in offspring longissimus muscle, specifically metabolites involved in lipid and amino metabolism. These changes may impact post-natal skeletal muscle metabolism, possibly altering energy efficiency and long-term health.

Keywords: gestation, maternal diet, metabolism, muscle, offspring

INTRODUCTION

Poor maternal nutrition during gestation can negatively impact offspring growth and development pre- and post-natally. Both restricted- and over-feeding during gestation can lead to alterations in body size and birth weight of offspring, as well as impaired muscle growth, changes in adiposity, and altered metabolism in multiple species which have long-lasting and detrimental effects on offspring growth and health (Hales and Barker, 2001; Wu et al., 2006; Reed et al., 2014; Hoffman et al., 2017). These long-lasting post-natal effects can persist into adulthood, and are likely the result of fetal programming, which is defined as changes in the maternal environment that alter the pre-natal development and post-natal growth trajectory of the developing offspring (Nathanielsz et al., 2007). Additionally, the impacts of poor maternal nutrition on offspring metabolism are linked with increased incidence of metabolic dysregulation and disease in the adult (Hales and Ozanne, 2003).

Because fiber number is determined during fetal development, muscle tissue is particularly vulnerable to intrauterine conditions, such as changes in maternal nutrition. Although there is an increase in net muscle mass after birth due to muscle fiber hypertrophy, the number of muscle fibers is set during gestation and no fiber hyperplasia occurs post-natally (Rowe and Goldspink, 1969; Beermann et al., 1978; Wigmore and Stickland, 1983; White et al., 2010). Currently, knowledge of the effects of maternal diet on muscle are primarily focused on phenotypic changes. For example, restricted-feeding dams during gestation increased offspring muscle fiber cross-sectional area (CSA) of semitendinosus muscle fibers at birth but resulted in reduced post-natal growth and smaller muscle fiber CSA at 3 months of age (Reed et al., 2014). Further, 8-mo-old lambs born to nutrient deficient mothers had fewer total muscle fibers than control animals (Zhu et al., 2006). Maternal over-feeding also increased muscle and whole-body adiposity in the offspring during fetal development, at birth, and post-natally (Daniel et al., 2007; Tong et al., 2009; Reed et al., 2014). In addition, maternal over-feeding during gestation decreased the number of muscle fibers formed during development and the size of those fibers pre-natally and post-natally (Cerisuelo et al., 2009; Tong et al., 2009; Reed et al., 2014). Muscle has an integral role in metabolism and inter-organ crosstalk due to its involvement with glucose and protein utilization and is susceptible to fetal programming in response to poor maternal nutrition. Skeletal muscle comprises 40–50% of body mass, making it the most abundant insulin-sensitive tissue (DeFronzo et al., 1985; Baron et al., 1988; Zurlo et al., 1990). Further, skeletal muscle is responsible for 75–95% of insulin-mediated glucose disposal and 20–30% of whole-body oxygen consumption (DeFronzo et al., 1985; Baron et al., 1988; Zurlo et al., 1990). Skeletal muscle also serves as an amino acid reservoir that sustains protein synthesis within the muscle and whole body (Wolfe, 2006). Changes to muscle mass, metabolic rate, hormone concentrations, or other circulating factors affecting muscle could significantly alter energy substrate use.

The altered uterine environment resulting from poor maternal nutrition during gestation may result in lasting changes to muscle metabolism and function, affecting post-natal muscle growth and whole-body metabolism. We hypothesized that poor maternal nutrition during gestation (over- and restricted-feeding) would alter the offspring muscle metabolome at mid- and late-gestation, and within 24 h of birth.

MATERIALS AND METHODS

Animals

All animal procedures were reviewed and approved by the University of Connecticut Institutional Animal Care and Use Committee (A13-059). Full experimental details were previously reported in Pillai et al. (2017). Briefly, multiparous Western White-faced ewes (n = 47) were estrus synchronized using a controlled intravaginal drug release device (CIDR; Easi-Breed CIDR Sheep Insert, Zoetis, Parsippany, NJ, United States) and an intramuscular injection of $PGF_{2\alpha}$ [Lutalyse, 5 mg/mL; Zoetis, Inc.; (Knights et al., 2001)]. Ewes were bred to 1 of 4 related Dorset rams. Day 0 of pregnancy was determined when ewes received a rump mark and showed no further evidence of remarking. Twenty days later, ewes were moved to individual pens and transitioned over a 7-day period to a complete pelleted feed based on National Research Council (NRC) requirements for ewes gestating with twins. Ewes were confirmed pregnant using transabdominal ultrasound on day 28.5 $\pm$ 0.4 (Jones et al., 2016). Pregnant ewes (n = 5 to 7 per treatment per time point) were fed either a control- (100% NRC), restricted- (60% NRC), or over-fed diet (140% NRC) starting at day 30.2 $\pm$ 0.2 of gestation based on the NRC requirement for total digestible nutrients (TDN; National Research Council, 1985) and adjusted weekly for individual changes in body weight. Offspring from control-, restricted-, or over-fed ewes are denoted as CON, RES, and OVER, respectively. Diets effectively altered maternal body weight, with restricted-fed ewes having lighter body weights than control- and over-fed ewes as early as day 45 of gestation (Pillai et al., 2017). At birth, restricted-fed ewes weighed 12% less than control-fed ewes, and over-fed ewes were 11% heavier than control ewes (Pillai et al., 2017).

Sample Collection

On days 90 and 135 of gestation, ewes (n = 5 to 7 per treatment per time point) were euthanized by an intravenous injection of Beuthanasia-D Special (Merck Animal Health; Summit, NJ, United States) containing 390 mg/mL sodium pentobarbital and 50 mg/mL phenytoin based on body weight, and exsanguinated. The fetuses were removed following a hysterectomy for necropsy and tissue collection. A subset of ewes was allowed to undergo parturition (birth; n = 5–7 per dietary treatment). Whole blood was obtained from live lambs via jugular venipuncture within 24 h of parturition and processed for serum (Hoffman et al., 2014). Subsequently, lambs were weighed and euthanized with an i.v. overdose of Beuthanasia-D Special (390 ng/mL sodium pentobarbital and 50 mg/mL phenytoin based on body weight), and exsanguinated. For the purposes of these experiments, a total of 72 offspring (n = 8 per treatment per time point) from 47 ewes at days 90 and 135, and within 24 h of birth were included in the final analysis. These time points represent mid-gestation, which is the time period of secondary myogenesis, late gestation, during which muscle growth is primarily through muscle hypertrophy, and just after parturition. Offspring body weight was not different at day 90 or day 135 of gestation, but RES offspring were lighter at birth than CON and OVER (p = 0.03; Pillai et al., 2017). Longissimus muscle (LM) samples from each offspring at days 90, 135, and birth were collected immediately after euthanasia and snap frozen in liquid nitrogen. The longissimus muscle is economically relevant as a dietary protein source. Samples were stored at −80°C until further use.

C2C12 Cell Culture

C2C12 cells (ATCC CRL-1772, Manassas, VA, United States) were cultured in growth media containing Dulbecco's modified Eagle media (DMEM) with 4 g/L D-glucose (Gibco Laboratories, Gaithersburg, MD, United States) and 10% fetal bovine serum (FBS), 1% penicillin/streptomycin, 0.3% fungizone, and 0.2% gentamycin. Cells were passed once and plated on 24-well plates at a density of 3,000 cells per well. After 24 h, the media was changed so that, instead of FBS, the growth media contained 10% offspring serum collected at birth from CON (n = 8), RES (n = 8), or OVER (n = 8) lambs. After 48 h, cells were pulsed with 5-bromo-2′-deoxyuridine (BrdU) for 30 min (Click-iT EdU Alexa Fluor 488 Imaging Kit, Invitrogen, Carlsbad, CA, United States), fixed with 4% paraformaldehyde, and immunostained according to manufacturer's recommendations. Cells were incubated with Hoescht 33342 for 1 h to visualize nuclei. The cells were imaged using a Zeiss Observer, and 5 random images per well were taken. The percentage of proliferating cells was determined by the number of BrdU(+) cells divided by the total number of nuclei and multiplied by 100.

To analyze myoblast differentiation, C2C12 cells were cultured in growth media on 24-well plates. After reaching 100% confluency, growth media was replaced with differentiation media containing 2% offspring serum, 1% penicillin/streptomycin, 0.3% fungizone, and 0.2% gentamycin in DMEM with 1 g/L glucose. C2C12 cells were allowed to differentiate in treatment media for 5 days. Myotubes were fixed with 4% paraformaldehyde and blocked in 5% horse serum in phosphate buffered saline (PBS) and 0.1% triton-X. Cells were incubated with anti-Myosin heavy chain (MyHC; MF20, Developmental Hybridoma Core) overnight at 4°C. After extensive washing in PBS, cells were incubated with secondary antibody (Alexa Fluor 488; 1:500) for 1 h. Hoescht 33342 was used to visualize nuclei. The cells were imaged using a Zeiss Observer, and 5 random images per well were taken. Fusion index was calculated as the number of nuclei within multinucleated MyHC-positive myotubes divided by the number of total number of nuclei and multiplied by 100. Fiber diameter was measured in 3 places per myofiber and averaged per fiber.

Mitochondrial and Glycolytic Stress Assays

Mitochondrial and glycolytic stress were evaluated using the Seahorse XFe24 Extracellular Flux Analyzer (Seahorse Bioscience; North Billerica, MA, United States) following manufacturer's instructions and protocol. In brief, C2C12 cells were plated onto XFe24 culture plates at a density of 15,000 cells per well and cultured in 10% offspring serum in growth media [CON (n = 6), RES (n = 6), or OVER (n = 6)] for 24 h. Twelve hours before the assay, the XFe24 sensor cartridges were hydrated with Seahorse Bioscience XFe24 Calibrant (pH 7.4) and stored at 37°C.

For the Cell Mito Stress Test Assay, 1 mM pyruvate (Sigma-Aldrich, St. Louis, MO, United States), 2 mM glutamine (Sigma-Aldrich), and 10 mM glucose (Sigma-Aldrich) were added to the assay media, warmed to 37°C, pH was adjusted to 7.4 with 0.1 N NaOH, and the media was sterile filtered. Oligomycin, carbonyl cyanide-4 (trifluoromethoxy) phenylhydrazone (FCCP), and rotenone/antimycin A were prepared in assay media. The injection ports were loaded using the constant volume method described in the manufacturer's protocol. The growth media was removed, and each well was rinsed twice with assay media. Assay media (525 μL) was added to each well, and the cell culture plate was incubated at 37°C without CO_2 for 60 min. The plate was then loaded into the Seahorse XFe24 Extracellular Flux Analyzer and the standard operating procedure for Cell Mito Stress Test Assay for the machine was followed according to manufacturer's protocol to measure oxygen consumption rate (OCR).

For the Glycolysis Stress Test Assay, 2 mM glutamine was added to Seahorse XF Assay Media (Seahorse Bioscience). The media was warmed to 37°C, pH was adjusted to 7.4 with 0.1 N NaOH, and the media was filter sterilized. The injection ports were loaded using the constant volume method described in the manufacturer's protocol. The growth media was removed and each well was rinsed twice with assay media. Assay media (525 μL) was added to each well, and the cell culture plate was incubated at 37°C without CO_2 for 60 min. The plate was then loaded into the Seahorse XFe24 Extracellular Flux Analyzer. Standard operating procedure for Glycolysis Stress Test Assay for the machine was followed according to manufacturer's protocol to measure extracellular acidification rate (ECAR).

The DNA content in individual wells on the XFe24 cell culture plates was quantified to account for variations in cell density

using Macherey-Nagel NucleoSpin Tissue kits (Macherey-Nagel Inc., Bethlehem, PA, United States), according to manufacturer's protocol. The OCR and ECAR measurements were adjusted for total DNA content in each well.

Metabolome Analysis

Sample Preparation

Longissimus dorsi samples (200 ng; n = 8 per treatment per time point) were shipped on dry ice to Metabolon, Inc. (Morrisville, NC, United States) for metabolome analysis. Samples were prepared using the automated MicroLab STAR® system (Hamilton Company, Reno, NV, United States). Several recovery standards were added before the first step in the extraction process for quality control (QC) purposes. To remove protein, dissociate small molecules bound to protein or trapped in the precipitated protein matrix, and to recover chemically diverse metabolites, proteins were precipitated with methanol under vigorous shaking for 2 min (Glen Mills GenoGrinder 2000, SPEX Sample Prep, Metuchen, NJ, United States) followed by centrifugation. The resulting extract was divided into five fractions: two for analysis by two separate reverse phase (RP)/ultra-performance liquid chromatography-tandem mass spectrometry (UPLC-MS/MS) methods with positive ion mode electrospray ionization (ESI), one for analysis by RP/UPLC-MS/MS with negative ion mode ESI, one for analysis by Hydrophilic Interaction Chromatography (HILIC)/UPLC-MS/MS with negative ion mode ESI, and one sample was reserved for backup. Samples were placed briefly on a TurboVap (Zymark, Hopkinton, MA, United States) to remove the organic solvent. The sample extracts were stored overnight under nitrogen before preparation for analysis.

Ultrahigh Performance Liquid Chromatography-Tandem Mass Spectroscopy (UPLC-MS/MS)

All methods utilized a Waters ACQUITY UPLC and a Thermo Scientific Q-Exactive high resolution/accurate mass spectrometer interfaced with a heated electrospray ionization (HESI-II) source and Orbitrap mass analyzer operated at 35,000 mass resolution. The sample extract was dried, then reconstituted in solvents compatible with each of the four methods. Each reconstitution solvent contained a series of standards at fixed concentrations to ensure injection and chromatographic consistency. One aliquot was analyzed using acidic positive ion conditions, chromatographically optimized for more hydrophilic compounds. In this method, the extract was gradient eluted from a C18 column (Waters UPLC BEH C18-2.1 × 100 mm, 1.7 μm) using water and methanol, containing 0.05% perfluoropentanoic acid (PFPA) and 0.1% formic acid (FA). Another aliquot was also analyzed using acidic positive ion conditions; however, it was chromatographically optimized for more hydrophobic compounds. In this method, the extract was gradient eluted from the same afore mentioned C18 column using methanol, acetonitrile, water, 0.05% PFPA and 0.01% FA, and was operated at an overall greater organic content. Another aliquot was analyzed using basic negative ion optimized conditions using a separate dedicated C18 column. The basic extracts were gradient eluted from the column using methanol and water, however, with 6.5 mM Ammonium Bicarbonate at pH 8. The fourth aliquot was analyzed via negative ionization following elution from a HILIC column (Waters UPLC BEH Amide 2.1 × 150 mm, 1.7 μm) using a gradient consisting of water and acetonitrile with 10 mM Ammonium Formate, pH 10.8. Quality control was achieved using four separate controls: a pooled matrix sample generated by taking a small volume of each experimental sample served as a technical replicate throughout the data set; extracted water samples served as process blanks; and a cocktail of QC standards that were chosen not to interfere with the measurement of endogenous compounds were spiked into every analyzed sample allowed instrument performance monitoring and aided chromatographic alignment. Instrument variability was determined by calculating the median relative standard deviation (RSD) for the standards that were added to each sample prior to injection into the mass spectrometers. Overall process variability was determined by calculating the median RSD for all endogenous metabolites (i.e., non-instrument standards) present in 100% of the pooled matrix samples. Experimental samples were randomized across the platform run with QC samples spaced evenly among the injections. The mass spectrometer analysis alternated between mass spectrometer (MS) and data-dependent sequential mass spectrometry (MSn) scans using dynamic exclusion. The scan range varied slighted between methods but covered 70–1,000 m/z.

Data Extraction and Compound Identification

Raw data were extracted, peak-identified, and QC processed using Metabolon's hardware and software. Compounds were identified by comparison with library entries of purified standards or recurrent unknown entities. Metabolon maintains a library based on authenticated standards that contains the retention time/index (RI), mass to charge ratio (m/z), and chromatographic data (including MS/MS spectral data) on all molecules present in the library. Furthermore, biochemical identifications are based on three criteria: retention index within a narrow RI window of the proposed identification, accurate mass match to the library ±10 ppm, and the MS/MS forward and reverse scores between the experimental data and authentic standards. The MS/MS scores are based on a comparison of the ions present in the experimental spectrum to the ions present in the library spectrum. While there may be similarities between these molecules based on one of these factors, the use of all three data points can be utilized to distinguish and differentiate compounds. More than 3,300 commercially available purified standard compounds have been acquired and registered into the laboratory information management system (LIMS) for analysis on all Metabolon platforms for determination of their analytical characteristics.

Statistical Analysis

Cell culture data were analyzed using PROC MIXED (SAS Institute Inc., Cary, NC, United States; version 9.4). Main effects of treatment, sex, and their interaction were analyzed and differences between means were determined using the pdiff

statement in LSMEANS. Data are reported as least square mean ± SE with significance at $p \leq 0.05$.

Following log transformation and imputation of missing values with the minimum observed value for each compound, ANOVA contrasts were used to identify metabolites that differed significantly between diet, time and the interaction of diet and time. Statistical significance is declared for $p \leq 0.05$ with false discovery rate $q < 0.05$. A principal component analysis was performed in Array Studio to find hierarchical clusterings of the data. Morpheus was used to generate heat maps using relative abundance (fold change) data[1].

RESULTS

Effects of RES and OVER Offspring Serum on Myoblast Characteristics

Serum from RES offspring increased proton leak 49% compared with CON ($p = 0.01$; **Table 1**), but serum from OVER offspring had no effect on proton leak compared with CON ($p = 0.58$). Serum from RES and OVER offspring did not significantly affect basal respiration, ATP production, maximal respiration, spare respiratory capacity, or non-mitochondrial respiration compared with CON ($p \geq 0.15$). Serum from RES and OVER offspring did not significantly affect C2C12 glycolytic function ($p \geq 0.36$; **Table 2**). There was no effect of sex ($p \geq 0.22$) or interaction of treatment and sex ($p \geq 0.48$) for any of the variables analyzed for mitochondrial or glycolytic function. Serum collected from RES and OVER offspring had no effect on BrdU incorporation ($p \geq 0.39$; CON = 24.89 ± 3.03%, RES = 24.06 ± 3.03%, OVER = 27.74 ± 3.03%), myofiber fusion index ($p \geq 0.15$; CON = 15.70 ± 2.87%, RES = 9.55 ± 3.23%, OVER = 10.97 ± 3.03%) or myofiber diameter ($p \geq 0.70$; CON = 15.38 ± 1.33 μm, RES = 14.88 ± 1.46 μm, OVER = 15.25 ± 1.38 μm) compared with CON.

TABLE 1 | Serum from offspring born to restricted-fed ewes increases C2C12 proton leak[1].

	Maternal diet				
Variable[2]	**CON**	**RES**	**OVER**	**SEM**	***p*-value**
Basal respiration	34.32	44.87	35.38	3.88	0.32
ATP production	19.33	22.54	18.94	3.21	0.69
Maximal respiration	177.15	303.21	182.58	49.83	0.17
Spare respiratory capacity	142.83	258.34	147.19	47.79	0.19
Proton leak	14.98[a]	22.33[b]	16.45[a]	1.81	0.01
Non-mitochondrial respiration	11.75	25.22	16.77	5.42	0.25

[1]C2C12 cells were cultured in serum collected from offspring of control-fed (CON, n = 6), restricted (RES, n = 6), or over-fed (OVER, n = 6) ewes at birth. [2]Measured as oxygen consumption rate (pmol $O_2 \cdot min^{-1} \cdot \mu g\ DNA^{-1}$). [a,b]Values with different letters are significantly different, $p < 0.05$.

TABLE 2 | Serum from offspring of poorly nourished ewes does not alter C2C12 glycolytic function[1].

	Maternal diet				
Variable[2]	**CON**	**RES**	**OVER**	**SEM**	***p*-value**
Glycolysis	48.03	45.21	41.39	4.08	0.27
Glycolytic capacity	51.41	52.35	47.85	4.75	0.51
Glycolytic reserve	3.38	7.14	6.46	1.91	0.19
Non-glycolytic acidification	15.63	16.69	14.33	1.93	0.40

[1]C2C12 cells were cultured in serum collected from offspring of control-fed (CON, n = 6), restricted (RES, n = 6), or over-fed (OVER, n = 6) ewes at birth. [2]Measured as extracellular acidification rate (mpH $\cdot$ $min^{-1} \cdot \mu g\ DNA^{-1}$).

Muscle Metabolome Analysis

A total of 612 metabolites were identified in LM samples (**Supplementary Table S1**). Principle component analysis of LM samples (**Figure 1**) demonstrated clustering within day of gestation, indicating that gestational development is the primary driver of variance between samples. Accordingly, day of gestation altered metabolite abundance within each diet group (**Table 3**). However, maternal diet also altered metabolite abundance at each time point (**Table 4**). Maternal over- and restricted-feeding differentially altered metabolites in the 8 major metabolic pathways (amino acid, lipid, peptide, carbohydrate, energy, nucleotide, cofactors and vitamins, xenobiotics; **Table 5**). Maternal over-feeding altered 63 of 161 (39%) of identified metabolites in the amino acid metabolism pathways compared with CON, in contrast to RES offspring which demonstrated 53 of 161 (33%) metabolites altered compared with CON. Maternal restricted-feeding altered 89 of 268 (33%) identified metabolites in lipid metabolism compared with CON, in contrast to OVER offspring, in which 70 of 268 (26%) identified metabolites in lipid metabolism compared with controls. Because of the importance of amino acid metabolism in maintaining energy homeostasis in fetal offspring (Battaglia and Meschia, 1978), and transition to lipid metabolism during early post-natal life, we chose to focus on these classes of metabolites.

Maternal Restricted-Feeding Alters Lipid Metabolism in the Offspring Longissimus Muscle

Throughout gestation and immediately following parturition, RES demonstrated reduced abundance of phosphatidylcholines, phosphatidylethanolamines, and lysophospholipids compared with CON ($p < 0.05$; **Figure 2**). In particular, phosphatidylcholine and phosphatidylethanolamine metabolites were decreased in RES compared with CON at day 90 of gestation ($p < 0.05$). Several lysophospholipid metabolites (**Figure 2**) were decreased in RES at each time point ($p < 0.05$), with the exception of 1-oleyl-glycerophosphoserine, which was increased at birth in RES compared with CON ($p < 0.02$). Acetyl carnitine and 3-hydroxybutyrylcarnitine were increased at birth, and 3-hydroxybutyrate was increased at day 135 in RES compared with CON ($p < 0.04$). Maternal restricted-feeding during gestation decreased abundance of 16 of 31 identified sphingomyelin metabolites at day 90 of gestation ($p < 0.05$; **Figure 2**). Abundance of two sphingolipid metabolites [sphingomyelin (d18:2/14:0, d18:1/14:1) and sphingomyelin (d18:2/24:2)] was increased in RES at day 135 compared with CON ($p < 0.02$). Coupled with changes in sphingomyelin

[1]https://software.broadinstitute.org/morpheus

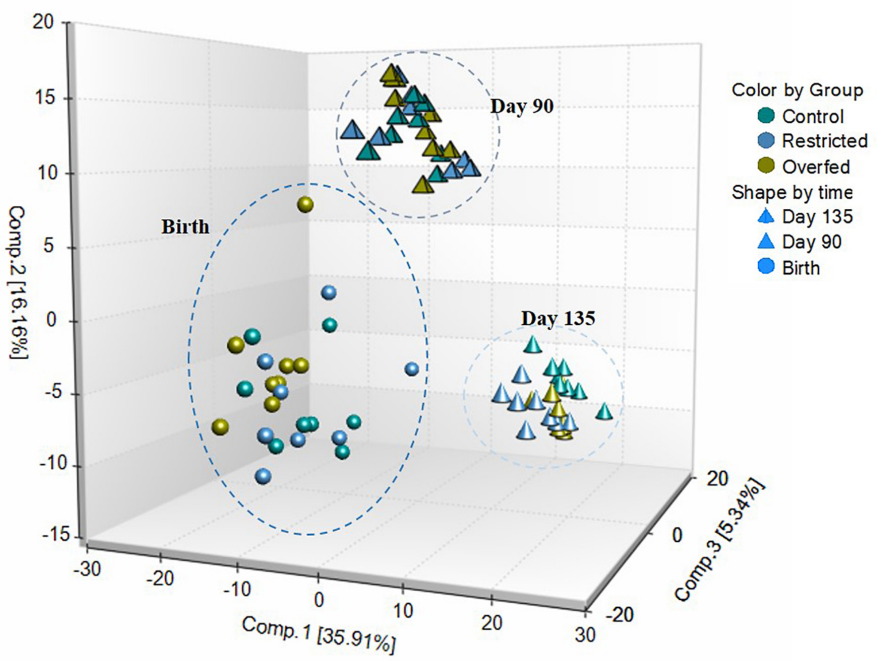

FIGURE 1 | Principle component analysis (PCA) and hierarchical clustering obtained from employing metabolic concentration of all metabolites detected in longissimus muscle (LM). PCA of LM samples indicates that time is the primary driver of variance between samples. LM samples (n = 72; 8 per treatment per time point) were collected from offspring born to ewes fed control- (100%), restricted- (60%), or over-fed (140%) diets at days 90 or 135 of gestation, or within 24 h of birth were analyzed by UPLC-MS/MS. Offspring from control-, restricted-, or over-fed ewes are denoted as CON, RES, and OVER, respectively.

metabolites were decreases in 7 of 10 identified ceramide metabolites at day 90; although abundance was similar to CON by day 135 of gestation.

Maternal Restricted-Feeding Alters Amino Acid Metabolism in the Offspring Longissimus Muscle

While the largest number of metabolites altered as a result of maternal restricted-feeding occurred in the lipid metabolism subpathways, maternal nutrient restriction also altered the abundance of metabolites in the amino acid metabolism subpathways (**Figure 2**). In the histidine metabolism subpathway, 1-methylhistidine, 3-methylhistidine, n-acetyl-1-methylhistidine, and anserine abundance was increased at day 135 relative to CON, while carnosine abundance was decreased ($p < 0.03$). At birth, abundance of carnosine, anserine, and 1-methyl-4-imidazoleacetate was decreased compared with CON ($p < 0.05$). Metabolites in the methionine, cysteine, SAM and taurine subpathway were also altered by restricted maternal nutrition. Specifically, *N*-acetylmethionine abundance was increased at day 90 of gestation ($p = 0.03$), while *N*-formylmethionine and taurocyamine abundance was decreased relative to CON at day 135 and birth ($p < 0.02$). Interestingly, reduced glutathione (GSH) was increased at day 90 ($p = 0.01$) with no change in oxidized glutathione ($p = 0.74$). 2-aminobutyrate was also decreased at day 90 of gestation but increased at day 135 of gestation relative to CON ($p < 0.01$).

Maternal Over-Feeding Alters Lipid Metabolism in the Offspring Longissimus

Maternal over-feeding during gestation altered the lipid metabolite profile in offspring muscle but affected fewer lipid metabolites than maternal restricted-feeding (**Figure 2**). In particular, four fatty acids [propionylcarnitine (C3); 5-dodecenoylcarnitine (C12:1); myristoleoylcarnitine (C14:1); behenoylcarnitine (C22)] were decreased in OVER at birth relative to CON ($p < 0.02$). Further, five phosphatidylethanolamines [1-palmitoyl-2-oleoyl-GPE (16:0/18:1); 1-palmitoyl-2-arachidonoyl-GPE (16:0/20:4); 1-stearoyl-2-oleoyl-GPE (18:0/18:1); 1,2-dioleoyl-GPE (18:1/18:1); 1-oleoyl-2-linoleoyl-GPE (18:1/18:2)] and eight lysophospholipids [1-palmitoleoyl-GPC (16:1); 1-oleoyl-GPC (18:1); 1-linoleoyl-GPC (18:2); 1-palmitoyl-GPE (16:0); 1-oleoyl-GPE (18:1); 1-arachidonoyl-GPE (20:4n6); 1-palmitoyl-GPI (16:0); 1-stearoyl-GPI (18:0)] metabolites were decreased at birth in OVER ($p < 0.05$). No fatty acid, phosphatidylethanolamine, or lysophospholipids increased in OVER compared with CON at birth ($p > 0.05$).

Maternal Over-Feeding Alters Amino Acid Metabolism in the Offspring Longissimus Muscle

Increased maternal nutrient consumption during gestation altered amino acid metabolites in a variety of metabolic pathways (**Figure 2**). Of interest, 1-methylhistidine, 3-methylhistidine, *N*-acetyl-1-methylhistidine were all reduced in OVER offspring

TABLE 3 | Number of fetal metabolites in longissimus muscle altered by day of gestation.

		Metabolites[1]		
Diet[2]	Time	Total	Increased	Decreased
CON	day 90 vs. day 135	362	200	162
	day 90 vs. Birth	436	191	245
	day 135 vs. Birth	374	127	247
RES	day 90 vs. day 135	376	211	165
	day 90 vs. Birth	441	189	252
	day 135 vs. Birth	374	129	245
OVER	day 90 vs. day 135	374	219	155
	day 90 vs. Birth	441	230	211
	day 135 vs. Birth	365	160	205

[1]Significance is determined at $p \leq 0.05$. [2]Offspring from ewes fed a control (100% NRC), restricted (60% NRC), or OVER (140% NRC) diet. Offspring from control-, restricted-, or over-fed ewes are denoted as CON, RES, and OVER, respectively.

TABLE 4 | Number of fetal metabolites in longissimus muscle altered by maternal diet.

		Metabolites[1]		
Diet[2]	Time	Total	Increased	Decreased
RES vs. CON	day 90	86	19	67
	day 135	72	22	50
	Birth	64	14	50
OVER vs. CON	day 90	78	49	29
	day 135	27	18	9
	Birth	102	15	87
RES vs. OVER	day 90	104	20	84
	day 135	118	38	80
	Birth	117	85	32

[1]Significance is determined at $p \leq 0.05$. [2]Offspring from ewes fed a CON (100% NRC), RES (60% NRC), or OVER (140% NRC) diet. Offspring from control-, restricted-, or over-fed ewes are denoted as CON, RES, and OVER, respectively.

compared with CON at day 90 of gestation ($p < 0.02$) while 1-methylhistamine was decreased at birth ($p = 0.03$). Branched chain amino acid (BCAA) metabolites, beta-hydroxyisovalerate, 3-methylglutaconate, and 3-hydroxyisobutyrate, were increased at day 90 and day 135 of gestation in OVER compared with CON ($p < 0.02$). Beta-hydroxyisovaleroylcarnitine was increased at day 90 ($p < 0.02$) but not day 135 or birth in OVER compared with CON. However, 4-methyl-2-oxopentanoate was decreased at day 90 of gestation in OVER compared with CON ($p = 0.04$). Metabolites involved in methionine, cysteine, and taurine metabolism were also increased in OVER compared with CON ($p < 0.05$). Specifically, *S*-methylcysteine was increased at all three time points in OVER compared with CON ($p < 0.01$). Taurine and *S*-methylcysteine sulfoxide were increased at day 135 ($p < 0.02$). Methionine sulfone was increased at birth ($p = 0.05$), and *S*-methylmethionine was increased at day 90 and birth ($p < 0.02$), but not day 135 compared with CON. In contrast, *N*-acetylmethionine was decreased in OVER at birth compared with CON ($p < 0.01$). Offspring of over-fed ewes also demonstrated alterations to glutathione metabolism. Specifically, GSH was increased at day 90 of gestation ($p < 0.01$) with no difference in oxidized glutathione. However, at day 90, cysteine-glutathione disulfide and 2-aminobutyrate were decreased in OVER compared with CON ($p < 0.04$). Ophthalmate was decreased at day 135 and *S*-methylglutathione was decreased at birth compared with CON ($p < 0.05$).

TABLE 5 | Number of metabolites in major pathways altered by maternal diet across time points[1].

Major metabolic pathway	Total number of metabolites[2]	Pathway metabolites altered[3]		
		RES vs. CON	OVER vs. CON	RES vs. OVER
Amino acid	161	53 (33%)	63 (39%)	69 (43%)
Peptide	17	4 (24%)	6 (35%)	9 (53%)
Carbohydrate	39	8 (21%)	12 (31%)	9 (23%)
Energy	11	1 (9%)	1 (9%)	3 (27%)
Lipid	268	89 (33%)	70 (26%)	118 (44%)
Nucleotide	56	16 (29%)	10 (18%)	16 (29%)
Cofactors and vitamins	31	12 (39%)	15 (48%)	13 (42%)
Xenobiotics	29	13 (45%)	10 (34%)	14 (48%)

[1]Offspring from ewes fed a CON (100% NRC), RES (60% NRC), or OVER (140% NRC) diet. Offspring from control-, restricted-, or over-fed ewes are denoted as CON, RES, and OVER, respectively. [2]Number of metabolites identified within each pathway. [3]Number of metabolites within each pathway altered between treatments, percent of total number of pathway metabolites is in parentheses. Significance is determined at $p \leq 0.05$.

Maternal Over- and Restricted-Feeding Result in Different Metabolite Profiles in the Offspring

The different amino acid and lipid metabolite profiles in offspring as a result of restricted- or over-feeding in the dam are most notable when comparing the two groups directly with each other (**Figure 2**). In particular, RES offspring demonstrate increased 1-methylhistidine, 3-methylhistidine, *N*-acetyl-1-methylhistidine, and anserine at day 90 and day 135 compared with OVER offspring ($p < 0.02$), yet decreased imidazole propionate and imidazole lactate at all three time points compared with OVER offspring ($p < 0.05$; **Figure 2**). Branched chain amino acid metabolites were decreased overall in RES compared with OVER. Specifically, beta-hydroxyisovalerate, 3-methylglutaconate, and 3-hydroxyisobutyrate were decreased at day 90 and day 135 in RES compared with OVER ($p < 0.02$). In contrast, beta-hydroxyisovaleroylcarnitine was decreased at day 90 ($p < 0.01$) but increased at birth in RES compared with OVER ($p < 0.01$). Methionine, cysteine, and taurine metabolites were also altered in RES compared with OVER offspring. For example, S-methylcysteine was decreased in RES compared with OVER at all three time points ($p < 0.01$). Both reduced and oxidized glutathione were decreased at day 135 in RES compared with CON ($p < 0.05$). In contrast, *S*-methylglutathione was increased at birth ($p < 0.02$), 2-aminobutyrate was increased at day 135 ($p < 0.01$), and ophthalmate was increased at day 90 and day 135 in RES compared with OVER ($p < 0.02$).

Restricted maternal nutrition during gestation increased abundance of 118 of 268 (44%) identified lipid metabolites in

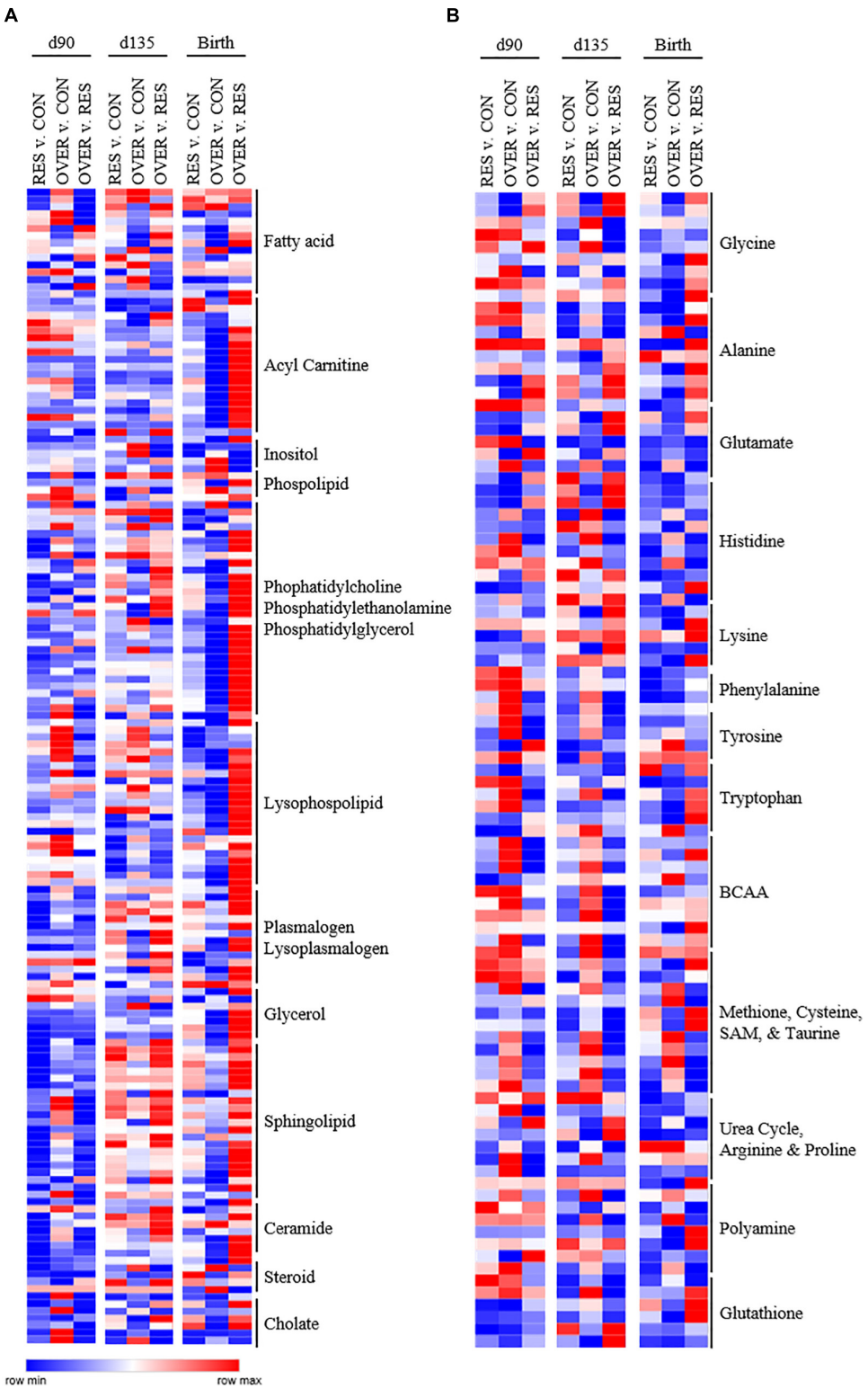

FIGURE 2 | Poor maternal diet alters relative abundance of lipid **(A)** and amino acid **(B)** metabolites in the offspring longissimus muscle in a diet and time dependent manner. Offspring from ewes fed a control (CON; 100% NRC), over-fed (OVER; 140% NRC), or restricted-fed (RES; 60% NRC) diet were sampled at days 90 or 135 of gestation, or within 24 h of birth. Identified names are metabolite sub-pathways. Cells represent fold changes of abundance by color range, from red (row max) to white (row average) and blue (row minimum) between treatment groups.

RES compared with OVER (**Figure 2**). In particular, abundance of the polyunsaturated fatty acids eicosapentaenoate (EPA) and docosapentaenoate (n3 DPA) were increased in RES compared with OVER at all three time points ($p < 0.02$). Further, 10 fatty acid metabolites involved in acyl carnitine metabolism were increased in RES offspring compared with OVER at birth ($p < 0.05$). The ketone body 3-hydroxybutyrate was decreased at day 90 and increased at day 135 in RES offspring compared with CON ($p < 0.04$). Seventeen sphingolipid metabolites were reduced in RES compared with OVER at day 90 of gestation; however, sphingomyelin (d18:2/24:2) was increased compared with OVER at all three time points ($p \leq 0.02$). Ceramide metabolites were also reduced at day 90 of gestation in RES offspring compared with OVER; however, glycosyl-*N*-stearoyl-sphingosine (d18:1/18:0) was increased in RES offspring compared with OVER at birth ($p = 0.03$).

DISCUSSION

Fetal programming of muscle metabolism has potential consequences for post-natal growth and risk of several metabolic diseases in adulthood. Here, we investigated the effects of maternal diet on offspring muscle metabolism using two approaches. First, we assessed myoblast function in the presence of serum from RES and OVER offspring, allowing us to investigate if systemic factors in these offspring have an inhibitory effect on myoblast metabolism using a standard cell line. Second, we performed untargeted metabolomics on offspring LM to identify metabolic pathways impacted by maternal diet. Using these approaches, we found that (1) serum from RES offspring increased myoblast proton leak, indicating that maternal nutrient restriction changes circulating serum factors that result in redox imbalance of myoblasts; and (2) maternal over- and restricted-nutrition altered the offspring lipid and amino acid metabolite profile, but result in distinct metabolite profiles in offspring muscle (**Figure 3**).

Proton leak is associated with energy efficiency in the mitochondria, with increased leak correlated with reduced mitochondrial coupling and therefore, reduced efficiency in generating ATP (Rolfe et al., 1999). Proton pumping across the mitochondrial membrane and proton leak contribute to a cycle that dissipates redox energy (Rolfe et al., 1999). Additionally, the mitochondrial proton cycle contributes approximately 15% of the standard metabolic rate in skeletal muscle (Rolfe et al., 1999). Increased myoblast proton leak from RES serum could result in increased basal metabolic rate, thereby decreasing energetic efficiency. This may be a result of factors in the serum which increase oxidative stress and/or the inflammatory response in the muscle, altering mitochondrial function and/or efficiency. The serum contains a rich milieu of factors which could result in this change, which is an area for future study. Further, increased proton leak is associated with redox imbalance, and has been linked to increased oxidative stress as well as increased inflammatory responses (Li et al., 2017), which can result in reduced muscle growth. The lack of change in myoblast differentiation in response to fetal serum was not surprising, given that there are no differences in muscle weight or muscle fiber cross-sectional area at birth in response to poor maternal diet in the same experimental cohort (Gauvin et al., unpublished). However, in a similar model, we have demonstrated that over- and restricted-feeding during gestation results in decreased post-natal muscle growth in the early post-natal period (Reed et al., 2014). The use of serum in this model allowed us to determine if factors in the serum influenced muscle growth

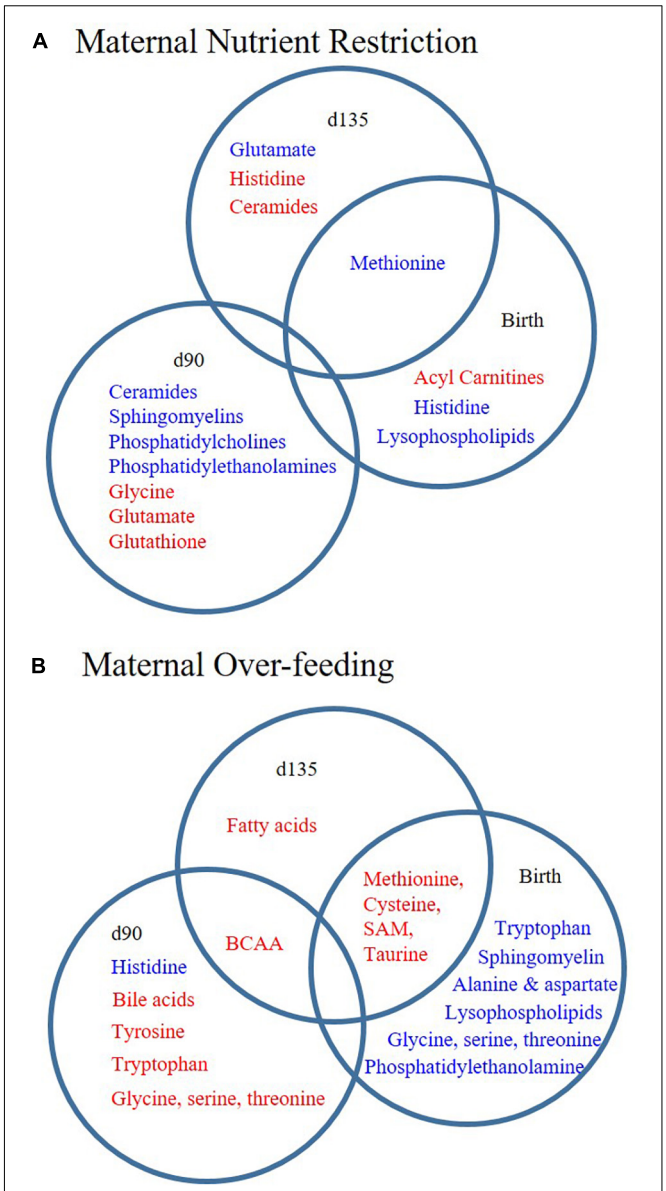

FIGURE 3 | Poor maternal diet results in distinct lipid and amino acid metabolite profiles in offspring longissimus. Offspring from ewes fed a control (CON; 100% NRC), over-fed (OVER; 140% NRC), or restricted-fed (RES; 60% NRC) diet were sampled at days 90 or 135 of gestation, or within 24 h of birth. Metabolite sub-pathways increased (red) or decreased (blue) in abundance at each time point in RES vs. CON **(A)** or OVER vs. CON **(B)**. BCAA, branched chain amino acid; SAM, *S*-adenosyl methionine.

and/or metabolism, or if the changes in muscle are due to other influences, such as programmed changes in the myogenic precursor cells (pre- or post-natally) or the local muscle environment.

Metabolome analysis demonstrated that both maternal diet and day of gestation drive changes in LM metabolite abundance, including changes to amino acid, lipid, carbohydrate, and energy pathways. Samples within each time point (day 90, day 135, and birth) exhibited an overall similar metabolite composition. These observations suggest, that at the time points evaluated that the stage of development is a stronger regulator of metabolism than maternal nutrition. This is not unexpected given the vast changes in fetal muscle metabolism during gestation (Battaglia and Meschia, 1978). The fetus relies primarily on carbohydrates and amino acids for energy, rather than lipids, during pre-natal development. These metabolites provide an energy source for oxidative metabolism, protein synthesis, and structural development that occurs in muscle throughout gestation (Battaglia and Meschia, 1978). While lipid oxidation for energy is limited relative to carbohydrate and amino acid utilization, lipid uptake into muscle is critical for establishing cellular membranes and maintaining cellular integrity. Birth represents a change in nutrient availability and energy substrate utilization (Girard, 1990; Hillman et al., 2012). At birth, the maternal glucose supply is removed, and the diet becomes richer in lipid. Therefore, changes to tissue utilization reflect the change in fuel availability to increase lipid oxidation post-natally (Girard, 1990; Hillman et al., 2012).

Offspring of restricted-fed ewes exhibited significant changes in the lipid metabolite profile, including changes in ceramide, sphingolipid, and phospholipid metabolites. Sphingolipids are an essential part of lipid membranes (including the mitochondrial membrane) and serve as second messengers for signal transduction in pathways affecting cell growth, differentiation, stress responses, and apoptosis (Merrill et al., 1997; Khavandgar and Murshed, 2015). Complex sphingolipids, such as sphingomyelins, are formed from ceramide in the Golgi complex by the action of sphingomyelin synthases (Kudo et al., 2008; Villani et al., 2008). Catabolism of sphingomyelin is catalyzed by sphingomyelinase and results in the generation of free phosphocholine and ceramide. The roles for ceramide and sphingomyelins in muscle are varied and not completely understood. Sphingolipid signaling (via production of sphingolipid-1-phosphate from sphingomyelin) mediates entry of satellite cells into the cell cycle from quiescence, supporting post-natal muscle growth and repair (Nagata et al., 2006). While reduced presence of sphingomyelins in developing muscle at day 90 suggests inhibited muscle development, we did not identify any difference in the number of Pax7-positive muscle progenitor cells or the muscle fiber CSA in the LM (Gauvin et al., unpublished), which suggests alternate roles for sphingomyelins at this time point. For example, the sphingomyelin pathway has been implicated in insulin resistance. At day 90 of gestation, the reduction in ceramide and sphingolipid abundance in RES offspring compared with CON may indicate altered insulin dynamics in an attempt to adapt to restricted nutrient availability. Although these changes were not observed at birth, we and others have demonstrated altered insulin sensitivity in offspring during postnatal growth suggesting that early alterations to sphingomyelin metabolites may be a mechanism that programs offspring muscle for altered insulin sensitivity later in life.

Potential changes in insulin dynamics during late gestation and early post-natal life are supported by the increases in 3-hydroxybutrylcarnitine and acetyl carnitine at birth. In rats, 3-hydroxybutryl-carnitine is increased during periods of insulin resistance induced by fasting and high fat diet feeding (An et al., 2004). 3-hydroxybutyrl-carnitine was also increased during fasting-induced ketosis in adult males and in patients with type 2 diabetes (Soeters et al., 2012; Mai et al., 2013). The total amount of 3-hydroxybutyrl-carnitine correlated with the 3-hydroxybutyrate rate of appearance, suggesting that 3-hydroxybutyrl-carnitine concentration is related to 3-hydroxybutyrate flux (Soeters et al., 2012). Indeed, 3-hydroxybutyrl-carnitine is formed from 3-hydroxybutyrate in a coenzyme A and ATP dependent manner. Increased concentration of 3-hydroxybutyrl-carnitine may reflect a limitation of ketone body oxidation or may be a mechanism to prevent mitochondrial accumulation or prevent ketoacidosis (Boudin et al., 1976; Ramsay et al., 2001). Further, acetyl carnitine concentration was increased in patients with impaired glucose tolerance or type 2 diabetes and was positively correlated with increased body fat and waist to hip ratio (Mai et al., 2013; Abu Bakar and Sarmidi, 2017). Insulin dependent uptake of 2-deoxyglucose in cultured myotubes was inhibited by the acetyl carnitine in a dose dependent manner, suggesting that acetyl carnitine contributes to insulin resistance in skeletal muscle (Miyamoto et al., 2016). Further, in myotubes with increased mitochondrial dysfunction (induced by Antimycin A), acyl carnitine metabolites were increased, potentially due to incomplete beta oxidation by the mitochondria (Abu Bakar and Sarmidi, 2017). Together, these data suggest that the fetus attempts to adapt to the restricted nutrient environment by altering insulin sensitivity during mid-gestation.

Offspring of over-fed dams demonstrated significant changes in amino acid metabolism. Muscle is the primary storage site for amino acids in the body, and protein accretion during late gestation and post-natal growth is the primary mechanism for muscle hypertrophy. In the fetus, amino acids serve as a source of energy but also as building blocks for protein accretion. The amino acids present in the muscle depend on the provision of amino acids via circulation as well as the balance of *de novo* synthesis and catabolism of amino acids in the muscle itself. During periods of fetal stress, protein catabolism increases in the hind limb muscle, mainly due to increased metabolism of BCAA (Liechty and Lemons, 1984; Liechty et al., 1987). Amino acid supplementation to fetuses in late gestation increased leucine oxidation but did not increase muscle protein accretion in control offspring (Brown et al., 2012). In humans, maternal BMI was positively associated with BCAA abundance and their metabolic byproducts, which are associated with the development of obesity and insulin resistance (Newgard et al., 2009; Wang et al., 2011). Leucine is metabolized to generate alanine and glutamine. Alanine concentrations were increased at day 90

of gestation in offspring of over-fed dams, consistent with increases in BCAA metabolites reflecting leucine degradation (e.g., beta-hydroxyisovalerate and 3-methylglutaconate), some of which remained increased at day 135 of gestation. Further, increased abundance of 3-hydroxyisobutyrate as a result of BCAA catabolism is associated with fatty acid uptake and lipid accumulation in muscle, leading to insulin resistance in mice (Jang et al., 2016). Thus, alterations in BCAA may predispose offspring of over-fed dams to obesity and metabolic dysregulation at later stages of development.

The complex interplay between metabolism and epigenetics is just now beginning to be understood (reviewed in Etchegaray and Mostoslavsky, 2016); however, fluctuations in metabolite abundance are associated with alterations in histone methylation and acetylation. Decreased abundance of N6-acetyllysine in offspring of over-fed ewes at birth suggests the occurrence of epigenetic changes in the muscle as a result of poor maternal diet. Acetylation of lysine on specific residues in the N-terminal domains of histones is recognized as a marker of active gene transcription (Crane-Robinson et al., 1997). Decreased abundance of N6-acetyllysine suggest a closed chromatin structure and decreased gene transcription in the offspring of over-fed dams compared with controls. Acetylmethionine abundance was also decreased at birth, further suggesting altered epigenetic activity, as methionine is the penultimate methyl group donor (Chen and Riggs, 2011). Further, the availability of flavin adenine dinucleotide (FAD) in adipocytes regulates the methylation status (and therefore transcription) of genes associated with energy expenditure such as PGC-1α and the pyruvate dehydrogenase kinase 4 (PDK4) through the activity of lysine-specific demethylase-1 (LSD1; Hino et al., 2012). In our data, at day 90 of gestation, offspring of over-fed dams demonstrated increased concentrations of FAD, suggesting altered methylation status of LSD1 target genes and possibly other epigenetic modifications.

Additionally, at day 90 of gestation, glucose-6-phosphate (G-6-P) and Coenzyme A were increased coupled with reduced adenosine and adenosine monophosphate. The increased G-6-P may contribute to the increased GSH at this time point through the pentose phosphate pathway, which uses G-6-P to generate NADPH via glucose-6-phosphate dehydrogenase (Diaz-Flores et al., 2006). Glutathione reductase then uses NADPH as an electron donor cofactor to generate reduced glutathione (GSH). This may be a protective mechanism against oxidative stress as a result of maternal over-nutrition. Indeed, GSH was increased at day 90 of gestation in response to increased maternal nutrient intake. Together, these data suggest that over-feeding during gestation alters muscle protein metabolism in the offspring in ways that likely predispose the offspring for reduced protein synthesis, increased oxidative stress, and altered post-natal muscle metabolism. Importantly, these changes may be programmed by epigenetic mechanisms, resulting in long-lasting effects that may span multiple generations.

As expected, the metabolite profiles of offspring of restricted- and over-fed dams were divergent in lipid and amino acid metabolism. For example, BCAA metabolites were reduced at day 90 of gestation and increased at birth in RES offspring compared with OVER offspring. Acyl carnitine moieties were increased in RES compared with OVER offspring at birth, suggesting divergent fatty acid metabolism. Further, sphingomyelins and ceramides were decreased in RES compared with OVER, suggesting alterations in fatty acid metabolism as well as insulin sensitivity. These data highlight the vast differences in the metabolic response of the muscle, despite similar phenotypes observed in offspring of poorly nourished ewes (Reed et al., 2014). Importantly, this demonstrates that despite similar phenotypic outcomes, over- and restricted-feeding during gestation result in distinct muscle metabolite profiles.

CONCLUSION

Poor maternal nutrition during gestation can negatively affect muscle and offspring development. We demonstrate here that over- and restricted-feeding during gestation alters metabolite abundance in the offspring muscle in a diet-specific manner. Together, these data suggest that poor maternal diet during gestation causes metabolic changes in offspring skeletal muscle, which likely have long-lasting effects on the potential for muscle growth, muscle metabolism, and importantly, whole body metabolism and energy efficiency.

ETHICS STATEMENT

This study was carried out in accordance with the recommendations of the University of Connecticut Institutional Animal Care and Use Committee. The protocol was approved by the University of Connecticut Institutional Animal Care and Use Committee.

AUTHOR CONTRIBUTIONS

DM participated in design and coordination, analyzed data, and drafted the manuscript. AJ, SP, MH, KM, KG, and SZ participated in design and coordination and critically evaluated the manuscript. SR conceived of the study, participated in design and coordination, analyzed data, and drafted the manuscript. All authors read and approved the final manuscript.

FUNDING

This work was supported by USDA National Institute of Food and Agriculture AFRI grant numbers 2013-01919 (to SZ) and 2016-67016-24863 (to SR) and the Storrs Agricultural Experiment Station.

ACKNOWLEDGMENTS

The authors thank V. Delaire and the UConn Livestock staff for their technical assistance, and T. Hoagland and the University of

Connecticut Animal Science undergraduate students for animal care during the duration of this experiment. The authors also thank Zoetis (Florham Park, NJ, United States) for their kind donation of the controlled intravaginal release devices used for estrous synchronization of ewes during breeding.

SUPPLEMENTARY MATERIAL

The Supplementary Material for this article can be found online at: https://www.frontiersin.org/articles/10.3389/fphys.2019.00515/full#supplementary-material

REFERENCES

Abu Bakar, M. H., and Sarmidi, M. R. (2017). Association of cultured myotubes and fasting plasma metabolite profiles with mitochondrial dysfunction in type 2 diabetes subjects. *Mol. Biosyst.* 13, 1838–1853. doi: 10.1039/c7mb00333a

An, J., Muoio, D. M., Shiota, M., Fujimoto, Y., Cline, G. W., Shulman, G. I., et al. (2004). Hepatic expression of malonyl-CoA decarboxylase reverses muscle, liver and whole-animal insulin resistance. *Nat. Med.* 10, 268–274. doi: 10.1038/nm995

Baron, A. D., Brechtel, G., Wallace, P., and Edelman, S. V. (1988). Rates and tissue sites of non-insulin- and insulin-mediated glucose uptake in humans. *Am. J. Physiol.* 255, E769–E774.

Battaglia, F. C., and Meschia, G. (1978). Principal substrates of fetal metabolism. *Physiol. Rev.* 58, 499–527. doi: 10.1152/physrev.1978.58.2.499

Beermann, D. H., Cassens, R. G., and Hausman, G. J. (1978). A second look at fiber type differentiation in porcine skeletal muscle. *J. Anim. Sci.* 46, 125–132. doi: 10.2527/jas1978.461125x

Boudin, G., Mikol, J., Guillard, A., and Engel, A. G. (1976). Fatal systemic carnitine deficiency with lipid storage in skeletal muscle, heart, liver and kidney. *J. Neurol. Sci.* 30, 313–325. doi: 10.1016/0022-510x(76)90137-4

Brown, L. D., Rozance, P. J., Thorn, S. R., Friedman, J. E., and Hay, W. W. Jr. (2012). Acute supplementation of amino acids increases net protein accretion in IUGR fetal sheep. *Am. J. Physiol. Endocrinol. Metab.* 303, E352–E364. doi: 10.1152/ajpendo.00059.2012

Cerisuelo, A., Baucells, M. D., Gasa, J., Coma, J., Carrion, D., Chapinal, N., et al. (2009). Increased sow nutrition during midgestation affects muscle fiber development and meat quality, with no consequences on growth performance. *J. Anim. Sci.* 87, 729–739. doi: 10.2527/jas.2007-0677

Chen, Z. X., and Riggs, A. D. (2011). DNA methylation and demethylation in mammals. *J. Biol. Chem.* 286, 18347–18353. doi: 10.1074/jbc.R110.205286

Crane-Robinson, C., Hebbes, T. R., Clayton, A. L., and Thorne, A. W. (1997). Chromosomal mapping of core histone acetylation by immunoselection. *Methods* 12, 48–56. doi: 10.1006/meth.1997.0446

Daniel, Z. C., Brameld, J. M., Craigon, J., Scollan, N. D., and Buttery, P. J. (2007). Effect of maternal dietary restriction during pregnancy on lamb carcass characteristics and muscle fiber composition. *J. Anim. Sci.* 85, 1565–1576. doi: 10.2527/jas.2006-743

DeFronzo, R. A., Gunnarsson, R., Bjorkman, O., Olsson, M., and Wahren, J. (1985). Effects of insulin on peripheral and splanchnic glucose metabolism in noninsulin-dependent (type II) diabetes mellitus. *J. Clin. Invest.* 76, 149–155. doi: 10.1172/jci111938

Diaz-Flores, M., Ibanez-Hernandez, M. A., Galvan, R. E., Gutierrez, M., Duran-Reyes, G., Medina-Navarro, R., et al. (2006). Glucose-6-phosphate dehydrogenase activity and NADPH/NADP+ ratio in liver and pancreas are dependent on the severity of hyperglycemia in rat. *Life Sci.* 78, 2601–2607. doi: 10.1016/j.lfs.2005.10.022

Etchegaray, J. P., and Mostoslavsky, R. (2016). Interplay between metabolism and epigenetics: a nuclear adaptation to environmental changes. *Mol. Cell.* 62, 695–711. doi: 10.1016/j.molcel.2016.05.029

Girard, J. (1990). Metabolic adaptations to change of nutrition at birth. *Biol. Neonate* 58(Suppl. 1), 3–15. doi: 10.1159/000243294

Hales, C. N., and Barker, D. J. (2001). The thrifty phenotype hypothesis. *Br. Med. Bull.* 60, 5–20. doi: 10.1093/bmb/60.1.5

Hales, C. N., and Ozanne, S. E. (2003). For debate: fetal and early postnatal growth restriction lead to diabetes, the metabolic syndrome and renal failure. *Diabetologia* 46, 1013–1019. doi: 10.1007/s00125-003-1131-7

Hillman, N. H., Kallapur, S. G., and Jobe, A. H. (2012). Physiology of transition from intrauterine to extrauterine life. *Clin. Perinatol.* 39, 769–783. doi: 10.1016/j.clp.2012.09.009

Hino, S., Sakamoto, A., Nagaoka, K., Anan, K., Wang, Y., Mimasu, S., et al. (2012). FAD-dependent lysine-specific demethylase-1 regulates cellular energy expenditure. *Nat. Commun.* 3:758. doi: 10.1038/ncomms1755

Hoffman, M. L., Reed, S. A., Pillai, S. M., Jones, A. K., McFadden, K. K., Zinn, S. A., et al. (2017). PHYSIOLOGY AND ENDOCRINOLOGY SYMPOSIUM:The effects of poor maternal nutrition during gestation on offspring postnatal growth and metabolism. *J. Anim. Sci.* 95, 2222–2232. doi: 10.2527/jas.2016.1229

Hoffman, M. L., Rokosa, M. A., Zinn, S. A., Hoagland, T. A., and Govoni, K. E. (2014). Poor maternal nutrition during gestation in sheep reduces circulating concentrations of insulin-like growth factor-I and insulin-like growth factor binding protein-3 in offspring. *Domest. Anim. Endocrinol.* 49, 39–48. doi: 10.1016/j.domaniend.2014.05.002

Jang, C., Oh, S. F., Wada, S., Rowe, G. C., Liu, L., Chan, M. C., et al. (2016). A branched-chain amino acid metabolite drives vascular fatty acid transport and causes insulin resistance. *Nat. Med.* 22, 421–426. doi: 10.1038/nm.4057

Jones, A. K., Gately, R. E., McFadden, K. K., Zinn, S. A., Govoni, K. E., and Reed, S. A. (2016). Transabdominal ultrasound for detection of pregnancy, fetal and placental landmarks, and fetal age before Day 45 of gestation in the sheep. *Theriogenology* 85, 939–945.e1. doi: 10.1016/j.theriogenology.2015.11.002

Khavandgar, Z., and Murshed, M. (2015). Sphingolipid metabolism and its role in the skeletal tissues. *Cell. Mol. Life Sci.* 72, 959–969. doi: 10.1007/s00018-014-1778-x

Knights, M., Maze, T. D., Bridges, P. J., Lewis, P. E., and Inskeep, E. K. (2001). Short-term treatment with a controlled internal drug releasing (CIDR) device and FSH to induce fertile estrus and increase prolificacy in anestrous ewes. *Theriogenology* 55, 1181–1191. doi: 10.1016/s0093-691x(01)00476-9

Kudo, N., Kumagai, K., Tomishige, N., Yamaji, T., Wakatsuki, S., Nishijima, M., et al. (2008). Structural basis for specific lipid recognition by CERT responsible for nonvesicular trafficking of ceramide. *Proc. Natl. Acad. Sci. U.S.A.* 105, 488–493. doi: 10.1073/pnas.0709191105

Li, X., Fang, P., Yang, W. Y., Chan, K., Lavallee, M., Xu, K., et al. (2017). Mitochondrial ROS, uncoupled from ATP synthesis, determine endothelial activation for both physiological recruitment of patrolling cells and pathological recruitment of inflammatory cells. *Can. J. Physiol. Pharmacol.* 95, 247–252. doi: 10.1139/cjpp-2016-0515

Liechty, E. A., and Lemons, J. A. (1984). Changes in ovine fetal hindlimb amino acid metabolism during maternal fasting. *Am. J. Physiol.* 246, E430–E435.

Liechty, E. A., Polak, M. J., and Lemons, J. A. (1987). Branched-chain amino acid carbon and nitrogen arteriovenous concentration differences across the ovine fetal hindlimb. *Pediatr. Res.* 21, 44–48. doi: 10.1203/00006450-198701000-00011

Mai, M., Tonjes, A., Kovacs, P., Stumvoll, M., Fiedler, G. M., and Leichtle, A. B. (2013). Serum levels of acylcarnitines are altered in prediabetic conditions. *PLoS One* 8:e82459. doi: 10.1371/journal.pone.0082459

Merrill, A. H. Jr., Schmelz, E. M., Dillehay, D. L., Spiegel, S., Shayman, J. A., Schroeder, J. J., et al. (1997). Sphingolipids–the enigmatic lipid class: biochemistry, physiology, and pathophysiology. *Toxicol. Appl. Pharmacol.* 142, 208–225. doi: 10.1006/taap.1996.8029

Miyamoto, Y., Miyazaki, T., Honda, A., Shimohata, H., Hirayama, K., and Kobayashi, M. (2016). Retention of acetylcarnitine in chronic kidney disease causes insulin resistance in skeletal muscle. *J. Clin. Biochem. Nutr.* 59, 199–206. doi: 10.3164/jcbn.15-146

Nagata, Y., Partridge, T. A., Matsuda, R., and Zammit, P. S. (2006). Entry of muscle satellite cells into the cell cycle requires sphingolipid signaling. *J. Cell Biol.* 174, 245–253. doi: 10.1083/jcb.200605028

Nathanielsz, P. W., Poston, L., and Taylor, P. D. (2007). In utero exposure to maternal obesity and diabetes: animal models that identify and characterize implications for future health. *Clin. Perinatol.* 34, 515–526. doi: 10.1016/j.clp.2007.09.005

National Research Council (1985). "Nutrient requirements of sheep," in *National Research Council (NRC)*. Washington, DC: National Academic Press.

Newgard, C. B., An, J., Bain, J. R., Muehlbauer, M. J., Stevens, R. D., Lien, L. F., et al. (2009). A branched-chain amino acid-related metabolic signature that differentiates obese and lean humans and contributes to insulin resistance. *Cell. Metab.* 9, 311–326. doi: 10.1016/j.cmet.2009.02.002

Pillai, S. M., Jones, A. K., Hoffman, M. L., McFadden, K. K., Reed, S. A., Zinn, S. A., et al. (2017). Fetal and organ development at gestational days 45, 90, 135 and at birth of lambs exposed to under- or over-nutrition during gestation. *Transl. Anim. Sci.* 1, 16–25.

Ramsay, R. R., Gandour, R. D., and van der Leij, F. R. (2001). Molecular enzymology of carnitine transfer and transport. *Biochim. Biophys. Acta* 1546, 21–43. doi: 10.1016/s0167-4838(01)00147-9

Reed, S. A., Raja, J. S., Hoffman, M. L., Zinn, S. A., and Govoni, K. E. (2014). Poor maternal nutrition inhibits muscle development in ovine offspring. *J. Anim. Sci. Biotechnol.* 5:43. doi: 10.1186/2049-1891-5-43

Rolfe, D. F., Newman, J. M., Buckingham, J. A., Clark, M. G., and Brand, M. D. (1999). Contribution of mitochondrial proton leak to respiration rate in working skeletal muscle and liver and to SMR. *Am. J. Physiol.* 276, C692–C699. doi: 10.1152/ajpcell.1999.276.3.C692

Rowe, R. W., and Goldspink, G. (1969). Muscle fibre growth in five different muscles in both sexes of mice. *J. Anat.* 104, 519–530.

Soeters, M. R., Serlie, M. J., Sauerwein, H. P., Duran, M., Ruiter, J. P., Kulik, W., et al. (2012). Characterization of D-3-hydroxybutyrylcarnitine (ketocarnitine): an identified ketosis-induced metabolite. *Metabolism* 61, 966–973. doi: 10.1016/j.metabol.2011.11.009

Tong, J. F., Yan, X., Zhu, M. J., Ford, S. P., Nathanielsz, P. W., and Du, M. (2009). Maternal obesity downregulates myogenesis and beta-catenin signaling in fetal skeletal muscle. *Am. J. Physiol. Endocrinol. Metab.* 296, E917–E924. doi: 10.1152/ajpendo.90924.2008

Villani, M., Subathra, M., Im, Y. B., Choi, Y., Signorelli, P., Del Poeta, M., et al. (2008). Sphingomyelin synthases regulate production of diacylglycerol at the Golgi. *Biochem. J.* 414, 31–41. doi: 10.1042/BJ20071240

Wang, T. J., Larson, M. G., Vasan, R. S., Cheng, S., Rhee, E. P., McCabe, E., et al. (2011). Metabolite profiles and the risk of developing diabetes. *Nat. Med.* 17, 448–453. doi: 10.1038/nm.2307

White, R. B., Bierinx, A. S., Gnocchi, V. F., and Zammit, P. S. (2010). Dynamics of muscle fibre growth during postnatal mouse development. *BMC Dev. Biol.* 10:21. doi: 10.1186/1471-213X-10-21

Wigmore, P. M., and Stickland, N. C. (1983). Muscle development in large and small pig fetuses. *J. Anat.* 137(Pt 2), 235–245.

Wolfe, R. R. (2006). The underappreciated role of muscle in health and disease. *Am. J. Clin. Nutr.* 84, 475–482. doi: 10.1093/ajcn/84.3.475

Wu, G., Bazer, F. W., Wallace, J. M., and Spencer, T. E. (2006). Board-invited review: intrauterine growth retardation: implications for the animal sciences. *J. Anim. Sci.* 84, 2316–2337. doi: 10.2527/jas.2006-156

Zhu, M. J., Ford, S. P., Means, W. J., Hess, B. W., Nathanielsz, P. W., and Du, M. (2006). Maternal nutrient restriction affects properties of skeletal muscle in offspring. *J. Physiol.* 575, 241–250. doi: 10.1113/jphysiol.2006.112110

Zurlo, F., Larson, K., Bogardus, C., and Ravussin, E. (1990). Skeletal muscle metabolism is a major determinant of resting energy expenditure. *J. Clin. Invest.* 86, 1423–1427. doi: 10.1172/jci114857

Conflict of Interest Statement: The authors declare that the research was conducted in the absence of any commercial or financial relationships that could be construed as a potential conflict of interest.

Copyright © 2019 Martin, Jones, Pillai, Hoffman, McFadden, Zinn, Govoni and Reed. This is an open-access article distributed under the terms of the Creative Commons Attribution License (CC BY). The use, distribution or reproduction in other forums is permitted, provided the original author(s) and the copyright owner(s) are credited and that the original publication in this journal is cited, in accordance with accepted academic practice. No use, distribution or reproduction is permitted which does not comply with these terms.

frontiers in Physiology

ORIGINAL RESEARCH
published: 24 May 2019
doi: 10.3389/fphys.2019.00562

Sex-Specific Effects of Nanoparticle-Encapsulated MitoQ (nMitoQ) Delivery to the Placenta in a Rat Model of Fetal Hypoxia

*Esha Ganguly[1,2,3], Mais M. Aljunaidy[1,2,3], Raven Kirschenman[2,3], Floor Spaans[2,3], Jude S. Morton[2,3], Thomas E. J. Phillips[4], C. Patrick Case[5], Christy-Lynn M. Cooke[2,3] and Sandra T. Davidge[1,2,3]**

[1]Department of Physiology, University of Alberta, Edmonton, AB, Canada, [2]Department of Obstetrics and Gynaecology, University of Alberta, Edmonton, AB, Canada, [3]Women and Children's Health Research Institute, University of Alberta, Edmonton, AB, Canada, [4]Dementia Research Institute, Cardiff University, Cardiff, United Kingdom, [5]Musculoskeletal Research Unit, University of Bristol, Bristol, United Kingdom

OPEN ACCESS

Edited by:
Dane Alan Crossley II, University of North Texas System, United States

Reviewed by:
Turk Rhen, University of North Dakota, United States
Jayanth Ramadoss, Texas A&M University, United States

***Correspondence:**
Sandra T. Davidge
sdavidge@ualberta.ca

Specialty section:
This article was submitted to Embryonic and Developmental Physiology, a section of the journal Frontiers in Physiology

Received: *04 March 2019*
Accepted: *24 April 2019*
Published: *24 May 2019*

Citation:
Ganguly E, Aljunaidy MM, Kirschenman R, Spaans F, Morton JS, Phillips TEJ, Case CP, Cooke C-LM and Davidge ST (2019) Sex-Specific Effects of Nanoparticle-Encapsulated MitoQ (nMitoQ) Delivery to the Placenta in a Rat Model of Fetal Hypoxia. Front. Physiol. 10:562. doi: 10.3389/fphys.2019.00562

Pregnancy complications associated with chronic fetal hypoxia have been linked to the development of adult cardiovascular disease in the offspring. Prenatal hypoxia has been shown to increase placental oxidative stress and impair placental function in a sex-specific manner, thereby affecting fetal development. As oxidative stress is central to placental dysfunction, we developed a placenta-targeted treatment strategy using the antioxidant MitoQ encapsulated into nanoparticles (nMitoQ) to reduce placental oxidative/nitrosative stress and improve placental function without direct drug exposure to the fetus in order to avoid off-target effects during development. We hypothesized that, in a rat model of prenatal hypoxia, nMitoQ prevents hypoxia-induced placental oxidative/nitrosative stress, promotes angiogenesis, improves placental morphology, and ultimately improves fetal oxygenation. Additionally, we assessed whether there were sex differences in the effectiveness of nMitoQ treatment. Pregnant rats were intravenously injected with saline or nMitoQ (100 µl of 125 µM) on gestational day (GD) 15 and exposed to either normoxia (21% O_2) or hypoxia (11% O_2) from GD15 to 21. On GD21, placentae from both sexes were collected for detection of superoxide, nitrotyrosine, nitric oxide, CD31 (endothelial cell marker), and fetal blood spaces, *Vegfa* and *Igf2* mRNA expression in the placental labyrinth zone. Prenatal hypoxia decreased male fetal weight, which was not changed by nMitoQ treatment; however, placental efficiency (fetal/placental weight ratio) decreased by hypoxia and was increased by nMitoQ in both males and females. nMitoQ treatment reduced the prenatal hypoxia-induced increase in placental superoxide levels in both male and female placentae but improved oxygenation in only female placentae. Nitrotyrosine levels were increased in hypoxic female placentae and were reduced by nMitoQ. Prenatal hypoxia reduced placental *Vegfa* and *Igf2* expression in both sexes, while nMitoQ increased *Vegfa* and *Igf2* expression only in hypoxic female placentae. In summary, our study suggests that nMitoQ treatment could be pursued as a potential preventative strategy against placental oxidative stress and programming of adult cardiovascular disease in

offspring exposed to hypoxia *in utero*. However, sex differences need to be taken into account when developing therapeutic strategies to improve fetal development in complicated pregnancies, as nMitoQ treatment was more effective in placentae from females than males.

Keywords: placenta, hypoxia, MitoQ, nanoparticles, sex difference

INTRODUCTION

Chronic fetal hypoxia, a common consequence of pregnancy complications (e.g., placental insufficiency), has been linked to the development of cardiovascular and metabolic diseases in the adult offspring. The placenta serves as feto-maternal interface for the exchange of nutrients and oxygen to the fetus. Placental insufficiency is often associated with placental oxidative and nitrosative stress (i.e., formation of reactive oxygen/nitrogen species; ROS/RNS). An imbalance in ROS/RNS levels caused by excessive generation of ROS and/or a fall in endogenous antioxidants such as superoxide dismutase (SOD) can lead to impaired placental development and altered placental function (reviewed in Al-Gubory et al., 2010; Schoots et al., 2018). One impact of excessive superoxide anions is the resultant scavenging of nitric oxide (NO) to produce RNS (e.g., peroxynitrite; Myatt and Cui, 2004); therefore, increased superoxide levels could reduce NO bioavailability and impair the important contribution of NO in feto-placental angiogenesis (Webster et al., 2008).

Interestingly, the placental response to oxidative stress appears to be different in placentae from males compared with females (reviewed in Rosenfeld, 2015). Human studies have shown that the placental oxidative stress response to adverse maternal environments (such as oxidative/nitrosative stress and reduced levels of antioxidants) in general appears to be more pronounced in male versus female placentae (Stark et al., 2011; Sedlmeier et al., 2014; Muralimanoharan et al., 2015; Evans and Myatt, 2017). In rodents, similar results were found, where adverse maternal environments (such as prenatal hypoxia) altered placental morphology, placental gene expression, and enzymes for epigenetic modifications (e.g., DNA methylation) in a sexually dimorphic manner (Mao et al., 2010; Gabory et al., 2012; Kim et al., 2014; Thompson et al., 2018). Therefore, examining sex-specific differences in the placental responses to adverse maternal environments or placental phenotypes as an outcome of the adverse environments is warranted.

As the placenta lacks both autonomic and cholinergic innervation, placental morphology and function are dependent on locally derived growth factors such as vascular endothelial growth factor A (VEGFA) and insulin-like growth factor 2 (IGF2; Reynolds and Redmer, 2001; Marzioni et al., 2004). Expression of the pro-angiogenic factor VEGFA is regulated by the oxygen sensing family of transcription factors such as hypoxia-inducible factor-1 alpha (HIF-1α; Cuffe et al., 2014). Placental hypoxia has been shown to impair feto-placental vascular development *via* VEGFA and HIF-1α (Kulandavelu et al., 2013). Decreased IGF2 expression is also associated with intrauterine growth restriction (IUGR) and critical to placental morphology and nutrient transfer to the fetus (Coan et al., 2008). In addition, hypoxia and placental oxidative/nitrosative stress may cause mitochondrial dysfunction, DNA damage, or reduced expression of the antioxidant system, all of which can affect normal placental function and potentially reduce oxygen and nutrient delivery, thus impairing fetal development (Droge, 2002; Lappas et al., 2010; Thompson and Al-Hasan, 2012). Therefore, given that oxidative stress is a central mediator of placental dysfunction in fetal hypoxia, prenatal treatment of placental oxidative stress could potentially prevent the long-term effects of fetal hypoxia on adult offspring.

Mitochondria are a major source of cellular ROS (as reviewed in Holland et al., 2017), and human placental tissues from complicated pregnancies were shown to have increased mitochondrial content, decreased respiratory chain complex expression, and impaired mitochondrial function (as reviewed in Mando et al., 2014; Chiaratti et al., 2015; McCarthy and Kenny, 2016). Therefore, our lab and others have been studying the potential use of the mitochondrial-targeted antioxidant MitoQ to target placental oxidative stress in complicated pregnancies (Phillips et al., 2017; Aljunaidy et al., 2018; Nuzzo et al., 2018). MitoQ consists of a ubiquinone moiety linked to a positively charged lipophilic cation allowing for accumulation on the inner mitochondrial membrane, making it highly effective in preventing mitochondrial oxidative stress (Smith et al., 1999; Ross et al., 2005; Murphy and Smith, 2007). Indeed, in a rat model of prenatal hypoxia, MitoQ treatment prevented the increase in mitochondrial stress markers in the placental labyrinth zone (Nuzzo et al., 2018). Recently, we have shown that MitoQ encapsulated into polymeric nanoparticles (nMitoQ) is a delivery approach to access the placental syncytium without crossing the placental basal membrane to reach the fetus (Aljunaidy et al., 2017; Phillips et al., 2017). With this treatment strategy, we showed that maternal treatment with nMitoQ in a rat model of prenatal hypoxia prevented placental oxidative stress, increased fetal weight in female fetuses, improved neuronal development, and had sex-dependent beneficial effects on *in vivo* cardiovascular function in prenatally hypoxic adult offspring (Phillips et al., 2017; Aljunaidy et al., 2018). Furthermore, nMitoQ treatment of human preeclamptic placental explants improved neuronal development *in vitro* (Scott et al., 2018). However, the effect of nMitoQ treatment on placental morphology, the mechanisms *via* which reduced placental oxidative stress might improve placental function and fetal growth, and any potential sex differences are still under investigation.

In the current study, we aimed to further identify the effect of nMitoQ treatment on placental function and oxidative stress, and the sex-specific effects of the treatment, in a rat model of prenatal hypoxia. We hypothesized that antioxidant nMitoQ treatment would decrease prenatal hypoxia-induced oxidative/nitrosative stress along with increasing VEGFA expression, improving placental morphology, increasing IGF2 expression, and ultimately resulting in improved fetal growth. Moreover, since it has been shown that placentae from male and female fetuses respond to prenatal stress differently, we hypothesized that there is a sex-specific divergence in the placental response to prenatal hypoxia-induced oxidative/nitrosative stress and the effectiveness of nMitoQ treatment.

MATERIALS AND METHODS

Ethics Approval

All procedures described were approved by the University of Alberta Animal Policy and Welfare Committee and were in accordance with the guidelines of the Canadian Council on Animal Care (AUP #242).

Preparation of Nanoparticle Encapsulated MitoQ (nMitoQ)

MitoQ loaded nanoparticles were synthesized as previously described (Phillips et al., 2017; Aljunaidy et al., 2018). Briefly, an amphiphilic copolymer of poly (γ-glutamic acid) and L-phenylalanine ethyl ester (γ-PGA-Phe) was synthesized as described previously (Kim et al., 2009). γ-PGA-Phe (10 mg/ml) dissolved in dimethyl sulfoxide (DMSO) was added to an equivalent volume of sodium chloride (NaCl; 0.15 M), dialyzed against distilled water using a dialysis membrane, freeze-dried, and resuspended in phosphate-buffered Saline (PBS; 10 mg/ml). Nanoparticles were then measured by dynamic light scattering (Zetasizer Nano ZS, Malvern Instruments, UK) as diameter (180 nm), zeta potential (−20 mV), and polydispersity index (0.12). γ-PGA-Phe nanoparticles (10 mg/ml) were mixed with MitoQ (2 mg/ml) at equivalent volume in NaCl (0.2 M). Nanoparticles were isolated by centrifugation, washed, and resuspended in PBS (10 mg/ml). The amount of MitoQ (278 nm), which was adsorbed to nanoparticles, was evaluated by UV absorption measurement, as previously described (Phillips et al., 2017).

Prenatal Hypoxia Rat Model

Female Sprague-Dawley rats, 3 months of age (weighing 250–275 g), were obtained from Charles River (Quebec, Canada) and housed in a temperature and light controlled room (10:14 h light/dark cycle) with *ad libitum* access to food and water. Females were housed with Sprague-Dawley males overnight, and pregnancy was confirmed the following morning by the presence of sperm in a vaginal smear, which was defined as gestational day (GD) 0 of pregnancy. On GD15, pregnant dams were randomly assigned into two groups that were exposed to either prenatal hypoxia (11% O_2) by placing them in a Plexiglas hypoxic chamber from GD15 to 21 or were housed at atmospheric oxygen (21% O_2) as controls. Pregnant dams received an intravenous injection *via* the tail vein on GD15 with either saline or nMitoQ (100 µl of 125 µM nMitoQ). As nMitoQ is recycled and lasts up to 1 week *in vivo*, the nMitoQ treatment protocol consisted only of a single injection (Phillips et al., 2017). The dose of nMitoQ was based on our previous studies (Phillips et al., 2017; Aljunaidy et al., 2018). As our study is focused on nMitoQ, as a single entity, we have a saline control rather than a nanoparticle along group as the properties may be different without the MitoQ and, ultimately, nanoparticles alone would never be used in practice. Previous studies have demonstrated that these nanoparticles are inert (Phillips et al., 2017; Scott et al., 2018). At the end of gestation, on GD21, rats were euthanized prior to parturition and fetal and placental weights were measured. Whole placentae (labyrinth and junctional zone) from male and female fetuses (two/sex/litter) were processed and embedded in either paraffin or optimal cutting temperature (OCT) compound for immunofluorescent and other staining procedures, as listed below. In other placentae (two/sex/litter), the placental labyrinth zones were isolated and snap frozen in liquid nitrogen for RNA and DNA methylation analysis.

Dihydroethidium Staining for Superoxide Production and Diaminofluorescein-FM (DAF-FM) for Nitric Oxide Levels

Placental cryostat sections (10 µm) were thawed, washed three times with Hank's balanced salt solution (HBSS), and incubated with dihydroethidium (DHE) to measure superoxide levels (200 µM, Biotium, Burlington, Canada) or DAF-FM to measure nitric oxide levels (10 µM, Thermo Fisher Scientific, Eugene, OR, USA) in HBSS at 37°C for 30 min. Sections were washed with HBSS (3 × 2 min) and covered with a drop of 4′,6-diamidino-2-phenylindole (DAPI) (Vector Laboratories). Sections were protected from light, and pictures were immediately taken to prevent photobleaching.

Immunofluorescent Nitrotyrosine Staining for Placental Peroxynitrite Levels and CD31 Staining to Assess Placental Labyrinth Feto-Placental Vascular Capillaries

Nitrotyrosine residues are the molecular footprint of peroxynitrite generation and can be used as a marker of peroxynitrite (Webster et al., 2008). CD31 was used as an endothelial marker (Newman, 1997) to assess placental vascularization. Placental cryostat sections (8 µm) were thawed, fixed in ice-cold acetone for 10 min, washed thrice in PBS, and non-specific binding was blocked using 2% bovine serum albumin (BSA) in PBS for 60 min. Sections were incubated overnight at 4°C with a primary antibody for nitrotyrosine (1:10; mouse-anti-tyrosine, NOVUS Biologicals, Oakville, ON, Canada) or CD31 (1:200 mouse-anti-CD31/PECAM-1,

NOVUS Biologicals) in 2% BSA/PBS. The next day, sections were washed thrice with PBS and incubated with secondary antibody [1:250 in 2% BSA/PBS; donkey anti-mouse IgG (H + L), AF488, Alexa, Invitrogen] for 1 h at room temperature. Sections were washed with PBS thrice, mounting medium containing DAPI was added (Vector Laboratories; Burlingame, CA, U.S.A) and slides were covered, protected from light and left to dry overnight. Images were taken the next day.

Immunofluorescent Staining for Placental HIF-1α Expression

Placental levels of the transcription factor hypoxia-inducible factor-1α (HIF-1α) were measured as a marker of hypoxia. Placental PFA-fixed sections (8 μm) were dewaxed in xylene and rehydrated in ethanol (100, 95 and 80%). Endogenous peroxidase activity was blocked using 10% H_2O_2 in distilled water for 10 min and incubated in sodium citrate buffer supplemented with 0.05% Tween 20 at 90°C for 20 min for antigen retrieval. Non-specific staining was blocked with 2% BSA/PBS for 60 min at room temperature and incubated overnight at 4°C with a primary antibody against HIF-1α (1:250; rabbit-anti-HIF1 alpha, NOVUS Biologicals, Oakville, ON, Canada) in 2% BSA/PBS. The next day, sections were washed twice with Tris buffered saline containing 0.05% Tween 20 (TBS-T) and incubated with secondary antibody [1:250; goat-anti-rabbit IgG (H + L)-AF546, Invitrogen, Carlsbad, CA, USA] in TBS-T for 60 min at room temperature. After incubation with secondary antibody, sections were washed twice in TBS-T, once in distilled water and mounted using mounting medium containing DAPI (Vector Laboratories). Slides were protected from light and left to dry overnight. Images were taken the next day.

Immunofluorescent Staining for Placental and Fetal Tissue Oxygenation

In a separate group of dams, tissue oxygenation levels were assessed by intraperitoneal (i.p.) injection of either pimonidazole hydrochloride (60 mg/kg) (Hypoxyprobe™-1, Burlington, USA) or an equivalent volume of vehicle (saline) as a control on GD20. Six hours post injection, dams were euthanized, and placentae, fetal hearts, and fetal liver were collected and snap frozen. Pimonidazole levels in placental tissues and fetal cardiac and hepatic tissues from both sexes were assessed by immunostaining. Pimonidazole hydrochloride (also known as 2-nitroimidazoles) distributes to all tissues but is activated by reduction in cells exposed to oxygen concentration less than 14 micromolar, which is equivalent to a partial pressure pO_2 = 10 mmHg at 37°C. The activated intermediate forms stable adducts with proteins containing thiol groups (i.e., reduced pimonidazole, the staining product). Placental cryosections (8 μm) were fixed in acetone (10 min) and washed in PBS thrice, and non-specific staining was blocked using 2% BSA/PBS for 1 h. Sections were incubated overnight at 4°C with monoclonal anti-pimonidazole antibody (1:200; Hypoxyprobe™ Kit) in 2% BSA/PBS. The next day, sections were washed thrice in PBS and incubated with secondary antibody [1:250; donkey anti-mouse IgG (H + L), AF488, Alexa, Invitrogen] in 2% BSA/PBS for 60 min. Sections were washed with PBS three times and mounted using mounting medium containing DAPI (Vector Laboratories). Slides were protected from light and left to dry overnight. Images were taken the next day.

Morphological Analysis of Placenta

Using an established hematoxylin and eosin (H&E) staining protocol, placental PFA-fixed sections (8 μm) were dewaxed in histoclear, rehydrated, stained with filtered Harris's hematoxylin for 3 min, washed with distilled water, and then put into filtered eosin for 30 s. The placental sections were washed in cold water, covered, and left to dry overnight.

Image Analysis

All images were taken on an Olympus IX81 fluorescence microscope with CellSens Dimensions software (Olympus, Japan) with TRITC at 532 nm (for DHE, HIF-1α staining) or FITC at 488 nm (for nitrotyrosine, DAF-FM and CD31 staining) wavelength, respectively. Three representative pictures of the placental labyrinth zone were randomly taken from each of the tissue section at 20× magnification. All pictures were corrected to the blank controls (i.e., samples without DHE, or samples incubated only with secondary antibodies) to remove background staining. Fluorescent images were analyzed using ImageJ 1.48 software (National Institutes of Health, Bethesda, MD, USA) to determine mean fluorescence intensity (MFI). MFI values from the DHE, nitrotyrosine, and pimonidazole staining were normalized to the nuclei counts per image. The average MFI of the three representative images per experimental group was taken.

For placental morphological analysis, images were taken with a digital camera mounted on a bright field microscope (EVOS XL Core Imaging System, Thermo Fisher Scientific, Canada) at a 2× magnification. For the other assessments, three randomly selected representative fields from each placenta were obtained at a magnification of 40×. Then, using ImageJ software, placental blood space area in each field of view was converted into black and remaining placental tissue into white for quantification. Total area of fetal blood space per field of view was calculated using ImageJ software, and the values were averaged per experimental group. Briefly, images were opened in ImageJ and converted into 16 bit binary images. Following which a threshold was set automatically by the program, which converted the placental blood space area into black and remaining placental tissue into white. Particle count of placental blood space was analyzed on ImageJ using the option of "analyze particles" in the software, which resulted in a surface area value for the black space, i.e., the placental blood space.

Real-Time RT-PCR for Placental Gene Expression of IGF and VEGFA

Total RNA was isolated from the placental labyrinth using RNeasy plus Mini Kit (QIAGEN Inc., Ontario, Canada).

Total RNA was reverse transcribed to cDNA using the High Capacity cDNA Reverse Transcription Kit (AB Applied Biosystems, Warrington, UK) according to the manufacturer's instructions. Using gene-specific primers for *Igf2, Igf2P0, Igf1r, Igf2r,* and *Vegfa,* quantitative real time RT-PCR (qPCR) was performed using iQ™ SYBR Green Supermix (Bio-Rad, Hercules, CA, USA; see **Table 1** for primers). Briefly, thermal cycling was initiated by a 5 min. Denaturation at 95°C, followed by 40 cycles of 95°C for 30 s, annealing at 60°C for 15 s, and 72°C for 30 s. Samples without reverse transcriptase (RT) using the same PCR primers were done as a control for the presence of genomic DNA. The gene expression levels in each sample (absolute quantification) were calculated from the standard curve (for each primer set) and normalized to rat Cyclophilin A (PPIA) expression.

Statistical Analysis

Statistical analyses were performed using GraphPad Prism 7.04 software (GraphPad Software, U.S.A.). All data are expressed as mean ± SEM. All data were analyzed using a two-way ANOVA, with hypoxia and nMitoQ treatment as the two independent factors, followed by Sidak's multiple comparison *post hoc* tests. A value of $p < 0.05$ was considered significant.

TABLE 1 | Quantitative real-time PCR primers.

Gene	Forward primer (5′–3′)	Reverse primer (5′–3′)
Igf2	TGT CTA CCT CTC AGG CCG TAC TT	TCC AGG TGT CGA ATT TGA AGA A
Igf2P0	GAT CAT CGT CCA GGC AAT TT	GTT GCG TAG TTC CCG AAG TT
Igf1r	AAG GAT GGC GTC TTC ACC A	GAG TGG CGA TCT CCC AGA G
Igf2r	CTG CAG GCG GGA AAG	TTC CAC TCT TAT CCA CAG CAC
Vegfa	GTG CAC TGG ACC CTG GCT TT	TTC ACC ACT TCA TGG GCT TTC TG
Ppia	AGC ATA CAG GTC CTG GCA TC	TTC ACC TTC CCA AAG ACC AC

RESULTS

Offspring and Placental Characteristics

In male fetuses, prenatal hypoxia decreased fetal weight and abdominal girth without affecting placental weight (**Table 2**). nMitoQ treatment increased male abdominal girth in the prenatal hypoxia exposed group, while no effects of nMitoQ treatment were observed on fetal or placental weights in males (**Table 2**). Prenatal hypoxia reduced placental efficiency and expressed as ratio of fetal weight/placental weight in male fetuses, which was not significantly improved by nMitoQ treatment; however, placental efficiency in the hypoxia/nMitoQ group was no longer significantly different than normoxia/saline controls (**Table 2**), suggesting an effect of nMitoQ treatment. Crown-to-rump length was similar between all experimental groups in male fetuses (**Table 2**).

In female fetuses, prenatal hypoxia had no effect on fetal weight or abdominal girth but increased placental weight, which was significantly reduced by nMitoQ treatment (**Table 3**). nMitoQ treatment had no effect on female fetal weight or abdominal girth (**Table 3**). Prenatal hypoxia reduced placental efficiency and expressed as ratio of fetal weight/placental weight in female fetuses, which was not significantly improved by nMitoQ treatment; however, placental efficiency in the hypoxia/nMitoQ group was no longer significantly different normoxia/saline controls (**Table 3**). Crown-to-rump length was similar between all experimental groups in female fetuses (**Table 3**).

nMitoQ Treatment Improved Placental Oxidative/Nitrosative Stress in Female Offspring

Superoxide and peroxynitrite levels were assessed as markers of oxidative/nitrosative stress. In male offspring, superoxide levels were significantly increased in offspring exposed to prenatal hypoxia compared to normoxic control offspring (**Figure 1A**). nMitoQ treatment significantly decreased placental superoxide generation in prenatally hypoxic male offspring and had no effect in the control group (**Figure 1A**). Nitrotyrosine levels (**Figure 1B**) or nitric oxide levels (**Figure 1C**) were not

TABLE 2 | Fetal and placental characteristics of male offspring.

Variables	Normoxia		p-Hypoxia		Main effect		
	Saline	nMitoQ	Saline	nMitoQ	p-Hypoxia	nMitoQ	Interaction
Fetal weight (g)	5.81 ± 0.24	5.6 ± 0.15	5.21 ± 0.19	5.13 ± 0.26	*	–	–
Placental weight (g)	0.61 ± 0.04	0.58 ± 0.03	0.61 ± 0.02	0.62 ± 0.03	–	–	–
Fetal weight/placental weight	9.05 ± 0.39	9.76 ± 0.50	7.96 ± 0.78	8.69 ± 0.56	–	–	–
Abdominal girth (cm)	3.87 ± 0.08	3.72 ± 0.05	3.32 ± 0.13	**3.82 ± 0.13**†	*	–	**
Crown-rump length (cm)	4.78 ± 0.09	4.92 ± 0.12	4.47 ± 0.18	4.82 ± 0.13	–	–	–

Body weight, placental weight, placental efficiency (body weight/placental weight), abdominal girth, and crown-rump length from male fetuses collected on GD21. Data are represented as mean ± SEM. All groups were compared using a two-way ANOVA followed by Sidak's post hoc test.

**p < 0.05 overall group effect of prenatal hypoxia.*

***p < 0.01 interaction between prenatal hypoxia and nMitoQ treatment.*

†p < 0.05 versus corresponding hypoxia-saline group. Exact p-value is p = 0.006.

affected by prenatal hypoxia or nMitoQ treatment in placentae from male offspring.

In female offspring, superoxide levels significantly increased in offspring exposed to prenatal hypoxia were significantly decreased by nMitoQ treatment in prenatally hypoxic offspring and had no effect in the control group (**Figure 1D**). Nitrotyrosine levels tended to be increased in the placentae of prenatally hypoxic female offspring (**Figure 1E**). Moreover, there was a significant interaction between nMitoQ treatment and prenatal hypoxia exposure in which nMitoQ treatment decreased

TABLE 3 | Fetal and placental characteristics of female offspring.

Variables	Normoxia		p-Hypoxia		Main effect		
	Saline	nMitoQ	Saline	nMitoQ	p-Hypoxia	nMitoQ	Interaction
Fetal weight (g)	5.16 ± 0.29	5.81 ± 0.14	5.17 ± 0.16	5.26 ± 0.09	–	–	–
Placental weight (g)	0.56 ± 0.01	0.59 ± 0.01	0.62 ± 0.02	**0.56 ± 0.01**†	–	–	*
Fetal weight/placental weight	9.06 ± 0.54	9.7 ± 0.31	7.7 ± 0.62	8.72 ± 0.44	–	–	–
Abdominal girth (cm)	3.67 ± 0.11	3.77 ± 0.13	3.38 ± 0.13	3.7 ± 0.12	–	–	–
Crown-rump length (cm)	4.7 ± 0.15	4.8 ± 0.10	4.56 ± 0.14	4.63 ± 0.07	–	–	–

Body weight, placental weight, placental efficiency (body weight/placental weight), abdominal girth, and crown-rump length from female fetuses collected on GD21. Data are represented as mean ± SEM. All groups were compared using a two-way ANOVA followed by Sidak's post hoc test.

**$p < 0.05$ overall group effect of prenatal hypoxia.*

†$p < 0.05$ versus corresponding hypoxia-saline group. Exact p-value is $p = 0.04$

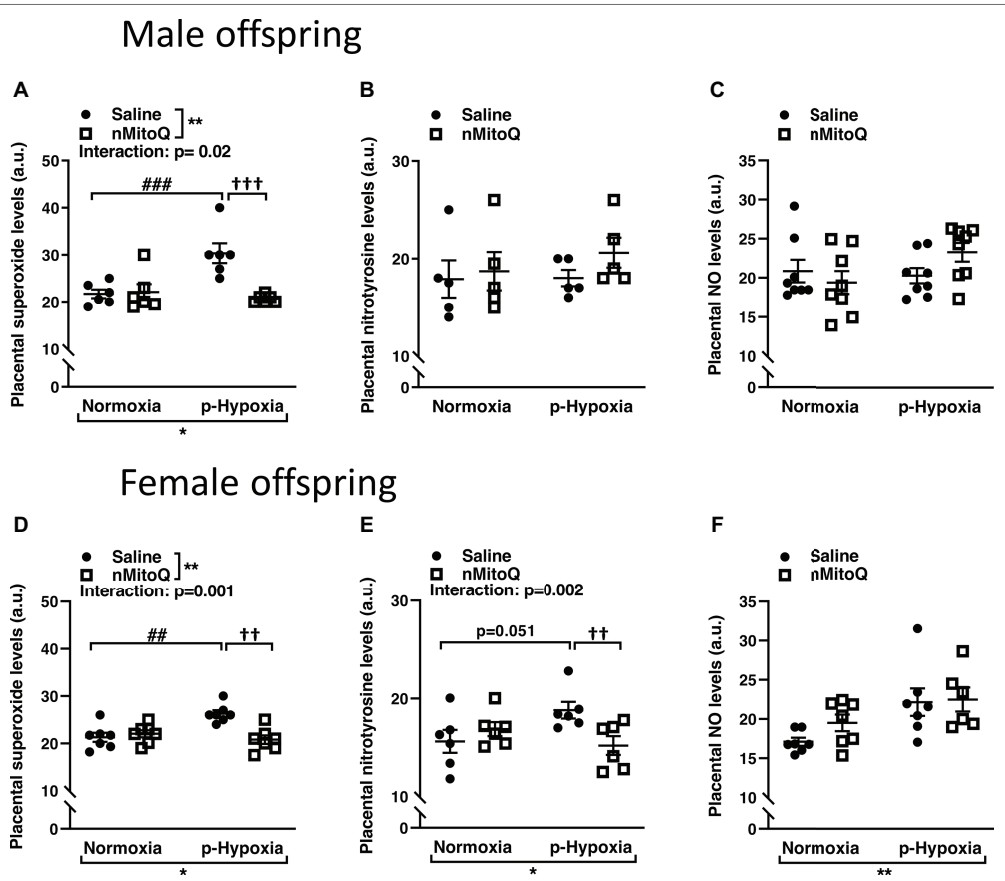

FIGURE 1 | Effects of nMitoQ treatment on placental superoxide, peroxynitrite, and NO levels in normoxic and hypoxic placentae of both male and female offspring. Normoxic and hypoxic dams were treated with nMitoQ or saline, and superoxide levels were assessed by DHE staining in placentae from male **(A)** and female **(D)** fetuses; peroxynitrite levels were detected by staining for nitrotyrosine (the footprint of peroxynitrite production) in placentae from male **(B)** and female **(E)** fetuses, and NO levels were assessed by DAF-FM staining in placentae from male **(C)** and female **(F)** fetuses on GD21. Data are represented as mean ± SEM. a.u.: arbitrary units. All groups were compared using a two-way ANOVA followed by Sidak's *post hoc* test (n = 6–7/group). *$p < 0.05$, **$p < 0.01$ group effect of prenatal hypoxia or nMitoQ treatment; $^{\#\#}p < 0.01$, $^{\#\#\#}p < 0.001$ compared to normoxia-saline; $^{\dagger\dagger}p < 0.01$, $^{\dagger\dagger\dagger}p < 0.001$ compared to hypoxia-saline group.

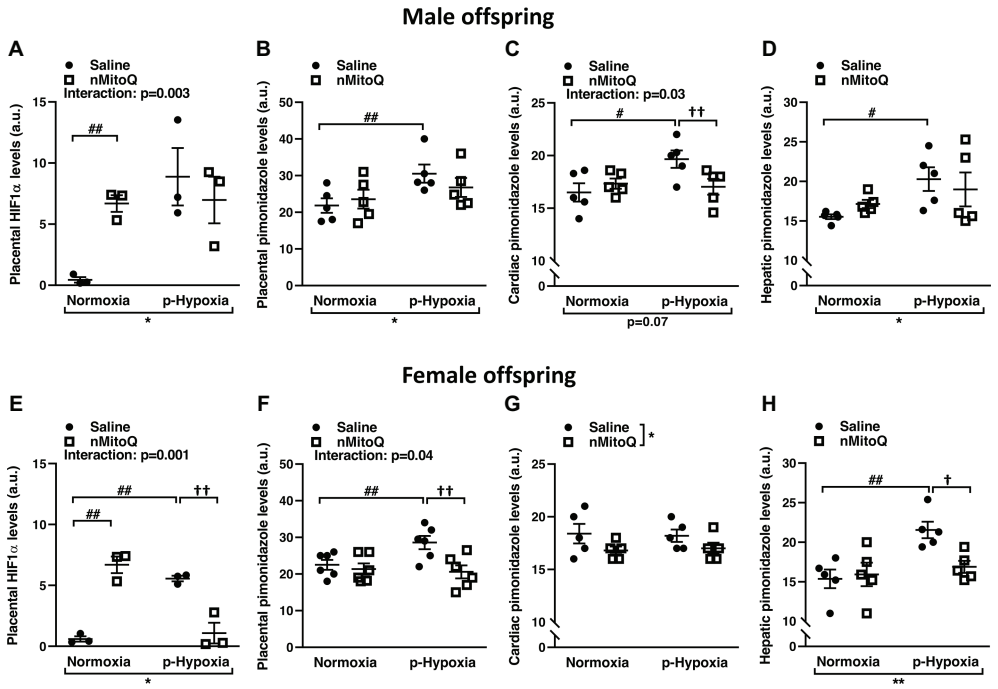

FIGURE 2 | Effects of nMitoQ treatment on placental and fetal hypoxia. Expression of HIF1-α protein, a marker for tissue hypoxia in placentae obtained from male **(A)** and female **(E)** fetuses on GD21. Oxygenation levels as assessed by pimonidazole staining in the placentae of male **(B)** and female **(F)**, the cardiac tissues of male (**C**) and female **(G)** and hepatic tissues of male **(D)** and female **(H)** fetuses on GD21. Data are represented as mean ± SEM. a.u.: arbitrary units. All groups were compared using a two-way ANOVA followed by Sidak's *post hoc* test (n = 5–6/group). $^{*}p < 0.05$, $^{**}p < 0.01$ group effect of prenatal hypoxia and nMitoQ treatment; $^{\#}p < 0.05$, $^{\#\#}p < 0.01$ compared to normoxia-saline; $^{\dagger}p < 0.05$, $^{\dagger\dagger}p < 0.01$ compared to hypoxia-saline group.

nitrotyrosine levels in placentae of only female hypoxic offspring (**Figure 1E**). However, hypoxia significantly increased nitric oxide levels in placentae from female offspring, but there was no effect of nMitoQ treatment (**Figure 1F**).

nMitoQ Treatment Decreased Markers of Placental and Fetal Hypoxia in Female Offspring

We next assessed HIF1-α protein levels as a marker for tissue hypoxia and confirmed placental oxygenation levels by pimonidazole staining. HIF1-α expression was significantly increased in prenatal hypoxia-exposed placentas from male offspring, which was not reduced by nMitoQ treatment (**Figure 2A**). There was a significant interaction between nMitoQ treatment and prenatal hypoxia in male placentae, whereby nMitoQ increased HIF1-α expression in placentae from normoxic male offspring (**Figure 2A**). Placental oxygenation was decreased (as shown by increased pimonidazole staining) in placentae of male offspring, which was unaffected by nMitoQ treatment (**Figure 2B**). Prenatal hypoxia decreased oxygenation in fetal hearts of only male offspring, while nMitoQ increased oxygenation in only prenatally hypoxic hearts of male offspring (**Figure 2C**). Hepatic oxygenation was reduced in livers of male offspring, but nMitoQ treatment had no effect (**Figure 2D**).

Prenatal hypoxia significantly increased placental HIF1-α expression in female offspring (**Figure 2E**). nMitoQ treatment decreased HIF1-α expression in placentae from female offspring exposed to prenatal hypoxia (**Figure 2E**). There was a significant interaction between nMitoQ treatment and prenatal hypoxia in female placentae, whereby nMitoQ increased HIF1-α expression in placentae from normoxic female offspring (**Figure 2E**). Placental oxygenation was also decreased (as shown by increased pimonidazole staining) in placentae of female offspring exposed to prenatal hypoxia (**Figure 2F**). nMitoQ treatment significantly increased oxygenation in placenta of only female offspring exposed to prenatal hypoxia (**Figure 2F**). There was no effect of prenatal hypoxia on oxygenation in fetal hearts of female offspring, while nMitoQ increased oxygenation in hearts of female offspring (**Figure 2G**). Hepatic oxygenation was reduced in livers of prenatally hypoxic female offspring, and nMitoQ treatment increased oxygenation in livers of only female offspring exposed to prenatal hypoxia (**Figure 2H**).

nMitoQ Treatment Increased Angiogenesis and Vascularization in Placentae of Female Offspring

Placental hypoxia is commonly associated with altered expression of the placental pro-angiogenic peptide vascular endothelial growth factor (VEGF; Lyall et al., 1997; Roh et al., 2005). In male offspring, prenatal hypoxia decreased placental *Vegf* mRNA expression, which was not altered by nMitoQ treatment (**Figure 3A**). Prenatal hypoxia also reduced

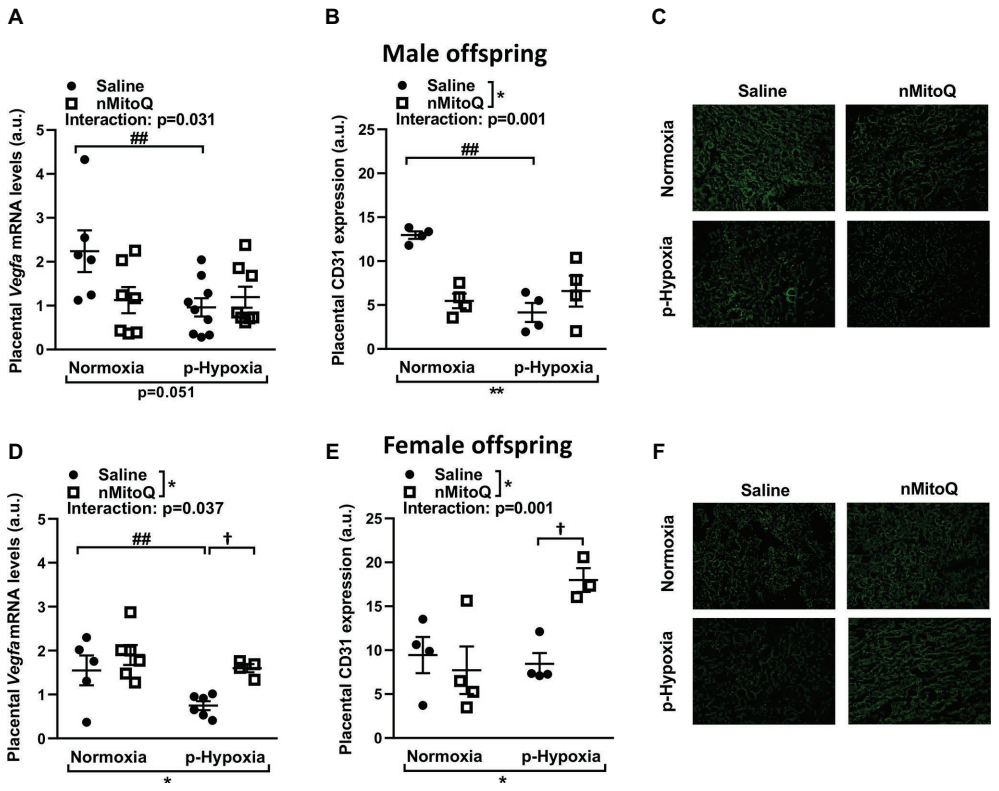

FIGURE 3 | Effects of nMitoQ treatment on markers of angiogenesis and vascularization in prenatally hypoxic placentae of both male female offspring. Proangiogenic factor *Vegfa* mRNA levels were assessed by qPCR in placental tissue obtained from male **(A)** and female **(D)** fetuses on GD21. Feto-placental vascular capillaries as assessed by CD31 staining in placentae obtained from male **(B)** and female **(E)** fetuses. Representative images of CD31 stained placental labyrinth sections in placentae of male **(C)** and female offspring **(F)**. Data are represented as mean ± SEM. a.u.: arbitrary units. All groups were compared using a two-way ANOVA followed by Sidak's *post hoc* test (n = 5–9/group). $^{*}p < 0.05$, $^{**}p < 0.01$ group effect of prenatal hypoxia and nMitoQ treatment; $^{\#\#}p < 0.01$ compared to normoxia-saline; $^{\dagger}p < 0.05$ compared to hypoxia-saline group.

CD31-positive area of staining (i.e., the fetal capillaries; **Figures 3B,C**). There was a significant interaction between nMitoQ treatment and prenatal hypoxia in male placentae, whereby nMitoQ reduced both *Vegf* and CD31 staining in placentae from normoxic male offspring (**Figures 3A,B**).

In female offspring, prenatal hypoxia decreased placental *Vegf* mRNA expression, which was increased by nMitoQ treatment in placentae from prenatally hypoxic female offspring (**Figure 3D**). CD31-positive area of staining (i.e., the fetal capillaries) was reduced by prenatal hypoxia in placentae from female offspring (**Figures 3E,F**). Similar to the *Vegf* expression pattern, there was a significant interaction between nMitoQ treatment and prenatal hypoxia in female placentae, whereby nMitoQ increased CD31 staining only in the placentae from prenatal hypoxic female offspring (**Figure 3E**).

Sufficient fetal blood space in the placental labyrinth zone is essential for oxygen and nutrient exchange between the maternal and fetal circulations (Burton and Fowden, 2015). We found that prenatal hypoxia reduced fetal and maternal blood space area in placentae from only male offspring (**Figures 4A,B**). nMitoQ did not change fetal and maternal blood space area in placentae from males (**Figure 4A**); however, in female offspring, nMitoQ treatment increased fetal blood space area in placentae exposed to prenatal hypoxia (**Figures 4C,D**).

nMitoQ Treatment Increased Placental *Igf2* in Female Offspring

IGF2 plays an important role in placental development (Fowden et al., 2006), and total placental *Igf2* and *Igf2* expressed only in the placental labyrinth region (i.e., *Igf2P0*) were shown to regulate the nutrient exchange characteristics of the placenta (Sibley et al., 2004). In male offspring, prenatal hypoxia decreased total *Igf2* and placental-specific *Igf2* expression, which was not affected by nMitoQ treatment (**Figures 5A,B**). In placentae from female offspring, total *Igf2* and placental-specific *Igf2* expression were significantly decreased by prenatal hypoxia (**Figures 5C,D**). Moreover, nMitoQ treatment increased *Igf2* expression in the prenatal hypoxia-exposed female placentae only (**Figure 5C**). Expression levels of the IGF2 receptors, *Igf1r* and *Igf2r*, were decreased in placentae of both prenatally hypoxic male and female offspring but were not affected by nMitoQ treatment (**Figures 6A–D**).

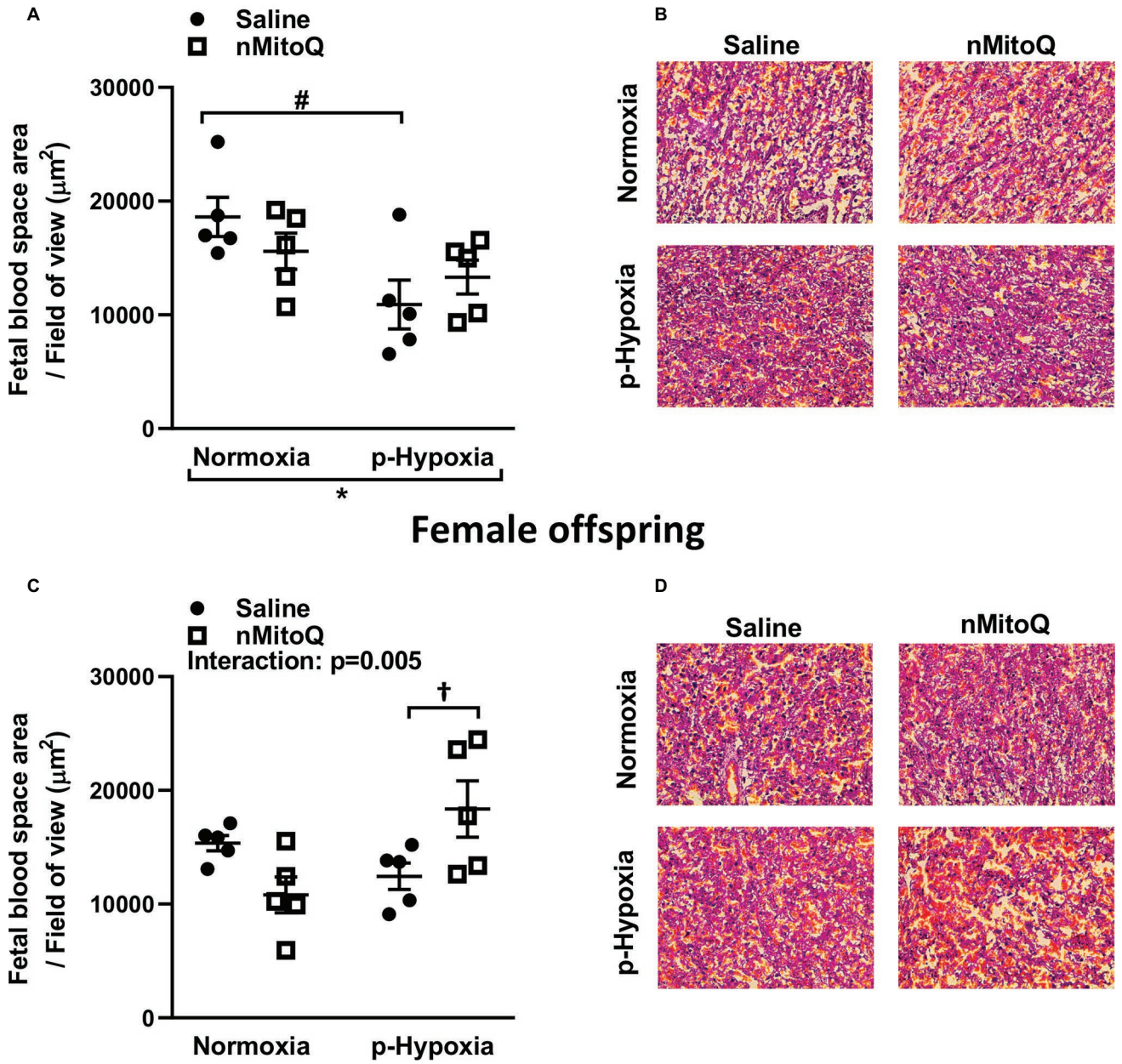

FIGURE 4 | Effects of nMitoQ treatment on fetal blood space area in prenatally hypoxic placentae of both male and female offspring. Fetal blood space area per field of view in labyrinth zones of placenta obtained from male **(A)** and female **(C)** fetuses on GD21. Representative images of H&E stained placental labyrinth sections in placentae of males **(B)** and females **(D)**. Data are represented as mean ± SEM. All groups were compared using a two-way ANOVA followed by Sidak's *post hoc* test (n = 5/group). $^{*}p < 0.05$ group effect of prenatal hypoxia, $^{\#}p < 0.05$ compared to normoxia-saline, $^{\dagger}p < 0.05$ compared to hypoxia-saline group.

DISCUSSION

In the current study, we hypothesized the sex-specific effects of preventing placental oxidative/nitrosative stress using nMitoQ, with a specific focus on placental morphology. This is of particular interest because oxidative stress in the placenta has been implicated to play a key role in the etiology of pregnancy complications such as fetal hypoxia and IUGR. Hence, our study was designed to elucidate possible mechanism(s) in the placenta that may account for differences in placental and fetal oxygenation and weights following a hypoxic insult and the sexually dimorphic effects of nMitoQ treatment. We showed that a reduction in

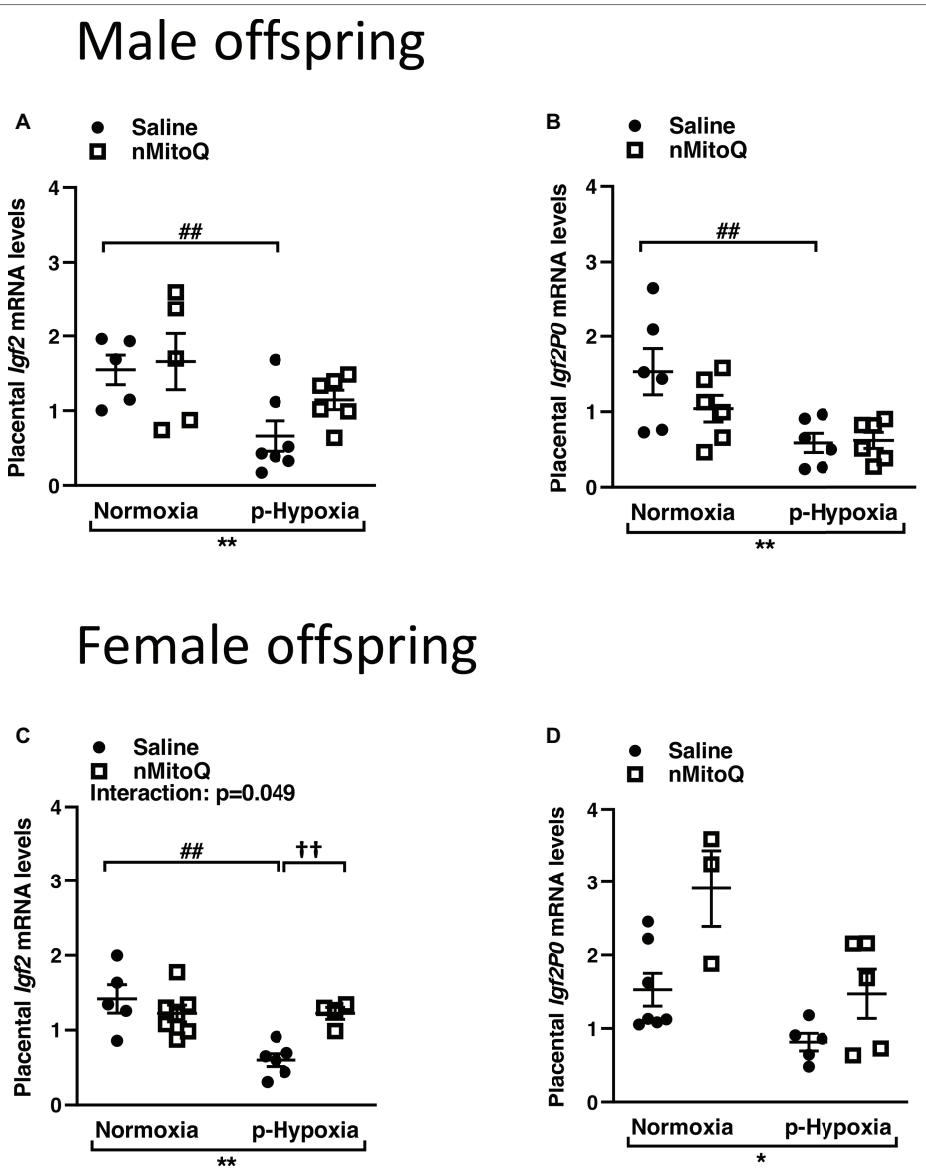

FIGURE 5 | Effects of nMitoQ on placental *Igf2* mRNA expression in prenatally hypoxic placentae of both male and female offspring. Growth factor *Igf2* **(A,C)** and *Igf2p0* **(B,D)** mRNA levels as assessed by qPCR in placentae obtained from male **(A,B)** and female **(C,D)** fetuses on GD21. Data are represented as mean ± SEM. All groups were compared using a two-way ANOVA followed by Sidak's *post hoc* test (n = 5–9/group). $^{*}p < 0.05$, $^{**}p < 0.01$ group effect of prenatal hypoxia; $^{\#\#}p < 0.01$ compared to normoxia-saline; $^{\dagger\dagger}p < 0.01$ compared to hypoxia-saline group.

placental ROS/RNS by nMitoQ treatment improved oxygenation, increased expression of VEGFA (known to affect placental morphology), and increased expression of *Igf2*. Moreover, nMitoQ treatment was more effective in placentae of female offspring than males. Our data demonstrated that the placental response to prenatal hypoxia is different in males versus females and that within the same dams, the response of the placentae to nMitoQ treatment is sexually dimorphic, resulting in sex differences in the effect of nMitoQ treatment on placental oxidative stress, vascularization, and placental and fetal growth.

Given that oxidative stress is a central mediator of placental dysfunction, we and others have studied the use of an antioxidant to protect the placenta against oxidative stress (Phillips et al., 2017; Nuzzo et al., 2018). Recently, the antioxidant benefits of MitoQ treatment on placental adaptations from hypoxic pregnancies were extensively studied in male offspring (Nuzzo et al., 2018). Nuzzo et al. showed that MitoQ given daily to hypoxic pregnant dams in drinking water from GD6 to GD20 restored placental efficiency to control levels, increased absolute placental volume, fetal capillary surface area in placental labyrinth zone, and maternal blood spaces related to placentae from normoxic pregnancies (Nuzzo et al., 2018). The placental morphological adaptations (i.e., increased placental weight, increased fetal capillary surface area) to early-onset hypoxia (GD6–GD20) demonstrated in males were contrary to the placental morphological phenotype (i.e., unchanged placental weight and reduced fetal capillary area)

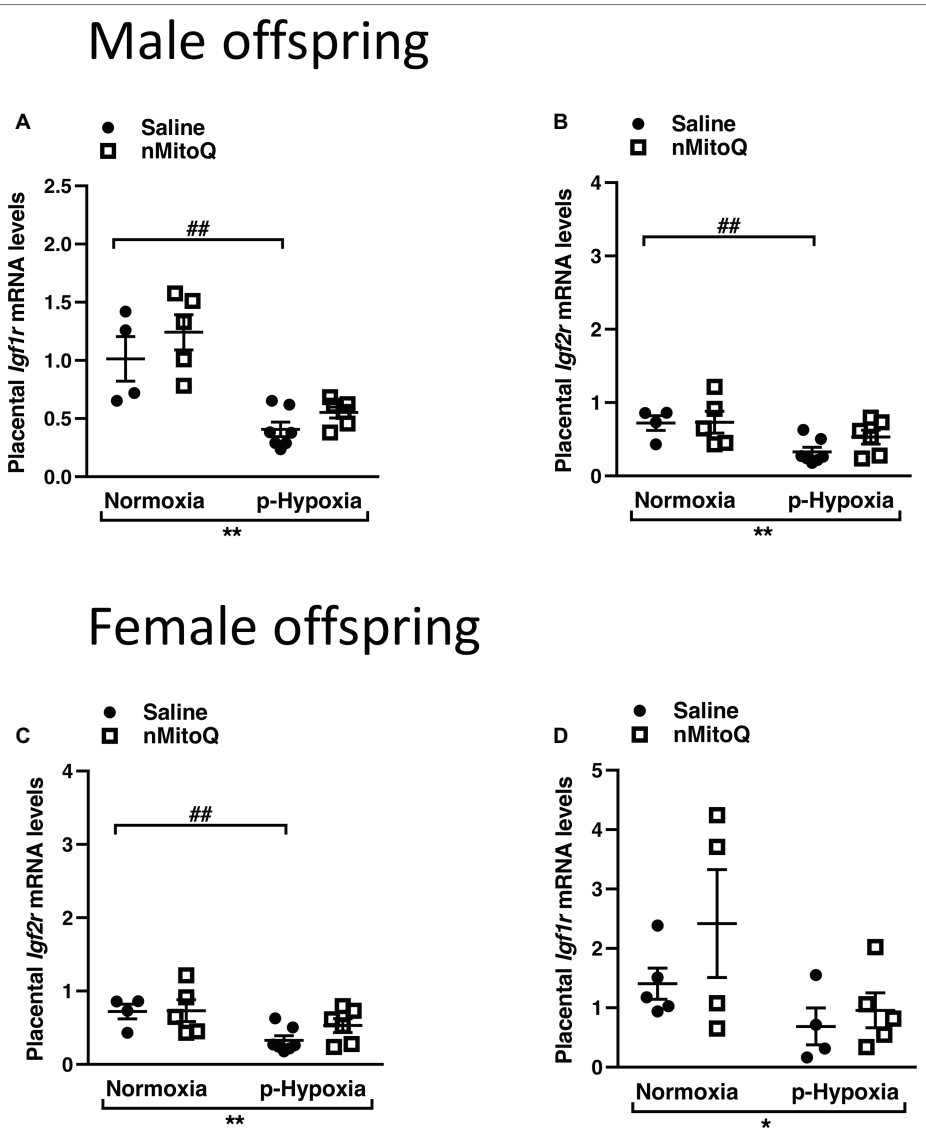

FIGURE 6 | Effects of nMitoQ treatment on *Igf1r* and *Igf2r* mRNA expression in prenatally hypoxic placentae of both male and female offspring. Receptors for IGF2, *Igf1r* **(A,C)** and *Igf2r* **(B,D)** mRNA levels were assessed by qPCR in the labyrinth zones of placentae taken from male **(A,B)** and female **(C,D)** fetuses on GD21. Data are represented as mean ± SEM. All groups were compared using a two-way ANOVA followed by Sidak's *post hoc* test (n = 4/group). $^{*}p < 0.05$, $^{**}p < 0.01$ group effect of prenatal hypoxia or nMitoQ treatment; $^{\#\#}p < 0.01$ compared to normoxia-saline.

observed in our model of late-onset hypoxia (GD15 –GD21) in male offspring. Thus, diverse prenatal hypoxia insults can affect pregnancies differently, which need to be taken into consideration for clinical translation of findings. In our study, using MitoQ encapsulated in nanoparticles (nMitoQ) to target the placenta in order to limit direct drug exposure to the fetus and avoid potential off-target effects during fetal development, we also observed beneficial effects; however, nMitoQ treatment was more effective in placentae of female offspring than males.

In our model of prenatal hypoxia, placental efficiency (fetal weight/placental weight) was reduced in both male and female fetuses, which was partially improved by nMitoQ treatment in both males and females. Interestingly, fetal weight was reduced by prenatal hypoxia only in males but not females, indicating that males may be more severely affected by prenatal hypoxia than females, as has been suggested in other studies (Stark et al., 2011; Muralimanoharan et al., 2015; Evans and Myatt, 2017). This reduction in fetal weight suggests insufficient oxygen and nutrient delivery to the fetus in the hypoxia exposed dams. Interestingly, in females, prenatal hypoxia increased placental weight, which was prevented by nMitoQ treatment. This may suggest that females, in compensation for the hypoxic environment, increased placental growth in order to increase oxygen and nutrient supply to the fetus and prevent growth restriction, which was indeed successful, as fetal weights in the females were not affected by prenatal hypoxia.

We showed that prenatal hypoxia increased oxidative stress (superoxide generation in male and female placentae), as

demonstrated previously (Richter et al., 2012; Aljunaidy et al., 2018; Nuzzo et al., 2018), and nitrosative stress (peroxynitrite formation in only female placentae). Oxidative and nitrosative stresses can inhibit normal placental development in various ways (e.g., inhibit mitochondrial electron transport and oxidation of DNA) and potentially reduce oxygen and nutrient delivery, thus impairing fetal development (Droge, 2002; Thompson and Al-Hasan, 2012). The nMitoQ treatment was therefore specifically designed to prevent oxidative stress in the placenta, and indeed, nMitoQ treatment significantly decreased placental superoxide and peroxynitrite levels. This supports our hypothesis that using MitoQ loaded nanoparticles as a targeted delivery system to the placenta is an effective treatment against the generation of reactive oxygen/nitrogen species in the placenta in compromised pregnancies. Interestingly, in female offspring, we observed that the increased superoxide/peroxynitrite levels by prenatal hypoxia coincided with increased NO levels. Under normal pregnancy conditions, NO bioavailability promotes feto-placental vasodilation and induces angiogenesis (Cooke, 2003; Kwon et al., 2004). The placental circulation lacks autonomic and cholinergic innervation, thus feto-placental angiogenesis and placental vascular resistance and function are dependent on locally derived vasoactive factors (e.g., NO) and growth factors (e.g., VEGF and IGF2; Pacher et al., 2007; Krause et al., 2011; Kulandavelu et al., 2013). In the human placenta, all nitric oxide synthase (NOS) isoforms are expressed but differentially within the tissues. Endothelial NOS (eNOS) isoform is predominantly expressed in syncytiotrophoblasts and endothelial cells (reviewed by Aban et al., 2018), while neuronal NOS (nNOS) and inducible NOS (iNOS) isoforms are expressed in the placental smooth muscle cells, syncytiotrophoblasts, extravillous trophoblasts, and hofbauer cells of the villous stroma (reviewed by Krause et al., 2011). Moreover, studies have correlated increased placental vascular resistance and placental dysfunction to decreased eNOS and increased inducible NOS (iNOS) isoform expression, leading to increased nitrosative stress (Casanello and Sobrevia, 2002; Giannubilo et al., 2008). Interestingly, IUGR has been associated with higher levels of placental NO, together with increased nitrosative stress and inadequate feto-placental vascularization (Lyall et al., 1996; Tikvica et al., 2008; Myatt, 2010). Therefore, the increased NO levels in female placentae may be an immediate adaptive mechanism to prenatal hypoxia, which may be associated with placental vascular dysfunction. Although we have not assessed NOS isoforms and the contribution of various cell types to the increased placental NO levels in females, the above studies may suggest that increased iNOS expression and/or activity could be a potential source for increased placental NO observed in our model of prenatal hypoxia.

We found that prenatal hypoxia decreased placental and fetal oxygenation (in males and females), which coincided with an increase in HIF-1α levels in both sexes. Systemic and placental responses to hypoxia are orchestrated by hypoxia-inducible factors (such as HIF-1α), and being a marker of hypoxia, this finding is in accordance with the reduced placental oxygenation we observed. Notably, in only the female prenatally hypoxic placentae, nMitoQ treatment effectively improved placental oxygenation. Moreover, the effect of prenatal hypoxia on oxygenation was more pronounced in the female fetal liver than the fetal heart, as previously reported by our laboratory, but only in male offspring (Rueda-Clausen et al., 2011). Interestingly, nMitoQ treatment improved oxygenation in the hearts of both male and female fetuses, but in the liver, only female fetuses showed improved oxygenation with nMitoQ. Moreover, placental HIF-1α was only decreased by nMitoQ in the female placentae. This may explain why the female fetuses did not show any signs of significant growth restriction, as nMitoQ effectively decreased oxidative stress and HIF-1α and reduced placental weight in the female placentae. The underlying mechanisms for reduced effectiveness of nMitoQ treatment in males are not fully understood and remain to be further studied. A possible explanation might be that males show greater growth rate *in utero* (Parker et al., 1984); therefore, the higher oxygen and nutrient demand by the male fetus may predispose them to a greater risk of adverse developmental outcomes following the oxygen deprivation (Ozaki et al., 2001).

Oxidative stress is known to contribute to abnormal placental growth, function, and angiogenesis (Burton et al., 2009). As mentioned above, the placenta lacks autonomic innervation, and locally derived NO and growth factors such as the pro-angiogenic factor VEGF play essential roles in placental vascular development and function (Kulandavelu et al., 2013). HIF-1α (in hypoxic conditions) has been shown to increase VEGFA expression, while a reduction in VEGF has been observed in placentae from complicated pregnancies such as preeclampsia (Andraweera et al., 2012; Abe et al., 2013). Therefore, placental angiogenesis is dependent on locally derived VEGFA. Our study showed that prenatal hypoxia decreased *Vegfa* mRNA expression and the area of fetal blood capillaries (measured by endothelial cell marker CD31) in placentae of both male and female offspring, suggesting decreased angiogenesis and vascularization. The decreased *Vegfa* mRNA expression could be due to decreased binding of HIF-1α to the hypoxia responsive element (HRE) on the *Vegfa* gene, which was previously shown by Myatt et al. to decrease *Vegfa* expression in preeclamptic placentae with increased ROS (Muralimanoharan et al., 2012). Interestingly, nMitoQ treatment only improved *Vegfa* mRNA expression, the area of fetal blood capillaries, and the placental blood space in the female placentae but not in the male placentae. The specific mechanisms remain to be investigated, but it may be speculated that this could be mediated in part by increased placental NO levels present in the prenatally hypoxic placentae, which were not affected by nMitoQ treatment and could increase VEGFA. However, the effects of NO on VEGFA expression vary for different tissues and cell types (Abe et al., 2013); therefore, NO mediated VEGFA expression within the placenta may be highly dependent on the different cell types. Our data are in accordance with the previous studies, where MitoQ (not bound to nanoparticles) was shown to increase maternal blood space surface area in the placenta in males only (Nuzzo et al., 2018). Taken together, our data could suggest that reduction of superoxide by nMitoQ could lead to enhanced angiogenesis *via* increased *Vegfa* expression and fetal capillary area and blood space in placentae of female offspring.

Another important growth factor for placental morphogenesis is IGF2 (Sferruzzi-Perri et al., 2017). In humans, decreased placental IGF2 has been associated with IUGR (Diplas et al., 2009). In mice, genetic knockouts of *Igf2* showed impaired placental development and fetal growth with reduced placental transfer of nutrients to the fetus (Constancia et al., 2005; Coan et al., 2008). We observed that prenatal hypoxia decreased expression of *Igf2* and *Igf2P0* in the labyrinth zone of both male and female offspring. This is in line with the previous studies showing that maternal exposure to hypoxia has direct effects on total *Igf2* expression in the placenta: maternal exposure to 10–12% oxygen during late gestation decreased *Igf2* expression, which affected the labyrinth layer morphology and decreased maternal blood space (Cuffe et al., 2014; Higgins et al., 2016). Hence, the reduction in placental *Igf2* expression could also explain the decreased fetal blood spaces by prenatal hypoxia that we observed. The expression of *Igf2* is regulated by methylation of the *Igf2* gene at the imprinting control region (ICR) and the differentially methylated region 2 (DMR2). Recent studies suggest that a suboptimal intrauterine environment leads to epigenetic changes in the *Igf2* gene and associated *Igf2* expression in growth restricted offspring of rats exposed to bilateral uterine artery ligation (Gonzalez-Rodriguez et al., 2016). Interestingly, hypoxic stress responses in general appear to be driven by epigenetic changes (Cerda and Weitzman, 1997). For example, prenatal hypoxia increased placental ROS and DNA methylation enzymes (Gheorghe et al., 2007). Therefore, we speculate that the methylation status at ICR and DMR2 may differ in a sex-specific manner, and changes in DNA methylation could account for the altered *Igf2* expression, which will be the focus for our future investigations.

It is well known that the placenta functions and adapts to an adverse intrauterine environment in a sex-specific manner (reviewed by Clifton, 2010). Furthermore, generation of oxidative stress differs in both male and female fetuses and placentae under conditions of adverse prenatal stress (Chaudhari et al., 2014). Our current study further demonstrates a dichotomous sex-specific and nMitoQ-specific effect on the placenta and ultimately fetal development. Overall, our data suggested that nMitoQ treatment decreased oxidative/nitrosative stress, improved oxygenation, was effective in bringing *Vegfa* and *Igf2* expression back to control levels, and increased fetal blood space only in female placentae, thereby showing that nMitoQ treatment may protect offspring from the detrimental effects of a hypoxic insult in a sexually dimorphic manner with increased effectiveness in females. Of note, our data showed that nMitoQ treatment also affected the placenta in the control groups. For example, in normoxic controls, nMitoQ treatment increased HIF-1α expression in both male and female placentae and reduced CD31 area in the male offspring. Previous studies have demonstrated that maternal antioxidant supplementation with ascorbic acid in normal pregnancies was associated with vascular dysfunction and weight gain (Richter et al., 2012). Therefore, continuing these studies we need to keep in mind that this treatment is specifically designed to treat pregnancies complicated by fetal hypoxia and be aware that there might be detrimental effects of maternal antioxidant intervention during normal pregnancy.

To conclude, we demonstrated that nMitoQ treatment reduced placental nitrosative stress and improved oxygenation and placental morphology *via* increased VEGFA and IGF2 expression in a sex-specific manner, showing more effectiveness in placentae from female offspring. Moreover, our study shows that male fetuses appear to be more susceptible to an adverse *in utero* environment. Although the exact mechanism(s) remain to be further investigated, a higher pro-oxidant state with reduced antioxidant capacity in the male placentae may explain the increased susceptibility of the male offspring under adverse conditions. In addition, our current study illustrates that the placenta is a contributing factor in the sexual dimorphism that has been observed in fetal programming. Thus, sex differences will need to be taken into account when developing placental-targeted therapeutic interventions to prevent fetal hypoxia and ultimately optimize fetal development in complicated pregnancies.

DATA AVAILABILITY

The datasets generated for this study are available on request to the corresponding author.

ETHICS STATEMENT

All procedures described were approved by the University of Alberta Animal Policy and Welfare Committee and were in accordance with the guidelines of the Canadian Council on Animal Care (AUP #242).

AUTHOR CONTRIBUTIONS

EG, MA, FS, JM, TP, CPC, C-LC, and SD contributed to experimental design. EG, MA, and RK participated in data acquisition. EG, MA, FS, JM, C-LC, and SD analyzed the data. EG, FS, C-LC, and SD were involved in drafting of the manuscript. EG, MA, FS, JM, TP, CPC, C-LC, and SD revised the final version of the manuscript. TP and CPC provided the study materials.

FUNDING

This research was funded by grants from the Canadian Institutes of Health Research (CIHR FS 154313) and the Women and Children's Health Research Institute (WCHRI) through the generosity of the Stollery Children's Hospital Foundation and supporters of the Lois Hole Hospital for Women. SD is a Canada research chair in the Maternal and Perinatal Cardiovascular Health and a distinguished university professor at the University of Alberta. FS was supported by a Postgraduate Fellowship Award from the Alberta Innovates – Health Solutions (AIHS) and a Molly Towell

Fellowship Award from the Molly Towell Perinatal Research Foundation. EG was supported by the Faculty of Medicine & Dentistry 75th Anniversary Awards and WCHRI Graduate Studentship Program.

ACKNOWLEDGMENTS

MitoQ was generously provided to TP and CPC by Dr. Michael Murphy, University of Cambridge, UK.

REFERENCES

Aban, C. E., Accialini, P. L., Etcheverry, T., Leguizamon, G. F., Martinez, N. A., and Farina, M. G. (2018). Crosstalk between nitric oxide and endocannabinoid signaling pathways in normal and pathological placentation. *Front. Physiol.* 9:1699. doi: 10.3389/fphys.2018.01699

Abe, H., Ishikawa, W., Kushima, T., Nishimura, T., Mori, C., Onuki, A., et al. (2013). Nitric oxide induces vascular endothelial growth factor expression in the rat placenta in vivo and in vitro. *Biosci. Biotechnol. Biochem.* 77, 971–976. doi: 10.1271/bbb.120923

Al-Gubory, K. H., Fowler, P. A., and Garrel, C. (2010). The roles of cellular reactive oxygen species, oxidative stress and antioxidants in pregnancy outcomes. *Int. J. Biochem. Cell Biol.* 42, 1634–1650. doi: 10.1016/j.biocel.2010.06.001

Aljunaidy, M. M., Morton, J. S., Cooke, C. M., and Davidge, S. T. (2017). Prenatal hypoxia and placental oxidative stress: linkages to developmental origins of cardiovascular disease. *Am. J. Physiol. Regul. Integr. Comp. Physiol.* 313, R395–R399. doi: 10.1152/ajpregu.00245.2017

Aljunaidy, M. M., Morton, J. S., Kirschenman, R., Phillips, T., Case, C. P., Cooke, C. M., et al. (2018). Maternal treatment with a placental-targeted antioxidant (MitoQ) impacts offspring cardiovascular function in a rat model of prenatal hypoxia. *Pharmacol. Res.* 134, 332–342. doi: 10.1016/j.phrs.2018.05.006

Andraweera, P. H., Dekker, G. A., Laurence, J. A., and Roberts, C. T. (2012). Placental expression of VEGF family mRNA in adverse pregnancy outcomes. *Placenta* 33, 467–472. doi: 10.1016/j.placenta.2012.02.013

Burton, G. J., and Fowden, A. L. (2015). The placenta: a multifaceted, transient organ. *Philos. Trans. R. Soc. Lond. Ser. B Biol. Sci.* 370:20140066. doi: 10.1098/rstb.2014.0066

Burton, G. J., Yung, H. W., Cindrova-Davies, T., and Charnock-Jones, D. S. (2009). Placental endoplasmic reticulum stress and oxidative stress in the pathophysiology of unexplained intrauterine growth restriction and early onset preeclampsia. *Placenta* 30(Suppl. A), S43–S48.

Casanello, P., and Sobrevia, L. (2002). Intrauterine growth retardation is associated with reduced activity and expression of the cationic amino acid transport systems y+/hCAT-1 and y+/hCAT-2B and lower activity of nitric oxide synthase in human umbilical vein endothelial cells. *Circ. Res.* 91, 127–134. doi: 10.1161/01.RES.0000027813.55750.E7

Cerda, S., and Weitzman, S. A. (1997). Influence of oxygen radical injury on DNA methylation. *Mutat. Res.* 386, 141–152.

Chaudhari, H. N., Kim, S. W., and Yun, J. W. (2014). Gender-dimorphic regulation of antioxidant proteins in response to high-fat diet and sex steroid hormones in rats. *Free Radic. Res.* 48, 587–598. doi: 10.3109/10715762.2014.896003

Chiaratti, M. R., Malik, S., Diot, A., Rapa, E., Macleod, L., Morten, K., et al. (2015). Is placental mitochondrial function a regulator that matches fetal and placental growth to maternal nutrient intake in the mouse? *PLoS One* 10:e0130631. doi: 10.1371/journal.pone.0130631

Clifton, V. L. (2010). Review: sex and the human placenta: mediating differential strategies of fetal growth and survival. *Placenta* 31(Suppl), S33–S39. doi: 10.1016/j.placenta.2009.11.010

Coan, P. M., Fowden, A. L., Constancia, M., Ferguson-Smith, A. C., Burton, G. J., and Sibley, C. P. (2008). Disproportional effects of Igf2 knockout on placental morphology and diffusional exchange characteristics in the mouse. *J. Physiol.* 586, 5023–5032. doi: 10.1113/jphysiol.2008.157313

Constancia, M., Angiolini, E., Sandovici, I., Smith, P., Smith, R., Kelsey, G., et al. (2005). Adaptation of nutrient supply to fetal demand in the mouse involves interaction between the Igf2 gene and placental transporter systems. *Proc. Natl. Acad. Sci. USA* 102, 19219–19224. doi: 10.1073/pnas.0504468103

Cooke, J. P. (2003). NO and angiogenesis. *Atheroscler. Suppl.* 4, 53–60. doi: 10.1016/S1567-5688(03)00034-5

Cuffe, J. S., Walton, S. L., Singh, R. R., Spiers, J. G., Bielefeldt-Ohmann, H., Wilkinson, L., et al. (2014). Mid- to late term hypoxia in the mouse alters placental morphology, glucocorticoid regulatory pathways and nutrient transporters in a sex-specific manner. *J. Physiol.* 592, 3127–3141. doi: 10.1113/jphysiol.2014.272856

Diplas, A. I., Lambertini, L., Lee, M. J., Sperling, R., Lee, Y. L., Wetmur, J., et al. (2009). Differential expression of imprinted genes in normal and IUGR human placentas. *Epigenetics* 4, 235–240. doi: 10.4161/epi.9019

Droge, W. (2002). Free radicals in the physiological control of cell function. *Physiol. Rev.* 82, 47–95. doi: 10.1152/physrev.00018.2001

Evans, L., and Myatt, L. (2017). Sexual dimorphism in the effect of maternal obesity on antioxidant defense mechanisms in the human placenta. *Placenta* 51, 64–69. doi: 10.1016/j.placenta.2017.02.004

Fowden, A. L., Sibley, C., Reik, W., and Constancia, M. (2006). Imprinted genes, placental development and fetal growth. *Horm. Res.* 65(Suppl. 3), 50–58. doi: 10.1159/000091506

Gabory, A., Ferry, L., Fajardy, I., Jouneau, L., Gothie, J. D., Vige, A., et al. (2012). Maternal diets trigger sex-specific divergent trajectories of gene expression and epigenetic systems in mouse placenta. *PLoS One* 7:e47986. doi: 10.1371/journal.pone.0047986

Gheorghe, C. P., Mohan, S., Oberg, K. C., and Longo, L. D. (2007). Gene expression patterns in the hypoxic murine placenta: a role in epigenesis? *Reprod. Sci.* 14, 223–233. doi: 10.1177/1933719107302860

Giannubilo, S. R., Menegazzi, M., Tedeschi, E., Bezzeccheri, V., Suzuki, H., and Tranquilli, A. L. (2008). Doppler analysis and placental nitric oxide synthase expression during fetal growth restriction. *J. Matern. Fetal. Neonatal. Med.* 21, 617–622. doi: 10.1080/14767050802214774

Gonzalez-Rodriguez, P., Cantu, J., O'neil, D., Seferovic, M. D., Goodspeed, D. M., Suter, M. A., et al. (2016). Alterations in expression of imprinted genes from the H19/IGF2 loci in a multigenerational model of intrauterine growth restriction (IUGR). *Am. J. Obstet. Gynecol.* 214, 625.e621–625.e611. doi: 10.1016/j.ajog.2016.01.194

Higgins, J. S., Vaughan, O. R., Fernandez De Liger, E., Fowden, A. L., and Sferruzzi-Perri, A. N. (2016). Placental phenotype and resource allocation to fetal growth are modified by the timing and degree of hypoxia during mouse pregnancy. *J. Physiol.* 594, 1341–1356. doi: 10.1113/JP271057

Holland, O., Dekker Nitert, M., Gallo, L. A., Vejzovic, M., Fisher, J. J., and Perkins, A. V. (2017). Review: placental mitochondrial function and structure in gestational disorders. *Placenta* 54, 2–9. doi: 10.1016/j.placenta.2016.12.012

Kim, H., Akagi, T., and Akashi, M. (2009). Preparation of size tunable amphiphilic poly(amino acid) nanoparticles. *Macromol. Biosci.* 9, 842–848. doi: 10.1002/mabi.200800367

Kim, D. W., Young, S. L., Grattan, D. R., and Jasoni, C. L. (2014). Obesity during pregnancy disrupts placental morphology, cell proliferation, and inflammation in a sex-specific manner across gestation in the mouse. *Biol. Reprod.* 90:130. doi: 10.1095/biolreprod.113.117259

Krause, B. J., Hanson, M. A., and Casanello, P. (2011). Role of nitric oxide in placental vascular development and function. *Placenta* 32, 797–805. doi: 10.1016/j.placenta.2011.06.025

Kulandavelu, S., Whiteley, K. J., Bainbridge, S. A., Qu, D., and Adamson, S. L. (2013). Endothelial NO synthase augments fetoplacental blood flow, placental vascularization, and fetal growth in mice. *Hypertension* 61, 259–266. doi: 10.1161/HYPERTENSIONAHA.112.201996

Kwon, H., Wu, G., Meininger, C. J., Bazer, F. W., and Spencer, T. E. (2004). Developmental changes in nitric oxide synthesis in the ovine placenta. *Biol. Reprod.* 70, 679–686. doi: 10.1095/biolreprod.103.023184

Lappas, M., Mitton, A., and Permezel, M. (2010). In response to oxidative stress, the expression of inflammatory cytokines and antioxidant enzymes are impaired in placenta, but not adipose tissue, of women with gestational diabetes. *J. Endocrinol.* 204, 75–84. doi: 10.1677/JOE-09-0321

Lyall, F., Greer, I. A., Young, A., and Myatt, L. (1996). Nitric oxide concentrations are increased in the feto-placental circulation in intrauterine growth restriction. *Placenta* 17, 165–168. doi: 10.1016/S0143-4004(96)80009-9

Lyall, F., Young, A., Boswell, F., Kingdom, J. C., and Greer, I. A. (1997). Placental expression of vascular endothelial growth factor in placentae from pregnancies complicated by pre-eclampsia and intrauterine growth restriction does not support placental hypoxia at delivery. *Placenta* 18, 269–276. doi: 10.1016/S0143-4004(97)80061-6

Mando, C., De Palma, C., Stampalija, T., Anelli, G. M., Figus, M., Novielli, C., et al. (2014). Placental mitochondrial content and function in intrauterine growth restriction and preeclampsia. *Am. J. Physiol. Endocrinol. Metab.* 306, E404–E413. doi: 10.1152/ajpendo.00426.2013

Mao, J., Zhang, X., Sieli, P. T., Falduto, M. T., Torres, K. E., and Rosenfeld, C. S. (2010). Contrasting effects of different maternal diets on sexually dimorphic gene expression in the murine placenta. *Proc. Natl. Acad. Sci. USA* 107, 5557–5562. doi: 10.1073/pnas.1000440107

Marzioni, D., Tamagnone, L., Capparuccia, L., Marchini, C., Amici, A., Todros, T., et al. (2004). Restricted innervation of uterus and placenta during pregnancy: evidence for a role of the repelling signal Semaphorin 3A. *Dev. Dyn.* 231, 839–848. doi: 10.1002/dvdy.20178

McCarthy, C. M., and Kenny, L. C. (2016). Mitochondrial [dys]function; culprit in pre-eclampsia? *Clin. Sci.* 130, 1179–1184. doi: 10.1042/CS20160103

Muralimanoharan, S., Guo, C., Myatt, L., and Maloyan, A. (2015). Sexual dimorphism in miR-210 expression and mitochondrial dysfunction in the placenta with maternal obesity. *Int. J. Obes.* 39, 1274–1281. doi: 10.1038/ijo.2015.45

Muralimanoharan, S., Maloyan, A., Mele, J., Guo, C., Myatt, L. G., and Myatt, L. (2012). MIR-210 modulates mitochondrial respiration in placenta with preeclampsia. *Placenta* 33, 816–823. doi: 10.1016/j.placenta.2012.07.002

Murphy, M. P., and Smith, R. A. (2007). Targeting antioxidants to mitochondria by conjugation to lipophilic cations. *Annu. Rev. Pharmacol. Toxicol.* 47, 629–656. doi: 10.1146/annurev.pharmtox.47.120505.105110

Myatt, L. (2010). Review: reactive oxygen and nitrogen species and functional adaptation of the placenta. *Placenta* 31(Suppl), S66–S69. doi: 10.1016/j.placenta.2009.12.021

Myatt, L., and Cui, X. (2004). Oxidative stress in the placenta. *Histochem. Cell Biol.* 122, 369–382. doi: 10.1007/s00418-004-0677-x

Newman, P. J. (1997). The biology of PECAM-1. *J. Clin. Invest.* 100, S25–S29.

Nuzzo, A. M., Camm, E. J., Sferruzzi-Perri, A. N., Ashmore, T. J., Yung, H. W., Cindrova-Davies, T., et al. (2018). Placental adaptation to early-onset hypoxic pregnancy and mitochondria-targeted antioxidant therapy in a rodent model. *Am. J. Pathol.* 188, 2704–2716. doi: 10.1016/j.ajpath.2018.07.027

Ozaki, T., Nishina, H., Hanson, M. A., and Poston, L. (2001). Dietary restriction in pregnant rats causes gender-related hypertension and vascular dysfunction in offspring. *J. Physiol.* 530, 141–152. doi: 10.1111/j.1469-7793.2001.0141m.x

Pacher, P., Beckman, J. S., and Liaudet, L. (2007). Nitric oxide and peroxynitrite in health and disease. *Physiol. Rev.* 87, 315–424. doi: 10.1152/physrev.00029.2006

Parker, A. J., Davies, P., Mayho, A. M., and Newton, J. R. (1984). The ultrasound estimation of sex-related variations of intrauterine growth. *Am. J. Obstet. Gynecol.* 149, 665–669. doi: 10.1016/0002-9378(84)90255-2

Phillips, T. J., Scott, H., Menassa, D. A., Bignell, A. L., Sood, A., Morton, J. S., et al. (2017). Treating the placenta to prevent adverse effects of gestational hypoxia on fetal brain development. *Sci. Rep.* 7:9079. doi: 10.1038/s41598-017-06300-1

Reynolds, L. P., and Redmer, D. A. (2001). Angiogenesis in the placenta. *Biol. Reprod.* 64, 1033–1040. doi: 10.1095/biolreprod64.4.1033

Richter, H. G., Camm, E. J., Modi, B. N., Naeem, F., Cross, C. M., Cindrova-Davies, T., et al. (2012). Ascorbate prevents placental oxidative stress and enhances birth weight in hypoxic pregnancy in rats. *J. Physiol.* 590, 1377–1387. doi: 10.1113/jphysiol.2011.226340

Roh, C. R., Budhraja, V., Kim, H. S., Nelson, D. M., and Sadovsky, Y. (2005). Microarray-based identification of differentially expressed genes in hypoxic term human trophoblasts and in placental villi of pregnancies with growth restricted fetuses. *Placenta* 26, 319–328. doi: 10.1016/j.placenta.2004.06.013

Rosenfeld, C. S. (2015). Sex-specific placental responses in fetal development. *Endocrinology* 156, 3422–3434. doi: 10.1210/en.2015-1227

Ross, M. F., Kelso, G. F., Blaikie, F. H., James, A. M., Cocheme, H. M., Filipovska, A., et al. (2005). Lipophilic triphenylphosphonium cations as tools in mitochondrial bioenergetics and free radical biology. *Biochemistry* 70, 222–230. doi: 10.1007/s10541-005-0104-5

Rueda-Clausen, C. F., Morton, J. S., Lopaschuk, G. D., and Davidge, S. T. (2011). Long-term effects of intrauterine growth restriction on cardiac metabolism and susceptibility to ischaemia/reperfusion. *Cardiovasc. Res.* 90, 285–294. doi: 10.1093/cvr/cvq363

Schoots, M. H., Gordijn, S. J., Scherjon, S. A., Van Goor, H., and Hillebrands, J. L. (2018). Oxidative stress in placental pathology. *Placenta* 69, 153–161. doi: 10.1016/j.placenta.2018.03.003

Scott, H., Phillips, T. J., Stuart, G. C., Rogers, M. F., Steinkraus, B. R., Grant, S., et al. (2018). Preeclamptic placentae release factors that damage neurons: implications for foetal programming of disease. *Neuronal Signaling* 2. doi: 10.1042/NS20180139

Sedlmeier, E. M., Brunner, S., Much, D., Pagel, P., Ulbrich, S. E., Meyer, H. H., et al. (2014). Human placental transcriptome shows sexually dimorphic gene expression and responsiveness to maternal dietary n-3 long-chain polyunsaturated fatty acid intervention during pregnancy. *BMC Genomics* 15:941. doi: 10.1186/1471-2164-15-941

Sferruzzi-Perri, A. N., Sandovici, I., Constancia, M., and Fowden, A. L. (2017). Placental phenotype and the insulin-like growth factors: resource allocation to fetal growth. *J. Physiol.* 595, 5057–5093. doi: 10.1113/JP273330

Sibley, C. P., Coan, P. M., Ferguson-Smith, A. C., Dean, W., Hughes, J., Smith, P., et al. (2004). Placental-specific insulin-like growth factor 2 (Igf2) regulates the diffusional exchange characteristics of the mouse placenta. *Proc. Natl. Acad. Sci. USA* 101, 8204–8208. doi: 10.1073/pnas.0402508101

Smith, R. A., Porteous, C. M., Coulter, C. V., and Murphy, M. P. (1999). Selective targeting of an antioxidant to mitochondria. *Eur. J. Biochem.* 263, 709–716. doi: 10.1046/j.1432-1327.1999.00543.x

Stark, M. J., Hodyl, N. A., Wright, I. M., and Clifton, V. L. (2011). Influence of sex and glucocorticoid exposure on preterm placental pro-oxidant-antioxidant balance. *Placenta* 32, 865–870. doi: 10.1016/j.placenta.2011.08.010

Thompson, L. P., and Al-Hasan, Y. (2012). Impact of oxidative stress in fetal programming. *J. Pregnancy* 2012:582748. doi: 10.1155/2012/582748

Thompson, L. P., Chen, L., Polster, B. M., Pinkas, G., and Song, H. (2018). Prenatal hypoxia impairs cardiac mitochondrial and ventricular function in guinea pig offspring in a sex-related manner. *Am. J. Physiol. Regul. Integr. Comp. Physiol.* 315, R1232–R1241. doi: 10.1152/ajpregu.00224.2018

Tikvica, A., Kusan Jukic, M., Pintaric, I., Medic, M., Hudicek-Martincic, G., Kosec, V., et al. (2008). Nitric oxide synthesis in placenta is increased in intrauterine growth restriction and fetal hypoxia. *Coll. Antropol.* 32, 565–570.

Webster, R. P., Roberts, V. H., and Myatt, L. (2008). Protein nitration in placenta - functional significance. *Placenta* 29, 985–994. doi: 10.1016/j.placenta.2008.09.003

Conflict of Interest Statement: The University of Bristol (TP and CC) has submitted a patent application for the nanoparticle formulation used in this study and its application to preeclampsia and related diseases.

The remaining authors declare that the research was conducted in the absence of any commercial or financial relationships that could be construed as a potential conflict of interest.

Copyright © 2019 Ganguly, Aljunaidy, Kirschenman, Spaans, Morton, Phillips, Case, Cooke and Davidge. This is an open-access article distributed under the terms of the Creative Commons Attribution License (CC BY). The use, distribution or reproduction in other forums is permitted, provided the original author(s) and the copyright owner(s) are credited and that the original publication in this journal is cited, in accordance with accepted academic practice. No use, distribution or reproduction is permitted which does not comply with these terms.

frontiers in Physiology

ORIGINAL RESEARCH
published: 18 June 2019
doi: 10.3389/fphys.2019.00754

Immediate and Persistent Effects of Temperature on Oxygen Consumption and Thermal Tolerance in Embryos and Larvae of the Baja California Chorus Frog, *Pseudacris hypochondriaca*

Casey A. Mueller, Julie Bucsky, Lindsey Korito and Samantha Manzanares*

Department of Biological Sciences, California State University San Marcos, San Marcos, CA, United States

OPEN ACCESS

Edited by:
Gina Galli,
The University of Manchester, United Kingdom

Reviewed by:
Frank Seebacher,
The University of Sydney, Australia
Holly Shiels,
The University of Manchester, United Kingdom

***Correspondence:**
Casey A. Mueller
cmueller@csusm.edu

Specialty section:
This article was submitted to Embryonic and Developmental Physiology, a section of the journal Frontiers in Physiology

Received: *02 March 2019*
Accepted: *31 May 2019*
Published: *18 June 2019*

Citation:
Mueller CA, Bucsky J, Korito L and Manzanares S (2019) Immediate and Persistent Effects of Temperature on Oxygen Consumption and Thermal Tolerance in Embryos and Larvae of the Baja California Chorus Frog, Pseudacris hypochondriaca. Front. Physiol. 10:754. doi: 10.3389/fphys.2019.00754

The developmental environment has significant immediate effects on phenotypes, but it may also persistently or permanently shape phenotypes across life history. This study examined how developmental temperature influenced embryonic and larval phenotypes of Baja California chorus frog (*Pseudacris hypochondriaca*), an abundant amphibian in southern California and northern Baja California. We collected egg clutches from native ponds in northern San Diego County within 24 h of fertilization, and clutches were separated and distributed between constant temperatures of 10, 15, 20, and 25°C for incubation. Oxygen consumption rate ($\dot{V}O_2$), developmental stage, and embryo and yolk masses were measured throughout development. Time to 50% hatch, survival at 50% hatch, and hatch duration were determined. Development rate was strongly affected by temperature, with warmer temperatures reducing time to hatch and hatch duration. Survival to hatch was high across all temperatures, >90%. Mass-specific $\dot{V}O_2$ of embryos either remained constant or increased throughout development, and by hatching energy demand was significantly increased at higher temperatures. There were limited temperature effects on growth, with embryo and yolk dry mass similar between temperatures throughout embryonic development. To examine long-term effects of embryonic temperature, we reared hatchlings from each temperature until onset of larval feeding. Once feeding, larvae were acclimated to 20 or 25°C (>2 weeks). Following acclimation to 20 or 25°C, we measured larval mass-specific $\dot{V}O_2$ and critical thermal maximum (CTMax) at a common developmental stage (Gosner stages 32–36, "hindlimb toe differentiation"). Embryonic temperature had persistent effects on larval $\dot{V}O_2$ and CTMax, with warmer temperatures generally resulting in similar or higher $\dot{V}O_2$ and CTMax. This partially supported a "warmer is better" effect of embryonic incubation temperature. These results suggest that in a thermally robust amphibian species, temperature may program the phenotype during early development to construct traits in

thermal tolerance and energy use that may persist. Overall, *P. hypochondriaca* displays a thermally robust phenotype, and it is possible that amphibians that possess a wider range of phenotypic plasticity will be relatively more successful mitigating effects of climate change.

Keywords: amphibian, carry-over effects, development, energy use, phenotypic plasticity, temperature

INTRODUCTION

The environment is a driving force that exerts immediate and long-term effects on phenotypes. However, animals are not passive entities, and phenotypic plasticity is an important avenue by which animals respond to the environment (Garland and Kelly, 2006; Mueller et al., 2015a). Phenotypic plasticity is a modification in phenotype to adjust and respond to the environment, occurring through changes in physiology, morphology and/or biochemistry (West-Eberhard, 1989; Pigliucci et al., 2006). Plasticity is particularly important for responses to temperature, which affects nearly all physiological processes. In particular, the embryonic and larval/juvenile period for vertebrates are typically very sensitive developmental periods in an organism's life history, marked by fundamental shifts in size, morphology, and physiology (Mueller et al., 2015a,b; Smith et al., 2015). Responses to temperature during these stages may have significant implications for species success, particularly in response to increased temperatures predicted with climate change (Cayan et al., 2008; van Vliet et al., 2013; IPCC, 2014).

The effect of temperature in shaping developing phenotypes comprises a very important area of current comparative physiological research, particularly for amphibians, as higher global temperatures are contributing to unprecedented worldwide declines in many groups of amphibians (Stuart et al., 2004; Pounds et al., 2006; Cohen et al., 2018). Embryonic ectothermic vertebrates are often exposed to wide fluctuations in temperature, and a species' ability to phenotypically respond to the environment may have profound consequences. Temperature drives development rate and growth of embryonic and larval amphibians and fish (Harkey and Semlitsch, 1988; Seymour et al., 1991; Mitchell and Seymour, 2000; Watkins, 2000; Mueller et al., 2011, 2015b; Smith et al., 2015), and can alter embryonic oxygen consumption rate ($\dot{V}O_2$), heart rate, yolk-conversion efficiency (YCE), and hatching survival (Mueller et al., 2011, 2015b; Eme et al., 2015). For example, embryonic incubation at warmer temperatures results in persistently higher $\dot{V}O_2$ values in embryonic and larval moss frogs (*Bryobatrachus nimbus*) and embryonic lake whitefish (*Coregonus clupeaformis*) (Mitchell and Seymour, 2003; Eme et al., 2015).

There is evidence that embryonic temperature has impacts on amphibian physiology beyond hatching. Such alterations in performance due to previous life history or conditions have been referred to as "carry-over effects" (O'Connor et al., 2014; Yagi and Green, 2018). Amphibians have shown carry-over/persistent effects from the thermal conditions of embryonic and/or larval development. For example, over test temperature ranges of 5°C–35°C, pre-metamorphic *Pseudacris regilla* (previously *Hyla regilla*) reared at 15°C as embryos swam faster and had higher myofibrillar ATPase activity than larvae reared at 25°C (Watkins, 2000). Similarly, sprint speed of larval *Bombina orientalis* was higher when larvae developed at relatively cooler temperatures (Parichy and Kaplan, 1995). *Rana sylvatica* that developed at 21°C as embryos compared to 15°C, swam slower when both developed at 21°C as larvae. However, embryonic development at 21°C and larval development at 18°C resulted in similar swimming speed compared to embryonic development at 15°C and larval development at 21°C, indicative of temperature exposure interactions across developmental time points (Watkins and Vraspir, 2005). Embryonic and larval acclimation temperatures showed interactive effects on swimming performance curves of *Limnodynastes peronii* larvae, with larvae incubated and acclimated at 25°C performing best in terms of breadth and peak of burst swimming speed when tested between 10 to 30°C (Seebacher and Grigaltchik, 2014). In contrast, *L. peronii* larvae incubated as embryos at 15°C did not show differences in larval $\dot{V}O_2$ compared to those incubated at 25°C, despite higher $\dot{V}O_2$ following larval acclimation to 15°C (Seebacher and Grigaltchik, 2014). Collectively, these studies suggest that within a range of acclimation temperatures, which may vary from species to species, relatively cooler or warmer temperatures during development of poikilothermic ectotherms may confer lower or higher performance during the larval stage, depending on the variable measured, supporting for example either the "warmer is better" or "colder is better" hypothesis of phenotypic plasticity (Huey et al., 1999). Furthermore, benefits of relatively cooler temperatures on performance are often reduced or absent at higher test temperatures (Wilson and Franklin, 1999; Watkins, 2000; Wilson et al., 2000; Seebacher and Grigaltchik, 2014), supporting the "beneficial acclimation hypothesis" that development at one temperature may be beneficial for performance at that temperature, but not at others (Huey et al., 1999). These previous studies examine function at one life history stage (e.g., larval stage) following embryonic and/or larval development under different temperatures. However, a deeper understanding of how temperature shapes developing phenotypes requires assessment of physiological function at *both* embryonic and larval life history stages.

The Baja California chorus frog (*Pseudacris hypochondriaca*) experiences a variable thermal environment across its life history. The chorus frog inhabits a wide range of environments throughout its latitudinal range (∼1400 km) from Santa Barbara County, California to Baja California, Mexico (Recuero et al., 2006), including deserts, grasslands, mountains and forests, that differ fundamentally in seasonal temperatures and elevation (∼3000 m) (Jameson et al., 1970; Schaub and Larsen, 1978). *P. hypochondriaca* reproduces in a variety of water bodies, some

of which are temporary, and males initiate mating calls at a wide range of water temperatures, between 4 and 20°C (Brattstrom and Warren, 1955; Cunningham and Mullally, 1956), though it is likely they also call at even higher temperatures (Mueller, unpublished data). Previous observations indicated embryos develop successfully between 8 and 29°C, and larvae between 0 and 33°C (Brattstrom and Warren, 1955; Brown, 1975). Adult chorus frogs also appear to tolerate a wide range of temperatures (Cunningham and Mullally, 1956), but how developmental temperature may shape the physiological phenotype of this eurythermal amphibian is unknown.

The goal of this study was to determine immediate and possibly persistent effects of temperature on embryonic and larval *P. hypochondriaca*. Embryos were incubated in constant temperatures of 10, 15, 20, or 25°C until hatching to determine the immediate influence of temperature on survival, development rate, growth and energy use of embryos. We hypothesized that embryonic survival would be high across temperatures, similar to a previous study that did not see a decrease in survival until approximately 30°C (Brown, 1975). We also predicted that embryonic development rate would increase as temperature increased, and that hatchlings would be smaller at higher temperatures with greater residual yolk. We hypothesized that embryonic mass-specific oxygen consumption rate ($\dot{V}O_2$) would remain constant or decrease throughout development prior to a marked increase for hatched animals, similar to previous data for embryonic and larval fish (Rombough, 1994; Eme et al., 2015). We also hypothesized that $\dot{V}O_2$ would be greater at higher temperatures in later embryonic stages due to temperature dependent effects observed in ectotherm metabolism. Larvae from each embryonic temperature treatment (10, 15, 20, or 25°C) were acclimated to 20 or 25°C to assess the possibility that effects of embryonic environment carried-over into larval phenotypes (**Figure 1**). We predicted that embryonic temperature would have persistent effects on larval aerobic metabolism, with larvae incubated as embryos in colder temperatures showing higher mass-specific $\dot{V}O_2$ at both larval acclimation temperatures, a "colder is better" result similar to a previous study showing such trends for $\dot{V}O_2$ and aerobic enzyme activities (Huey et al., 1999; Seebacher and Grigaltchik, 2014). We also predicted that incubation at warmer temperature as embryos would confer greater thermal tolerance for larvae at the same acclimation temperature, a "warmer is better" result similar to a previous study that showed similar trends for swimming speed (Huey et al., 1999; Seebacher and Grigaltchik, 2014). Lastly, we hypothesized that acclimation to 25°C would result in lower mass-specific $\dot{V}O_2$ and greater thermal tolerance of larvae compared to acclimation to 20°C.

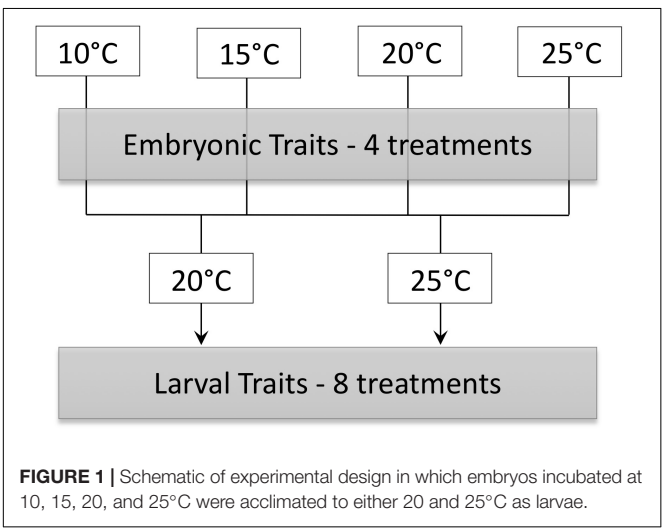

FIGURE 1 | Schematic of experimental design in which embryos incubated at 10, 15, 20, and 25°C were acclimated to either 20 and 25°C as larvae.

MATERIALS AND METHODS

Field Collection and Embryo Incubation

Eggs were collected from ponds on the California State University San Marcos campus (33°07′58.4″N/117°09′38.0″W, 200 m elevation) during January–February 2017 and January–March 2018. Eggs were collected during mid-late gastrulation (Gosner (1960) stages 8–9), indicating embryos were likely laid the night before and thus were within 24 h of fertilization. Eggs were cleaned of debris in water in the lab under a microscope (Zoom Stereo Trinocular Microscope, Amscope, Irvine, CA, United States). Eggs were collected, cleaned and incubated in 230 ml plastic Ziploc®containers with identically sourced water, tap water that had been aged by bubbling with air for 48 h before use. Eggs were initially collected and cleaned with aged water that was identical in temperature to field water (13–16°C). Clutches were separated and distributed between four temperatures: 10, 15, 20, and 25°C. The 10°C and 15°C embryos were incubated in wine coolers (Newair AWC-330E, Huntington Beach, CA, United States), 20°C embryos were incubated in a Thermo Scientific Precision Incubator (Marietta, OH, United States), and 25°C embryos were incubated in an environmental growth chamber (Chagrin Falls, Ohio, United States). A Thermochron iButton®data logger (Model DS1922L, iButtonLink, Whitewater, WI, United States) recorded temperature every 30 min in a separate container with the same volume of water as the embryo containers. Temperature was recorded every 30 min, and average daily temperatures were used to generate a grand mean for each temperature: 10°C = 10.0 ± 0.1°C, 15°C = 15.0 ± 0.1°C, 20°C = 19.9 ± 0.1°C, 25°C = 25.1 ± 0.1°C. Clutches were observed for mortality and first hatching, and the number of hatchlings was recorded each day until all embryos had hatched. Survival at 50% hatch, average time to 50% hatch, and hatch window duration (days from initial to final hatchling) were determined across clutches (10°C = 6 clutches, 15°C = 13 clutches, 20°C = 10 clutches, 25°C = 9 clutches).

Embryo Oxygen Consumption Rate ($\dot{V}O_2$)

Oxygen consumption rate ($\dot{V}O_2$) was measured at Gosner embryonic stages 16, 18, 20, and 22 (hatch) in independent embryos at the temperature in which embryos were incubated (n = 8 per stage for each treatment). $\dot{V}O_2$ was determined from the decrease in partial pressure of oxygen (PO_2) in a closed respirometry system. Individual embryos/hatchlings were placed in respiratory chambers (volume: 0.94–1.17 ml) containing a

5 mm O_2 sensor spot (Loligo System, Tjele, Denmark). Four chambers were housed in a recirculating water bath thermostated to the target temperature by a recirculating heater/chiller (Thermo Fisher Scientific, IsotempTM 6200, Waltham, MA, United States). The sensor spot in each chamber was read by a fiber optic cable (PreSens Precision Sensing, GmbH, Regensbury, Germany) connected to a Witrox 4 oxygen meter (Loligo Systems, Tjele, Denmark) with a computer running Autoresp^{TM} software (Loligo Systems, Tjele, Denmark). Oxygen levels of each chamber was read every 5 min for approximately 120 min. The first ∼40 min was excluded from $\dot{V}O_2$ calculation to account for handling and allow embryos to reach a steady state of oxygen consumption. The lowest recorded oxygen levels in chambers were 12 kPa, and $\dot{V}O_2$ was always stable (linear) over the 120 min measurement period, indicating O_2 levels were above those likely to adversely affect $\dot{V}O_2$. $\dot{V}O_2$ (μl h^{-1}) was calculated using the following equation:

$$\dot{V}O_2 = \left(\frac{PO_{2(t2)} - PO_{2(t1)}}{t_2 - t_1}\right) * \beta * V$$

where $PO_{2(t2)}$–$PO_{2(t1)}$ is the decrease in PO_2 (kPa) in the chamber over the time period (t_2–t_1, h), β is the capacitance of the water at the relevant temperature (μl O_2 μl^{-1} kPa^{-1}), and V is the chamber volume minus the embryo volume (μl, estimated from mass). Each chamber was calibrated with a fresh anoxic solution of 10 mg sodium sulfite in 1 ml of water (0%) and air equilibrated water (100%). All $\dot{V}O_2$ values were corrected for $\dot{V}O_2$ of the empty chamber to account for any microbial oxygen consumption. Mass-specific $\dot{V}O_2$ (μl h^{-1} mg^{-1}) was calculated by dividing $\dot{V}O_2$ by dry yolk-free mass.

Embryo Mass

Individuals used for $\dot{V}O_2$ determination and other embryos selected at embryonic stages 16, 18, 20, and 22 (hatch) were placed in 4% paraformaldehyde (PFA) in phosphate buffered saline (PBS; pH = 7.4) in microcentrifuge tubes. After fixation in 4% PFA for 36 ± 1 d, embryos/hatchlings were removed from their chorion (if not already so) and photographed under a dissecting microscope (10-15X, Zoom Stereo Trinocular Microscope, Amscope, Irvine, CA, United States) with a USB 3.0 digital camera (Amscope, Irvine, CA, United States). The yolk was then carefully dissected away from the embryo, and the embryo and yolk weighed to ± 0.01 mg (XA105DU, Mettler-Toledo, Columbus, OH, United States). The embryo and yolk were dried at 65°C for 24 h (model 10 oven, Quincy Lab, Inc., Chicago, IL, United States) and reweighed. The stage of each embryo was confirmed from photographs.

Larval Incubation

A subset of embryos were allowed to hatch and were maintained at each embryo temperature treatment until 5–7 d after first feeding. Larvae in each temperature were then randomly separated into two groups and acclimated to 20 or 25°C. Temperature of the larvae was increased at a rate of 1–2.5°C day^{-1}. This created 8 larval temperature treatments (**Figure 1**). Larvae were maintained at each temperature in aged tap water in 2 L rectangular plastic containers at a density of 5–8 larvae L^{-1} and a 12 h: 12 h light: dark regime. Twice weekly, containers were cleaned of waste, 30% of the water replaced with fresh aged water, and larvae fed boiled lettuce *ad libitum*.

Larval Routine Oxygen Consumption Rate and Critical Thermal Maximum

Larval development was monitored until Gosner (1960) stages 32–36, which represents hindlimb toe differentiation. Larvae were acclimated to 20 or 25°C for a minimum of 2 weeks prior to reaching these stages. The average acclimation period for each temperature treatment prior to experimentation was as follows: 10–20°C: 52 ± 3 d, 15–20°C: 46 ± 2 d, 20–20°C: 40 ± 3 d, 25–20°C: 31 ± 2 d, 10–25°C: 53 ± 1 d, 15–25°C: 34 ± 3 d, 20–25°C: 27 ± 2 d, and 25–25°C: 32 ± 3 d.

Once the larva had reached the representative stage, routine $\dot{V}O_2$ was measured at the acclimation temperature using intermittent respirometry (n = 6–16 per treatment). Individual larvae were placed in ∼8.2 ml respirometry chambers containing a 5 mm O_2 sensor spot (Loligo System, Tjele, Denmark) and read as described above for embryonic $\dot{V}O_2$. An intermittent cycle of 60 s flush, 240 s wait and 300 s measure periods was controlled by a Daq-M and Autoresp^{TM} software (Loligo Systems, Tjele, Denmark). This intermittent cycle resulted in PO_2 of the chambers never falling below 17 kPa. Trials were performed for a minimum of 120 min, and the first ∼40 min was excluded from $\dot{V}O_2$ calculation to account for handling and allow larvae to reach a steady state of oxygen consumption. Each chamber was calibrated with a fresh anoxic solution of 10 mg sodium sulfite in 1 ml of water (0%) and air equilibrated water (100%). It was not possible to keep larvae completely stationary during trials, so measurements represent routine metabolic rate (i.e., $\dot{V}O_2$ that represents O_2 consumed during relatively low levels of activity). All $\dot{V}O_2$ values were corrected for $\dot{V}O_2$ of empty chambers to account for any microbial oxygen consumption. Following $\dot{V}O_2$ determination, larvae were euthanized in MS-222, staged, weighed and fixed in 4% PFA in PBS. After fixation for ∼30 days, the gut was dissected from the larvae and wet and dry masses determined as described above for embryos.

Critical thermal maximum (CTMax) was determined for a separate subset of larvae (n = 5–14 per treatment) at the same developmental stages as $\dot{V}O_2$ measurement. For each CTMax trial, individual larvae were placed in 250 ml tri-corner plastic beakers (Globe Scientific, Inc., Paramus, NJ, United States) filled with aged tap water at the appropriate temperature. Beakers were suspended in a polystyrene frame within a 20 L polystyrene-insulated plastic water bath that was heated continuously during the trial by two 150W aquarium heaters (EHEIM GmbH) and bath water circulated with an aquarium pump (15 L min^{-1}, Lifeguard Aquatics, Cerritos, CA, United States). All individual test chambers were provided with moderate aeration to prevent thermal stratification. Beaker water temperatures were measured with a VWR®Traceable®Ultra waterproof thermometer (± 0.1°C) (VWR, Radnor, PA, United States). Temperatures were increased at 0.33 ± 0.01°C min^{-1}. Temperature increase continued until larvae exhibited

loss of equilibrium (LOE), defined as the inability to respond to mechanical stimulation and dorso-ventral orientation, and thus failure to show an escape response (Cupp, 1980; Sherman and Levitis, 2003). As tadpoles reached LOE, beaker temperature was recorded, and the temperature corrected based on a calibrated VWR®Traceable®Digital Thermometer (precision ± 0.0001°C; accuracy ± 0.05°C; Avantor, VWR, Radnor, PA, United States). Following LOE, larvae were immediately removed from the CTMax chamber and returned to their acclimation temperature. Larvae were allowed to recover for ≥1 h, after which they were euthanized in MS-222, dried and weighed to 0.01 mg. 90% of larvae survived for ≥1 h following trials, and only CTMax values for those that survived were included in analyses.

Statistical Analyses

Data were tested for normality and homogeneity of variances using the Shapiro-Wilk and O'Brien test, respectively, and appropriate parametric or non-parametric tests used. Non-parametric analyses were used as no transformations ensured non-parametric data met parametric assumptions. Time to 50% hatch, hatch duration, survival at 50% hatch were compared across embryonic incubation temperature using a Kruskal-Wallis test with *post hoc* Steel-Dwass comparisons. Wet mass, dry mass, and water content of embryos and yolk across developmental stages and temperature were examined using a Friedman's non-parametric 2-way ANOVA with developmental stage, temperature, and the interaction between developmental stage and temperature as the effects. Mass-specific $\dot{V}O_2$ across developmental stages and temperature were examined with a 2-way ANOVA with developmental stage, temperature, and the interaction between developmental stage and temperature as the effects. *Post hoc* Tukey HSD comparisons were used when effects were significant.

Larval mass-specific $\dot{V}O_2$ were compared across temperature treatments using a two-way ANOVA with embryonic temperature, larval acclimation temperature, and the interaction between embryonic and larval temperatures as the effects. Tukey HSD comparisons were used when effects were significant. Larval CTMax was compared across temperature treatments using a 2-way ANCOVA with embryonic temperature and larval acclimation temperature as the main effects and dry mass as a covariate. Data are presented as mean ± SEM, and differences were accepted as statistically significant at $\alpha = 0.05$.

RESULTS

Embryonic Development, Growth and Oxygen Consumption

All embryos hatched at Gosner (1960) stage 22. Survival (%) was high throughout embryonic development and not affected by temperature, with 92–97% survival at 50% hatch across all temperatures ($\chi^2_3 = 3.8$, $P = 0.28$, **Figure 2A**). As temperature increased, time to 50% hatch significantly decreased from 21 days post-fertilization (dpf) at 10°C to 5 dpf at 25°C ($\chi^2_3 = 34.2$, $P < 0.0001$, **Figure 2B**). Q_{10} for development rate was 2.8 for 10–15°C, 3.1 for 15–20°C and 2.0 for 20–25°C, with an overall Q_{10} of 2.5 for 10–25°C. Hatch duration (d) also significantly decreased with an increase in incubation temperature, but did not significantly differ between 20 and 25°C ($\chi^2_3 = 27.5$, $P < 0.0001$, **Figure 2C**).

Embryo wet mass increased with developmental stage ($F_{3,387} = 87.7$, $P < 0.0001$), and was influenced by the interaction of stage and temperature ($F_{9,387} = 5.5$, $P < 0.0001$), but not temperature ($F_{3,387} = 1.4$, $P = 0.26$) (**Figure 3A**). Embryo wet mass was similar across temperatures at stage 16, 18, and 20. At stage 22 (hatching) embryo wet mass was higher at 25°C compared to other temperatures, and embryo wet mass at 15°C was higher than at 20°C. Embryo dry mass at hatching for all temperatures combined was significantly higher compared to earlier stages ($F_{3,380} = 2.7$, $P = 0.04$), but was not affected by temperature ($F_{3,380} = 1.4$, $P = 0.24$), or the interaction of stage and temperature ($F_{9,380} = 1.7$, $P = 0.08$) (**Figure 3B**). The majority of the increase in wet mass during development was due to an increase in water content, which increased with stage ($F_{3,380} = 113.8$, $P < 0.0001$), and was also significantly affected by temperature ($F_{3,380} = 14.9$, $P < 0.0001$) and the interaction of stage and temperature ($F_{9,380} = 6.8$, $P < 0.0001$) (**Figure 3C**). The significant interaction occurred due to lower embryo water content at stage 18 for 25°C embryos compared to other temperatures, and lower water content at stage 20 for 10 and 15°C embryos. Differences were absent by stage 22.

Yolk wet mass decreased with stage ($F_{3,384} = 20.2$, $P < 0.0001$) and was influenced by temperature ($F_{3,384} = 4.7$, $P < 0.01$), but not the interaction of stage and temperature ($F_{9,384} = 1.8$, $P = 0.07$) (**Figure 3D**). For all stages combined yolk wet mass was higher at 10°C compared to other temperatures. Yolk dry mass decreased with stage ($F_{3,379} = 46.1$, $P < 0.0001$), and was affected by temperature ($F_{3,379} = 4.0$, $P < 0.01$) and the interaction of stage and temperature ($F_{3,379} = 3.3$, $P < 0.001$) (**Figure 3E**). The significant interaction was due to higher yolk dry mass at hatching for 10°C embryos compared to 15 and 25°C. Yolk water content was lowest at stage 20 compared to stage 16 and 22 for all temperatures combined ($F_{3,379} = 5.0$, $P < 0.01$), but was not affected by temperature ($F_{3,379} = 2.7$, $P = 0.09$) or the interaction of stage and temperature ($F_{9,379} = 1.5$, $P = 0.14$) (**Figure 3F**).

Embryonic mass-specific $\dot{V}O_2$ was influenced by stage ($F_{3,130} = 38.7$, $P < 0.0001$) and temperature ($F_{3,130} = 35.5$, $P < 0.0001$) and the interaction of stage and temperature ($F_{9,130} = 4.4$, $P < 0.0001$) (**Figure 4**). The interaction occurred because mass-specific $\dot{V}O_2$ did not significantly change across stages for embryos incubated at 10 and 15°C, but did increase across development at 20 and 25°C. Mass-specific $\dot{V}O_2$ was not affected by temperature at stage 16. However, as development progressed mass-specific $\dot{V}O_2$ diverged, and it was significantly different for 10 and 15°C embryos compared to 20 and 25°C at stages 18 and 20. At hatch (stage 22) mass-specific $\dot{V}O_2$ increased with temperature, except for statistically similar values at 10 and 15°C. Q_{10} values for mass-specific $\dot{V}O_2$ at hatching were 1.2 for 10–15°C, 3.8 for

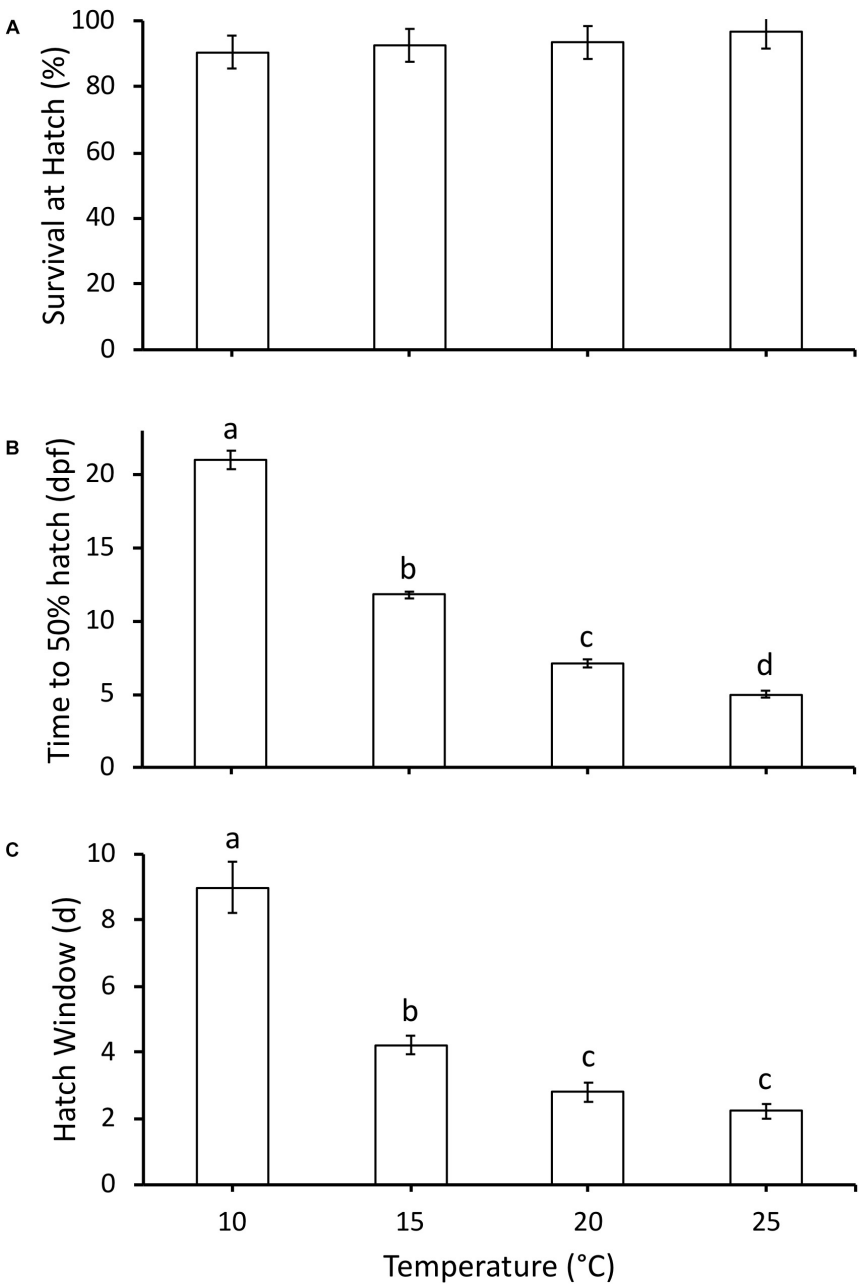

FIGURE 2 | (A) Survival at hatch (%), **(B)** time to 50% hatch (days post-fertilization, dpf), and **(C)** hatch window (days from first to last hatch) of hatchlings incubated at different temperatures. Data presented as mean ± SEM, n for each temperature as follows: 10°C = 6, 15°C = 13, 20°C = 10, 25°C = 9. Different letters indicate significant differences between temperatures based on Kruskal-Wallis test and Steel-Dwass *post hoc* comparisons.

15–20°C and 2.0 for 20–25°C, with an overall Q_{10} of 2.1 for 10–25°C.

Larval Oxygen Consumption Rate and Critical Thermal Maximum

Larval mass-specific $\dot{V}O_2$ was influenced by embryonic temperature ($F_{3,75}$ = 2.5, P = 0.035), larval acclimation temperature ($F_{1,75}$ = 7.9, $P < 0.01$), and the interaction between embryonic and larval temperatures ($F_{3,75}$ = 2.8, P = 0.044) (**Figure 5A**). Embryonic temperature influenced mass-specific $\dot{V}O_2$ only at the larval acclimation temperature of 25°C. Following acclimation to 25°C, larvae incubated at 20°C as embryos demonstrated higher mass-specific $\dot{V}O_2$ than larvae incubated at 10°C as embryos.

Critical thermal maximum was significantly affected by embryonic temperature ($F_{3,58}$ = 7.0, $P < 0.001$), larval acclimation temperature ($F_{1,58}$ = 44.0, $P < 0.0001$), the

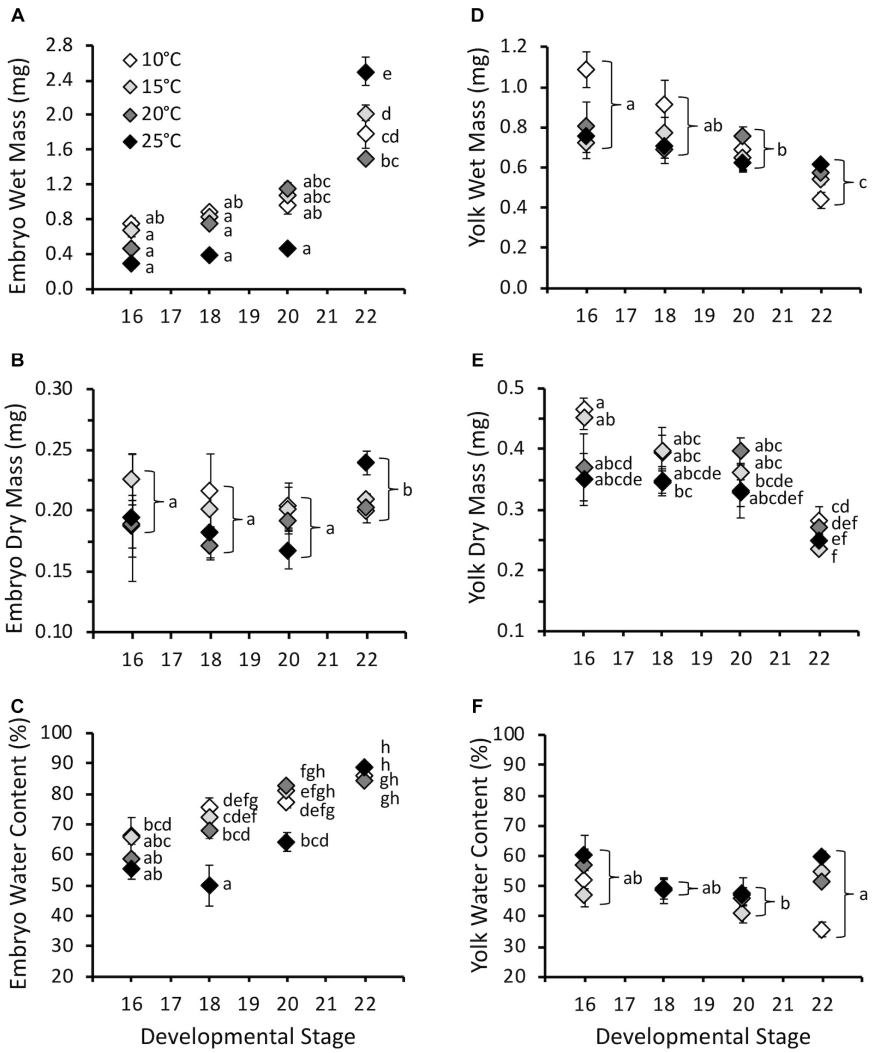

FIGURE 3 | (A) Embryo wet mass (mg), **(B)** embryo dry mass (mg), **(C)** embryo water content (%), **(D)** yolk wet mass (mg), **(E)** yolk dry mass (mg), and **(F)** yolk water content (%) throughout embryonic development at different incubation temperatures. Developmental stages based on Gosner (1960). Data presented as mean ± SEM, n = 5–11 for stage 16, 7–20 for stage 18, 8–16 for stage 20, 39–121 for stage 22. Letters on **A**, **C,** and **E** indicate significant differences based on interaction between development stage and temperature (two-way ANOVA, Tukey *post hoc* comparisons). Letters on **B**, **D,** and **F** indicate significant differences between stages for all temperatures combined (two-way ANOVA, Tukey *post hoc* comparisons).

interaction between embryonic and larval temperatures ($F_{3,58}$ = 3.5, P = 0.028), but not dry mass ($F_{1,58}$ = 2.9, P = 0.1). Mean CTMax was 1.8°C higher at an acclimation temperature of 25°C compared to 20°C (**Figure 5B**). However, embryonic temperature had persistent effects in certain cases. At the tadpole acclimation temperature of 20°C, larvae incubated at 20°C as embryos had lower CTMax than larvae incubated at 25°C. In contrast, CTMax was similar across all embryonic temperature treatments at 25°C acclimation.

DISCUSSION

One of the most dynamic sources of physiological phenotypic plasticity is environmental temperature early in development, and predicting persistent physiological consequences for organisms across taxa is an area of significant current research interest (Kim et al., 2017; Noble et al., 2018; Ruthsatz et al., 2018; Warner et al., 2018). We explored this central idea in comparative physiology using *P. hypochondriaca*, an amphibian that experiences a broad range of temperatures throughout its life history. We demonstrated that temperature during embryonic development had both immediate embryonic effects as well as carry-over larval effects that influenced physiological function. Increased temperature during embryonic development did not reduce survival or mass, despite an increased energy demand that supported faster development. Acclimation to higher temperature during larval development generally caused increased thermal tolerance, whereas aerobic metabolism showed no change or a modest increase with higher larval acclimation

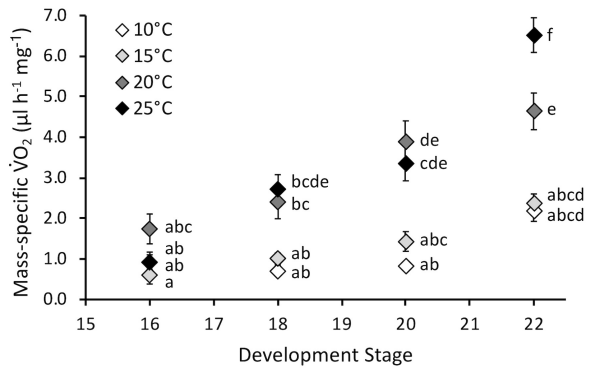

FIGURE 4 | Mass-specific oxygen consumption rate ($\dot{V}O_2$, µl h^{-1} mg^{-1}) of embryos incubated at different temperatures. Developmental stages based on Gosner (1960). Data presented as mean ± SEM, n = 8 for all data points. Letters indicate significant differences based on interaction between development stage and temperature (two-way ANOVA, Tukey *post hoc* comparisons).

temperature. Embryonic incubation temperature had certain persistent effects. Namely, embryonic temperature of 10°C resulted in reduced $\dot{V}O_2$ at a larval acclimation temperature of 25°C, and embryonic development at 25°C resulted in high thermal tolerance in 20°C acclimated larvae. Therefore, in a thermally robust species such as *P. hypochondriaca* the developmental environment has long-term impacts on phenotype. This is particularly important in relation to temperature, as it may provide valuable insight into species responses to a changing climate.

Immediate Effects of Temperature During Embryonic Development

The embryonic responses to temperature in *P. hypochondriaca* demonstrated broad thermal tolerance of the species. Development until hatching was highly successful across the temperature range (10 – 25°C) studied (**Figure 2A**), matching previous studies that indicate successful embryonic development at temperatures up to 29°C (Brown, 1975). However, it was somewhat surprising that survival remained so high (97%) at 25°C. This temperature has been rarely recorded in the field location from which the eggs were collected (Mueller, unpublished data), yet the embryos show no apparent adverse effects. While survival was consistent across treatments, temperature did drive a step-wise increase in embryonic development rate, as reflected in a decrease in time to 50% hatch (**Figure 2B**) and a reduction in hatch window (**Figure 2C**). Increased development rate with temperature was an expected result, and has been observed in many amphibians (McLaren and Cooley, 1972; Kuramoto, 1975; Bradford, 1990; Seymour et al., 1991; Mitchell and Seymour, 2000). The Q_{10} for development rate was 2.5 across the temperature range studied, which is in the lower range of Q_{10} values (2.0 to 4.5) measured in other amphibians across the same temperature range (Kuramoto, 1975). A relatively low Q_{10} indicates that temperature has less of an effect on development rate compared to other species, which provides additional support for the broad thermal tolerance of *P. hypochondriaca*. Together, the survival and development rate results highlight the eurythermal nature of the embryos and suggests that *P. hypochondriaca* is likely to be of least concern even if air temperatures increase by 1.6–4.4°C, and water temperatures increase by 0.5–2.5°C by 2099, as predicted by different climate models for southern California (Cayan et al., 2008; van Vliet et al., 2013).

Despite the effect of temperature on development rate, temperature had limited influence on masses throughout embryonic development (**Figure 3**). This result does not support our hypothesis that warmer embryos would be smaller at hatch, as has been observed in other amphibian and fish species (Rombough, 1988; Kamler et al., 1998; Mueller et al., 2015b; Eme et al., 2018). However, other species have also shown no change in body mass with temperature, so this is not unique to *P. hypochondriaca* (Watkins and Vraspir, 2005; Mueller et al., 2011). While embryo wet mass increased throughout embryonic development, this was largely due to an increase in water content, and there was limited increase in dry mass only at hatching. In contrast, both wet and dry yolk mass decreased, while yolk water content was relatively stable. The lack of substantial somatic growth prior to hatch has been observed in other amphibians (Mitchell, 2001; Mueller et al., 2012). The limited growth at these stages is likely to limit the influence that temperature may have in how energy is allocated to mass. However, we did not observe differences in larvae mass when larval $\dot{V}O_2$ and CTMax were measured, and therefore the limited temperature effect on mass appears to persist throughout larval development at the temperatures examined.

Contrary to our hypothesis, mass-specific $\dot{V}O_2$ increased throughout embryonic development at higher temperatures, and this matched increased development rate (**Figure 4**). Overall Q_{10} values for development rate (2.5) and mass-specific $\dot{V}O_2$ (2.1) were similar, indicating comparable temperature sensitivity for these two important developmental rates. Thus, immediate effects of temperature on embryonic development, namely faster development at increased temperature, is largely correlated with increased energy use. There does not appear to be a decrease in energy efficiency with development at higher temperatures. These findings further indicated that temperatures up to 25°C appeared to have no significant immediate negative impact on *P. hypochondriaca* embryos. Examining energy allocation during development to the processes such as development, growth and maintenance, which can be modeled with dynamic energy budget theory (Mueller et al., 2012), would be a fruitful area of future study in this species.

Interactive Effects of Embryonic Temperature and Larval Acclimation Temperature

Our investigation of larval function revealed the effects of larval acclimation temperature and persistent effects of embryonic temperature. We examined both mass-specific $\dot{V}O_2$ and CTMax during hindlimb toe differentiation [Gosner (1960) stages 32–36] across all temperature treatments. By nature of temperature

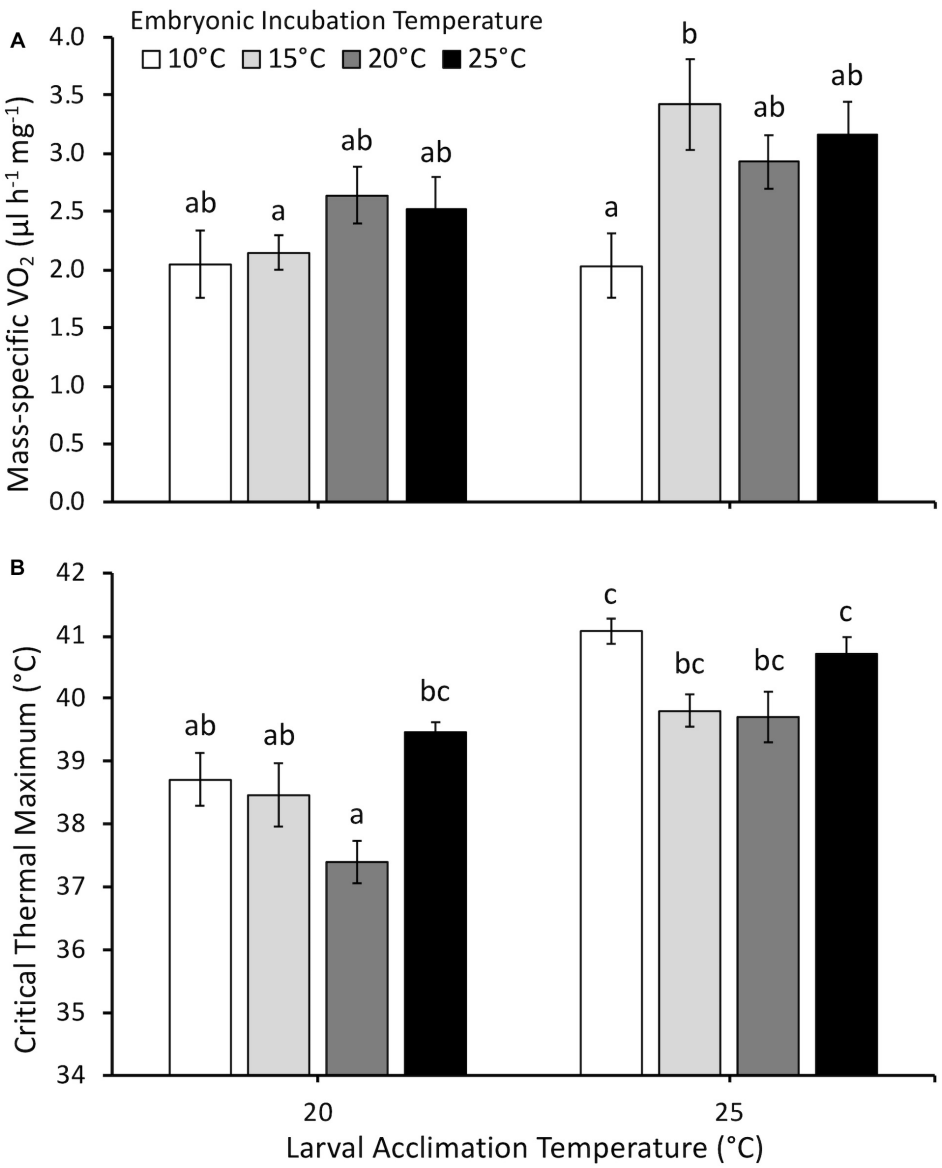

FIGURE 5 | (A) Mass-specific oxygen consumption rate ($\dot{V}O_2$, $\mu l\ h^{-1}\ mg^{-1}$) and **(B)** critical thermal maximum (°C) of larvae acclimated to either 20 or 25°C following embryonic incubation at different temperatures. Larvae measured at Gosner (1960) stage 32–36 (hind limb toe differentiation). Data presented as mean ± SEM, n = 6–16 for $\dot{V}O_2$, n = 5–14 for CTMax. Different letters indicate significant differences across all embryonic incubation and larval acclimation treatments (two-way ANOVA, Tukey *post hoc* comparisons).

influencing development rate, the period of acclimation prior to reaching these stages was shorter at higher temperatures, and there is a possibility this may have influenced the results observed. However, *P. hypochondriaca* shows variation in larval development duration within temperatures (Mueller, unpublished data), and every animal measured was acclimated to its larval temperature for at least 2 weeks. Instead, we hypothesized that the developmental status of an individual is more likely to have an impact on function, and thus we performed our measurements within a narrow range of developmental stages, which resulted in comparable larval sizes across treatments.

Persistent effects of the embryonic environment on larval mass-specific $\dot{V}O_2$ or CTMax depended upon larval acclimation temperature, with both measurements supporting a "warmer is better" effect of embryonic incubation temperature (Huey et al., 1999). Larval mass-specific $\dot{V}O_2$ measured following acclimation to 20°C showed no significant persistent effects of embryonic temperature (**Figure 5A**). However, at the acclimation temperature of 25°C, we observed that larvae incubated at 10°C as embryos had reduced mass-specific $\dot{V}O_2$ compared to larvae incubated at 15°C. This result is in contrast to our hypothesis that embryonic incubation at colder temperatures would cause higher mass-specific $\dot{V}O_2$ at

later developmental stages (i.e., "colder is better"). Our data showed that larval mass-specific $\dot{V}O_2$ either increases or does not change at the higher larval acclimation temperature of 25°C compared to 20°C. Seebacher and Grigaltchik (2014) showed that *Limnodynastes peronii* larvae displayed higher $\dot{V}O_2$ when acclimated to 15°C compared to 25°C, particularly when measured at 20, 25 and 30°C (Seebacher and Grigaltchik, 2014). The present studies' acclimation temperatures were only 5°C apart compared to 10°C used by Seebacher and Grigaltchik (2014), and the general trend in *P. hypochondriaca* was for higher acclimation temperature to result in higher $\dot{V}O_2$. It is possible that different larval acclimation periods (∼2–8 weeks for this study, 6 weeks for *L. peronii*) can result in different observations for the effect of embryonic incubation temperature on $\dot{V}O_2$.

It is also possible that any persistent effects of embryonic incubation temperatures are species-specific and/or trait-specific. Only the present study and Seebacher and Grigaltchik (2014) measured multiple whole animal performance or enzymatic data, and both studies show separate dependent variables that support either cooler (Seebacher and Grigaltchik, 2014 $\dot{V}O_2$ and aerobic enzyme assays) or warmer (Seebacher and Grigaltchik, 2014 anaerobic enzyme assays; and present study, $\dot{V}O_2$) incubation temperatures conferring a higher energy use phenotype for larvae. Seebacher and Grigaltchik (2014) also showed persistently higher values for a performance trait (swimming speed) following warmer embryonic incubation, similar to our finding for $\dot{V}O_2$ and CTMax data. However, *R. sylvatica* that developed at cooler temperatures swam faster than warmer incubated embryos, when measured as larvae, suggesting cooler temperatures are better for larval performance measurements (Watkins and Vraspir, 2005).

Similar to mass-specific $\dot{V}O_2$, interactive effects between embryonic temperature and larval acclimation temperature resulted in changes in larval thermal tolerance. Most treatments in the present study showed that acclimation to a higher temperature conferred greater thermal tolerance in *P. hypochondriaca* larvae (**Figure 5B**). At the larval acclimation temperature of 20°C, larvae incubated at 20°C as embryos had the lowest CTMax, significantly lower than larvae incubated at 25°C as embryos. In fact, CTMax of larvae incubated at 25°C as embryos was relatively high compared to other treatments at this acclimation temperature, and was not significantly different from CTMax measured at 25°C. These larvae were the only treatment in which the change from embryonic to larval temperature involved a decrease in temperature rather than an increase or no change. The increased embryonic temperature appears to have conferred a higher thermal tolerance that was retained, even following larval acclimation to a colder temperature. Thus, this treatment supported our hypothesis that warmer embryonic temperatures would result in increased thermal tolerance of larvae. Future experiments could examine a decrease in larval compared to embryonic temperature to provide insight into effects on thermal tolerance.

Thermal tolerance of larval *P. hypochondriaca* is within the range measured in similar species, but was more responsive to acclimation compared to previous studies. Our CTMax values at an acclimation temperature of 20°C (38–39°C) were similar to *Pseudacris triseriata*, *R. sylvatica*, *R. temporaria,* and *Xenopus laevis*, but lower than values (41–43°C) observed in *Bufo americanus*, *B. woodhousei*, *B. marinus,* and *Gastrophryne carolinenus* at the same acclimation temperature (Cupp, 1980; Floyd, 1983; Sherman and Levitis, 2003; Enriquez-Urzelai et al., 2019). Thus, thermal tolerance of *P. hypochondriaca* larvae tends to match other species that breed during the winter months. Across embryonic treatments, a 5°C increase in acclimation temperature resulted in an average 1.8°C increase in CTMax (slope of change in temperature tolerance for every 1°C increase in acclimation temperature = 0.36). This is a greater gain of tolerance that observed in other species. For example, when measured at the same developmental stages, *R. temporaria* gains 0.8°C with a 7°C increase in acclimation temperature (slope = 0.11), while *R. catesbeiana* and *B. marinus* gain approximately 0.7 and 1°C, respectively, with a 10°C increase in acclimation temperature (slopes = 0.07 and 0.1, respectively) (Menke and Claussen, 1982; Floyd, 1983; Enriquez-Urzelai et al., 2019). Performing similar experiments in species that vary in their temperature ranges during development may help to fully understand the effects of acclimation and potential carry-over effects of temperature on thermal tolerance.

SUMMARY

This study confirmed the thermally tolerant nature of *P. hypochondriaca* during its embryonic and larval life stages, and we demonstrated that the embryonic environment can have persistent effects at the larval stage. We observed that embryonic temperature of 10°C resulted in reduced $\dot{V}O_2$ at a larval acclimation temperature of 25°C, whereas CTMax was higher in larvae incubated at 25°C and acclimated to 20°C. Thus, under what conditions carry-over effects of developmental temperature emerge in the phenotype are likely to be trait-specific. It remains unclear what the implications of changes in energy use and thermal tolerance are for *P. hypochondriaca* beyond the larval stage. Future studies should examine phenotypes across the metamorphic transition to see if carry-over effects emerge even following significant morphological and physiological changes such as those occurring during amphibian metamorphosis. Higher larval temperatures generally produce smaller and younger metamorphs (see meta-analysis by Ruthsatz et al., 2018), but the functional consequences of this beyond metamorphosis is unclear; in our present study high embryonic incubation temperature did not affect hatchling size of these eurythermal frogs. Larval density has been shown to influence size and digestive morphology after metamorphosis (Bouchard et al., 2016; Yagi and Green, 2018). A recent study with *R. temporaria* suggests larval thermal tolerance may not persist beyond metamorphosis, and therefore water temperature exposure during larval development may not confer protective or deleterious effects on juveniles (Enriquez-Urzelai et al., 2019).

Future studies exploring physiology in multiple amphibian species are required to elucidate general patterns in phenotypic responses to developmental temperature. Our study partially supported a "warmer is better" effect of embryonic incubation temperature (similar or higher $\dot{V}O_2$ and CTMax for larvae incubated in warmer embryonic conditions), whereas Seebacher and Grigaltchik (2014) showed support for the "colder is better" hypothesis (higher $\dot{V}O_2$ and aerobic enzyme activities for larvae incubated in colder embryonic conditions (Huey et al., 1999; Seebacher and Grigaltchik, 2014). Moving forward, comparisons of stenothermal versus eurythermal species, and studies including amphibians that differ in their geographic ranges and temperatures they experience during development are needed to understand the factors that influence persistent phenotypic changes. Amphibians with restricted geographic distributions show increased stress responses compared to generalist species with larger distributions (Assis et al., 2018), and it is likely that stenothermal amphibians may also show stronger persistent phenotypic changes in response to temperature compared to eurythermal species such as *P. hypochondriaca*. Examining effects of developmental temperature across life history of numerous species will provide us with a more comprehensive understanding of how temperature shapes phenotypes, and this will be invaluable for predicting species responses to a changing climate.

DATA AVAILABILITY

The datasets generated for this study are available on request to the corresponding author.

ETHICS STATEMENT

This study was carried out in accordance with the recommendations of the Office for Laboratory Animal Welfare, the National Institutes of Health, and the California State University San Marcos Institutional Animal Care and Use Committee. The protocol was approved by the California State University San Marcos Institutional Animal Care and Use Committee.

AUTHOR CONTRIBUTIONS

CM conceived and designed the study, performed the experiments, and wrote the manuscript. JB, LK, and SM performed the experiments and collated the data. All authors approved final version of the manuscript.

FUNDING

This work was partly supported by startup funds from the California State University San Marcos to CM.

ACKNOWLEDGMENTS

We thank John Eme and the two reviewers for their helpful comments on an earlier version of this manuscript. We also thank the California Department of Fish and Wildlife for the scientific collecting permit to collect eggs (permit #13473).

REFERENCES

Assis, V. R., Titon, S. C. M., and Gomes, F. R. (2018). Acute stress, steroid plasma levels, and innate immunity in Brazilian toads. *Gen. Comp. Endocrinol.* 273, 86–97. doi: 10.1016/j.ygcen.2018.05.008

Bouchard, S. S., O'Leary, C. J., Wargelin, L. J., Charbonnier, J. F., and Warkentin, K. M. (2016). Post-metamorphic carry-over effects of larval digestive plasticity. *Funct. Ecol.* 30, 379–388. doi: 10.1111/1365-2435.12501

Bradford, D. F. (1990). Incubation time and rate of embryonic development in amphibians: the influence of ovum size, temperature, and reproductive mode. *Physiol. Zool.* 63, 1157–1180. doi: 10.1086/physzool.63.6.30152638

Brattstrom, B. H., and Warren, J. W. (1955). Observations on the ecology and behavior of the Pacific treefrog. *Hyla regilla*. *Copeia* 1955, 181–191.

Brown, H. A. (1975). Embryonic temperature adaptations of the Pacific treefrog. *Hyla regilla*. *Comp. Biochem. Physiol. A* 51, 863–873. doi: 10.1016/0300-9629(75)90067-5

Cayan, D. R., Maurer, E. P., Dettinger, M. D., Tyree, M., and Hayhoe, K. (2008). Climate change scenarios for the California region. *Clim. Change* 87, 21–42. doi: 10.1007/s10584-007-9377-6

Cohen, J. M., Civitello, D. J., Venesky, M. D., McMahon, T. A., and Rohr, J. R. (2018). An interaction between climate change and infectious disease drove widespread amphibian declines. *Global Change Biol.* 25, 927–937. doi: 10.1111/gcb.14489

Cunningham, J. D., and Mullally, D. P. (1956). Thermal factors in the ecology of the Pacific treefrog. *Herpetologica* 12, 68–79.

Cupp, P. V. Jr. (1980). Thermal tolerance of five salientian amphibians during development and metamorphosis. *Herpetologica* 36, 234–244.

Eme, J., Mueller, C. A., Lee, A. H., Melendez, C., Manzon, R. G., Somers, C. M., et al. (2018). Daily, repeating fluctuations in embryonic incubation temperature alter metabolism and growth of Lake whitefish (*Coregonus clupeaformis*). *Comp. Biochem. Physiol. A* 226, 49–56. doi: 10.1016/j.cbpa.2018.07.027

Eme, J., Mueller, C. A., Manzon, R. G., Somers, C. M., Boreham, D. R., and Wilson, J. Y. (2015). Critical windows in embryonic development: shifting incubation temperatures alter heart rate and oxygen consumption of Lake Whitefish (*Coregonus clupeaformis*) embryos and hatchlings. *Comp. Biochem. Physiol. A* 179, 71–80. doi: 10.1016/j.cbpa.2014.09.005

Enriquez-Urzelai, U., Sacco, M., Palacio, A. S., Pintanel, P., Tejedo, M., and Nicieza, A. G. (2019). Ontogenetic reduction in thermal tolerance is not alleviated by earlier developmental acclimation in *Rana temporaria*. *Oecologia* 189, 385–394. doi: 10.1007/s00442-019-04342-y

Floyd, R. B. (1983). Ontogenetic change in the temperature tolerance of larval *Bufo marinus* (Anura: Bufonidae). *Comp. Biochem. Physiol. A* 75, 267–271. doi: 10.1016/0300-9629(83)90081-6

Garland, T., and Kelly, S. A. (2006). Phenotypic plasticity and experimental evolution. *J. Exp. Biol.* 209, 2344–2361. doi: 10.1242/jeb.02244

Gosner, K. L. (1960). A simplified table for staging anuran embryos and larvae with notes on identification. *Herpetologica* 16, 183–190.

Harkey, G. A., and Semlitsch, R. D. (1988). Effects of temperature on growth, development, and color polymorphism in the ornate chorus frog *Pseudacris ornata*. *Copeia* 1988, 1001–1007.

Huey, R. B., Berrigan, D., Gilchrist, G. W., and Herron, J. C. (1999). Testing the adaptive significance of acclimation: a strong inference approach. *Am. Zool.* 39, 323–336. doi: 10.1093/icb/39.2.323

IPCC (2014). "Climate change 2014: synthesis report," in *Proceedings of the Contribution of Working Groups I, II and III to the Fifth Assessment Report of the Intergovernmental Panel on Climate Change*. eds R. K. Pachauri and L. A. Meyer (Geneva: IPCC).

Jameson, D. L., Taylor, W., and Mountjoy, J. (1970). Metabolic and morphological adaptation to heterogenous environments by the Pacific tree toad, *Hyla regilla*. *Evolution* 24, 75–89. doi: 10.1111/j.1558-5646.1970.tb01741.x

Kamler, E., Keckeis, H., and Bauer-Nemeschkal, E. (1998). Temperature-induced changes of survival, development and yolk partitioning in *Chondrostoma nasus*. *J. Fish Biol.* 53, 658–682. doi: 10.1111/j.1095-8649.1998.tb01009.x

Kim, S.-Y., Metcalfe, N. B., da Silva, A., and Velando, A. (2017). Thermal conditions during early life influence seasonal maternal strategies in the three-spined stickleback. *BMC Ecol.* 17:34. doi: 10.1186/s12898-017-0144-x

Kuramoto, M. (1975). Embryonic temperature adaptation in development rate of frogs. *Physiol. Zool.* 48, 360–366. doi: 10.1086/physzool.48.4.30155661

McLaren, I. A., and Cooley, J. M. (1972). Temperature adaptation of embryonic development rate among frogs. *Physiol. Zool.* 45, 223–228. doi: 10.1086/physzool.45.3.30152501

Menke, M. E., and Claussen, D. L. (1982). Thermal acclimation and hardening in tadpoles of the bullfrog, *Rana catesbeiana*. *J. Therm. Biol.* 7, 215–219. doi: 10.1016/0306-4565(82)90027-4

Mitchell, N. J. (2001). The energetics of endotrophic development in the frog *Geocrinia vitellina* (Anura: Myobatrachidae). *Physiol. Biochem. Zool.* 74, 832–842. doi: 10.1086/323989

Mitchell, N. J., and Seymour, R. S. (2000). Effects of temperature on the energy cost and timing of embryonic and larval development of the terrestrially breeding moss frog, *Bryobatrachus nimbus*. *Physiol. Biochem. Zool.* 73, 829–840. doi: 10.1086/318097

Mitchell, N. J., and Seymour, R. S. (2003). The effects of nest temperature, nest substrate and clutch size on the oxygenation of embryos and larvae of the Australian moss frog, *Bryobatrachus nimbus*. *Physiol. Biochem. Zool.* 76, 60–71. doi: 10.1086/345486

Mueller, C. A., Augustine, S., Kooijman, S. A. L. M., Kearney, M. R., and Seymour, R. S. (2012). The trade-off between maturation and growth during accelerated development in frogs. *Comp. Biochem. Physiol. A* 163, 95–102. doi: 10.1016/j.cbpa.2012.05.190

Mueller, C. A., Eme, J., Burggren, W. W., Rundle, S. D., and Roghair, R. D. (2015a). Challenges and opportunities in integrative developmental physiology. *Comp. Biochem. Physiol. A* 184, 113–124. doi: 10.1016/j.cbpa.2015.02.013

Mueller, C. A., Eme, J., Manzon, R. G., Somers, C. M., Boreham, D. R., and Wilson, J. Y. (2015b). Embryonic critical windows: changes in incubation temperature alter survival, hatchling phenotype and cost of development in Lake whitefish (*Coregonus clupeaformis*). *J. Comp. Physiol. B* 185, 315–331. doi: 10.1007/s00360-015-0886-8

Mueller, C. A., Joss, J. M. P., and Seymour, R. S. (2011). The energy cost of embryonic development in fishes and amphibians, with emphasis on new data from the Australian lungfish, *Neoceratodus forsteri*. *J. Comp. Physiol. B* 181, 43–52. doi: 10.1007/s00360-010-0501-y

Noble, D. W., Stenhouse, V., and Schwanz, L. E. (2018). Developmental temperatures and phenotypic plasticity in reptiles: a systematic review and meta-analysis. *Biol. Rev.* 93, 72–97. doi: 10.1111/brv.12333

O'Connor, C. M., Norris, D. R., Crossin, G. T., and Cooke, S. J. (2014). Biological carryover effects: linking common concepts and mechanisms in ecology and evolution. *Ecosphere* 5, 1–11.

Parichy, D., and Kaplan, R. (1995). Maternal investment and developmental plasticity: functional consequences for locomotor performance of hatchling frog larvae. *Funct. Ecol.* 9, 606–617.

Pigliucci, M., Murren, C. J., and Schlichting, C. D. (2006). Phenotypic plasticity and evolution by genetic assimilation. *J. Exp. Biol.* 209, 2362–2367. doi: 10.1242/jeb.02070

Pounds, J. A., Bustamante, M. R., Coloma, L. A., Consuegra, J. A., Fogden, M. P., Foster, P. N., et al. (2006). Widespread amphibian extinctions from epidemic disease driven by global warming. *Nature* 439, 161–167. doi: 10.1038/nature04246

Recuero, E., Martínez-Solano, Í, Parra-Olea, G., and García-París, M. (2006). Phylogeography of *Pseudacris regilla* (Anura: Hylidae) in western North America, with a proposal for a new taxonomic rearrangement. *Mol. Phylogenet. Evol.* 39, 293–304. doi: 10.1016/j.ympev.2005.10.011

Rombough, P. J. (1988). Growth, aerobic metabolism, and dissolved oxygen requirements of embryos and alevins of steelhead, *Salmo gairdneri*. *Can. J. Zool.* 66, 651–660. doi: 10.1139/z88-097

Rombough, P. J. (1994). Energy partitioning during fish development: additive or compensatory allocation of energy to support growth? *Funct. Ecol.* 8, 178–186.

Ruthsatz, K., Peck, M. A., Dausmann, K. H., Sabatino, N. M., and Glos, J. (2018). Patterns of temperature induced developmental plasticity in anuran larvae. *J. Therm. Biol.* 74, 123–132. doi: 10.1016/j.jtherbio.2018.03.005

Schaub, D. L., and Larsen, J. H. Jr. (1978). The reproductive ecology of the Pacific treefrog (*Hyla regilla*). *Herpetologica* 34, 409–416.

Seebacher, F., and Grigaltchik, V. S. (2014). Embryonic developmental temperatures modulate thermal acclimation of performance curves in tadpoles of the frog *Limnodynastes peronii*. *PLoS One* 9:e106492. doi: 10.1371/journal.pone.0106492

Seymour, R. S., Geiser, F., and Bradford, D. F. (1991). Metabolic cost of development in terrestrial frog eggs (*Pseudophryne bibronii*). *Physiol. Zool.* 64, 688–696. doi: 10.1086/physzool.64.3.30158201

Sherman, E., and Levitis, D. (2003). Heat hardening as a function of developmental stage in larval and juvenile *Bufo americanus* and *Xenopus laevis*. *J. Therm. Biol.* 28, 373–380. doi: 10.1016/s0306-4565(03)00014-7

Smith, G. D., Hopkins, G. R., Mohammadi, S., Skinner, H. M., Hansen, T., Brodie, E. D., et al. (2015). Effects of temperature on embryonic and early larval growth and development in the rough-skinned newt (*Taricha granulosa*). *J. Therm. Biol.* 51, 89–95. doi: 10.1016/j.jtherbio.2015.03.010

Stuart, S. N., Chanson, J. S., Cox, N. A., Young, B. E., Rodrigues, A. S. L., Fischman, D. L., et al. (2004). Status and trends of amphibian declines and extinctions worldwide. *Science* 306, 1783–1786. doi: 10.1126/science.1103538

van Vliet, M. T., Franssen, W. H., Yearsley, J. R., Ludwig, F., Haddeland, I., Lettenmaier, D. P., et al. (2013). Global river discharge and water temperature under climate change. *Global Environ. Change* 23, 450–464. doi: 10.1016/j.gloenvcha.2012.11.002

Warner, D. A., Du, W. G., and Georges, A. (2018). Introduction to the special issue-Developmental plasticity in reptiles: physiological mechanisms and ecological consequences. *J. Exp. Zool. A Ecol. Int. Physiol.* 329, 153–161. doi: 10.1002/jez.2199

Watkins, T. B. (2000). The effects of acute and developmental temperature on burst swimming speed and myofibrillar ATPase activity in tadpoles of the Pacific tree frog, Hyla regilla. *Physiol. Biochem. Zool.* 73, 356–364. doi: 10.1086/316744

Watkins, T. B., and Vraspir, J. (2005). Both incubation temperature and posthatching temperature affect swimming performance and morphology of wood frog tadpoles (*Rana sylvatica*). *Physiol. Biochem. Zool.* 79, 140–149. doi: 10.1086/498182

West-Eberhard, M. J. (1989). Phenotypic plasticity and the origins of diversity. *Annu. Rev. Ecol. Syst.* 20, 249–278. doi: 10.1146/annurev.ecolsys.20.1.249

Wilson, R., and Franklin, C. (1999). Thermal acclimation of locomotor performance in tadpoles of the frog *Limnodynastes peronii*. *J. Comp. Physiol. B* 169, 445–451. doi: 10.1007/s003600050241

Wilson, R., James, R., and Johnston, I. (2000). Thermal acclimation of locomotor performance in tadpoles and adults of the aquatic frog *Xenopus laevis*. *J. Comp. Physiol. B* 170, 117–124. doi: 10.1007/s003600050266

Yagi, K. T., and Green, D. M. (2018). Post-metamorphic carry-over effects in a complex life history: behavior and growth at two life stages in an amphibian, *Anaxyrus fowleri*. *Copeia* 106, 77–85. doi: 10.1643/ce-17-593

Conflict of Interest Statement: The authors declare that the research was conducted in the absence of any commercial or financial relationships that could be construed as a potential conflict of interest.

Copyright © 2019 Mueller, Bucsky, Korito and Manzanares. This is an open-access article distributed under the terms of the Creative Commons Attribution License (CC BY). The use, distribution or reproduction in other forums is permitted, provided the original author(s) and the copyright owner(s) are credited and that the original publication in this journal is cited, in accordance with accepted academic practice. No use, distribution or reproduction is permitted which does not comply with these terms.

frontiers in Physiology

ORIGINAL RESEARCH
published: 03 July 2019
doi: 10.3389/fphys.2019.00816

A Transcriptomic Model of Postnatal Cardiac Effects of Prenatal Maternal Cortisol Excess in Sheep

*Andrew Antolic[1], Elaine M. Richards[1,2], Charles E. Wood[2] and Maureen Keller-Wood[1]**

[1] Department of Pharmacodynamics, University of Florida, Gainesville, FL, United States, [2] Department of Physiology and Functional Genomics, University of Florida, Gainesville, FL, United States

In utero treatment with glucocorticoids have been suggested to reprogram postnatal cardiovascular function and stress responsiveness. However, little is known about the effects of prenatal exposure to the natural corticosteroid, cortisol, on postnatal cardiovascular system or metabolism. We have demonstrated an increased incidence of stillbirth in sheep pregnancies in which there is mild maternal hypercortisolemia caused by infusion of 1 mg/kg/d cortisol. In order to model corticosteroid effects in the neonate, we created a second model in which cortisol was infused for 12 h per day for a daily infusion of 0.5 mg/kg/d. In this model we had previously found that neonatal plasma glucose was increased and plasma insulin was decreased compared to those in the control group, and that neonatal ponderal index and kidney weight were reduced and left ventricular wall thickness was increased in the 2 week old lamb. In this study, we have used transcriptomic modeling to better understand the programming effect of this maternal hypercortisolemia in these hearts. This is a time when both terminal differentiation and a shift in the metabolism of the heart from carbohydrates to lipid oxidation are thought to be complete. The transcriptomic model indicates suppression of genes in pathways for fatty acid and ketone production and upregulation of genes in pathways for angiogenesis in the epicardial adipose fat (EAT). The transcriptomic model indicates that RNA related pathways are overrepresented by downregulated genes, but ubiquitin-mediated proteolysis and protein targeting to the mitochondria are overrepresented by upregulated genes in the intraventricular septum (IVS) and left ventricle (LV). In IVS the AMPK pathway and adipocytokine signaling pathways were also modeled based on overrepresentation by downregulated genes. Peroxisomal activity is modeled as increased in EAT, but decreased in LV and IVS. Our results suggest that pathways for lipids as well as cell proliferation and cardiac remodeling have altered activity postnatally after the *in utero* cortisol exposure. Together, this model is consistent with the observed increase in cardiac wall thickness at necropsy and altered glucose metabolism observed *in vivo*, and predicts that *in utero* exposure to excess maternal cortisol will cause postnatal cardiac hypertrophy and altered responses to oxidative stress.

Keywords: cortisol, pregnancy, maternal stress, cardiac metabolism, adipose, lipid

OPEN ACCESS

Edited by:
Sonnet Jonker,
Oregon Health & Science University, United States

Reviewed by:
George David Giraud,
Oregon Health & Science University, United States
Adam John Watkins,
University of Nottingham, United Kingdom

***Correspondence:**
Maureen Keller-Wood
kellerwd@cop.ufl.edu

Specialty section:
This article was submitted to Embryonic and Developmental Physiology, a section of the journal Frontiers in Physiology

Received: *04 March 2019*
Accepted: *11 June 2019*
Published: *03 July 2019*

Citation:
Antolic A, Richards EM, Wood CE and Keller-Wood M (2019) A Transcriptomic Model of Postnatal Cardiac Effects of Prenatal Maternal Cortisol Excess in Sheep. Front. Physiol. 10:816. doi: 10.3389/fphys.2019.00816

INTRODUCTION

Cortisol plays an important role in the maturation of many fetal organs, and in primates and many other mammalian species, including the sheep, is essential for the normal maturation of organs such as the lung which are essential for the transition to ex utero life (Liggins, 1994). The heart is one of the organs in which cortisol appears to play a vital role in maturation (Rog-Zielinska et al., 2013). However, excess glucocorticoids or repeated exogenous glucocorticoid treatments, have been found to reduce birth weight (Newnham and Moss, 2001; Davis et al., 2009), increase postnatal blood pressure (Dodic et al., 1998, 2001, 2002a,b), and alter postnatal glucose metabolism (Moss et al., 2001; Sloboda et al., 2002; Antolic et al., 2015).

Late gestation is a critical period for maturation of cardiomyocytes. During this period cardiomyocytes transition from primarily mononucleated and proliferative cells to binucleated, terminally differentiated cardiomyocytes (Jonker et al., 2007b). Circulating factors that stimulate proliferation include angiotensin II, cortisol, and insulin-like growth factor-1, while atrial natriuretic peptide (ANP) and tri-iodo-L-thyronine (T3) suppress proliferation (Sundgren et al., 2003a,b; Giraud et al., 2006; Chattergoon et al., 2007; OTierney et al., 2010b). Hemodynamic forces also influence cardiomyocyte proliferation; proliferation is stimulated by increased arterial pressure and suppressed with reduced systolic load (Jonker et al., 2007a; OTierney et al., 2010a). After birth there are substantial changes that occur in cardiac metabolism as the nutrient supply dramatically changes. Throughout gestation and immediately after birth the heart relies almost entirely on glycolysis and lactate oxidation, with minimal contribution from β-oxidation of fatty acids due to their limited supply (Werner and Sicard, 1987; Lopaschuk et al., 1991; Bartelds et al., 1998, 2000). However, in the newborn period, there is a gradual shift in the reliance on glucose and lactate for carbon sources to β-oxidation of fatty acids supplied in the mother's milk (Werner and Sicard, 1987; Ascuitto et al., 1989; Lopaschuk and Spafford, 1990; Lopaschuk et al., 1991). Thus, changes in myocyte maturation, but also afterload and metabolism all occur in the immediate neonatal period. In our previous studies in pregnant ewes, we have shown that increased levels of maternal cortisol in late gestation, similar to levels expected in a chronically stressed animal, alter the trajectory of cardiac gene expression and indicated that metabolic pathways were overrepresented in the differentially expressed genes in fetuses near term (Richards et al., 2014). In our sheep model, a chronic doubling of maternal cortisol over the last month of fetal life was associated with a dramatic increase in stillbirth in the immediate perinatal period (Keller-Wood et al., 2014), and with significantly lower heart rate in the last hour before birth (Antolic et al., 2017). The newborns of cortisol-treated ewes also have changes in the cardiac transcriptome and in the cardiac and serum metabolomes (Antolic et al., 2019; Walejko et al., 2019); these data have suggested that metabolism of lipids and the TCA cycle are altered in the fetuses of ewes with higher than normal cortisol concentrations. Transcriptomic modeling of pathways in the heart altered after maternal cortisol treatment also indicated increased expression of genes associated with the TGFβ pathway, consistent with the observed increase in collagen deposition and wall thickness of the left ventricular free wall in the newborns after maternal cortisol treatment (Antolic et al., 2019).

To determine postnatal effects of increased *in utero* cortisol exposure, we used a model in which ewes were treated with cortisol for 12 h per day, starting in the evening and continuing into the next morning. This model is less severe than the model in which ewes are continuously infused with cortisol, but the design mimics the pattern of cortisol in Cushing's syndrome in which evening cortisol levels fail to fall (Laudat et al., 1988; Raff et al., 1998; Scharnholz et al., 2010). Although sheep do not have a circadian rhythm in cortisol (Bell et al., 1991), in most animal housing situations we expect a morning rise in cortisol during feeding and husbandry, with lower levels in the evening and overnight hours. We found that in newborns of this experimental paradigm, there was an increase in the relative thickness of the LV wall at 2 weeks of age relative to that of 2 week old lambs of control ewes. There is an increase in the glucose to insulin ratio in the offspring of the cortisol-treated ewes, which may also modify cardiac metabolism. We used a transcriptomic approach to model the effects of the *in utero* exposure to assess which pathways in the postnatal heart are altered by the prior exposure. Specifically, we were interested in whether pathways related to carbohydrate or fatty acid oxidation, or to structural changes in the heart were significantly over-represented. Because our previous studies with more chronic exposure to high maternal cortisol (continuous infusion at 1 mg/kg/d to the ewe) produced effects on cardiac transcriptomics and metabolomics suggesting altered energy utilization, we included samples from the epicardial fat depot to assess the changes in gene expression in that tissue, and model the pathways altered in the epicardial adipose with those in the nearby cardiac tissue. These studies were designed to inform future studies in offspring from this model of maternal stress, by using gene expression patterns to provide an untargeted and unbiased insight into changes in the offspring heart.

MATERIALS AND METHODS

Experimental Design

All animal use was approved by the Institutional Animal Care and Use Committee at the University of Florida. Black-faced ewes with singleton (13) or twin pregnancies (2) were studied in late gestation. During study, ewes were housed indoors in a facility with temperature and humidity-controlled rooms, and with controlled light cycle (lights on 0700 to 1900 h), and animals were housed in pens that allowed them free movement throughout the pregnancy and postpartum period. Ewes were of similar body condition and were fed a diet of pelleted feed at a weight within NRC standards for the ewe's body weight, fetal number and gestational age, with supplementation with alfalfa hay from 140 day onward. Ewes were prepared with chronic indwelling femoral arterial and venous catheters at approximately day 115 of pregnancy under isoflurane anesthesia as previously described (Antolic et al., 2015). Ewes were randomly assigned at

surgery to one of two groups: control with no infusion (Control; $n = 7$ ewes), or cortisol- infused (CORT, $n = 10$ ewes; Cortisol (Solu-Cortef, Pfizer, Inc.). Cortisol was infused intravenously using a syringe pump into the maternal femoral arterial catheter at a total dose of 0.5 mg/kg/d; the pumps were controlled with a timer (Chronotrol, ChronTrol Corporation, San Diego, CA, United States) to restrict the infusions to 2100 to 0900 h. All infusions were delivered to the ewes in their pens using a tether system for the infusion; this allows the ewes to freely move about their pens throughout the period of the study. The cortisol infusion was discontinued after delivery of the lamb(s). Lambs were housed with their ewes in the same pen; on day 3 after birth the pen was opened to an adjacent pen to allow the ewe and her lamb additional space.

The *in vivo* data and morphometrics at 2 weeks of age in the control and cortisol-treated ewes and their lambs has been previously reported (Antolic et al., 2015). The average morning cortisol concentration during the infusion was 22.0 ± 4.0 ng/ml in CORT ewes and 9.5 ± 2.6 ng/ml in the Control ewes. Two lambs in the CORT group were stillborn. One set of twins were born in each group of ewes. Seven control ewes delivered four male and four female lambs at 144–149 days gestation; eight CORT ewes delivered four male and five female lambs at 142–146 days. Ewes were sampled before birth, and lambs were sampled after birth using a jugular line which was placed on the day of birth, as previously described. As previously reported, there was no effect of this maternal cortisol infusion on the lambs' body temperature, or body weight at birth or on the following days. Although ponderal index was reduced overall in the lambs in the CORT group, this effect was only significant in the male lambs. Although morning maternal cortisol concentrations were increased in the ewes prior to birth, plasma cortisol concentrations were not different postpartum in the ewes or between the two groups of lambs. There was an overall effect of CORT to increase plasma glucose and decrease plasma insulin concentrations in the postnatal lambs, and therefore average glucose to insulin ratio was increased in the CORT lambs, as previously reported (Antolic et al., 2015).

On postnatal day 14–15, the lambs were killed via intravenously administered Euthasol solution (Euthasol; Fort Worth, TX, United States). Organ weights were measured at necropsy. As previously reported (Antolic et al., 2015) cardiac weight was not significantly altered by CORT, but the ratio of left ventricular free wall thickness relative to tibial length was increased (control: 0.445 ± 0.017 mm/cm vs. CORT: 0.496 ± 0.019 mm/cm). There were no significant differences in relative septal wall thickness (control: 0.512 ± 0.030 mm/cm vs. CORT: 0.530 ± 0.021 mm/cm) or relative right ventricular wall thickness (control: 0.235 ± 0.018 mm/cm vs. CORT: 0.253 ± 0.010 mm/cm).

Tissue Collection for Transcriptomic Analysis

At necropsy, the hearts were quickly removed and dissected using sterile instruments and gloves ($n = 8$ per group). Tissue samples taken from the interventricular septum (IVS), left ventricular free wall (LV) and the epicardial adipose depot (EAT) were snap frozen and stored at −80°C until analysis.

Messenger RNA from homogenized samples of lamb left ventricular free wall, septa, and epicardial adipose were extracted using Trizol and then purified with on-column DNase digestion (Qiagen RNeasy Plus kits; Qiagen Sciences, Germantown, MD, United States). RNA integrity numbers (RIN) for the RNA samples were between 7.3 and 8.3 for LV, 7.7–8.6 for IVS ($n = 8$ control and 8 CORT for each section of the heart) and 7.1–7.7 for EAT samples ($n = 7$ control, $n = 9$ CORT). RNA (500 ng) was labeled with Cy5 using the Agilent QuickAmp Labeling kit; hybridization was performed using previously described methods (Richards et al., 2014). We used the Agilent-019921 Sheep Gene Expression Microarray 8 × 15 k, G4813A (GPL14112) platform. Our group has described the annotation for this array platform in previous publications (Richards et al., 2014; Chang et al., 2018). The raw normalized array data for this experiment have been deposited in the National Center for Biotechnology Information's Gene Expression Omnibus (GEO) and are accessible through GEO Series accession number GSE131537 for the cardiac samples, and GEO Series accession number GSE119254 for the epicardial fat samples.

Microarray Data Analysis

Raw microarray data was processed using the Limma package in R software (R Development Core Team, 2008), to perform background correction and data normalization using the quantile method. Probes with low expression and microarray control probes were excluded as well as those probes that were less than 10% brightness of the negative controls. The remaining probes were then retained for further statistical analysis.

Statistical Analysis

In order to identify differentially expressed genes in the LV and IVS the Limma package was utilized to analyze the processed microarray data using a moderated *t*-test that employs an empirical Bayes method ($P < 0.05$). The effect of cortisol was analyzed by comparing the gene expression in tissues collected from CORT lambs compared to Control lambs.

Network and Enrichment Analysis

Webgestalt was used to identify overrepresented biological processes, molecular functions, and cellular components associated with the differentially regulated genes. $P = 0.05$ was used as the criterion for statistical significance after Benjamini-Hochberg multiple test correction of the *p*-value, with a minimum of two genes per category (Zhang et al., 2005; Wang et al., 2013). This approach included all genes that were significant at $p < 0.05$ without correction for multiple comparisons, and corrects for the false discovery in the pathway analyses by using the Benjamini-Hochberg correction for false discovery due to multiple testing. GeneMANIA, BiNGO, and ClueGO plugins of Cytoscape, were used to perform network inference of the differentially regulated genes, gene ontology analysis, and generate enriched gene-gene interaction networks from GO and KEGG databases (Shannon et al., 2003; Bindea et al., 2009;

Montojo et al., 2010; Mlecnik et al., 2018). The results of these analyses were considered significantly different between the CORT and Control tissues using $p < 0.05$ corrected for false discovery rate.

RESULTS

Genes Altered by Maternal Cortisol Infusion in the Left Ventricular Free Wall of the Postnatal Lamb

We found 115 genes were upregulated and 145 genes were downregulated in the LV of the 14-day-old lambs of cortisol-treated ewes as compared to lambs of control ewes (**Supplementary Table 1**). Webgestalt analysis found that the only major molecular function upregulated in the left ventricle by overnight maternal cortisol was peptidyl-prolyl *cis-trans* isomerase activity (4 genes; adj. $P = 7.30E-03$). Overrepresented cellular components represented by upregulated genes in the lamb LV after maternal cortisol infusion included cytoplasm (26 genes), mitochondria (22 genes), peroxisome (4 genes), and nucleus (51 genes). More specific components include mitochondrial outer membrane translocase complex (2 genes; adj. $P = 6.60E-03$), intrinsic to mitochondrial outer membrane (2 genes; adj. $P = 1.56E-02$), integral to peroxisomal membrane (2 genes; adj. $P = 1.47E-02$), and nuclear lumen (27 genes; adj. $P = 1.68E-02$). Gene Ontology analysis identified negative regulation of transforming growth factor beta receptor signaling pathway (4 genes; adj. $P = 4.78E-02$, including NR3C1 encoding GR), protein targeting mitochondrion (4 genes; adj. $P = 4.78E-02$, including TOMM40, TIMM8A, TOMM5, and MFN2), and response to arsenic-containing substance (3 genes; adj. $P = 4.78E-02$), ribonucleotide and ribonucleoside biosynthetic process (5 genes; adj. $P = 4.78E-02$), cellular protein modification process (31 genes; adj. $P = 4.78E-02$), fatty acid oxidation (2 genes; adj. $P = 4.78E-02$) as pathways overrepresented by upregulated genes in the LV in CORT lambs compared to Control lambs. KEGG pathway analysis (**Table 1**) identified pathways associated with the upregulated genes in the postnatal lamb LV of the CORT lambs compared to Control lambs. The identified pathways were ubiquitin mediated proteolysis, metabolic pathways, peroxisome, drug metabolism-other enzymes, insulin signaling pathway, RIG-I-Like receptor signaling pathway, and phosphatidylinositol signaling system.

Overrepresented cellular components reflected by downregulated genes in the LV of CORT lambs compared to Control lambs were macromolecular complex (46 genes), cytosol (29 genes), nucleoplasm (23 genes) and nucleolus (24 genes). The only overrepresented biological processes related to the downregulated genes in the CORT lambs compared to Control lambs were macromolecular catabolic processes (70 genes; $P = 4.53E-02$) and RNA processing (15 genes, $p = 4.53E-02$). There were no molecular functions associated with downregulated pathways in the LV of CORT lambs. Pathways identified for the downregulated genes in CORT lambs compared to Control lambs were neuro ligand-receptor interaction, RNA transport, ribosome biogenesis in eukaryotes, circadian rhythm-mammal, phagosome, RNA degradation, gap junction, base excision repair, pathogenic E. coli infection, amyotrophic lateral sclerosis, hedgehog signaling pathway, calcium signaling pathway, metabolic pathways, salivary secretion, and ribosome (**Table 1**).

TABLE 1 | KEGG pathways significantly overrepresented in up and down-regulated genes in LV of 2-week-old lambs from cortisol-treated ewes (0.5 mg/kg/day) compared to lambs of control ewes ($n = 8$ lambs per group; 4 males and 4 females).

Up-regulated pathway names	**#Genes**	***P*-value**	**Genes**
Ubiquitin mediated proteolysis	6	2.90E-05	RCHY1, KLHL9, TCEB2, ANAPC13, BIRC6, UBA2.
Peroxisome	3	0.011	PEX13, SLC27A, AGPS
Metabolic pathways	8	0.0356	HPRT1, ACACB, AGPS, UCKL1, MMAB, PHOSPHO2, ALG1, NME2
Drug metabolism	2	0.0356	HPRT1, UCKL1
Insulin signaling pathway	3	0.0356	CALM2, ACACB, SREBF1
RIG-I-like receptor signaling pathway	2	0.0356	DDX3X, PIN1
Phosphatidylinositol signaling pathway	2	0.0356	CALM2, PIP4K2A
Down-regulated pathway names			
Neuroactive ligand-receptor interaction	5	0.007	THRB, PTGER3, TSPO, GHR, ADRB1
RNA transport	4	0.007	EIF4G1, EELAC1, EIF3A, POP7
Ribosome biogenesis in eukaryotes	3	0.007	DKC1, IMP4, POP7
Circadian rhythm – mammal	2	0.007	CLOCK, CSNK1E
Phagosome	4	0.007	TUBB2B, CYBA, TUR6, TUBB3
RNA degradation	3	0.007	EXOSC2, CNOT10, DCP2
Gap junction	3	0.0081	TUBB2B, ADRB1, TUBB3
Base excision repair	2	0.0119	MPG, NTHL1
Pathogenic *Escherichia coli* infection	2	0.0238	TUBB2B, TUBB3
Amyotrophic lateral sclerosis (ALS)	2	0.0238	DERL1, BAX
Hedgehog signaling pathway	2	0.0238	CSNK1G2, CSNK1E
Calcium signaling pathway	3	0.0302	PTGER3, PLCD1, ADRB1
Metabolic pathways	8	0.0412	GART, PIGT,PLCD1, ST6GAL1, PPAP2C, DHCR7, CYP27A1, CRYL1
Salivary secretion	2	0.0441	ATP1B3, ADRB1
Ribosome	2	0.0441	RPS8, RPS2

The 260 differentially regulated genes in the LV were entered into ClueGO, which recognized 255 genes as having functional annotations. The 255 genes were significantly associated with 40 gene ontology terms or KEGG pathways and further organized into 18 groups based on the similarity of their associated genes, which were used to create an enriched network based on gene-gene interactions. The most significant term from each group was used as the representative term (**Figure 1**). The group with the most terms associated to it was the negative regulation of transcription from RNA polymerase II promoter involved in smooth muscle cell differentiation (2 genes, adj. $P = 3.88E-04$).

Genes Altered by Maternal Cortisol Treatment in the Interventricular Septum of the Postnatal Lamb

We found 103 genes were upregulated and 153 were downregulated in the IVS of 14-day-old lambs of cortisol infused ewes compared with 14-day-old lambs of untreated ewes (**Supplementary Table 2**). Major cellular components associated with the genes upregulated in the CORT lambs compared to Control lambs were cytosol, mitochondria and ribosome. The only major molecular function modeled as upregulated by the maternal cortisol treatment was structural constituent of ribosome (6 genes; adj. $P = 1.07E-02$; this included expression of genes encoding 4 mitochondrial ribosomal proteins, L2, L33, S11, and S33). Gene Ontology analysis identified cellular protein transport (16 genes $p = 1.62E-20$) as a significantly altered biological process associated with upregulated genes in the CORT lambs compared to Control lambs, and more specifically identified protein targeting to the mitochondria (4 genes, $P = 2.56E-20$; including TIMM8A, TIMM8B, TOMM5, and MTX1) as well as chaperone-mediated protein transport (2 genes; adj. $P = 4.35E-02$), and regulation of protein ubiquitination (7 genes; adj. $P = 1.62E-02$) as upregulated in CORT lambs. KEGG pathway analysis (**Table 2**) indicated that this maternal cortisol infusion upregulated pathways in the postnatal lamb IVS involving protein processing in the endoplasmic reticulum, ubiquitin-mediated proteolysis, p53 signaling pathway, the ribosome, and mRNA surveillance pathway.

Cellular components associated with the genes down-regulated in the lambs in the CORT group compared to control

TABLE 2 | KEGG pathways significantly overrepresented in up and down-regulated genes in IVS of 2-week-old lambs from cortisol-treated (0.5 mg/kg/day) ewes compared to lambs of control ewes ($n = 8$ lambs per group; 4 males and 4 females).

Up-regulated pathway names	#Genes	*P*-value	Genes
Protein processing in endoplasmic reticulum	4	0.006	SEC13, ERP29, SEC24C, HERPUD1
Ubiquitin mediated proteolysis	3	0.0195	RCHY1, TCEB1, ANAPC11
p53 signaling pathway	2	0.0367	RCHY1, TSC2
Ribosome	2	0.039	UBA52, RPL13A
mRNA surveillance pathway	2	0.039	SYMPK, PABPC1
Down-regulated pathway names			
Spliceosome	7	9.18E-06	RBM17, PRPF3, SNRNP40, RBNP40, RBM25, PLRG1, SRSF1, PRPF40A,
Adipocytokine signaling pathway	3	0.0173	PRKAG2, CAMKK2, PRKAB2
RNA degradation	3	0.0173	EXOSC2, CNOT10, EXOSC10
Hypertrophic cardiomyopathy (HCM)	3	0.0202	PRKAG2, PRKAB2, TPM3,
RNA polymerase	2	0.0223	POLR3GL, POLR1B
Pathways in cancer	5	0.0223	LAMA4, RUNX1, RARA, TPM3, MITF
Base excision repair	2	0.0223	HMGB1, MBD4
Lysosome	3	0.0293	LGMN, CD63, MANBA
Osteoclast differentiation	3	0.0300	CYLD, MAP3K7, MITF
RNA transport	3	0.0404	TGS1, NMD3, EEF1A1
Acute myeloid leukemia	2	0.0404	RUNX1, RARA
Purine metabolism	3	0.0423	POLR3GL, POLR1B, PDE4B

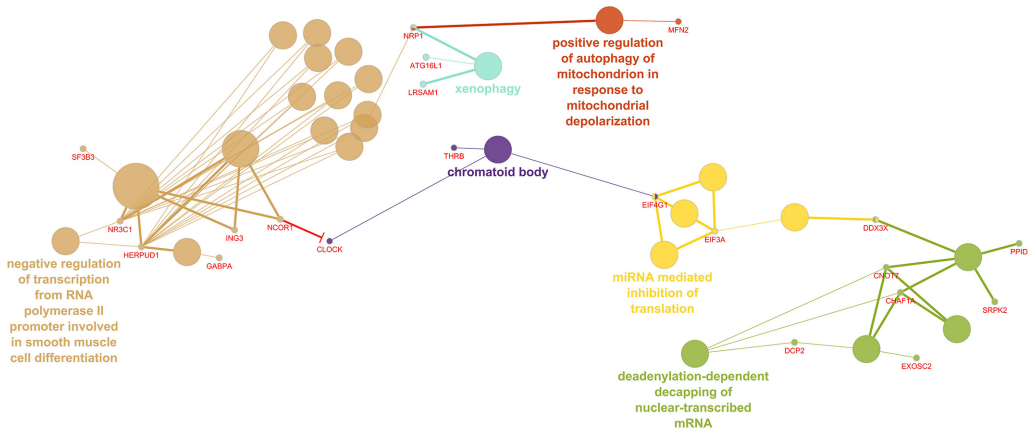

FIGURE 1 | Enriched ClueGO gene network from the left ventricular free wall. Similar gene ontology or KEGG pathway terms are clustered by color and the representative term for those clusters are presented. Gene names shown in red; Red lines with bars represent interactions involved in gene repression.

lambs were macromolecular processes, and intracellular parts. These included AMP-activated protein kinase complex (2 genes; adj. P = 8.30E-03), Ada2/Gcn5/Ada3 transcription activator complex (2 genes; adj. P = 3.09E-02), sarcoplasmic reticulum (3 genes, p = 4.17E-02), exosome (2 genes, P = 4.72E-02), autophagic vacuole membrane (2 genes, adj. P = 4.10E-02) spliceosome complex (6 genes; adj. P = 8.00E-03), and contractile fibers (5 genes, p = 4.72E-02). Also associated with downregulated genes in CORT lambs compared to Control lambs were the nucleus and chromosome, including the nucleolus (32 genes; adj. P = 9.39E-06), nuclear speck (7 genes; adj. P = 1.40E-03), and chromatin (7 genes, p = 4.72E-2). The major molecular functions associated with downregulated genes in the CORT lambs compared to Control lambs were protein kinase binding (11 genes; adj. P = 1.64E-02) and AMP-activated protein kinase activity (2 genes; adj. P = 4.59E-02). Cellular metabolic processes (95 genes) and macromolecular catabolic processes (84 genes) were the major biological processes associated with downregulated genes. More specifically, macromolecule catabolic process (19 genes; adj. P = 4.47E-02), mRNA splicing via spliceosome (8 genes; adj. P = 4.47E-02) and dosage compensation by inactivation of X chromosome (2 genes; adj. P = 4.47E-02) were identified as overrepresented biological processes that were downregulated by the maternal cortisol treatment. KEGG pathways implicated by the downregulated genes (**Table 2**) were the spliceosome, adipocytokine signaling, RNA degradation, hypertrophic cardiomyopathy, RNA polymerase, pathways in cancer, base excision repair, lysosome, osteoclast differentiation, RNA transport, acute myeloid leukemia, and purine metabolism.

ClueGO recognized 255 differentially expressed genes in the IVS, of which 252 had functional annotations. The 252 genes were significantly associated with 10 gene ontology terms or KEGG pathways and further organized into six groups, which were used to create an enriched network based on gene-gene interactions (**Figure 2**). The group with the most terms associated to it was the spliceosomal complex.

Genes Altered by Maternal Cortisol Infusion in the Epicardial Fat of the Postnatal Lamb

Modeling of the 93 upregulated genes by prior maternal cortisol in the epicardial adipose of the CORT lambs compared to Control lambs (**Supplementary Table 3**) did not identify any significant biological processes or molecular function. There were also no KEGG pathways identified as significantly represented by upregulated genes. This is likely because of the relatively small number of upregulated genes. Analysis using the Bingo plugin of Cytoscape, resulted in identification of blood vessel development, angiogenesis and negative regulation of endothelial cell differentiation as the upregulated processes in epicardial fat of CORT lambs compared to Control lambs. These pathways included increased expression of NOTCH3, NOTCH4, KDR, FLT1, MEOX1, and MMP14. However, each of these genes was only modestly upregulated, approximately 20–30%; only GBP2 (guanylate binding protein 2) was upregulated more than 2-fold. Together these indicate possible upregulation of blood vessel formation in the EAT of lambs of cortisol-treated ewes compared to the controls.

There were 176 genes with decreased expression in the EAT of the 2-week-old CORT lambs after prior maternal cortisol infusion (**Supplementary Table 3**). The mitochondrion was the cellular compartment most significantly associated with the downregulated genes in the CORT lambs compared to Control lambs (41 genes, 1.9E-05). Catalytic activity and oxido-reductase activity were identified as the molecular functions overrepresented in the downregulated genes in the CORT lambs compared to Control lambs: these pathways included cytochrome c oxidase activity (3 genes encoding subunits of this protein, p = 4.66E-02), superoxide dismutase activity (2

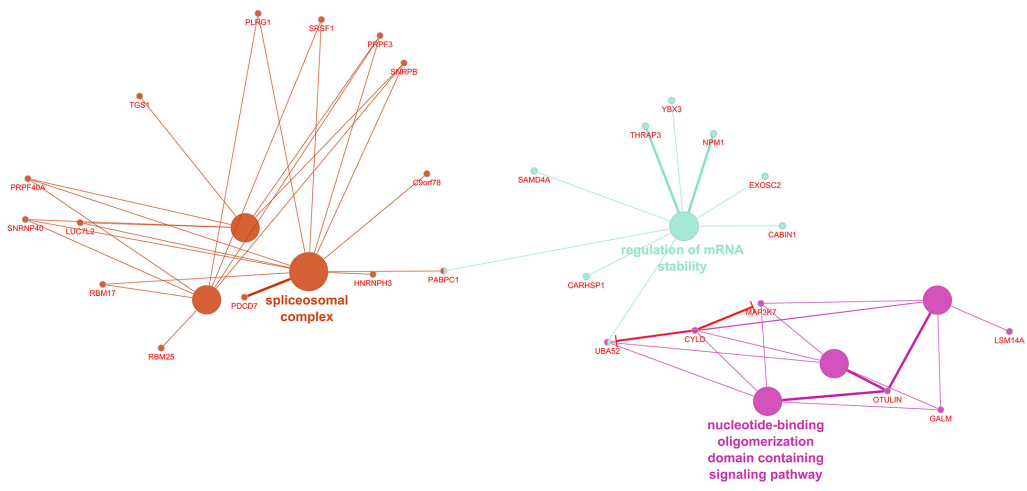

FIGURE 2 | Enriched ClueGO gene network from the interventricular septum. Similar gene ontology or KEGG pathway terms are clustered by color and the representative term for those clusters are presented. Gene names shown in red; Red lines with bars represent interactions involved in gene repression.

genes encoding SOD, p = 3.26E-02), oxidoreductase activity, acting on the CH-CH group of donors, NAD or NADP as acceptor (3 genes, p = 4.66E-02), enoyl-CoA hydratase activity (2 genes, p = 4.66E-02), and hydroxymethylglutaryl-CoA synthase (2 genes, p = 2.37E-02). The biological processes identified for the downregulated genes in CORT lambs were associated with small molecule metabolic processes (47 genes), including lipid metabolic processes (27 genes) and with oxido-reduction (18 genes); more specifically the processes were regulation of fatty acid metabolic processes (6 genes, p = 3.68E-02), cholesterol metabolic processes (5 genes, p = 4.83E-02), respiratory electron transport chain (7 genes, p = 1.62E-02) and coenzyme A metabolic processes (4 genes, p = 1.62E-2).

KEGG pathways associated with the differentially down-regulated genes in the CORT lambs compared to the Control lambs are pathways related to metabolism e.g., butanoate, propanoate, fructose and mannose, fatty acid elongation, peroxisome, TCA cycle, ketone bodies, and mitochondria (e.g., Parkinson's disease, Huntington's disease), with some overlap between these pathways (**Table 3**). Bingo analysis suggested that the downregulated genes also contained an overrepresentation of genes involved in iron ion homeostasis.

TABLE 3 | KEGG pathways significantly overrepresented in downregulated genes in EAT of 2-week-old lambs from cortisol-treated (0.5 mg/kg/day) (n = 9 lambs, 4 male and 5 female) compared to lambs of control ewes (n = 7, 3 male and 4 female).

Down-regulated pathway names	#Genes	*P*-value	Genes
Metabolic pathways	32	5.6E-05	HSD17B1, COX5B, COX6C, COX6B1, GK, HK1, ACACB, UCK1, CMBL, NDUFAB1, PIGP, EPHX2, ADA, HMGCS1, HMGCS2, TMZSF2, DLD, HADHB, POLR1B, GMDS, DTYMK, FBP2, PANK1, ECHS1, DLST, CRLS1, ALDH5A1, ALDH1A1, PON3, ACLY, MLYCD, PAFAH1B2
Peroxisome	6	0.004	MLYCD, PECR, SOD1, SOD2 PECR, PEX12, EPHX2
Butanoate metabolism	4	0.004	HMGCS1, HMGCS2, ECHS1, ALDH5A1
Huntington's disease	8	0.004	TFAM, SOD1, SOD2, VDAC1, COX5B, COX6C, COX6B1, NDUFAB1
Parkinson's disease	6	0.006	COX5B, COX6C, COX6B1, VDAC1, NDUFAB1, UBE2G2
Valine, leucine and isoleucine degradation	5	0.006	HMGCS1, HMHCS2, HADHB, DLD, ECHS1
Citrate cycle (TCA cycle)	3	0.030	DLST, DLD, ACLY
Propanoate metabolism	3	0.036	MLYCD, ACACB, ECHS1
Synthesis and degradation of ketone bodies	2	0.036	HMGCS1, HMHCS2
Fatty acid elongation in mitochondria	2	0.036	ECHS1, HADHB
Terpenoid backbone biosynthesis	2	0.046	HMGCS1, HMHCS2
Fructose and mannose metabolism	3	0.046	HK1, GMDS, FBP2

The 269 differentially regulated EAT genes were entered into ClueGO; 259 had functional annotations. The 259 genes were associated with 27 gene ontology terms or KEGG pathways and further organized into 4 groups that were used to create an enriched network based on gene-gene interactions. The most significant term from each group was used as the representative term (**Figure 3**). The group with the most terms associated to it was the acetyl-CoA metabolic process (7 genes, p = 6.38E-04).

Analysis of overlap of networks represented by differentially expressed genes in CORT lambs across the tissues showed relatively few genes were commonly regulated between EAT compared to either LV (14 genes) or IVS (17 genes), with only very general GO terms such as biological process or cell process associated with these commonly regulated genes. However, when we looked at the networks represented by genes differentially regulated in CORT lambs compared to Control lambs but regulated in the opposite direction in the different tissues, we found an association of some nodes between downregulated genes related to metabolic processes such as carboxylic acid, steroid or fatty acid metabolism and electron transport chain pathways in the EAT and upregulated genes related to cellular protein metabolic processes or protein transport pathways in the LV or related to protein targeting to mitochondria in IVS in CORT lambs (**Figures 4B,D**). In contrast the few upregulated networks in EAT did not associate with differentially downregulated genes in the LV or IVS in CORT lambs (**Figures 4A,C**).

DISCUSSION

As noted in our previous publication regarding these lambs, the majority of lambs of ewes treated with cortisol only at night survived the birth process, but at 2 weeks of life we noted a relative thickening of the left ventricular free wall. An increase in cardiac mass or wall thickness has also been previously observed in our studies with continuous maternal infusion of cortisol, which produces double the daily dose of that used in this study (Antolic et al., 2017), as well as in other models with dexamethasone treatment in sheep (Dodic et al., 2001). In the sheep heart, the cardiomyocytes are terminally differentiated by the time of birth (Jonker et al., 2007b). We do not know if the LV wall thickening occurred *in utero* during the cortisol exposure or only after birth; we also do not have data to determine if this occurs in response to higher arterial pressures postnatally in these lambs. With the higher dose of cortisol to the ewe, there was an increase in collagen deposition in the heart, and also an upregulation of the SMAD and TGFβ pathway (Antolic et al., 2019); the administration of 1 mg/kg/d to the ewe did not increase mean arterial pressure in the fetuses. However, in this current study in lambs, our transcriptomics do not model proliferation, nor do they indicate an increase in SMAD/TGFβ. We predict that the growth in these hearts is hypertrophic growth, and that any proliferation is that of fibroblasts or of endothelial cells.

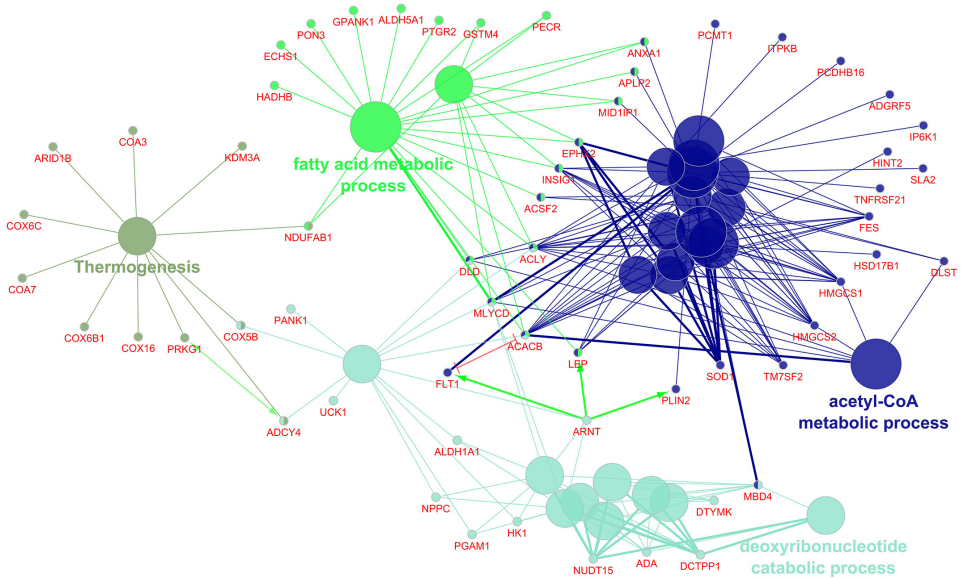

FIGURE 3 | Enriched ClueGO gene network from the epicardial adipose tissue. Similar gene ontology or KEGG pathway terms are clustered by color and the representative term for those clusters are presented. Gene names shown in red; Green lines with arrows represent gene activation interactions; Red lines with bars represent interactions involved in gene repression.

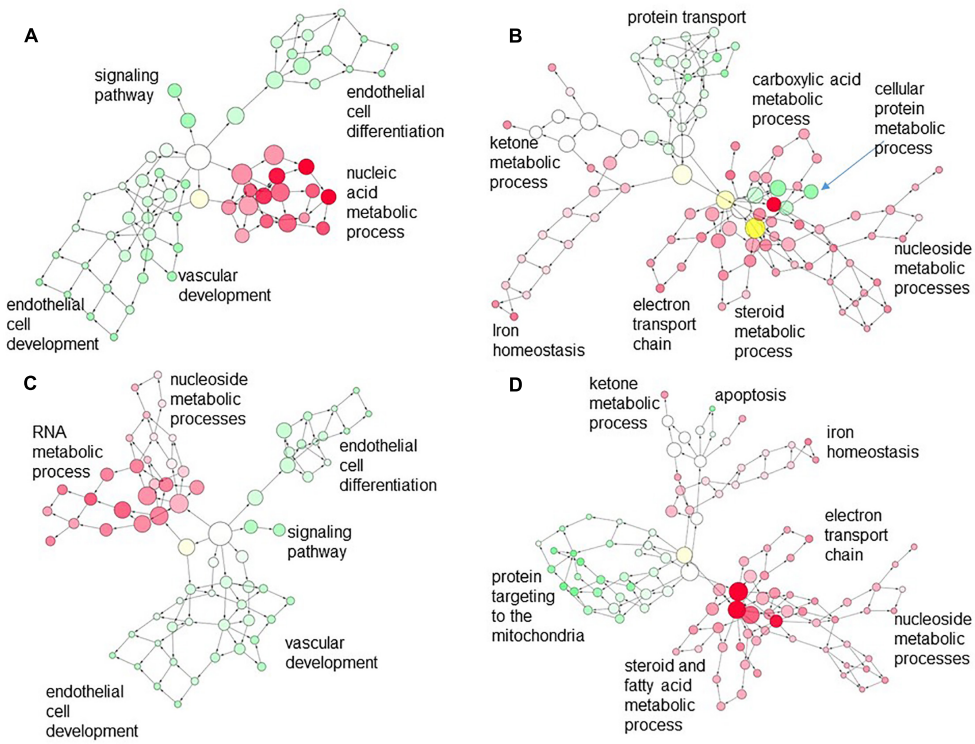

FIGURE 4 | Merged network created in Cytoscape depicting interaction of the gene ontology (GO) terms associated with **(A)** down-regulated genes in the LV (red) and upregulated genes in the EAT (green); **(B)** upregulated genes in the LV (green) with downregulated genes in the EAT (red); **(C)** down-regulated genes in the IVS (red) with upregulated genes in the EAT (green); **(D)** upregulated genes in the IVS (green) with downregulated genes in the EAT (red). Each circle is a node that corresponds to a GO term. Nodes size is proportional to the number of genes associated with that GO term. Nodes are connected by edges; edge length is inversely proportional to the degree of association of the connected nodes. Density of the color in the nodes is proportional to the level of statistical significance. Higher order (most specific) GO terms appear at the periphery of the network.

Reports in human infants about the effects of *in utero* cortisol exposure are more conflicting; although postnatal steroid treatment in preterm infants appears to cause left ventricular hypertrophy during the period of therapy, other reports suggest that prenatal glucocorticoids might have either transitory or no effect (Mildenhall et al., 2006, 2009). It has been suggested that the observed hypertrophy may occur in a subset in which mothers also had gestational diabetes; which independently increases the incidence of ventricular enlargement in the newborn (Demiroren et al., 2005; Aman et al., 2011; Garcia-Flores et al., 2011). In our studies, we found that the lambs of the cortisol- treated ewes had increased glucose to insulin ratio compared to lambs of control ewes (Antolic et al., 2015), which may contribute to the mild hypertrophy we observed in these lambs.

Interestingly, in prior cohorts in which ewes were infused continuously with cortisol, producing high levels throughout the 24 h cycle, we have seen high rates of stillbirth (Keller-Wood et al., 2014), and transcriptomic modeling has suggested that the normal progression in patterns of gene transcription are altered by the maternal cortisol exposure (Richards et al., 2014; Antolic et al., 2019). In the model used here, we were able to study newborn lambs to 2 weeks of age, and use transcriptomic modeling to infer pathways altered by the effects of elevated maternal cortisol that should be further investigated in the neonate or as the offspring ages. The present study includes tissue samples that are non-homogeneous; in the left ventricular free wall and septum, this includes cardiomyocytes, Purkinje fibers, fibroblasts, endothelial cells and other components of the vascular walls. In the epicardial fat, in addition to adipose cells, there are also vascular cells and some fibroblasts. Interestingly, the transcriptomic modeling did not indicate disruption in gene expression in pathways critical for oxidative metabolism within IVS or LV as the major effect of the exposure. Although both metabolic pathways and insulin signaling were identified as KEGG pathways overrepresented by genes with increased expression in the LV in the CORT lambs as compared to the Control lambs, other metabolic pathways were associated with downregulated genes in CORT lambs, and there were few genes and no pathways that specifically relate to TCA cycle function, mitochondrial energetics, or fatty acid or glucose oxidation in the LV, nor in the IVS. This is in contrast to our transcriptomic model in the LV and IVS of the fetus at term after the higher dose, continuous maternal infusion of cortisol during the same period of gestation. In the present cohort, in both LV and IVS, pathways related to RNA transport, and RNA degradation were associated with downregulated genes in CORT lambs, and ubiquitin-mediated proteolysis and protein targeting to the mitochondria were identified as upregulated pathways in CORT lambs as compared to Control lambs. This suggests that protein synthesis and degradation may both be impacted in the lambs. In the IVS G1 to S phase transition was identified as a downregulated KEGG pathway in CORT lambs as compared to Control lambs, consistent with upregulation of genes associated with the ribosome and with endoplasmic reticulum protein processing, and suggesting cells remain in the G1 phase longer, which would be consistent with non-proliferative growth or with DNA repair, The AMPK pathway and adipocytokine signaling pathways were modeled as downregulated in IVS of CORT lambs compared to Control lambs (AMPK subunits: PRKAG2, PRKAB2, and CAMKK were downregulated). AMPK suppresses proliferative growth, and increases fatty acid oxidation, but also stimulates autophagy (Mihaylova and Shaw, 2011). Because our samples include cardiomyocytes, fibroblasts, endothelial cells and other cell types, it is not possible to determine in which cell type growth or autophagy might be altered, however, the angiogenic pathway was not identified as a pathway overrepresented by the differentially expressed genes, so that the model does not suggest any alterations in angiogenesis in the LV or IVS. Overall, the transcriptomic model is more consistent with structural remodeling in the offspring heart rather than disruption of energetics and oxidation of fatty acids, and suggests that there may be proliferation of non-myocyte cell types such as fibroblasts. Thus the study indicates that longer term studies of the offspring as they age should focus on cardiac remodeling and hypertrophy.

In EAT and LV there are indications of a functional intersection in differentially regulated pathways. Using Cytoscape, we can visualize the intersection of the networks modeled by the differentially regulated genes. In the case of LV and EAT, there appears to be a clustering of nodes (representing genes) in LV involved in cellular macromolecular and protein metabolic processes, which are upregulated in LV, with nodes in EAT for ketoacids and fatty acid metabolism, which are downregulated (**Figure 4B**). In our Webgestalt analysis, the models found that in both LV and EAT pathways associated with fatty acids were identified as overrepresented by the differentially regulated genes. In EAT, the pathways for fatty acid elongation (PECR, ECHS1, HADHB, and MLYCD), and ketone production (HMGCS1 and HMGCS2, encoding HMG-CoA synthase) were identified from downregulated genes. Interestingly, peroxisome was identified as a pathway with increased gene expression in LV and decreased in EAT. Peroxisomes are important for catabolism of long chain fatty acids and for production of the plasmalogens which are used in myelination, as structural phospholipids and to protect against oxidative stress, but not as substrates for mitochondrial oxidative phosphorylation (Dudda et al., 1996; Brosche and Platt, 1998; Sindelar et al., 1999). In EAT the peroxisomal genes downregulated were associated with responses to oxidative stress (SOD1, SOD2, encoding superoxide dismutases, and EPHX2, encoding epoxide hydrolase). The peroxisomal pathway genes upregulated in the LV were associated with fatty acid production [PEX13, important in peroxisomal biogenesis (Maxwell et al., 2003); SLC27A, acyl CoA synthetase [Reviewed in Soupene and Kuypers (2008)]; and ACACB, catalyzing production of malonyl CoA, a negative regulator of acyl CoA uptake (Brownsey et al., 2006)]. In a study in our laboratory in newborn lambs born to ewes treated continuously with 1 mg/kg/d cortisol, cardiac levels of plasmenyl-phosphatidylcholines (plasmenyl-PC), plasmanyl-phosphatidylethanolamines (plasmanyl-PE), and cardiolipins (CL) were reduced whereas triglycerides and diglycerides were elevated (Walejko et al., 2019). Oxidized plasmalogen products are elevated in a porcine model of myocardial infarction, and are thought to play a role in protection against oxidative

stress in the heart and in the brain (Schmid and Takahashi, 1968; Dudda et al., 1996; Brosche and Platt, 1998). Thus, these results suggest that the EAT in offspring hearts may be more susceptible to oxidative stress, and that the LV is perhaps upregulating adaptive responses to oxidative stress; thus the capacity of the offspring heart to respond to oxidative challenge would be important to test in further studies in more mature offspring.

In IVS, there was also some suggestions of overlap with EAT in the functional pathways that were differentially affected by the *in utero* cortisol exposure. The intersection of GO networks was less impressive, with only negative regulation of anti-apoptosis in the IVS being closely clustered to downregulation of genes associated with metabolic changes in the EAT. There is some suggestion that triglyceride uptake and production is altered; increased expression of DGAT2, encoding an enzyme responsible for *de novo* synthesis of triglycerides, as well as LSR, encoding the protein responsible for uptake of triglycerides, was identified in the IVS. In our previous study of the newborn cardiac metabolome after maternal cortisol exposure, we found higher levels of di and triglycerides (Walejko et al., 2019). DGAT2 expression is linked to insulin resistance in muscle fibers (Levin et al., 2007). Potentially the IVS may ectopically deposit triglycerides made from the precursor metabolites that should have been stored in the EAT but were not, due to the relative immaturity of the EAT adipocytes. Ectopic deposition of "fat" in the ventricles is linked to a variety of defects of heart function [for review see (Borén et al., 2013; Mazzali et al., 2015)], so this may have important health implications. However, further studies are needed to explore a possible link between EAT dysfunction and triglyceride deposition as the animals mature.

Iron ion homeostasis was an overrepresented gene ontology in the genes downregulated in the cortisol treatment group, and this is consistent with the role of iron in controlling levels of reactive oxygen species in mitochondria during respiration. The gene most significantly reduced by maternal cortisol treatment in the microarray analyses of EAT was lactotransferrin (LTF), or lactoferrin, one of the genes included in the iron ion homeostasis category modeled. However, iron also plays a role in adipogenesis, lipolysis, lipid peroxidation, insulin-mediated glucose uptake, and mitochondrial biogenesis (Rumberger et al., 2004; Green et al., 2006; Moreno-Navarrete et al., 2014a). The macrophages of adipose depots recycle iron for proper adipocyte function, but also manipulate storage during inflammation and resolution of inflammation (Hubler et al., 2015). Thus, although maternal cortisol treatment appears to affect iron homeostasis in EAT, the causes and consequences of this are unclear from our data. The expression of genes encoding ATP citrate lyase (ACLY) and adipose differentiation-related protein (PLIN2) were reduced in expression in the EAT of the cortisol treatment group. ACLY produces acetyl CoA for lipogenesis and cholesterol genesis, and PLIN2 is a marker of lipid vacuoles of mature adipocytes. Knockdown of LTF decrease adipogenic, lipogenic and insulin signaling-related gene expression in pre-adipocytes (Moreno-Navarrete et al., 2014b) and supplementation promotes lipolysis in cultured adipocytes (Ikoma-Seki et al., 2015), and endogenous lactoferrin, produced by adipocytes, is necessary for the differentiation of preadipocytes to adipocytes (Moreno-Navarrete et al., 2013). These gene expression changes suggest that the EAT of the treated lambs is still proliferating and or relatively undifferentiated compared to the EAT of lambs of untreated ewes. This is complemented by the continued angiogenesis modeled in the cortisol treatment group, together these imply continued growth of the EAT depot. We were technically unable to measure whether there was an increase in the size of this adipose tissue depot due to hyperplasia following maternal cortisol treatment. These data suggest a larger depot might be more evident in older animals than those used in this study when the depot has completely formed. A larger EAT depot could have important health consequences. For example, the thickness of human EAT is correlated at only 8 years of age with increased risk of higher corrected-BMI and metabolic syndrome (Barbaro et al., 2016), and the volume and density of EAT is associated with cardiovascular disease including hypertension (Börekçi et al., 2015), resistant hypertension (Erdogan et al., 2016), myocardial ischemia (Hell et al., 2016) and coronary artery calcification (Gauss et al., 2015).

The effects of maternal cortisol are substantially different than those of maternal nutrition (either over or under) or placental restriction, which effect changes in leptin, adiponectin, PPARγ signaling, and IGFs that parallel the plane of nutrient supply to the fetus (Muhlhausler et al., 2007; Duffield et al., 2008, 2009), suggesting that this effect is not secondary to a limitation in substrate ability to the heart *in utero*. Our results do suggest long-lasting effects of the maternal hypercortisolemia on the postnatal heart, and suggest that alterations in epicardial adipose maturation and function may contribute to changes in cardiac structure and function. The transcriptomic model is consistent with the phenotype of the lambs; they were healthy and grew normally, and had minor cardiac wall thickening (Antolic et al., 2015).

The importance of glucocorticoids for organ maturation in late gestation (Silver, 1990; Liggins, 1994; Fowden and Silver, 1995; Phillips et al., 1997; Rog-Zielinska et al., 2013; Agnew et al., 2018) is most evident in preterm babies, in whom antenatal glucocorticoid therapy is essential for improving lung maturation; however, this life-saving intervention may also increase the risk for developing cardiovascular disease later in life (Benediktsson et al., 1993; Seckl, 2004; Dalziel et al., 2005; McKinlay et al., 2015). Accumulating evidence now shows that glucocorticoids are also necessary for cardiac maturation, and that excessive *in utero* exposure to glucocorticoids can negatively impact the maturational process. Studies from our lab indicate that elevations in maternal cortisol concentration throughout late gestation alters the normal trajectory of cardiac gene expression in the ovine fetus (Richards et al., 2014; Antolic et al., 2019), which persists into postnatal development. Although the underlying mechanism(s) is still under investigation, it appears to involve multiple signaling pathways (particularly those involved in cardiac metabolism), transcription factors, and protein abundance and activity. As a consequence, perinatal exposure to glucocorticoids may program the cardiac transcriptome, leaving individuals

exposed during that developmental window susceptible to cardiovascular disease.

DATA AVAILABILITY

The datasets generated for this study can be found in the National Center for Biotechnology Information's and the Gene Expression Omnibus, GSE131537 and GSE119254.

ETHICS STATEMENT

This study was carried out in accordance with the recommendations of the NIH Guide for the Care and Use of Laboratory Animals. The protocol was approved by the University of Florida Institutional Care and Use Committee.

AUTHOR CONTRIBUTIONS

MK-W and ER designed the study. AA and ER carried out the array analysis. All authors analyzed and interpreted the data, and drafted and approved the final version of the manuscript. AA and MK-W prepared the figures.

FUNDING

This work was funded by the National Institutes of Health Grant Number HD057871.

SUPPLEMENTARY MATERIAL

The Supplementary Material for this article can be found online at: https://www.frontiersin.org/articles/10.3389/fphys.2019.00816/full#supplementary-material

REFERENCES

Agnew, E. J., Ivy, J. R., Stock, S. J., and Chapman, K. E. (2018). Glucocorticoids, antenatal corticosteroid therapy and fetal heart maturation. *J. Mol. Endocrinol.* 61, R61–R73. doi: 10.1530/JME-18-0077

Aman, J., Hansson, U., Ostlund, I., Wall, K., and Persson, B. (2011). Increased fat mass and cardiac septal hypertrophy in newborn infants of mothers with well-controlled diabetes during pregnancy. *Neonatology* 100, 147–154. doi: 10.1159/000323741

Antolic, A., Feng, X., Wood, C. E., Richards, E. M., and Keller-Wood, M. (2015). Increased maternal nighttime cortisol concentrations in late gestation alter glucose and insulin in the neonatal lamb. *Physiol. Rep.* 3:e12548. doi: 10.14814/phy2.12548

Antolic, A., Li, M., Richards, E. M., Curtis, C. W., Wood, C. E., and Keller-Wood, M. (2019). Mechanisms of in utero cortisol effects on the newborn heart revealed by transcriptomic modeling. *Am. J. Physiol. Regul. Integr. Comp. Physiol.* 316, R323–R337. doi: 10.1152/ajpregu.00322.2018

Antolic, A., Wood, C. E., and Keller-Wood, M. (2017). Chronic maternal hypercortisolemia in late gestation alters fetal cardiac function at birth. *Am. J. Physiol. Regul. Integr. Comp. Physiol.* 314, R342–R352. doi: 10.1152/ajpregu.00296.2017

Ascuitto, R. J., Ross-Ascuitto, N. T., Chen, V., and Downing, S. E. (1989). Ventricular function and fatty acid metabolism in neonatal piglet heart. *Am. J. Physiol.* 256(1 Pt 2), H9–H15.

Barbaro, G., Piedimonte, A., Podagrosi, M., Mercurio, R., Mosca, A., DAvanzo, M., et al. (2016). Epicardial adipose tissue and signs of metabolic syndrome in children. *Eat Weight Disord.* 21, 269–276. doi: 10.1007/s40519-015-0221-0

Bartelds, B., Gratama, J. W., Knoester, H., Takens, J., Smid, G. B., Aarnoudse, J. G., et al. (1998). Perinatal changes in myocardial supply and flux of fatty acids, carbohydrates, and ketone bodies in lambs. *Am. J. Physiol.* 274, H1962–H1969. doi: 10.1152/ajpheart.1998.274.6.H1962

Bartelds, B., Knoester, H., Smid, G. B., Takens, J., Visser, G. H., Penninga, L., et al. (2000). Perinatal changes in myocardial metabolism in lambs. *Circulation* 102, 926–931. doi: 10.1161/01.cir.102.8.926

Bell, M. E., Wood, C. E., and Keller-Wood, M. (1991). Influence of reproductive state on pituitary-adrenal activity in the ewe. *Domest Anim. Endocrinol.* 8, 245–254. doi: 10.1016/0739-7240(91)90060-w

Benediktsson, R., Lindsay, R. S., Noble, J., Seckl, J. R., and Edwards, C. R. (1993). Glucocorticoid exposure in utero: new model for adult hypertension. *Lancet* 341, 339–341. doi: 10.1016/0140-6736(93)90138-7

Bindea, G., Mlecnik, B., Hackl, H., Charoentong, P., Tosolini, M., Kirilovsky, A., et al. (2009). ClueGO: a cytoscape plug-in to decipher functionally grouped gene ontology and pathway annotation networks. *Bioinformatics* 25, 1091–1093. doi: 10.1093/bioinformatics/btp101

Börekçi, A., Gür, M., Şeker, T., Kalyoncu Uçar, A., Baykan, A. O., Elbasan, Z., et al. (2015). Epicardial fat thickness as associated with left ventricular myocardial performance in patients with newly diagnosed hypertension. *Turk Kardiyol. Dern. Ars.* 43, 705–713. doi: 10.5543/tkda.2015.95902

Borén, J., Taskinen, M. R., Olofsson, S. O., and Levin, M. (2013). Ectopic lipid storage and insulin resistance: a harmful relationship. *J. Intern. Med.* 274, 25–40. doi: 10.1111/joim.12071

Brosche, T., and Platt, D. (1998). The biological significance of plasmalogens in defense against oxidative damage. *Exp. Gerontol.* 33, 363–369. doi: 10.1016/s0531-5565(98)00014-x

Brownsey, R. W., Boone, A. N., Elliott, J. E., Kulpa, J. E., and Lee, W. M. (2006). Regulation of acetyl-CoA carboxylase. *Biochem. Soc. Trans.* 34(Pt 2), 223–227.

Chang, E. I., Zarate, M. A., Arndt, T. J., Richards, E. M., Rabaglino, M. B., Keller-Wood, M., et al. (2018). Ketamine reduces inflammation pathways in the hypothalamus and hippocampus following transient hypoxia in the late-gestation fetal sheep. *Front. Physiol.* 9:1858. doi: 10.3389/fphys.2018.01858

Chattergoon, N. N., Giraud, G. D., and Thornburg, K. L. (2007). Thyroid hormone inhibits proliferation of fetal cardiac myocytes in vitro. *J. Endocrinol.* 192, R1–R8.

Dalziel, S. R., Walker, N. K., Parag, V., Mantell, C., Rea, H. H., Rodgers, A., et al. (2005). Cardiovascular risk factors after antenatal exposure to betamethasone: 30-year follow-up of a randomized controlled trial. *Lancet* 365, 1856–1862. doi: 10.1016/s0140-6736(05)66617-2

Davis, E. P., Waffarn, F., Uy, C., Hobel, C. J., Glynn, L. M., and Sandman, C. A. (2009). Effect of prenatal glucocorticoid treatment on size at birth among infants born at term gestation. *J. Perinatol.* 29, 731–737. doi: 10.1038/jp.2009.85

Demiroren, K., Cam, L., Oran, B., Koç, H., Başpinar, O., Baysal, T., et al. (2005). Echocardiographic measurements in infants of diabetic mothers and macrosomic infants of nondiabetic mothers. *J. Perinat. Med.* 33, 232–235.

Dodic, M., Abouantoun, T., OConnor, A., Wintour, E. M., and Moritz, K. M. (2002a). Programming effects of short prenatal exposure to dexamethasone in sheep. *Hypertension* 40, 729–734. doi: 10.1161/01.hyp.0000036455.62159.7e

Dodic, M., Hantzis, V., Duncan, J., Rees, S., Koukoulas, I., Johnson, K., et al. (2002b). Programming effects of short prenatal exposure to cortisol. *FASEB J.* 16, 1017–1026. doi: 10.1096/fj.01-1045com

Dodic, M., May, C. N., Wintour, E. M., and Coghlan, J. P. (1998). An early prenatal exposure to excess glucocorticoid leads to hypertensive offspring in sheep. *Clin. Sci.* 94, 149–155. doi: 10.1042/cs0940149

Dodic, M., Samuel, C., Moritz, K., Wintour, E. M., Morgan, J., Grigg, L., et al. (2001). Impaired cardiac functional reserve and left ventricular hypertrophy in adult sheep after prenatal dexamethasone exposure. *Circ. Res.* 89, 623–629. doi: 10.1161/hh1901.097086

Dudda, A., Spiteller, G., and Kobelt, F. (1996). Lipid oxidation products in ischemic porcine heart tissue. *Chem. Phys. Lipids* 82, 39–51. doi: 10.1016/0009-3084(96)02557-1

Duffield, J. A., Vuocolo, T., Tellam, R., McFarlane, J. R., Kauter, K. G., Muhlhausler, B. S., et al. (2009). Intrauterine growth restriction and the sex specific programming of leptin and peroxisome proliferator-activated receptor gamma (PPARgamma) mRNA expression in visceral fat in the lamb. *Pediatr. Res.* 66, 59–65. doi: 10.1203/PDR.0b013e3181a7c121

Duffield, J. A., Vuocolo, T., Tellam, R., Yuen, B. S., Muhlhausler, B. S., and McMillen, I. C. (2008). Placental restriction of fetal growth decreases IGF1 and leptin mRNA expression in the perirenal adipose tissue of late gestation fetal sheep. *Am. J. Physiol. Regul. Integr. Comp. Physiol.* 294, R1413–R1419. doi: 10.1152/ajpregu.00787.2007

Erdogan, G., Belen, E., Sungur, M. A., Sungur, A., Yaylak, B., Güngör, B., et al. (2016). Assessment of epicardial adipose tissue thickness in patients with resistant hypertension. *Blood Press Monit.* 21, 16–20. doi: 10.1097/MBP.0000000000000149

Fowden, A. L., and Silver, M. (1995). Comparative development of the pituitary-adrenal axis in the fetal foal and lamb. *Reprod. Domest. Anim.* 30, 170–177. doi: 10.1111/j.1439-0531.1995.tb00141.x

Garcia-Flores, J., Jañez, M., Gonzalez, M. C., Martinez, N., Espada, M., and Gonzalez, A. (2011). Fetal myocardial morphological and functional changes associated with well-controlled gestational diabetes. *Eur. J. Obstet. Gynecol. Reprod. Biol.* 154, 24–26. doi: 10.1016/j.ejogrb.2010.08.002

Gauss, S., Klinghammer, L., Steinhoff, A., Raaz-Schrauder, D., Marwan, M., Achenbach, S., et al. (2015). Association of systemic inflammation with epicardial fat and coronary artery calcification. *Inflamm. Res.* 64, 313–319. doi: 10.1007/s00011-015-0809-x

Giraud, G. D., Louey, S., Jonker, S., Schultz, J., and Thornburg, K. L. (2006). Cortisol stimulates cell cycle activity in the cardiomyocyte of the sheep fetus. *Endocrinology* 147, 3643–3649. doi: 10.1210/en.2006-0061

Green, A., Basile, R., and Rumberger, J. M. (2006). Transferrin and iron induce insulin resistance of glucose transport in adipocytes. *Metabolism* 55, 1042–1045. doi: 10.1016/j.metabol.2006.03.015

Hell, M. M., Ding, X., Rubeaux, M., Slomka, P., Gransar, H., Terzopoulos, D., et al. (2016). Epicardial adipose tissue volume but not density is an independent predictor for myocardial ischemia. *J. Cardiovasc. Comput. Tomogr.* 10, 141–149. doi: 10.1016/j.jcct.2016.01.009

Hubler, M. J., Peterson, K. R., and Hasty, A. H. (2015). Iron homeostasis: a new job for macrophages in adipose tissue? *Trends Endocrinol. Metab.* 26, 101–109. doi: 10.1016/j.tem.2014.12.005

Ikoma-Seki, K., Nakamura, K., Morishita, S., Ono, T., Sugiyama, K., Nishino, H., et al. (2015). Role of LRP1 and ERK and cAMP signaling pathways in lactoferrin-induced lipolysis in mature rat adipocytes. *PLoS One* 10:e0141378. doi: 10.1371/journal.pone.0141378

Jonker, S. S., Faber, J. J., Anderson, D. F., Thornburg, K. L., Louey, S., and Giraud, G. D. (2007a). Sequential growth of fetal sheep cardiac myocytes in response to simultaneous arterial and venous hypertension. *Am. J. Physiol. Regul. Integr. Comp. Physiol.* 292, R913–R919.

Jonker, S. S., Zhang, L., Louey, S., Giraud, G. D., Thornburg, K. L., and Faber, J. J. (2007b). Myocyte enlargement, differentiation, and proliferation kinetics in the fetal sheep heart. *J. Appl. Physiol.* 102, 1130–1142. doi: 10.1152/japplphysiol.00937.2006

Keller-Wood, M., Feng, X., Wood, C. E., Richards, E., Anthony, R. V., Dahl, G. E., et al. (2014). Elevated maternal cortisol leads to relative maternal hyperglycemia and increased stillbirth in ovine pregnancy. *Am. J. Physiol. Regul. Integr. Comp. Physiol.* 307, R405–R413. doi: 10.1152/ajpregu.00530.2013

Laudat, M. H., Cerdas, S., Fournier, C., Guiban, D., Guilhaume, B., and Luton, J. P. (1988). Salivary cortisol measurement: a practical approach to assess pituitary-adrenal function. *J. Clin. Endocrinol. Metab.* 66, 343–348. doi: 10.1210/jcem-66-2-343

Levin, M. C., Monetti, M., Watt, M. J., Sajan, M. P., Stevens, R. D., Bain, J. R., et al. (2007). Increased lipid accumulation and insulin resistance in transgenic mice expressing DGAT2 in glycolytic (type II) muscle. *Am. J. Physiol. Endocrinol. Metab.* 293, E1772–E1781.

Liggins, G. C. (1994). The role of cortisol in preparing the fetus for birth. *Reprod. Fertil. Dev.* 6, 141–150.

Lopaschuk, G. D., and Spafford, M. A. (1990). Energy substrate utilization by isolated working hearts from newborn rabbits. *Am. J. Physiol.* 258(5 Pt 2), H1274–H1280.

Lopaschuk, G. D., Spafford, M. A., and Marsh, D. R. (1991). Glycolysis is predominant source of myocardial ATP production immediately after birth. *Am. J. Physiol.* 261(6 Pt 2), H1698–H1705.

Maxwell, M., Bjorkman, J., Nguyen, T., Sharp, P., Finnie, J., Paterson, C., et al. (2003). Pex13 inactivation in the mouse disrupts peroxisome biogenesis and leads to a Zellweger syndrome phenotype. *Mol. Cell Biol.* 23, 5947–5957. doi: 10.1128/mcb.23.16.5947-5957.2003

Mazzali, G., Fantin, F., Zoico, E., Sepe, A., Bambace, C., Faccioli, S., et al. (2015). Heart fat infiltration in subjects with and without coronary artery disease. *J. Clin. Endocrinol. Metab.* 100, 3364–3371. doi: 10.1210/jc.2015-b1787

McKinlay, C. J., Cutfield, W. S., Battin, M. R., Dalziel, S. R., Crowther, C. A., Harding, J. E., et al. (2015). Cardiovascular risk factors in children after repeat doses of antenatal glucocorticoids: an RCT. *Pediatrics* 135, e405–e415. doi: 10.1542/peds.2014-2408

Mihaylova, M. M., and Shaw, R. J. (2011). The AMPK signalling pathway coordinates cell growth, autophagy and metabolism. *Nat. Cell Biol.* 13, 1016–1023. doi: 10.1038/ncb2329

Mildenhall, L., Battin, M. R., Bevan, C., Kuschel, C., and Harding, J. E. (2009). Repeat prenatal corticosteroid doses do not alter neonatal blood pressure or myocardial thickness: randomized, controlled trial. *Pediatrics* 123, e646–e652. doi: 10.1542/peds.2008-1931

Mildenhall, L. F., Battin, M. R., Morton, S. M., Bevan, C., Kuschel, C. A., and Harding, J. E. (2006). Exposure to repeat doses of antenatal glucocorticoids is associated with altered cardiovascular status after birth. *Arch. Dis. Child Fetal Neonatal Ed.* 91, F56–F60.

Mlecnik, B., Galon, J., and Bindea, G. (2018). Comprehensive functional analysis of large lists of genes and proteins. *J. Proteomics* 171, 2–10. doi: 10.1016/j.jprot.2017.03.016

Montojo, J., Zuberi, K., Rodriguez, H., Kazi, F., Wright, G., Donaldson, S. L., et al. (2010). GeneMANIA cytoscape plugin: fast gene function predictions on the desktop. *Bioinformatics* 26, 2927–2928. doi: 10.1093/bioinformatics/btq562

Moreno-Navarrete, J. M., Ortega, F., Moreno, M., Ricart, W., and Fernández-Real, J. M. (2014a). Fine-tuned iron availability is essential to achieve optimal adipocyte differentiation and mitochondrial biogenesis. *Diabetologia* 57, 1957–1967. doi: 10.1007/s00125-014-3298-5

Moreno-Navarrete, J. M., Ortega, F., Moreno, M., Serrano, M., Ricart, W., and Fernández-Real, J. M. (2014b). Lactoferrin gene knockdown leads to similar effects to iron chelation in human adipocytes. *J. Cell Mol. Med.* 18, 391–395. doi: 10.1111/jcmm.12234

Moreno-Navarrete, J. M., Serrano, M., Sabater, M., Ortega, F., Serino, M., Pueyo, N., et al. (2013). Study of lactoferrin gene expression in human and mouse adipose tissue, human preadipocytes and mouse 3T3-L1 fibroblasts. Association with adipogenic and inflammatory markers. *J. Nutr. Biochem.* 24, 1266–1275. doi: 10.1016/j.jnutbio.2012.10.002

Moss, T. J., Sloboda, D. M., Gurrin, L. C., Harding, R., Challis, J. R., and Newnham, J. P. (2001). Programming effects in sheep of prenatal growth restriction and glucocorticoid exposure. *Am. J. Physiol. Regul. Integr. Comp. Physiol.* 281, R960–R970.

Muhlhausler, B. S., Duffield, J. A., and McMillen, I. C. (2007). Increased maternal nutrition increases leptin expression in perirenal and subcutaneous adipose tissue in the postnatal lamb. *Endocrinology* 148, 6157–6163. doi: 10.1210/en.2007-0770

Newnham, J. P., and Moss, T. J. (2001). Antenatal glucocorticoids and growth: single versus multiple doses in animal and human studies. *Semin. Neonatol.* 6, 285–292. doi: 10.1053/siny.2001.0064

OTierney, P. F., Anderson, D. F., Faber, J. J., Louey, S., Thornburg, K. L., and Giraud, G. D. (2010a). Reduced systolic pressure load decreases cell-cycle activity in the fetal sheep heart. *Am. J. Physiol. Regul. Integr. Comp. Physiol.* 299, R573–R578. doi: 10.1152/ajpregu.00754.2009

OTierney, P. F., Chattergoon, N. N., Louey, S., Giraud, G. D., and Thornburg, K. L. (2010b). Atrial natriuretic peptide inhibits angiotensin II-stimulated proliferation in fetal cardiomyocytes. *J. Physiol.* 588(Pt 15), 2879–2889. doi: 10.1113/jphysiol.2010.191098

Phillips, I. D., Anthony, R. V., Butler, T. G., Ross, J. T., and McMillen, I. C. (1997). Hepatic prolactin receptor gene expression increase in the sheep fetus before birth and after cortisol infusion. *Endocrinology* 138, 1351–1354. doi: 10.1210/en.138.3.1351

R Development Core Team (2008). *R: A Language and Environment for Statistical Computing*. Vienna: R Foundation for Statistical Computing.

Raff, H., Raff, J. L., and Findling, J. W. (1998). Late-night salivary cortisol as a screening test for Cushings syndrome. *J. Clin. Endocrinol. Metab.* 83, 2681–2686. doi: 10.1210/jc.83.8.2681

Richards, E. M., Wood, C. E., Rabaglino, M. B., Antolic, A., and Keller-Wood, M. (2014). Mechanisms for the adverse effects of late gestational increases in maternal cortisol on the heart revealed by transcriptomic analyses of the fetal septum. *Physiol. Genomics* 46, 547–559. doi: 10.1152/physiolgenomics.00009.2014

Rog-Zielinska, E. A., Thomson, A., Kenyon, C. J., Brownstein, D. G., Moran, C. M., Szumska, D., et al. (2013). Glucocorticoid receptor is required for foetal heart maturation. *Hum. Mol. Genet.* 22, 3269–3282. doi: 10.1093/hmg/ddt182

Rumberger, J. M., Peters, T., Burrington, C., and Green, A. (2004). Transferrin and iron contribute to the lipolytic effect of serum in isolated adipocytes. *Diabetes* 53, 2535–2541. doi: 10.2337/diabetes.53.10.2535

Scharnholz, B., Lederbogen, F., Feuerhack, A., Bach, A., Kopf, D., Frankhauser, P., et al. (2010). Does night-time cortisol excretion normalize in the long-term course of depression? *Pharmacopsychiatry* 43, 161–165. doi: 10.1055/s-0030-1248316

Schmid, H. H., and Takahashi, T. (1968). The alk-i-enyl ether and alkyl ether lipids of bovine heart muscle. *Biochim. Biophys. Acta* 164, 141–147. doi: 10.1016/0005-2760(68)90140-9

Seckl, J. R. (2004). Prenatal glucocorticoids and long-term programming. *Eur. J. Endocrinol.* 151(Suppl. 3), U49–U62.

Shannon, P., Markiel, A., Ozier, O., Baliga, N. S., Wang, J. T., Ramage, D., et al. (2003). Cytoscape: a software environment for integrated models of biomolecular interaction networks. *Genome Res.* 13, 2498–2504. doi: 10.1101/gr.1239303

Silver, M. (1990). Prenatal maturation, the timing of birth and how it is regulated in domestic animals. *Exp. Physiol.* 75, 285–307. doi: 10.1113/expphysiol.1990.sp003405

Sindelar, P. J., Guan, Z., Dallner, G., and Ernster, L. (1999). The protective role of plasmalogens in iron-induced lipid peroxidation. *Free Radic. Biol. Med.* 26, 318–324. doi: 10.1016/s0891-5849(98)00221-4

Sloboda, D. M., Newnham, J. P., and Challis, J. R. (2002). Repeated maternal glucocorticoid administration and the developing liver in fetal sheep. *J. Endocrinol.* 175, 535–543. doi: 10.1677/joe.0.1750535

Soupene, E., and Kuypers, F. A. (2008). Mammalian long-chain acyl-CoA synthetases. *Exp. Biol. Med.* 233, 507–521. doi: 10.3181/0710-MR-287

Sundgren, N. C., Giraud, G. D., Schultz, J. M., Lasarev, M. R., Stork, P. J., and Thornburg, K. L. (2003a). Extracellular signal-regulated kinase and phosphoinositol-3 kinase mediate IGF-1 induced proliferation of fetal sheep cardiomyocytes. *Am. J. Physiol. Regul. Integr. Comp. Physiol.* 285, R1481–R1489.

Sundgren, N. C., Giraud, G. D., Stork, P. J., Maylie, J. G., and Thornburg, K. L. (2003b). Angiotensin II stimulates hyperplasia but not hypertrophy in immature ovine cardiomyocytes. *J. Physiol.* 548(Pt 3), 881–891. doi: 10.1111/j..2003.t01-1-00881.x

Walejko, J. M., Antolic, A., Koelmel, J. P., Garrett, T. J., Edison, A. S., and Keller-Wood, M. (2019). Chronic maternal cortisol excess during late gestation leads to metabolic alterations in the newborn heart. *Am. J. Physiol. Endocrinol. Metab.* 316, E546–E556. doi: 10.1152/ajpendo.00386.2018

Wang, J., Duncan, D., Shi, Z., and Zhang, B. (2013). WEB-based GEne SeT analysis toolkit (WebGestalt): update 2013. *Nucleic Acids Res.* 41, W77–W83. doi: 10.1093/nar/gkt439

Werner, J. C., and Sicard, R. E. (1987). Lactate metabolism of isolated, perfused fetal, and newborn pig hearts. *Pediatr. Res.* 22, 552–556. doi: 10.1203/00006450-198711000-00016

Zhang, B., Kirov, S., and Snoddy, J. (2005). WebGestalt: an integrated system for exploring gene sets in various biological contexts. *Nucleic Acids Res.* 33, W741–W748.

Conflict of Interest Statement: The authors declare that the research was conducted in the absence of any commercial or financial relationships that could be construed as a potential conflict of interest.

Copyright © 2019 Antolic, Richards, Wood and Keller-Wood. This is an open-access article distributed under the terms of the Creative Commons Attribution License (CC BY). The use, distribution or reproduction in other forums is permitted, provided the original author(s) and the copyright owner(s) are credited and that the original publication in this journal is cited, in accordance with accepted academic practice. No use, distribution or reproduction is permitted which does not comply with these terms.

frontiers in Physiology

ORIGINAL RESEARCH
published: 05 July 2019
doi: 10.3389/fphys.2019.00857

Limited Support for Thyroid Hormone or Corticosterone Related Gene Expression as a Proximate Mechanism of Incubation Temperature-Dependent Phenotypes in Birds

Sydney F. Hope[1], Christopher R. Buenaventura[2], Zahabiya Husain[2], Sarah E. DuRant[3], Robert A. Kennamer[4], William A. Hopkins[1] and Christopher K. Thompson[2]*

[1] Department of Fish and Wildlife Conservation, Virginia Tech, Blacksburg, VA, United States, [2] School of Neuroscience, Virginia Tech, Blacksburg, VA, United States, [3] Department of Biological Sciences, University of Arkansas, Fayetteville, AR, United States, [4] Savannah River Ecology Laboratory, University of Georgia, Aiken, SC, United States

OPEN ACCESS

Edited by:
Dane Alan Crossley II, University of North Texas System, United States

Reviewed by:
Angela Leigh Cumberland, RMIT University, Australia
Edward M. Dzialowski, University of North Texas, United States

***Correspondence:**
Sydney F. Hope
shope@vt.edu

Specialty section:
This article was submitted to Embryonic and Developmental Physiology, a section of the journal Frontiers in Physiology

Received: *04 March 2019*
Accepted: *20 June 2019*
Published: *05 July 2019*

Citation:
Hope SF, Buenaventura CR, Husain Z, DuRant SE, Kennamer RA, Hopkins WA and Thompson CK (2019) Limited Support for Thyroid Hormone or Corticosterone Related Gene Expression as a Proximate Mechanism of Incubation Temperature-Dependent Phenotypes in Birds. Front. Physiol. 10:857. doi: 10.3389/fphys.2019.00857

The conditions that animals experience during early development can have profound consequences for health and fitness. In birds, one of the most important aspects of development is egg incubation temperature. A small decrease in average temperature leads to various impacts on offspring phenotype, such as smaller body sizes, slower growth rates, and less efficient metabolic activity. Little is known, however, about the proximate mechanisms underlying these incubation temperature-induced phenotypic changes. Two important hormones which could play a proximate role are thyroid hormone and corticosterone, which mobilize stored energy reserves and coordinate the normal growth of tissues, particularly in the brain. Previous research shows that circulating blood concentrations of both hormones are influenced by incubation temperature, but the mechanism by which incubation temperature may lead to these changes is unknown. We hypothesized that incubation temperature induces changes in thyroid hormone and corticosterone regulation, leading to changes in expression of hormone-sensitive genes in the brain. To test this, we incubated wood duck (*Aix sponsa*) eggs at three different temperatures within the natural range (35.0, 35.8, and 37.0°C). We measured mRNA expression of thyroid hormone-related neuroendocrine endpoints (deiodinase 2/3, thyroid hormone receptor α/β, neural regeneration related protein, and Krueppel-like factor 9) in newly hatched ducklings and corticosterone-related neuroendocrine endpoints (mineralocorticoid receptor, glucocorticoid receptor, cholecystokinin, and brain-derived neurotrophic factor) in 15 day-old ducklings using qPCR on brain tissue from the hippocampus and hypothalamus. Contrary to our predictions, we found that mRNA expression of thyroid hormone-related endpoints in both brain areas were largely unaffected by incubation temperature, although there was a trend for an inverse relationship between mRNA expression and incubation temperature for several genes in the hypothalamus. We also found that mineralocorticoid

receptor mRNA expression in the hypothalamus was lower in ducklings incubated at the low relative to the high temperatures. This study is the first to evaluate the effects of incubation temperature on mRNA expression of neuroendocrine endpoints in the developing avian brain and suggests that these particular endpoints may be largely resistant to changes in incubation temperature. Thus, further research into the proximate mechanisms for incubation temperature-induced developmental plasticity is needed.

Keywords: early developmental environment, parental effects, *Aix sponsa*, avian, hippocampus, hypothalamus, glucocorticoids, brain

INTRODUCTION

During early development, animals are particularly susceptible to changes in their environment, and these developmental conditions can have long-term consequences for health and fitness (Lindström, 1999; Monaghan, 2008). In some cases, changes in the early developmental environment can induce phenotypic changes that optimize offspring for their current or future environment. This type of developmental programming has been described in both ectothermic and endothermic vertebrates (Salinas and Munch, 2012; Mariette and Buchanan, 2016). Developmental plasticity can lead to negative consequences and disease, however, when there are mismatches between the developmental and adult environment, or when suboptimal developmental conditions lead to suboptimal phenotypes (Monaghan, 2008). On the other hand, some traits, especially those that are essential to survival, are more resistant to changes in the early developmental environment and exhibit little developmental plasticity (Waddington, 1942). Among vertebrates, parental behaviors that influence the early developmental environment play a key role in shaping offspring phenotypes. Currently, the underlying hormonal and neuroendocrinological mechanisms in the developing offspring that are affected by changing developmental conditions and contribute to these phenotypic outcomes are poorly understood.

In birds, one of the most important aspects of the environment during early development is egg incubation temperature. Factors such as weather, clutch size, and parental body condition can influence incubation temperatures both directly and indirectly through impacts on parental incubation behavior (Aldrich and Raveling, 1983; Haftorn and Reinertsen, 1985; Conway and Martin, 2000; Coe et al., 2015; Hope et al., 2018a). Thus, egg temperatures can vary substantially both among and within avian nests (Reid et al., 2000; Hepp et al., 2006; Boulton and Cassey, 2012; Coe et al., 2015; Hope et al., 2018a). Importantly, subtle differences (<1°C) in average incubation temperature result in a wide array of phenotypic changes in avian offspring (DuRant et al., 2010, 2011, 2012a,b, 2013a, 2014; Nord and Nilsson, 2011, 2016; Hepp and Kennamer, 2012; Hepp et al., 2015; Berntsen and Bech, 2016). In some cases, this developmental plasticity may be beneficial for offspring. For example, low incubation temperatures produce individuals that have slower growth rates (DuRant et al., 2010; Nord and Nilsson, 2011) and more proactive behaviors (Hope et al., 2018b), which may be advantageous in environments with low resource availability. However, in many cases, low incubation temperatures result in phenotypes that are likely not adaptive, such as reduced thermoregulatory ability (DuRant et al., 2012b, 2013a), reduced ability to fledge from the nest (Hope et al., 2019) and, notably, reduced survival (Hepp and Kennamer, 2012; Berntsen and Bech, 2016; Nord and Nilsson, 2016).

Although the effects of incubation temperature on avian phenotype are well-documented (DuRant et al., 2013b), little is known about the proximate mechanisms underlying these incubation temperature-induced phenotypic changes. Two important hormones that could play a proximate role are thyroid hormones and glucocorticoids. Both thyroid hormones (McNabb and King, 1993; Morreale de Escobar et al., 2004; McNabb, 2006) and glucocorticoids (McEwen, 2001; Kanagawa et al., 2006) are essential for neurogenesis and coordinating the normal growth of tissues in the developing vertebrate brain, which could then have downstream effects on other aspects of offspring phenotype. Indeed, altered levels of both thyroid hormones (Pop et al., 1999; Boelaert and Franklyn, 2005; Ahmed et al., 2008) and glucocorticoids (Maniam et al., 2014) during early development are related to disease and physiological and behavioral disorders in vertebrates. Importantly, incubation temperature is related to circulating levels of both thyroid hormone (DuRant et al., 2014) and corticosterone (DuRant et al., 2010), the major avian glucocorticoid, in juvenile birds. The mechanism by which incubation temperature leads to these changes in hormone levels, or how these changes in hormone levels may have lasting impacts on phenotype, however, is unknown. One possible underlying mechanism may be that incubation temperature influences the development of the major hormonal axes associated with these two hormones (i.e., hypothalamic-pituitary-thyroid [HPT] axis and hypothalamic-pituitary-adrenal [HPA] axis). For example, incubation temperature may induce changes in the expression of genes involved in the regulation of these two hormones, particularly in developing brain tissue. Furthermore, incubation temperature-induced changes in circulating hormones are likely to induce changes in the expression of hormone-sensitive genes in the developing brain, which will then have an impact on physiology and behavior, even if changes in hormone levels are transient. A better understanding of these mechanisms is critical for assessing the impact of altered environmental conditions on developing organisms.

In this study, we hypothesized that incubation temperature induces changes in thyroid hormone and corticosterone regulation, leading to changes in the expression of thyroid

hormone and corticosterone sensitive genes that are important for normal brain development. Some of the genes examined are also involved in regulating these hormone systems, particularly in the hypothalamus. To test this hypothesis, we incubated wood duck (*Aix sponsa*) eggs at three different temperatures within the natural range (35.0, 35.8, and 37.0°C; DuRant et al., 2013b). To measure gene expression, we used quantitative PCR (qPCR) on duckling brain tissue from the hippocampus and hypothalamus. We measured mRNA expression of the thyroid hormone-related genes deiodinase 2/3 (DIO2 and DIO3), thyroid hormone receptor α/β (TRα and TRβ), neural regeneration related protein (NREP), and Krueppel-like factor 9 (KLF9) in newly hatched ducklings. We measured mRNA expression of the corticosterone-related genes mineralocorticoid receptor (MR), glucocorticoid receptor (GR), cholecystokinin (CCK), and brain-derived neurotrophic factor (BDNF) in 15 day-old ducklings. Because previous research shows that ducklings incubated at lower temperatures have lower levels of the more active form of thyroid hormone (T_3; DuRant et al., 2014) and higher baseline and stress-induced corticosterone levels (DuRant et al., 2010) than those incubated at higher temperatures, we expected that mRNA expression would be altered by incubation temperature. Specifically, we predicted that the expression of genes that are stimulated by thyroid hormone (TRβ, DIO3, NREP, and KLF9) would be the lowest (Hu et al., 2016; Thompson and Cline, 2016), and genes that are downregulated by thyroid hormone signaling (TRα and DIO2) would be the highest in ducklings incubated at the lowest temperature (Bernal, 2007; Duarte-Guterman and Trudeau, 2010). Further, we predicted that the expression of genes related to the regulation and negative feedback of corticosterone (MR and GR) and those that are normally suppressed by corticosterone (BDNF) would be the lowest, and that genes that are related to HPA axis stimulation (CCK) would be highest in ducklings incubated at the lowest temperature (Murakami et al., 2005; Liu et al., 2010; Datson et al., 2012).

MATERIALS AND METHODS

Study Species and Site

The wood duck is a common North American duck that nests in tree cavities and nest boxes (Hepp and Bellrose, 2013). The wood duck breeding season begins in mid-February and lasts until mid-July, and re-nesting is common (Hepp and Bellrose, 2013). The female incubates the eggs without help from the male, and eggs hatch after ∼30 days of incubation (Hepp and Bellrose, 2013). Females spend most of the day incubating but usually take two 1–2 h recesses each day to forage (Manlove and Hepp, 2000). Incubation temperature varies among and within populations (Bellrose and Holm, 1994; Manlove and Hepp, 2000; Hepp et al., 2006), and within nests (Hope et al., 2018a). Incubation temperature is lower and more variable as clutch size increases (Hope et al., 2018a). Clutch sizes (average = 12 eggs; Bellrose and Holm, 1994) are variable within populations and can reach >40 eggs (Morse and Wight, 1969) due to conspecific brood parasitism (Semel and Sherman, 1986; Semel et al., 1988; Roy Nielsen et al., 2006). Offspring are precocial and can feed themselves once they leave the nest (Bellrose and Holm, 1994).

Egg Collection and Incubation

Our methods for egg collection and incubation are described fully in Hope et al. (2018b). Briefly, we collected unincubated wood duck eggs from nest boxes at the Department of Energy's Savannah River Site in South Carolina (33.1°N, 81.3°W) in March 2015. We incubated eggs in Grumbach incubators (model BSS 420, Asslar, Germany) at Virginia Tech. Eggs were incubated at three different average temperatures (35.0, 35.8, and 37.0°C). We chose these temperatures because they are within the natural range for wood ducks and have been shown to produce variation in a wide array of duckling phenotypes (DuRant et al., 2013b and references therein), including corticosterone levels (DuRant et al., 2010), thyroid hormone levels (DuRant et al., 2014), and behavior (Hope et al., 2018b). Incubators had two daily 75 min cool-down periods at 8:15 and 18:30 h to mimic natural conditions (Manlove and Hepp, 2000). During these cooling periods, the incubators turned off for 75 min, which produced different minimum temperatures for each treatment (average minimum temperatures ± SD for each treatment: 35.0°C: 32.9 ± 0.85°C; 35.8°C: 33.8 ± 0.89°C; 37.0°C: 33.5 ± 0.95°C). Temperature data from *i*Buttons® (Hygrochron, Maxim Integrated, CA, United States) within the incubators confirmed that they maintained the above mentioned average temperatures.

General Husbandry

For this study, 30 ducklings from 18 nests (8 incubated at 35.0°C, 11 at 35.8°C, and 11 at 37.0°C) were sacrificed at day 0, and 35 ducklings from 27 nests (11 incubated at 35.0°C, 12 at 35.8°C, and 12 at 37.0°C) were sacrificed on day 15 to collect brain tissue. Once hatched, day 0 ducklings were placed in a covered cage with a 50W infrared heat lamp with other similar-aged ducklings for <10 h, until they were euthanized. Day 15 ducklings were housed in cages with *ad lib* food and water, and underwent a series of behavioral trials as part of a different experiment. Complete animal husbandry methods for these ducklings are described in Hope et al. (2018b).

Tissue Collection

Ducklings were humanely euthanized via carbon dioxide asphyxiation and cervical dislocation. Immediately following euthanasia, whole brains were extracted from ducklings and flash-frozen on dry ice (≤12 min from start of euthanasia until brain completely frozen). Brains were then stored at −80°C until sectioning. Using a cryostat, brains were sectioned until the hippocampus and hypothalamus regions were visible. We took two punches from each brain region of each bird, and these two punches were pooled for each bird, producing one sample per brain region per bird. Punches were taken from only one side (i.e., right or left) of each brain, and we alternated which brain region we sampled for each bird to test for hemispheric differences. Punches were immediately placed in Trizol and frozen on dry ice. Samples were stored at −80°C until analysis.

Quantifying mRNA Expression

We investigated thyroid hormone-related mRNA expression in day 0 ducklings because thyroid hormone is important during early development and, in a previous study, wood duck ducklings incubated at different temperatures displayed different levels of circulating thyroid hormone on day 0, but not on day 4 or 10 (DuRant et al., 2014). We investigated corticosterone-related gene expression in day 15 ducklings because wood duck ducklings incubated at different temperatures display differences in corticosterone levels at day 9 (DuRant et al., 2010), and because post-mortem tissue samples were available at day 15 after a previous study (Hope et al., 2018b). Further, some animals undergo a refractory period shortly after hatch, where HPA axis function is dampened and individuals are unresponsive to stressors (Sapolsky and Meaney, 1986), thus we did not expect to find meaningful results for the HPA axis in day 0 ducklings. Although effects of incubation temperature on circulating levels of corticosterone appear to be absent by day 15 (Hope et al., 2018b), there are still lasting effects on behavior until day 15 (Hope et al., 2018b), and thus we postulated that transient elevations of corticosterone until day 9 would lead to changes in the HPA axis, including altered gene expression, that would be apparent at day 15.

We extracted RNA per the manufacturer's instructions for Trizol, measured the amount of RNA extracted on a NanoDrop, and reverse transcribed the mRNA using the iScript kit (Bio-Rad, CA, United States), using 1 ug of RNA per reaction. Tissue samples from each duckling were run individually. We performed qPCR using 8 ng cDNA per reaction using the iTaq Universal SYBR Green Supermix kit (Bio-Rad) on a Bio-Rad CFX384 thermocycler. All reactions were done with technical triplicates; outlier reactions (deviations more than 1.5 times the SD from the mean) within a set of triplicates were removed from analysis. We used a two-step reaction with a 10 s 95° melt step, followed by a 30 s 60° annealing and an extension step for 40 cycles, with fluorescence measured at the end of every 60° step. At the end of 40 cycles, we evaluated the melt curves for secondary products; none of the primers used in this study generated secondary products. We designed primers by blasting the genes of interest from mallard (*Anas platyrhynchos*) genome to the domestic goose (*Anser cygnoides domesticus*) genome and selecting regions of high homology using NCBI primer blast online tool. A list of primers is found in **Table 1**. Primer pairs were selected using PCR against wood duck cDNA and running out the product on a gel to ensure each primer pair generated the expected product size, only one product, and no primer-dimer production.

To evaluate the suitability of GAPDH and ACTB as reference genes, we used two basic forms of analysis. First, we examined if raw Ct (the cycle at which florescence intensity reached threshold) for each reference gene significantly varied across temperatures in each brain area. We found that temperature did not affect ACTB and GAPDH expression (p = 0.55 and 0.89, respectively). We also assessed reference gene stability using the geNorm and NormFinder analysis tools in Excel (Microsoft). GAPDH and ACTB met the criteria to be used as stable reference genes in these experimental conditions. We then used the $\Delta\Delta$Ct method to calculate change in expression relative to the average of the reference genes (GAPDH and ACTB). Last, we normalized expression data using the results from the 35°C hypothalamus group as a baseline. Fold change is a 10-base fold change because results were transformed using a square exponent (i.e., $2^{-\Delta\Delta Ct}$).

Statistical Analyses

We used GraphPad Prism to analyze our data for statistical differences. Data sets from individual brain areas were evaluated with one way ANOVA with temperature as the independent factor for each brain region and at each time point, and *post hoc* comparisons were made with Tukey's multiple comparisons test. We also tested for hemispheric (i.e., left vs. right) differences in mRNA expression in each brain region using one way ANOVAs. We were unable to use repeated measures ANOVA to include brain region as an additional factor because the data set was not completely balanced (i.e., some punches from some brain areas in some animals had poor RNA extraction/quality and therefore could not be compared using within-animals comparisons). However, we were able to make general observations about overall expression patterns across brain regions without respect to incubation temperature. Sample sizes for each analysis (reflecting individuals that were excluded due to poor RNA extraction/quality) are reported in **Table 2**.

RESULTS

mRNA Expression of Thyroid Hormone-Associated Neuroendocrine Endpoints

We evaluated changes in gene expression in six different thyroid hormone-related genes of interest in 0 day-old ducklings that were incubated at three different temperatures (**Figure 1**). A summary of these statistical results can be found in **Table 2**. In short, we did not observe statistically significant differences in gene expression across incubation temperatures in the two brain areas examined. There was a trend of elevated expression at lower incubation temperatures in the hypothalamus of several thyroid hormone-related neuroendocrine endpoints (**Figure 1**), but none of these results were statistically different.

mRNA Expression of Corticosterone-Associated Neuroendocrine Endpoints

We also evaluated changes in gene expression in four different corticosterone-related genes of interest in two different brain areas in 15 day-old ducklings that were incubated at three different temperatures (**Figure 2**). A summary of statistical results can be found in **Table 2**. We found that expression of MR was significantly lower in the hypothalamus at 35.0 and 35.8°C relative to 37.0°C ($p < 0.01$), with expression at about 2/3 of the levels seen at 37.0°C. Temperature did not appear to

TABLE 1 | Table of primers used for quantitative PCR.

Category	Gene	Gene name	Primer direction	Primer sequence	Amplicon size (bp)
Reference	ACTB	Actin beta	For	GCAGATGTGGATCAGCAAGC	98
			Rev	AGGGTGTGGGTGTTGGTAAC	
	GAPDH	Glyceraldehyde-3-phosphate dehydrogenase	For	TCTGGCAAAGTCCAAGTGGT	99
			Rev	CCGGAAGTGGCCATGAGTAG	
Thyroid Hormone	DIO2	Deiodinase 2	For	GATGCGTCAACAGGTGTGTC	118
			Rev	GTGTTCTCCTGCAATGATCTGA	
	DIO3	Deiodinase 3	For	GCGAGCTTTCGAGCAAGATG	82
			Rev	ACAGTATCGACAGAGCGTGG	
	KLF9	Kruppel-like factor 9	For	TGGTTCTTCAGAGCACTGCG	123
			Rev	CCCGCTTTTTCTCATCCAGC	
	NREP	Neuronal regeneration related protein	For	TGTGATGCTGCCACAGGATT	82
			Rev	CCATCAGAGCTACCTTGCCA	
	TRα	Thyroid hormone receptor α	For	TCTTCGACCTGGGCAAATCC	90
			Rev	TACCTGAGGACATGAGCAGC	
	TRβ	Thyroid hormone receptor β	For	CCACAGAACTCTTCCCTCCG	121
			Rev	TGAGAAGAGCTGGGCAATGG	
Corticosterone	GR	Nuclear receptor subfamily 3 group C member 1	For	GACCTCTCCAAGGCAGTGTC	138
			Rev	CAGGAGCCTGAAGTCCGTTT	
	MR	Nuclear receptor subfamily 3 group C member 2	For	ATTCGGAGGAAGAACTGCCC	79
			Rev	TGGACTTTCGGGCTCCTAGA	
	CCK	Cholecystokinin	For	GGGGCTCACACAATGACAAC	101
			Rev	TTTCAGGGGGCCAGTAGACA	
	BDNF	Brain derived neurotrophic factor	For	ATGTTCCACCAAGTGAGAAGAG	133
			Rev	GACCTGGGTAAGCCAAGCTG	

TABLE 2 | Summary of statistics.

Category	Gene	Gene name	Hippocampus			Hypothalamus		
			F	***N***	***p*-value**	***F***	***N***	***p*-value**
Thyroid Hormone	DIO2	Deiodinase 2	0.2634	29	0.7705	0.9964	28	0.3834
	DIO3	Deiodinase 3	0.4098	29	0.668	0.4087	28	0.6689
	KLF9	Kruppel-like factor 9	0.7097	29	0.5011	1.643	28	0.2135
	NREP	Neuronal regeneration related protein	0.1175	29	0.8897	1.689	28	0.2051
	TRα	Thyroid hormone receptor α	0.2331	29	0.7937	1.183	28	0.323
	TRβ	Thyroid hormone receptor β	0.2719	29	0.7641	0.0418	28	0.9591
Corticosterone	GR	Nuclear receptor subfamily 3 group C member 1	0.08396	28	0.9197	0.513	33	0.6038
	MR	Nuclear receptor subfamily 3 group C member 2	0.1609	28	0.8523	***5.744***	***32***	***0.0079***
	CCK	Cholecystokinin	0.08543	27	0.9184	1.952	30	0.1609
	BDNF	Brain derived neurotrophic factor	1.727	28	0.1984	1.58	32	0.2232

One way ANOVA across 3 temperature treatments within each brain region. Tukey's multiple comparisons test as a post hoc test for ANOVAs with $p < 0.05$.

affect gene expression in the three other genes evaluated (GR, CCK, and BDNF).

Comparisons Among Brain Regions

There were several general expression patterns observed in our study across brain regions without respect to temperature. First, we found that, in general, expression of thyroid hormone-related genes was substantially higher in the hypothalamus than in the hippocampus, particularly KLF9 (**Figure 1C**) and the receptors of thyroid hormone, TRα, and TRβ (**Figures 1E,F**) in 0 day-old ducklings. We also found that BDNF expression was much higher in the hippocampus than in the hypothalamus in 15 day-old ducklings (**Figure 2D**). We found that MR mRNA expression was significantly higher in the right hemisphere compared to the left hemisphere ($p = 0.015$) of the hypothalamus, but there were no other hemispheric differences in other genes/brain regions (all $p \geq 0.29$).

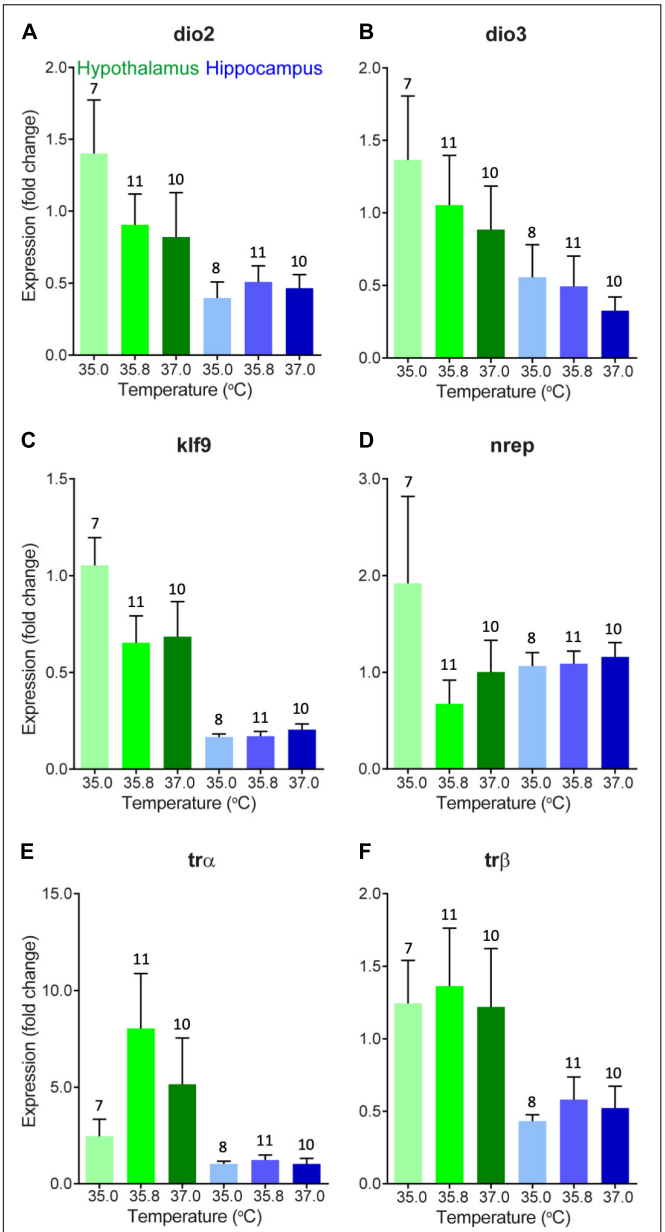

FIGURE 1 | Gene expression (mean fold change compared to 35°C hypothalamus group as a baseline) of **(A)** deiodinase 2, **(B)** deiodinase 3, **(C)** Krueppel-like factor 9, **(D)** neural regeneration related protein, **(E)** thyroid hormone receptor α, and **(F)** thyroid hormone receptor β in the hypothalamus (green) and hippocampus (blue) of newly hatched (day 0) wood duck ducklings incubated at three different incubation temperatures. Gene expression was measured using quantitative PCR of brain tissue. Fold change is a 10-base fold change because results were transformed using a square exponent (i.e., $2^{-\Delta\Delta Ct}$). Error bars indicate standard error. Numbers above bars indicate sample size.

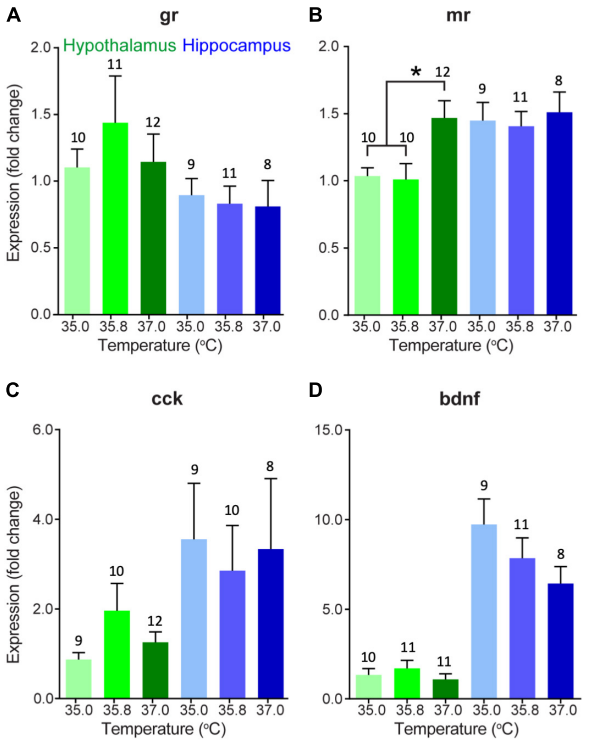

FIGURE 2 | Gene expression (mean fold change compared to 35°C hypothalamus group as a baseline) of **(A)** glucocorticoid receptor, **(B)** mineralocorticoid receptor, **(C)** cholecystokinin, and **(D)** brain-derived neurotrophic factor in the hypothalamus (green) and hippocampus (blue) of 15 day-old wood duck ducklings incubated at three different incubation temperatures. Gene expression was measured using quantitative PCR of brain tissue. Fold change is a 10-base fold change because results were transformed using a square exponent (i.e., $2^{-\Delta\Delta Ct}$). Error bars indicate standard error. Asterisk indicates significant effect of incubation temperature ($p < 0.05$), as determined by a one-way ANOVA and Tukey HSD test. Numbers above bars indicate sample size.

DISCUSSION

In this study, we investigated whether incubation temperature influences the expression of genes related to the regulation of thyroid hormone and corticosterone in the developing avian brain. We found that a 1–2°C decrease in average incubation temperature resulted in lower mRNA expression of MR in the hypothalamus of 15 day-old wood duck ducklings, which may have implications for regulation of corticosterone at baseline levels. Aside from this, we found no other significant differences in mRNA expression among incubation temperature treatments. This is surprising, considering the wide array of differences in phenotypes that are manifested as a result of small changes in incubation temperature in wood ducks and other species (DuRant et al., 2010, 2011, 2012a,b, 2013a, 2014; Nord and Nilsson, 2011, 2016; Hepp and Kennamer, 2012; Hepp et al., 2015; Berntsen and Bech, 2016), and suggests that altered expression of these particular genes at this developmental stage is likely not the mechanism underlying incubation temperature-induced developmental plasticity. On the contrary, this suggests that the expression of these genes in the brain may be robust to changes in the developmental environment, including fluctuations in circulating levels of thyroid hormone and corticosterone.

We found that MR mRNA expression in the hypothalamus was lower in ducklings incubated at 35.0 and 35.8°C than

those incubated at 37.0°C. MR has a higher affinity for corticosterone than GR and thus, mediates most of the effects of corticosterone at baseline levels (Kloet et al., 1998). Therefore, differences in MR mRNA expression may indicate the ability of ducklings to regulate normal rhythms of corticosterone levels (e.g., diurnal and circadian) and may underlie differences in baseline corticosterone levels that are seen in ducklings incubated at different temperatures (DuRant et al., 2010). Indeed, our result is consistent with what we would expect given the results from a previous study where ducklings incubated at low temperatures had higher corticosterone levels than those incubated at higher temperatures (DuRant et al., 2010). When circulating levels of corticosterone are high, we would expect that, in order to maintain homeostasis, the brain would respond by decreasing the expression of receptors to decrease its sensitivity to corticosterone. Because the effect of incubation temperature on circulating corticosterone levels is apparent on day 9 (DuRant et al., 2010), but appears to be absent by day 15 (Hope et al., 2018b), the change in MR mRNA expression that we find in this study at day 15 may be a long-term consequence of a transient surge in corticosterone prior to day 15. Given that we found this result in the hypothalamus but not in the hippocampus suggests that the paraventricular nucleus (located in the hypothalamus) has increased MR mRNA expression and may have begun to modulate circulating levels of corticosterone in the animals incubated at the highest temperature but not those incubated at the lower two temperatures. Interestingly, we did not find a significant effect of incubation temperature on GR mRNA expression in either brain region, which is important for regulation of corticosterone at stress-induced levels and negative feedback (Kloet et al., 1998). Thus, it is possible that decreased MR mRNA expression in just the hypothalamus does not translate into major differences in phenotype in these ducklings. Further research is needed to determine any causal relationships among gene expression and aspects of health and phenotype. For instance, experiments using *in situ* hybridization would shed light on any anatomical changes in expression that might be masked when using qPCR. In addition, experiments to assess rates of neurogenesis in the hippocampus may reveal an effect of incubation temperature-induced changes in corticosterone levels.

Although mRNA expression of most genes analyzed did not appear to be affected by differences in incubation temperature, we did identify some apparent differences in the expression of some genes between the hippocampus and the hypothalamus. Our results show that BDNF mRNA expression is very high in the hippocampus of day 15 ducklings relative to the expression in the hypothalamus. The hippocampus is likely undergoing substantial development at this stage, and elevated BDNF mRNA expression would contribute to cellular changes necessary for a functional hippocampus. Levels of neurogenesis are generally very high in the developing hippocampus of young Japanese quail chicks relative to older animals (Nkomozepi et al., 2018), and the same is to be expected in the wood duck hippocampus. Furthermore, there is relatively little neurogenesis in the young quail hypothalamus (Nkomozepi et al., 2018), which is consistent with our observations of higher BDNF expression in the hippocampus relative to hypothalamus.

In general, HPT-axis associated mRNA expression was higher in the hypothalamus than in the hippocampus in day 0 ducklings. This suggests that relative sensitivity to and ongoing molecular regulation of thyroid hormone signaling is likely higher in the hypothalamus than in the hippocampus at this stage in development. The elevated expression of HPT-axis associated neuroendocrine endpoints may suggest that the relative contribution of thyroid hormone to cellular and molecular mechanisms of brain development is higher in the hypothalamus and/or in the paraventricular nucleus, which regulates thyroid hormone synthesis by expression of thyrotropin releasing hormone already at this stage in development. Given the small size of regions of the hypothalamus, punches of heterogeneous populations of neurons across animals may have contributed to the variability observed in our results and masked specific differences observed in the trends noted above. Future experiments can address this issue using either single cell transcriptomics or laser capture of specific hypothalamic brain regions. In addition, circulating cerebral spinal fluid (CSF) levels of transthyretin (TTR), a choroid plexus-derived thyroid hormone distributor protein (Dickson et al., 1986; Richardson et al., 2015), may also be affected by temperature, which could allow for compensation of different circulating levels of thyroid hormone in plasma (DuRant et al., 2014). Future experiments could address this by directly measuring levels of TTR in CSF or examining the expression profile of TTR in the choroid plexus. Last, monocarboxylate transporter 8 (MCT8) transports thyroid hormone across the cell membrane, including transfer of thyroid hormone across the choroid plexus (Roberts et al., 2008). Thus, changes in expression of MCT8 or another MCT such as MCT10 in the hypothalamus, hippocampus, or choroid plexus, could be another compensatory mechanism for temperature-derived changes in circulating levels of thyroid hormone.

The aim of this study was to investigate if differences in HPT or HPA axis function, specifically the mRNA expression of genes related to thyroid hormone or corticosterone regulation, may be a mechanism underlying the pervasive effects of incubation temperature on avian offspring phenotype, health, and fitness (DuRant et al., 2013b). We found some evidence that incubation temperature influenced corticosterone-related gene expression (i.e., MR) but little evidence that it affected thyroid hormone-related gene expression. Thus, the mechanism by which developmental egg temperature leads to changes in phenotype is still largely unknown.

DATA AVAILABILITY

Datasets are available on request. The raw data supporting the conclusions of this manuscript will be made available by the authors, without undue reservation, to any qualified researcher.

ETHICS STATEMENT

This study was carried out in accordance with the recommendations of the Virginia Tech Institutional Animal Care

and Use Committee (VT IACUC). The protocol was approved by the VT IACUC.

AUTHOR CONTRIBUTIONS

SH, SD, RK, WH, and CT conceived the idea of the study. RK provided access to the field site and study system. SH conducted the field and captive animal work. SH, CB, ZH, and CT conducted the laboratory work. CT conducted the statistical analyses. SH and CT wrote the manuscript. All authors approved the final version of the manuscript.

FUNDING

This work was supported by the National Science Foundation Graduate Research Fellowship under the grant number 478969, the National Institutes of Environmental Health Sciences under the grant number R00ES022992, and is based upon the work financially supported by the United States Department of Energy under the award number DE-FC09-07SR22506 to the University of Georgia Research Foundation. The United States Department of Energy had no involvement in the study design, in collection, analysis, and interpretation of the data, or in the decision to publish this article. This work was also funded in part by the Sigma Xi Grants-in-Aid of Research, the Virginia Tech Institute for Critical Technologies and Applied Science, and the Virginia Tech Graduate Student Assembly Graduate Research Development Program. Funding for Open Access was provided by the Virginia Tech Open Access Subvention Fund and the Virginia Tech Department of Fish and Wildlife Conservation.

ACKNOWLEDGMENTS

We thank J. Hallagan, V. Alaasam, B. Vernasco, E. Lustig, A. Rhyne, K. Tugan, A. Lowe, M. C. Douglas, S. Lance, L. Bryan, and D. Scott for their immense help during the study. We also thank the Savannah River Ecology Laboratory for access to the wetlands and nest boxes. Eggs were collected under the 2015 South Carolina Department of Natural Resources Collecting Permit #05-2015.

REFERENCES

Ahmed, O. M., El-Gareib, A. W., El-bakry, A. M., Abd El-Tawab, S. M., and Ahmed, R. G. (2008). Thyroid hormones states and brain development interactions. *Int. J. Dev. Neurosci.* 26, 147–209. doi: 10.1016/j.ijdevneu.2007.09.011

Aldrich, T. W., and Raveling, D. G. (1983). Effects of experience and body weight on incubation behavior of Canada Geese. *Auk* 100, 670–679.

Bellrose, F. C., and Holm, D. J. (1994). *Ecology and Management of the Wood Duck*, eds G. C. Sanderson, R. E. McCabe, and A. Hodgins (Mechanicsburg, PA: Stackpole Books).

Bernal, J. (2007). Thyroid hormone receptors in brain development and function. *Nat. Rev. Endocrinol.* 3, 249–259. doi: 10.1038/ncpendmet0424

Berntsen, H. H., and Bech, C. (2016). Incubation temperature influences survival in a small passerine bird. *J. Avian Biol.* 47, 141–145. doi: 10.1111/jav.00688

Boelaert, K., and Franklyn, J. (2005). Thyroid hormone in health and disease. *J. Endocrinol.* 187, 1–15. doi: 10.1677/joe.1.06131

Boulton, R. L., and Cassey, P. (2012). How avian incubation behaviour influences egg surface temperatures: relationships with egg position, development and clutch size. *J. Avian Biol.* 43, 289–296. doi: 10.1111/j.1600-048X.2012.05657.x

Coe, B. H., Beck, M. L., Chin, S. Y., Jachowski, C. M. B., and Hopkins, W. A. (2015). Local variation in weather conditions influences incubation behavior and temperature in a passerine bird. *J. Avian Biol.* 46, 385–394. doi: 10.1111/jav.00581

Conway, J. C., and Martin, T. E. (2000). Effects of ambient termperature on avian incubation behavior. *Behav. Ecol.* 11, 178–188. doi: 10.1093/beheco/11.2.178

Datson, N. A., Speksnijder, N., Mayer, J. L., Steenbergen, P. J., Korobko, O., Goeman, J., et al. (2012). The transcriptional response to chronic stress and glucocorticoid receptor blockade in the hippocampal dentate gyrus. *Hippocampus* 22, 359–371. doi: 10.1002/hipo.20905

Dickson, P. W., Aldred, A. R., Marley, P. D., Bannister, D., and Schreiber, G. (1986). Rat choroid plexus specializes in the synthesis and the secretion of transthyretin (prealbumin). regulation of transthyretin synthesis in choroid plexus is independent from that in liver. *J. Biol. Chem.* 261, 3475–3478.

Duarte-Guterman, P., and Trudeau, V. L. (2010). Regulation of thyroid hormone-, oestrogen- and androgen-related genes by triiodothyronine in the brain of *Silurana tropicalis*. *J. Neuroendocrinol.* 22, 1023–1031. doi: 10.1111/j.1365-2826.2010.02047.x

DuRant, S., Carter, A., Denver, R., Hepp, G., and Hopkins, W. (2014). Are thyroid hormones mediators of incubation temperature-induced phenotypes in birds? *Biol. Lett.* 10:20130950. doi: 10.1098/rsbl.2013.0950

DuRant, S., Hepp, G., Moore, I., Hopkins, B., and Hopkins, W. (2010). Slight differences in incubation temperature affect early growth and stress endocrinology of wood duck (Aix sponsa) ducklings. *J. Exp. Biol.* 213, 45–51. doi: 10.1242/jeb.034488

DuRant, S., Hopkins, W., Carter, A., Stachowiak, C., and Hepp, G. (2013a). Incubation conditions are more important in determining early thermoregulatory ability than posthatch resource conditions in a precocial bird. *Physiol. Biochem. Zool.* 86, 410–420. doi: 10.1086/671128

DuRant, S., Hopkins, W., Hepp, G., and Walters, J. (2013b). Ecological, evolutionary, and conservation implications of incubation temperature-dependent phenotypes in birds. *Biol. Rev. Camb. Philos. Soc.* 88, 499–509. doi: 10.1111/brv.12015

DuRant, S., Hopkins, W., Hawley, D., and Hepp, G. (2012a). Incubation temperature affects multiple measures of immunocompetence in young wood ducks (Aix Sponsa). *Biol. Lett.* 8, 108–111. doi: 10.1098/rsbl.2011.0735

DuRant, S., Hopkins, W., Wilson, A., and Hepp, G. (2012b). Incubation temperature affects the metabolic cost of thermoregulation in a young precocial bird. *Funct. Ecol.* 26, 416–422. doi: 10.1111/j.1365-2435.2011.01945.x

DuRant, S., Hopkins, W., and Hepp, G. (2011). Embryonic developmental patterns and energy expenditure are affected by incubation temperature in Wood Ducks (Aix sponsa). *Physiol. Biochem. Zool.* 84, 451–457. doi: 10.1086/661749

Haftorn, S., and Reinertsen, R. E. (1985). The effect of temperature and clutch size on the energetic cost of incubation in a free-living blue tit (*Parus caeruleus*). *Auk* 102, 470–478.

Hepp, G. R., and Bellrose, F. C. (2013). "Wood Duck (Aix sponsa)," in *The Birds of North America*, ed. A. Poole (Ithaca, NY: Cornell Lab of Ornithology).

Hepp, G. R., DuRant, S. E., and Hopkins, W. A. (2015). "Influence of incubation temperature on offspring phenotype and fitness in birds," in *Nests, Eggs and Incubation: New Ideas About Avian Reproduction*, eds D. C. Deeming and S. J. Reynolds (New York, NY: Oxford University Press), 171–178. doi: 10.1093/acprof:oso/9780198718666.003.0014

Hepp, G. R., and Kennamer, R. A. (2012). Warm is better: incubation temperature influences apparent survival and recruitment of Wood Ducks (Aix sponsa). *PLoS One* 7:e047777. doi: 10.1371/journal.pone.0047777

Hepp, G. R., Kennamer, R. A., and Johnson, M. H. (2006). Maternal effects in Wood Ducks: incubation temperature influences incubation period and neonate phenotype. *Funct. Ecol.* 20, 307–314. doi: 10.1111/j.1365-2435.2006.01108.x

Hope, S., DuRant, S., Hallagan, J., Beck, M., Kennamer, R., and Hopkins, W. (2018a). Free-moving artificial eggs containing temperature loggers reveal

remarkable within-clutch variance in incubation temperature. *J. Avian Biol.* 49:e01685. doi: 10.1111/jav.01685

Hope, S., Kennamer, R., Moore, I., and Hopkins, W. (2018b). Incubation temperature influences the behavioral traits of a young precocial bird. *J. Exp. Zool. Part Ecol. Integr. Physiol.* 329, 1–12. doi: 10.1002/jez.2176

Hope, S. F., Kennamer, R. A., van Montfrans, S. G., and Hopkins, W. A. (2019). Incubation temperature and social context affect the nest exodus of precocial ducklings. *Behav. Ecol.* 30, 518–527. doi: 10.1093/beheco/ary192

Hu, F., Knoedler, J. R., and Denver, R. J. (2016). A mechanism to enhance cellular responsivity to hormone action: krüppel-like factor 9 promotes thyroid hormone receptor-β autoinduction during postembryonic brain development. *Endocrinology* 157, 1683–1693. doi: 10.1210/en.2015-1980

Kanagawa, T., Tomimatsu, T., Hayashi, S., Shioji, M., Fukuda, H., Shimoya, K., et al. (2006). The effects of repeated corticosteroid administration on the neurogenesis in the neonatal rat. *Am. J. Obstet. Gynecol.* 194, 231–238. doi: 10.1016/j.ajog.2005.06.015

Kloet, E. R. D., Vreugdenhil, E., Oitzl, M. S., and Ls, M. J. (1998). Brain corticosteroid receptor balance in health and disease. *Brain Corticost. Recept.* 19:33.

Lindström, J. (1999). Early development and fitness in birds and mammals. *Trends Ecol. Evol.* 14, 343–348. doi: 10.1016/s0169-5347(99)01639-0

Liu, Y., Yang, N., and Zuo, P. (2010). cDNA microarray analysis of gene expression in the cerebral cortex and hippocampus of BALB/c mice subjected to chronic mild stress. *Cell. Mol. Neurobiol.* 30, 1035–1047. doi: 10.1007/s10571-010-9534-8

Maniam, J., Antoniadis, C., and Morris, M. J. (2014). Early-life stress, HPA axis adaptation, and mechanisms contributing to later health outcomes. *Front. Endocrinol.* 5:73. doi: 10.3389/fendo.2014.00073

Manlove, C. A., and Hepp, G. R. (2000). Patterns of nest attendance in female wood ducks. *Condor* 102:286. doi: 10.2307/1369639

Mariette, M. M., and Buchanan, K. L. (2016). Prenatal acoustic communication programs offspring for high posthatching temperatures in a songbird. *Science* 353, 812–814. doi: 10.1002/jez.2022.Pre-

McEwen, B. S. (2001). Plasticity of the hippocampus: adaptation to chronic stress and allostatic load. *Ann. N. Y. Acad. Sci.* 933, 265–277. doi: 10.1111/j.1749-6632.2001.tb05830.x

McNabb, F. A., and King, D. B. (1993). "Thyroid hormone effects on growth, development, and metabolism," in *The Endocrinology of Growth, Development, and Metabolism in Vertebrates*, eds M. Schreibman, C. G. Scanes, and P. K. T. Pang (San Diego, CA: Academic Press, Inc.), 873–885.

McNabb, F. M. A. (2006). Avian thyroid development and adaptive plasticity. *Gen. Comp. Endocrinol.* 147, 93–101. doi: 10.1016/j.ygcen.2005.12.011

Monaghan, P. (2008). Early growth conditions, phenotypic development and environmental change. *Philos. Trans. R. Soc. Lond. B. Biol. Sci.* 363, 1635–1645. doi: 10.1098/rstb.2007.0011

Morreale de Escobar, G., Obregon, M., Escobar, and del Rey, F. (2004). Role of thyroid hormone during early brain development. *Eur. J. Endocrinol.* 151, U25–U37. doi: 10.1530/eje.0.151U025

Morse, T. E., and Wight, H. M. (1969). Dump nesting and its effect on production in wood ducks. *J. Wildl. Manag.* 33, 284–293.

Murakami, S., Imbe, H., Morikawa, Y., Kubo, C., and Senba, E. (2005). Chronic stress, as well as acute stress, reduces BDNF mRNA expression in the rat hippocampus but less robustly. *Neurosci. Res.* 53, 129–139. doi: 10.1016/j.neures.2005.06.008

Nkomozepi, P., Mazengenya, P., and Ihunwo, A. O. (2018). Changes in neurogenesis with post-hatching age in the male Japanese quail (*Cortunix japonica*) brain. *Acta Neurobiol. Exp.* 78, 173–186. doi: 10.21307/ane-2018-016

Nord, A., and Nilsson, J.-A. (2016). Long-term consequences of high incubation temperature in a wild bird population. *Biol. Rev. Camb. Philos. Soc.* 12:20160087. doi: 10.1098/rsbl.2016.0087

Nord, A., and Nilsson, J. -Å (2011). Incubation temperature affects growth and energy metabolism in blue tit nestlings. *Am. Nat.* 178, 639–651. doi: 10.1086/662172

Pop, V. J., Kuijpens, J. L., van Baar, A. L., Verkerk, G., van Son, M. M., de Vijlder, J. J., et al. (1999). Low maternal free thyroxine concentrations during early pregnancy are associated with impaired psychomotor development in infancy: maternal FT4 and psychomotor development in infancy. *Clin. Endocrinol.* 50, 149–155. doi: 10.1046/j.1365-2265.1999.00639.x

Reid, J. M., Monaghan, P., and Ruxton, G. D. (2000). The consequences of clutch size for incubation conditions and hatching success in starlings. *Funct. Ecol.* 14, 560–565. doi: 10.1046/j.1365-2435.2000.00446.x

Richardson, S. J., Wijayagunaratne, R. C., D'Souza, D. G., Darras, V. M., and Van Herck, S. L. (2015). Transport of thyroid hormones via the choroid plexus into the brain: the roles of transthyretin and thyroid hormone transmembrane transporters. *Front. Neurosci.* 9:66. doi: 10.3389/fnins.2015.00066

Roberts, L. M., Woodford, K., Zhou, M., Black, D. S., Haggerty, J. E., Tate, E. H., et al. (2008). Expression of the thyroid hormone transporters monocarboxylate transporter-8 (SLC16A2) and organic ion transporter-14 (SLCO1C1) at the blood-brain barrier. *Endocrinology* 149, 6251–6261. doi: 10.1210/en.2008-0378

Roy Nielsen, C. L., Gates, R. J., and Parker, P. G. (2006). Intraspecific nest parasitism of wood ducks in natural cavities: comparisons with nest boxes. *J. Wildl. Manag.* 70, 835–843. doi: 10.2193/0022-541x(2006)70%5B835:inpowd%5D2.0.co;2

Salinas, S., and Munch, S. B. (2012). Thermal legacies: transgenerational effects of temperature on growth in a vertebrate. *Ecol. Lett.* 15, 159–163. doi: 10.1111/j.1461-0248.2011.01721.x

Sapolsky, R. M., and Meaney, M. J. (1986). Maturation of the adrenocortical stress response: neuroendocrine control mechanisms and the stress hyporesponsive period. *Brain Res. Rev.* 11, 65–76. doi: 10.1016/s0006-8993(86)80190-1

Semel, B., and Sherman, P. W. (1986). Dynamics of nest parasitism in Wood Ducks. *Auk* 103, 813–816.

Semel, B., Sherman, P. W., and Byers, S. M. (1988). Effects of brood parasitism and nest-box placement on wood duck breeding ecology. *Condor* 90, 920–930. doi: 10.2307/1368849

Thompson, C. K., and Cline, H. T. (2016). Thyroid hormone acts locally to increase neurogenesis, neuronal differentiation, and dendritic arbor elaboration in the tadpole visual system. *J. Neurosci.* 36, 10356–10375. doi: 10.1523/JNEUROSCI.4147-15.2016

Waddington, C. (1942). Canalization of development and the inheritance of acquired traits. *Nature* 150, 563–565. doi: 10.1038/150563a0

Conflict of Interest Statement: The authors declare that the research was conducted in the absence of any commercial or financial relationships that could be construed as a potential conflict of interest.

Copyright © 2019 Hope, Buenaventura, Husain, DuRant, Kennamer, Hopkins and Thompson. This is an open-access article distributed under the terms of the Creative Commons Attribution License (CC BY). The use, distribution or reproduction in other forums is permitted, provided the original author(s) and the copyright owner(s) are credited and that the original publication in this journal is cited, in accordance with accepted academic practice. No use, distribution or reproduction is permitted which does not comply with these terms.

frontiers in Physiology

REVIEW
published: 22 January 2020
doi: 10.3389/fphys.2019.01634

Phenotypic Switching Resulting From Developmental Plasticity: Fixed or Reversible?

*Warren W. Burggren**

Developmental Integrative Biology, Department of Biological Sciences, University of North Texas, Denton, TX, United States

The prevalent view of developmental phenotypic switching holds that phenotype modifications occurring during critical windows of development are "irreversible" – that is, once produced by environmental perturbation, the consequent juvenile and/or adult phenotypes are indelibly modified. Certainly, many such changes appear to be non-reversible later in life. Yet, whether animals with switched phenotypes during early development are unable to return to a normal range of adult phenotypes, or whether they do not experience the specific environmental conditions necessary for them to switch back to the normal range of adult phenotypes, remains an open question. Moreover, developmental critical windows are typically brief, early periods punctuating a much longer period of overall development. This leaves open additional developmental time for reversal (correction) of a switched phenotype resulting from an adverse environment early in development. Such reversal could occur from right after the critical window "closes," all the way into adulthood. In fact, examples abound of the capacity to return to normal adult phenotypes following phenotypic changes enabled by earlier developmental plasticity. Such examples include cold tolerance in the fruit fly, developmental switching of mouth formation in a nematode, organization of the spinal cord of larval zebrafish, camouflage pigmentation formation in larval newts, respiratory chemosensitivity in frogs, temperature-metabolism relations in turtles, development of vascular smooth muscle and kidney tissue in mammals, hatching/birth weight in numerous vertebrates,. More extreme cases of actual reversal (not just correction) occur in invertebrates (e.g., hydrozoans, barnacles) that actually 'backtrack' along normal developmental trajectories from adults back to earlier developmental stages. While developmental phenotypic switching is often viewed as a permanent deviation from the normal range of developmental plans, the concept of developmental phenotypic switching should be expanded to include sufficient plasticity allowing subsequent correction resulting in the normal adult phenotype.

Keywords: development, plasticity, evolution, environment, critical window

OPEN ACCESS

Edited by:
Sonnet Jonker,
Oregon Health & Science University, United States

Reviewed by:
Ivan Gomez-Mestre,
Estación Biológica de Doñana (EBD), Spain
Kent L. Thornburg,
Oregon Health & Science University, United States

***Correspondence:**
Warren W. Burggren
burggren@unt.edu

Specialty section:
This article was submitted to Embryonic and Developmental Physiology, a section of the journal Frontiers in Physiology

Received: *16 September 2019*
Accepted: *27 December 2019*
Published: *22 January 2020*

Citation:
Burggren WW (2020) Phenotypic Switching Resulting From Developmental Plasticity: Fixed or Reversible? Front. Physiol. 10:1634. doi: 10.3389/fphys.2019.01634

DEVELOPMENT, PLASTICITY AND PHENOTYPE

That developing animals are shaped by their environment is not a new concept. Aristotle deserves first credit for recognizing that animals will develop different forms when raised in different environments (Aristotle, 350BC). Of course we now frame these observations as changes in gene expression influenced by environmental stressors. In this essay I first briefly expand upon the

Gene X Environment context to include development, epigenetics and other factors, and then consider whether the product of these interactions (e.g., modified phenotypes enabled by developmental plasticity) are fixed or reversible.

Moving Beyond the Gene–Environment Interaction Paradigm in the Context of Development

Phenotypic plasticity is a venerable, long-standing concept, and is often framed as the interactions of genes (G) by environment (E), creating a specific phenotype that is the result of so-called 'G × E' interactions. This concept has been reviewed dozens of times as both a general concept as well as in specific contexts such as human pathologies and disease – an entry into the voluminous literature can be gained from Moffitt et al. (2005), Manuck and McCaffery (2014), Halldorsdottir and Binder (2017), Josephs (2018), and Saltz et al. (2018). Much of the discussion of environmentally induced changes in gene expression resulting in modified phenotype does not explicitly involve a developmental component, though certainly much is known about developmental phenotypic plasticity in both plants and animals – for reviews see West-Eberhard (2005), Spicer and Rundle (2007), Uller (2008), de Jong and Leyser (2012), Bateson et al. (2014), Standen et al. (2014), Burggren and Mueller (2015), Bateson (2017), and Burggren (2018). Thus, for developing animals, the classic G × E framework is expanded to the more encompassing (Genes × Environment) × Development, or (G × E) × D. Note that it has been suggested that Time (T) and even allometry be a component of this construct (Pigliucci et al., 1996), but in this essay we consider development as a distinct sub-set of time (Dubansky, 2018).

It is becoming increasingly clear that, to this basic formula describing developmental phenotype, we must add an *epigenetic* component ('Epi') representing intragenerational and especially intergenerational environmental experiences resulting in modified gene expression (Skinner, 2011; Jablonka, 2013; Burggren and Crews, 2014; Skinner, 2015; Burggren, 2016, 2017). The influences of epigenetic readers, writers and erasers on the epigenetic markers that influence gene expression can result from changes ranging from minutes to across multiple generations. Thus, the formula G × E × D, which assumes that gene expression results from contemporaneous environmental conditions, can be expanded to G × (E + Epi) × D. This new expression now includes both within-life altered gene expression patterns as well as both known and unknown epigenetic factors from past parental/ancestral experiences through altered gene expression patterns in germ cells. These epigenetic changes, combined with ambient environmental affects on gene expression, contribute to the control of the phenotype that emerges during development. Importantly, these genomic/epigenomic interactions form the basis for the differing phenotypic outcomes that lead to successful survival in stressful environments.

Finally, an additional source of phenotype switching has been proposed to emerge from stochastically driven cell differentiation during early development that is amplified as tissue differentiation and growth progresses (Woods, 2014). Developing animals might then be a mosaic of both programed and stochastic development. As a consequence, the originally lauded but now limiting 'G × E' construct could be expanded to G × (E + Epi) × (D × S), where S represents the influence of stochasticity. In suggesting this, it is realized that there will doubtlessly be disagreement as to where the brackets are placed in this 'formula', whether the × symbols should in fact be + signs, etc. etc. The point of this or any other next-generation formulae encompassing these concepts is that the G × E paradigm is now more properly regarded as an overly simplistic, historical view of how animals interact with their environment during development and maturation.

All of these factors – genes, environment, development, epigentic markers and stochastic changes in the developmental plan – interact together in complex and sometimes unpredictable ways, and lead to modified phenotypes resulting from developmental phenotypic plasticity. Importantly, however, there is also a crucial element of *timing*, in that the expression of genes, appearance of stressors in the environment, progression of development, and the writing and erasing of epigenetic markers all march to the beat of a different drummer. No where is this more evident than in the concept of "critical windows" during development, which will now be explored.

Critical Windows, Developmental Plasticity, and Phenotype Switching

To heavily paraphrase T. Dobzhansky's famous phrase on biology and evolution (Dobzhansky, 1973), nothing in *development* makes sense except in the light of *critical windows* (also known as sensitive periods). The terms 'critical moment' and 'sensitive period' were first used in the early 20th century by the influential embryologist Charles Stockard, who showed that oxygen deprivation during certain specific periods of development created developmental anomalies in *Fundulus,* trout and frogs (Stockard, 1921). These observations helped explain the relationship between time in development and susceptibility to environmental influences, a relationship further explored in Nobel laureate Hans Spemann's *Embryonic Development and Induction* (Spemann, 1938). Likely drawing upon the analogy with biology, in the late 1950s neurologists Wilder Penfield and Lamar Roberts advanced the "critical period hypothesis" related to neural development and language acquisition (Penfield and Roberts, 1959). Lenneberg (1967) further promoted this notion for human development in his book *Biological Foundations of Language*. Noteworthy is that, somewhat in contrast to the embryological literature that focuses on maladaptations (usually morphological) emerging during critical windows, in the human linguistics and psychological literature, the critical window is often regarded as a period when certain environmental exposures are actually necessary and important for language development and other aspects of normal development, e.g., Hensch and Bilimoria (2012).

Currently, investigators typically describe a critical window as a specific, defined period during development when G × E × D (and, studied less often, [G × (E + Epi) × D] interactions result in subsequently switched (modified) phenotypes that differ from the normally expected range of developmental trajectory. Numerous authors have offered up similar definitions – e.g., Kunes and Zicha (2006), Ferner and Mortola (2009), Ali et al. (2011), Burggren and Reyna (2011), Vickers (2011), Voss (2013), Alvine and Burggren (2014), Burggren et al. (2014), Burggren and Mueller (2015), Eme et al. (2015), and Pelster and Burggren (2018).

The concept of critical window is the subject of considerable investigation in disciplines ranging from physiology to ecology to toxicology. Indeed, at the time of the writing of this article, the Pubmed data base listed >4400 articles evoking critical windows (the majority being in animal rather than plant development), and >32,000 articles describing sensitive periods in a human psychological context. While there is huge variation in observations and experiments on critical windows and their effects, **Table 1** outlines some of the key general characteristics of critical windows, along with some examples of resulting phenotype switching.

ARE CHANGES THAT ARE EVOKED DURING CRITICAL WINDOWS REVERSIBLE OR FIXED?

Definitions and Semantics

Most organisms typically have at least some capacity to counteract potentially negative effects of environmental fluctuations that they experienced during development or even later in life as adults. Yet, a commonly (though not universally) posited key characteristic of developmental phenotypic plasticity is that a switched phenotype produced specifically as a result of developmental plasticity is essentially *irreversible* – e.g., Wilson and Franklin (2002); West-Eberhard (2003), Matesanz et al. (2010, 2012), Utz et al. (2014), Woods (2014), Senner et al. (2015), Beaman et al. (2016), Slotsbo et al. (2016), and Noh et al. (2017). This view is especially held to be true when prevalent when phenotypic switching occurs during a narrow developmental window. Interestingly, Woods (2014) employs the term phenotypic *flexibility* for reversible (or additional new) phenotypic changes. Utz et al. (2014) uses the term *reversible* if a trait's phenotype "*. . .can be reversed to the original state.*" Some authors do not distinguish between 'plasticity' and 'flexibility' or even see the need to, whereas others painstakingly lay out their ground for the irreversibility of phenotypic modification during development – for discussion, see Debat and David (2001), Gabriel (2005), Woods (2014), and Sommer et al. (2017). Investigators studying cold hardening in developing insects have differentiated between irreversible "*developmental acclimation*" and reversible "*short-term acclimation*" (Noh et al., 2017). Finally, several studies have differentiated between 'developmental' and 'reversible' environmentally induced phenotypic modification (Angiletta, 2009; Munday et al., 2013; Utz et al., 2014; Donelson et al., 2017).

Regarding definitions, it is not the intention of this review to add to the existing definitional morass surrounding the definition of developmental phenotypic plasticity and resultant phenotypic switching[1] (Korzybski, 1933). Yet, perhaps the additional term 'correctable' should be inserted into the discussion of terms. Why? Correctable indicates that the normal range of adult phenotypes could still be achieved despite potentially transient phenotypic modification during development – that is, the switched phenotype can be corrected to the phenotype that would result if gene expression had not been modified by environmental or epigenetic influences. This would leave the term 'reversible' to apply to the unusual phenomenon of a true reversal (backtracking) along a developmental pathway (which can indeed occur, as discussed below). Yet, the problem with this reversible/correctable semantic conundrum is that the term 'correctable' suggests that the modified phenotype resulting from developmental plasticity is actually sub-optimal (i.e., needs to be 'corrected'). In fact, the modified phenotype emerging from (enabled by) developmental plasticity might, of course, actually be advantageous under current environmental conditions – e.g., Toth and Hettyey (2018); Bautista and Burggren (2019), and Mendez-Sanchez and Burggren (2019). Not being able to resolve this issue here, this essay will nonetheless use the commonly acceptable term reversible with a parenthetical inclusion of correctable to remind the reader of the complexity of developmental plasticity.

We Find What We Look For

Importantly, the prevailing view that phenotypic switching during critical windows of development is irreversible, likely emerges from a truth buried within developmental dogma. In fact, many of the described examples of phenotypic switching induced during an often-narrow critical window for a trait indeed appear to be irreversible (Burggren and Reyna, 2011; Daskalakis et al., 2013; Burggren and Mueller, 2015; Senner et al., 2015; Lloyd and Saglani, 2017). Moreover, stark examples such as the production of 2-headed frogs induced by hypoxia experienced during a critical window (Stockard, 1921) certainly contribute to the notion that switched phenotypes cannot be reversed. Yet, developmental critical windows are typically quite brief periods during a much longer period of overall development, and these extended developmental periods can potentially allow sufficient time for the animal to regain some or all of its normal phenotype.

[1]The philosopher Popper (1970) suggested that "*. . . we should altogether avoid, like the plague, discussing the meaning of words.*" While one can be sympathetic to his viewpoint, due diligence requires acknowledging differing definitions in the long-standing debate as to the reversibility of effects resulting from developmental plasticity. Underscoring this point, the two reviewers of this manuscript had differing opinions on whether the field viewed phenotypic switching as reversible or irreversible when it occurred during development. Ultimately, perhaps Alfred Korzybski (1879–1950), the father of the field of General Semantics, got it right when he posited that "*Whatever you say it is, it isn't*" (Korzybski, 1933).

TABLE 1 | Characteristics of critical windows for development.

Characteristics of critical windows	Description	Examples	References
Timing in Development of Critical Windows	Critical developmental windows can occur from shortly after egg fertilization until achievement of sexual maturity.	Human psychiatric illnesses frequently first manifest during critical windows in teenagers, potentially associated with gut microbiome dysfunction.	McVey Neufeld et al., 2016
		Human cardiovascular form and function impacted by environmental toxicants during critical windows starting as early as week 2 after conception	Lage et al., 2012
Duration ('Width') of Critical Window	Finite "width" to critical window – i.e., distinct onset and closing of window, but interpretation of critical window "edges" is dependent upon stressor dose	Cardiac development in chicken embryos primarily sensitive during week 2 of 3 weeks incubation	Chan and Burggren, 2005
		Gonad differentiation in zebrafish between 30–44 days post-fertilization	Quintaneiro et al., 2019
		Modeling of critical window as a 3D construct of time, dose and phenotype	Burggren and Mueller, 2015
Duration of Switched Phenotype	Phenotypic switching irreversible, persisting through subsequent life stages	Larval hypoxia has long-term effects on protein digestion and growth in juvenile European sea bass	Zambonino-Infante et al., 2017
		Chicken embryos show aberrant aortic arch morphogenesis when hemodynamic variables are manipulated specifically at Stage 21.	Kowalski et al., 2013
Number of Critical Windows Per Trait	Typically only one, but multiple critical windows can exist for same trait	Lipid and glucose metabolism in adult sheep is similarly affected by undernutrition early in gestation as well as immediately postnatally	Poore et al., 2010
		Correction of structural abnormalities in mouse brain cortex have multiple critical windows	Cox et al., 2018
Stressors Acting During Critical Window	Stressors can be intrinsic or extrinisic (environmental) factors.	Odors (aversive or attractive) in first week post-eclosion fruit fly larvae alter olfactory circuitry	Golovin and Broadie, 2016
		Hypoxia during middle third of avian incubation alters gross morphology and metabolic physiology	Dzialowski et al., 2002
Dose Effects During Critical Window	Phenotypic switching during critical windows is dose-dependent	Body mass changes in *Artemia* during early development are dependent on strength of environmental salinity	Mueller et al., 2016
		Hypoxia-induced alteractions of morphology and physiology of chicken embryo show differential responses to 13 and 15% oxygen	Zhang and Burggren, 2012
Sex Differences in Critical Window Susceptibility for Same Trait	Phenotypic switching during critical windows is sex-dependent	Prenatal critical window for oranotin toxicant exposure in rats results in greater permanent phenotype switching in males compared to females	Grote et al., 2009
		Prenatal critical window for particulate air pollution exposure causes phenotype switching in human male but not female children	Hsu et al., 2015
Organ System Differences in Critical Windows	Timing of development of window differs between organ systems within an organism	Critical window for hypoxic effects on heart mass and blood pressure are considerably different in timing and width in embryonic alligator hearts	Tate et al., 2015
		Critical windows for sensitivity to environmental toxicant differ in timing and duration for immune and respiratory systems in humans	Dietert et al., 2000
Population Differences in Critical Windows For Same Trait	Timing and width of critical window for a particular phenotypic trait varies between different populations – i.e., "heterokairy"	Human populations differ in critical window for infant weight gain and its effect on adult adiposity	Wells, 2014
		Hypersalinity delays onset of heartbeat and changes timing of foot attachment and eye spot formation in the euryhaline snail *Radix balthica*	Tills et al., 2010
Species Differences in Critical Windows For Same Trait	Timing of window for a particular phenotypic trait varies between different species – i.e., "heterochrony"	Critical windows for nephrogenesis and morphologica renal development differ between dog, pig, rabbit, monkey, mouse, and rat	Frazier, 2017
		Critical windows for motor activity and motor function performance identified by exposure to environmental neurotoxins differ in rats and mice	Ingber and Pohl, 2016
		Critical window for gut microbiome establishment differs between wood frogs, green frogs and bullfrogs	(Ingber and Pohl, 2016)

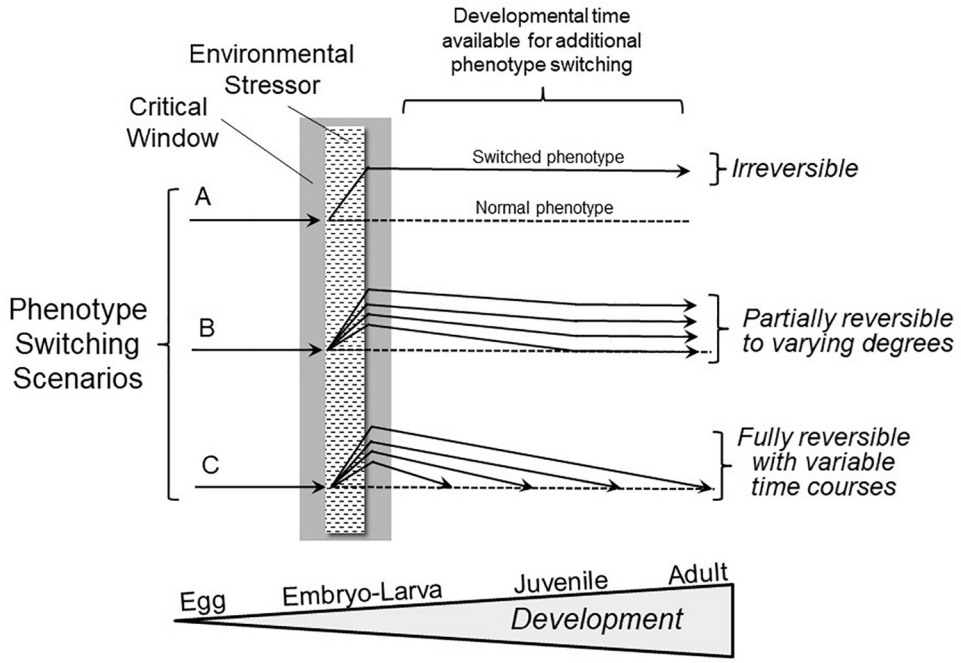

FIGURE 1 | Hypothetical outcomes involving phenotype switching scenarios following exposure to adverse environments during critical windows in development. Scenario A shows the conventional, highly discussed condition of irreversible switching of phenotype induced by an environmental stressor during the critical window. Scenario B depicts a far less frequently studied situation of phenotypic switching initiated during a critical window that, in fact, is reversible to varying degrees. Scenario C indicates that there may be complete reversibility of phenotypic modifications occurring at varying rates during subsequent development. The extent and rate of phenotype reversal may relate to the extent of the difference between the altered and normal (typical) juvenile/adult phenotypes. Importantly, either a single trait might show different degrees of reversibility, or multiple traits could show a range of degrees of reversal to the normal phenotype.

As Utz et al. (2014) comment, "*Most theoretical investigations on plasticity are restricted to irreversible plasticity. i.e., the expression of a specific phenotype is determined during development and remains unchanged during the whole life of an organism. . .*". As these authors go on to indicate, there are three categories of traits – non-plastic, irreversibly plastic, and reversibly plastic. An important point that Utz et al. (2014) make, and that I wish to underscore in this essay, is that most studies have focused on irreversible traits. Such traits are certainly in abundance, but do not represent the full picture of developmental phenotypic plasticity and phenotype switching. Consequently, a well populated database has been developed that is skewed toward non-reversible traits. Put differently, if one looks for irreversible phenotypic switching, one will most certainly find it. As a result, an overly restricted working definition of developmental phenotypic plasticity seems to have emerged in which the concept of reversibility has little or no traction. Against this backdrop, Lande (2014) advocates moving beyond previous theory that assumes a constant adult phenotype results from plasticity during development, to a more nuanced view that considers multiple factors. These include the cost of plasticity, the environmental variance and predictability, and developmental rates and characteristics (Lande, 2014).

Notably, an overly narrow definition has prevailed to date largely because we are not conducting experiments specifically designed to reveal reversible phenotype switching during development. Consider Hempel's and Popper's "Ravens Paradox," where finding a single white raven falsifies the hypothesis that all ravens are black (Hempel, 1945; Popper, 1959). Following their logic, we only need to find one example of a phenotypic modification occurring during a developmental critical window that can be subsequently reversed ("the white raven") to falsify the hypothesis that all phenotypic switching during development is irreversible ("all ravens are black"). If reversible phenotypic switching initially induced during the critical window were to occur, what would it actually look like? **Figure 1** presents a broad view of the expression of developmental plasticity that includes reversible phenotypic switching. In the most highly studied scenario (**Figure 1A**) changes evoked by an environmental stressor are deemed irreversible, and as indicated earlier, there are certainly many examples of this phenomenon. However, Scenarios B and C provide for varying degrees and rates of reversibility of phenotypes initially produced as a result of stressors during the critical window.

It is important to emphasize that there are no theoretical or practical objections to reversal of phenotypic switching originating during a developmental critical windows. But, if the field of developmental biology chooses to define that particular subset of clearly non-reversible phenotypic changes occurring during development as, in fact, representing all 'developmental phenotypic plasticity,' we exclude real phenomena that don't fit into that overly restrictive definition. Moreover, it means we would have to come up

with yet another term to cover those examples of reversible (correctable) phenotypic switching that are induced during the critical window for development. Perhaps more efficient is simply convincing the reader that there are, indeed, clear examples of reversible phenotypic switching resulting from developmental phenotypic plasticity. Let us now consider the considerable body of evidence for reversible phenotypic plasticity.

REVERSIBLE DEVELOPMENTAL PHENOTYPIC SWITCHING: THE EVIDENCE

Reversible (Correctable) Phenotypic Switching During Development

In the most common pattern of reversible phenotypic switching, a developing organism takes a novel developmental trajectory in response to an environmental stressor, producing a modified phenotype which may be either advantageous or deleterious. Then, when the stressor inducing this modified phenotype disappears, the organism takes a second novel developmental trajectory returning it to the pathway leading to the normal range of adult phenotypes that may well be more appropriate for the typical environmental condition (**Figures 1B,C**). Consider the following specific examples.

Invertebrates

Cold tolerance as adults can be acquired during cold exposure during early larval development in the fruit fly, *Drosophila melanogaster*. However, this modified, adaptive phenotype can be reversed during acclimation in the adult fly (Slotsbo et al., 2016). Interestingly, heat tolerance acquired during high temperature exposure as a fly larva is only partially reversible. This is reminiscent of Scenario B in **Figure 1**, where there can even be different degrees of reversibility for different phenotypic traits.

In the butterfly *Bicyclus anynana,* development temperature affects the size of the egg ultimately laid by the mature adults, with butterflies reared in cool temperatures producing larger eggs (Fischer et al., 2003). However, when the fully matured adults are switched to warmer temperatures for ∼10 days, they will revert to the phenotype that lays smaller eggs, as if they had been reared as larvae in cooler temperatures. Thus, these temperature-induced phenotype modifications originating in larval development are quite reversible (Brakefield et al., 2007).

Developmental phenotypic switching of mouth formation has been examined in the model nematode *Pristionchus pacificus* (Werner et al., 2017). Different culture conditions (e.g., liquid vs. agar) during development "toggle" one of two distinctive differences in mouth form phenotype. Importantly, these effects are both immediate as well as reversible when culture medium is switched, indicating that the developmental trajectory of mouth formation can be adjusted by each set of gene-environment interactions resulting from culture conditions.

Vertebrates

Larval newts (*Lissotriton boscai*) at stage 45–47 change pigmentation as they develop in response to different ambient backgrounds, with light, high-reflecting environments inducing depigmentation and dark, low-reflecting environments resulting in enhanced pigmentation. Yet, pigment induction is completely reversible in adults depending upon backgrounds (Polo-Cavia and Gomez-Mestre, 2017).

Temperature-metabolism relations in the turtle *Trachemys scripta elegans* are strongly affected by temperature regimes during egg incubation (Ligon et al., 2012). However, the metabolic compensation to temperature, evident in hatchlings through both measurements of resting metabolic rate and growth rate, can be later reversed irrespective of life stage and irrespective of the embryonic developmental stage at which temperature stimuli were delivered.

Nutrient restriction during the first week of development in larval *Xenopus laevis* results in the failure of neural progenitors to proliferate, but this effect can be corrected by a return to normal nutrition, affected by a subsequent 10-fold increase in cell proliferation stimulated by feeding (McKeown et al., 2017). Feeding also rescues nutrition restricted-induced decreases body length and brain tectal volume. Interestingly, the ability to rescue earlier developmental defects in the central nervous system induced by nutrient restriction during the CNS critical window (up to 7 days of development), does itself, have a critical window (≤9 days).

Numerous examples exist of reversal of modified phenotypes at the cellular and molecular levels in vertebrates. Branching morphogenesis in the renal ureteric bud/collecting duct involve new branches sprouting from the tips of existing branches rather than from the stalks of the branches. However, when the tips are removed, the stalks can form new tips, indicating that the developmental transition from tip to stalk morphology during branching is reversible (Sweeney et al., 2008). Vascular smooth muscle cells show both extensive phenotypic plasticity and diversity during development. Environmental cues (e.g., mechanical stress, oxygen partial pressure) and the genes that respond to them result in phenotypic switching of smooth muscle cells when experiencing vascular injury, for example. This phenotype switching of both form and function during development is, however, fully reversible, likely involving epigenetic markers (Owens, 2007).

Humans

A well-documented and readily understood example of the effects of an adverse environment during critical windows for development is so-called 'catch-up' or compensatory growth in infants and children. Though these terms are frequently used interchangeably, a stricter definitional approach in the non-clinical literature uses "compensatory" to apply to an acceleration of growth rate, while "catch-up" more broadly allows for a return to conspecific control levels, which can be achieved by an extended period of growth with actual growth rate remaining at optimal levels (Arendt, 1997; Hector and Nakagawa, 2012). In humans, uterine nutritional insufficiency (an environmental stressor for the fetus) can result in abnormally low birth

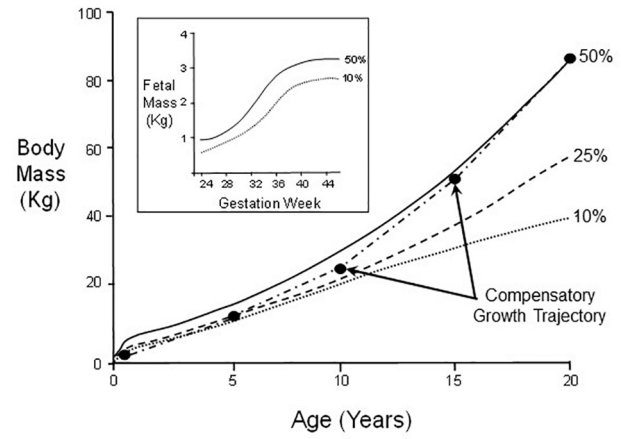

FIGURE 2 | Body mass changes in male humans between birth and age 20. Indicated are growth curves for 50th, 25th, and 10th percentiles of the population. A hypothetical example of catch-up growth is also indicated. Inset: Fetal mass as a function of gestation week for 50th and 10th percentiles.

weight. However, some low birth weight infants can exhibit compensatory growth, a post-natal period of greater than typical calorie acquisition and conversion to body mass at higher rates than a normally growing infant/child (**Figure 2**). Compensatory growth results in an atypical developmental trajectory that ultimately restores body mass to levels typical of its normal control cohort after a few years of early childhood (Cho and Suh, 2016; Martin et al., 2017). This is not "just" slowed growth, but rather an actual departure from normal range of phenotype for the infant's age, which is reversed (corrected) in later development.

Noteworthy is that while normal body mass *per se* is restored by adulthood (Scenario C in **Figure 1**), other general pathological phenotypic modifications resulting from nutrition restriction during critical windows for fetal development or early neonatal growth may not themselves be fully reversed (Scenario B in **Figure 1**). In the case of very low birth weight infants, this nutritional restriction during early development can lead to so-called "metabolic syndrome" in some adults, whereby increased risk exists for heart disease, stroke and type 2 diabetes (Martin et al., 2017). This underscores that any general phenotypic switching during development may simultaneously consist of both reversible *and* irreversible/pathological components (**Figure 1**). Consequently, experimenters need to be watchful for both categories of phenomena in experiments on developmental phenotypic switching, especially as there may be irreversible sub-components of a phenotype that are not revealed until development is complete.

Compensatory growth, and the related 'catch-up growth' during development, are not strictly a human or even mammalian phenomena. An extensive (but not exhaustive) meta-analysis identified these phenomena in 38 mammalian, 91 piscine, 39 avian and 30 arthropod species (Hector and Nakagawa, 2012). While not analyzed in this study, compensatory growth also occurs in amphibians and reptiles – e.g., Roark et al. (2009) and Burraco et al. (2019). Interestingly, the evolutionarily highly conserved nature of compensatory or catch-up growth suggests a high degree of biological significance. Yet, also important to note is that restoration of 'body mass' does not reflect appropriate restoration of all tissue types in proportion. In humans, the compensatory growth is often due to postnatal fat accumulation at the expense of muscle, in addition to the metabolic syndrome mentioned earlier (Okada et al., 2015). Thus, while body mass compensation may be obtained, the phenotype aberration caused by early undernutrition is not really fully corrected/reversed. Somewhat similarly, in lizards, regrowth of automized tails yields a structure with higher fat content than the original (Russell et al., 2015).

"Truly Reversible" Phenotypic Switching During and After Development

More extreme cases of true reversal involve an animal actually backtracking along the normal developmental trajectory. In the hydrozoans *Turritopsis dohrnii* (the 'immortal jellyfish') and *Hydractinia carnea*, for example, individuals follow one of several environment-dependent alternative developmental trajectories toward the adult medusa. Astonishingly, they can actually undergo an environmentally induced regression from the sexually mature medusa back into the polyp form when faced with stress in the form of starvation or elevated temperature or salinity. This regression can occur in as little as 3 days, increasing chances of survival in the face of environmental stress (Bavestrello et al., 2000; Schmich et al., 2007; Lisenkova et al., 2017).

Similar examples of such 'reversible acclimation' have been observed in the acorn barnacle, *Balanus glandula*. When adult barnacles reared in quiet water are transferred to elevated seawater flows, they can regain larval segments of their feeding legs lost during typical development (Kaji and Palmer, 2017).

Physiological reversal along developmental pathways has been documented in larvae and adults of the American bullfrog, *Lithobates catesbeianus* (Santin and Hartzler, 2016). Neuroventilatory responses to CO_2 and O_2 involved in modulating lung breathing were reduced in aquatic overwintering adult bullfrogs. More than just attenuated, however, the gas sensitivity profiles actually reverted to that of water larvae tadpoles.

Mature human osteoblasts subjected to simulated microgravity show altered pro-osteogenic determinants and a downregulation of bone differentiation marker and adhesive proteins. In a complete reversal of the normal developmental process, this pattern of cellular dedifferentiation allows reacquisition of migration potential by the primary osteoblasts (Gioia et al., 2018).

The examples of truly reversible development above bring into stark relief the many exceptions to the common viewpoint that modified phenotypes with their origins within developmental critical windows can, indeed, be reversible. Thus, a more comprehensive view of phenotypic switching enabled by developmental phenotypic plasticity is presented in

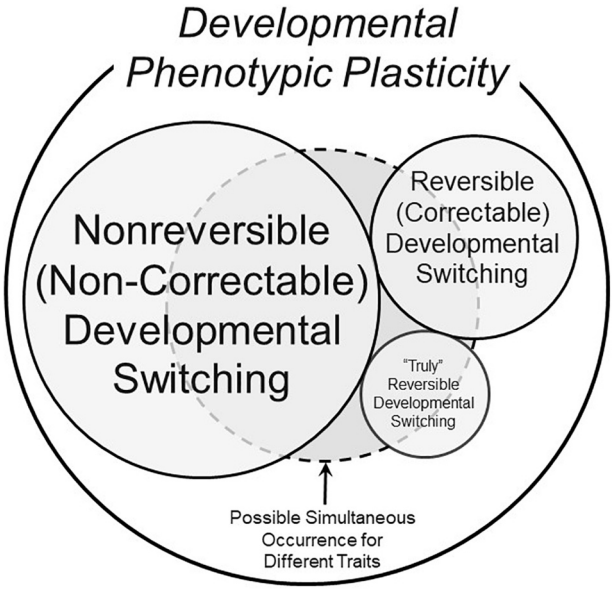

FIGURE 3 | A schematic of possible components of the overall phenomenon of developmental phenotypic plasticity. This Venn diagram makes the assumption that not all phenotypic changes induced by stressors during developmentally critical windows are non-reversible (non-correctable) – see text for further discussion of definitions. The different sizes of the circles and text are meant to convey the very approximate prevalence of the form of developmental switching. The dashed circle represents the fact that all three types of developmental phenotypic switching could occur simultaneously in an animal, each for a different trait.

Figure 3, which includes developmental phenotypic switching in three categories: traditional non-reversible (non-correctable), reversible (correctable) and "truly" reversible.

Non-exclusivity of Types of Phenotype Switching

Not all traits affected by development in a single animal necessarily follow the same pattern. As Lande (2014) indicates, "*. . .many phenotypic characters of an individual develop and fluctuate continuously and reversibly throughout life in response to environmental change.*" Important to note is that, all too often (at least to this animal physiologist), "phenotype" refers to easily observed morphological features (e.g., size, color). In fact, an organism could for example be switching its physiology, biochemistry and behavior but not its gross external physiology. There may also be complex, subtle differences between developing phenotypic traits in terms of rates of change and metabolic associated costs (Lande, 2019). Likely most animals undergoing phenotypic switching in heterogeneous environments are 'mosaics', with some characters changing and others not, depending on the environmental cues.

Yet, as also emphasized above, we know that some characters do appear to become fixed during developmental critical windows. None of these scenarios are mutually exclusive. The domain circumscribed by the dashed line in **Figure 3** indicates how, within a single animal, some traits could be non-reversible (non-correctable), others could be quite reversible (correctable), and still other traits might actually regress as an example of true reversibility.

As a conceptual example of multiple patterns of plasticity and subsequent phenotype switching within a single individual, consider an animal who's pulmonary morphometrics may be permanently altered during development because of hypoxic exposure during a critical window for lung development. However, the rate and depth at which they are ventilated at rest in the adult (physiology) could be a highly plastic physiological regulatory trait. As another example, a fish's musculature for swimming (morphology) could become fixed by experiences during development, but the characteristics of that fish's basic schooling (behavior) as an adult could be reset by changes in fish density – thus creating the phenotype switching 'mosaic' referred to above. Unfortunately, empirical evidence of such changes is scarce. We know that bullfrogs exposed to hypoxia at various stages in larval development and as adults show highly differential responses associated with the timing of the hypoxic exposure. Larvae show highly plastic morphological characters associated with gas exchange, but these characters become fixed in the adult and are no longer affected by hypoxia (Burggren and Mwalukoma, 1983). In contrast, the same hypoxic exposures cause little change in the red blood cell properties, including blood P_{50}, of larvae, whereas these variables remain high plastic in the adults (Pinder and Burggren, 1983). In the quail (*Coturnix coturnix*) and the chicken (*Gallus domesticus*), hypoxia experienced during different periods of embryonic incubation induces phenotypic switching of some morphological, physiological and hematological characters, but not others (Dzialowski et al., 2002; Chan and Burggren, 2005; Burggren and Elmonoufy, 2017). Certainly, more experiments designed to reveal specific patterns of phenotypic switching are warranted. To reiterate a point made earlier, if we start looking for these various forms of developmental phenotypic switching, we are likely to find them.

REVERSIBLE PHENOTYPE SWITCHING AS A BRIDGE DURING PERIODS OF UNPREDICTABLE CLIMATE CHANGE

Having made a case for reversible (correctable) phenotype switching enabled by developmental phenotypic plasticity, what might we speculate to be the selection pressures leading to its evolution? Advantages to *mature* organisms of reversible phenotype switching, as well as its evolution, have received considerable attention – for an entry into the literature see Gabriel (2005), Gabriel (2006), Piersma and van Gils (2010), Berman (2016), Chen et al. (2016), Pfab et al. (2016), Lazaro et al. (2019), and Ratikainen and Kokko (2019). Yet, as Beaman et al. (2016) state, "*. . .the evolution of reversible acclimation can no longer be viewed as independent from developmental processes.*" Indeed, the phenomenon of 'developmental bias' is increasingly becoming an important component of understanding evolutionary process (Uller et al., 2018; Parsons et al., 2019). Unfortunately, relatively few

studies have explicitly collected experimental data to determine the adaptive advantages of reversible phenotype switching in developing, as opposed to mature, organisms. Such data, if available, could then be used to infer and model the evolution of reversible (correctable) plasticity. Yet, we can still ask the question "*Why might such reversibility be important*"?

Many common environmental stressors are short-term, variable in magnitude and non-predictable in occurrence – e.g., Burggren (2018, 2019). Thus, the development of alternative traits may be adaptive for one set of environmental conditions, but maladaptive for another set which may quickly follow, especially if either the switched phenotype of the environmental conditions are extreme (Chevin et al., 2010; Chevin and Hoffmann, 2017; Burggren, 2018; Pelster and Burggren, 2018). For example, consider the development of the gills in a developing freshwater fish that typically dwells in air saturated water. The ability to develop enlarged branchial surfaces could be life-saving should temporary aquatic hypoxia occur. However, once the environment returns to its normal condition of air saturation, retaining an enlarged gas exchange surface into adulthood, or even into just the next developmental stage, is likely to be metabolically very costly. This additional cost arises from maintaining osmoregulatory balance that is challenged by the inward flood of water across the larger gill surface area. The ability to 'shed' a trait or suite of traits by reversing (correcting) a switched phenotype arising during development is likely to be highly adaptive to the developing animal or its adult form. In contrast, fixed phenotypes at the end of the developmental period are more likely to result in phenotype-environment mis-matches (Gomulkiewicz and Kirkpatrick, 1992; Padilla and Adolph, 1996; Dukas, 1998; Snell-Rood, 2012). Thus, one could anticipate a strong selection pressure for a form of plasticity that allowed reversible phenotype switching in developing organisms, especially when environmental stressors cycle at shorter frequencies than the life span of the organism (Gabriel, 2005, 2006). Mathematical modeling has shown that reversible phenotype switching can be beneficial, even in rhythmically and slowly changing environments (Pfab et al., 2016).

Reversibility of developmental phenotypic switching may be an important mechanism of surviving climate change. Simply put, the ability to reverse short-term phenotypic changes during development may be key to a species surviving short-term climate changes, especially when extreme and stochastic. **Figure 4** shows a hypothetical scenario of two different organisms,

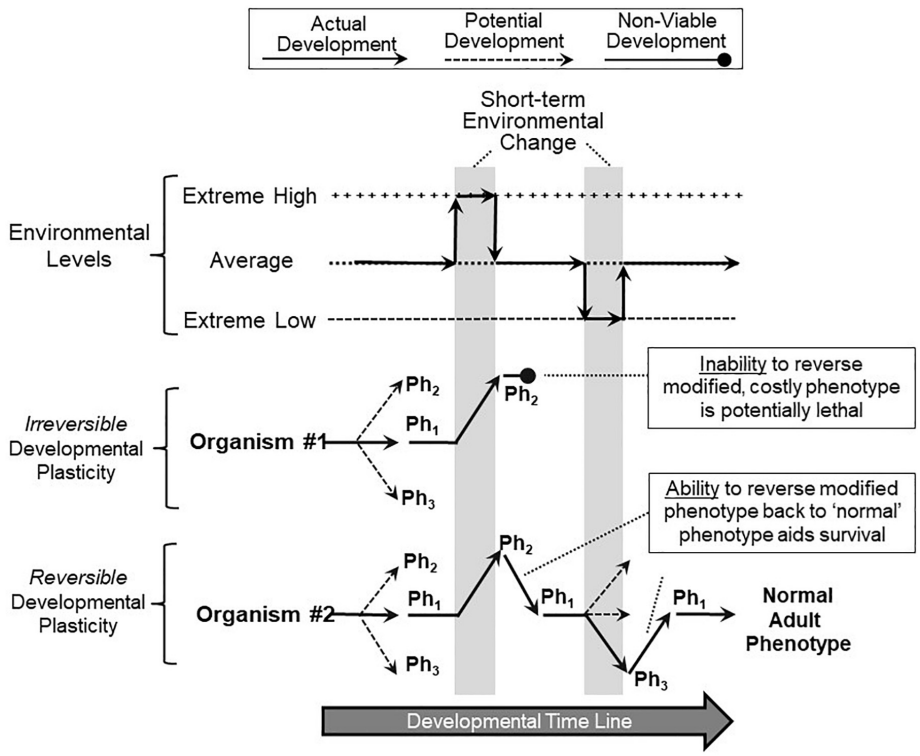

FIGURE 4 | Implications of reversible and non-reversible developmental phenotypic plasticity. In this scenario, two organisms are tracked during their development as they experience multiple, short-term extreme environmental changes (vertical gray bars). Both Organism #1 (red) and Organism #2 (blue) respond to the first extreme environmental change by switching from their normal range of phenotypes (Ph_1) to a specialized, adaptive phenotype (Ph_2) that allows continued survival in that environment. However, Organism #1, lacking the ability to reverse (correct) its phenotype that was suitable for the extreme high environment, is now non-viable when the environment reverts back to more typical conditions as development continues. Organism #2, which similarly responded to the first environmental change with a switched phenotype (Ph_2), has the ability to reverse or correct the costly or even lethal modified phenotype back to normal ranges (Ph_1) when the environment returns to normal, aiding its survival. Organism #2 can also move to other phenotypes (Ph_3) and revert back to normal ranges (Ph_1) as subsequent environmental swings occur. Thus, in this overall scenario, reversible phenotypic switching during development heavily favors survival of the developing organism.

both exhibiting developmental phenotypic plasticity, and both switching phenotype during development in response to the appearance of an adverse environment and its accompanying stressors. In this particular scenario, the short-term adverse environment then quickly and briefly returns to 'normal' (average) before actually changing to an adverse condition in the other direction. This might resemble extreme short-term weather events – for example, temperature swings – but could also mimic changes such as salinity or water availability. Let us further assume that the switched phenotype, essential for survival in a newly extreme environment, turns out to be costly, perhaps even lethal, for that organism when returned to a normally experienced or especially to a extreme low environment (as in the example of increased fish gill area, above). Under these circumstances, Organism #1, which is unable to reverse a switched phenotype, becomes non-viable and may even fail to develop (**Figure 4**). In contrast, Organism #2, capable of reversible phenotype switching, can revert to the original phenotype, continue development and live on to reproduce (**Figure 4**). Of course, there is a cost to all forms of plasticity (Snell-Rood, 2012; Lande, 2014; Pelster and Burggren, 2018), and not all phenotype switching is adaptive, especially in a stochastic environment (Padilla and Adolph, 1996; Burggren, 2018).

COSTS AND BENEFITS OF REVERSIBLE PHENOTYPIC SWITCHING

Having indicated that reversible phenotypic switching during development can indeed occur, a key question emerges: *How costly is reversible phenotypic switching between different developmental pathways or trajectories?* The answer hinges on the energetic/metabolic cost of developmental phenotypic switching between a modified phenotype and the normal range of phenotypes – and back. In a meta-analysis of phenotypic switching in 23 plant and animal species, the fitness costs of developmental plasticity were often found to be quite low (Van Buskirk and Steiner, 2009). Metabolic costs in particular of any magnitude can manifest themselves in terms of elevated metabolic levels or in the form of slowed growth. In fishes, physiological phenotype switching and reversal, occurring with acclimatization or laboratory acclimation, incurs variable degrees of metabolic costs (Jayasundara and Somero, 2013; Esbaugh et al., 2016). Phenotypic switching of behavioral phenotypes can be metabolically expensive given the high energetic cost of neural function and the additional neurons and neural connections that may be required (Hampson, 1991; Sporns et al., 2000; Snell-Rood, 2012; Karbowski, 2019). Changing morphological characters during development also has its costs, of course. For example, adaptive changes in head size in developing Australian tiger snakes (*Notechis scutatus*) resulted in slower rates of growth (Aubret and Shine, 2010). Morphological phenotype switching induced by predator cues in the developing freshwater crustacean *Daphnia pulex* had little apparent direct cost, but these may have been masked by an overall reduction in metabolic rate (Scheiner and Berrigan, 1998).

While in some instances the cost of a phenotypic switch and its reversal may not be prohibitively high, multiple cycles of switching caused by an environmental stressor followed by a reversal back to the normal range of phenotypes may be detrimental. Energetic reserves may be reduced or even exhausted, associated with oxidative stress being incurred. Developmental time and trajectories or even longevity even affected (Snell-Rood, 2012), to mention just a few negative consequences. Of course, the cost may pivot on the ability to acquire resources before, during and after each phenotype switching cycle.

CONCLUSION

Consideration of climate change in a developmental context becomes all the more useful when expanding the concept of developmental phenotypic switching to include switching that is reversible subsequent to the critical window. Appreciating the potentially reversible (correctable) nature of at least some traits evoked by abrupt, bidirectional environmental changes could prove to be key to understanding and predicting how individuals, populations and species will cope during climate change, especially when the changes are highly variable and unpredictable.

AUTHOR CONTRIBUTIONS

WB wrote this manuscript and constructed all figures.

FUNDING

This research was made possible by a grant (RECOVER 1 SA-15-20) from The Gulf of Mexico Research Initiative (GoMRI).

ACKNOWLEDGMENTS

Dr. Ed Dzialowski and Mr. Christopher Melendez provided many useful comments during the development of this manuscript.

REFERENCES

Ali, S., Champagne, D. L., Alia, A., and Richardson, M. K. (2011). Large-scale analysis of acute ethanol exposure in zebrafish development: a critical time window and resilience. *PLoS One* 6:e20037. doi: 10.1371/journal.pone.0020037

Alvine, T., and Burggren, W. W. (2014). Renal, metabolic and hematological effects of trans-retinoic acid during critical developmental windows in the embryonic chicken. *J. Comp. Physiol. B* 184, 107–123. doi: 10.1007/s00360-013-0777-9

Angiletta, M. J. J. (2009). *Thermal Adaptation: A Theoretical and Empirical Synthesis*. Oxford: Oxford University Press.

Arendt, J. D. (1997). Adaptive intrinsic growth rates: an invtegration across taxa. *Q. Rev. Biol.* 72, 149–177. doi: 10.1086/419764

Aristotle (350BC). *On the Parts of Animals*, trans. W. Ogle [The Internet Classics Archive]. Available at: http://classics.mit.edu//Aristotle/parts_animals.html

Aubret, F., and Shine, R. (2010). Fitness costs may explain the post-colonisation erosion of phenotypic plasticity. *J. Exp. Biol.* 213, 735–739. doi: 10.1242/jeb.040576

Bateson, P. (2017). Robustness and plasticity in development. *Wiley Interdiscip. Rev. Cogn. Sci.* 8, e1386.

Bateson, P., Gluckman, P., and Hanson, M. (2014). The biology of developmental plasticity and the Predictive Adaptive Response hypothesis. *J. Physiol.* 592, 2357–2368. doi: 10.1113/jphysiol.2014.271460

Bautista, N. M., and Burggren, W. W. (2019). Parental stressor exposure simultaneously conveys both adaptive and maladaptive larval phenotypes through epigenetic inheritance in the zebrafish (Danio rerio). *J. Exp. Biol.* 222:jeb208918. doi: 10.1242/jeb.208918

Bavestrello, G., Puce, S., Cerrano, C., and Sara, M. (2000). Phenotypic plasticity in hydrozoans: morph reversibility. *Riv. Biol.* 93, 283–294.

Beaman, J. E., White, C. R., and Seebacher, F. (2016). Evolution of plasticity: mechanistic link between development and reversible acclimation. *Trends Ecol. Evol.* 31, 237–249. doi: 10.1016/j.tree.2016.01.004

Berman, J. (2016). Ploidy plasticity: a rapid and reversible strategy for adaptation to stress. *FEMS Yeast Res.* 16:fow020. doi: 10.1093/femsyr/fow020

Brakefield, P. M., Pijpe, J., and Zwaan, B. J. (2007). Developmental plasticity and acclimation both contribute to adaptive responses to alternating seasons of plenty and of stress in Bicyclus butterflies. *J. Biosci.* 32, 465–475. doi: 10.1007/s12038-007-0046-8

Burggren, W. (2018). Developmental phenotypic plasticity helps bridge stochastic weather events associated with climate change. *J. Exp. Biol.* 221:jeb161984. doi: 10.1242/jeb.161984

Burggren, W., and Mwalukoma, A. (1983). Respiration during chronic hypoxia and hyperoxia in larval and adult bullfrogs (Rana catesbeiana). I. Morphological responses of lungs, skin and gills. *J. Exp. Biol.* 105, 191–203.

Burggren, W. W. (2016). Epigenetic inheritance and its role in evolutionary biology: re-evaluation and new perspectives. *Biology* 5:24. doi: 10.3390/biology5020024

Burggren, W. W. (2017). Epigenetics in insects: mechanisms, phenotypes and ecological and evolutionary implications. *Adv. Insect Physiol.* 53, 1–30. doi: 10.1016/bs.aiip.2017.04.001

Burggren, W. W. (2019). Inadequacy of typical physiological experimental protocols for investigating consequences of stochastic weather events emerging from global warming. *Am. J. Physiol. Regul. Integr. Comp. Physiol.* 316, R318–R322. doi: 10.1152/ajpregu.00307.2018

Burggren, W. W., Christoffels, V. M., Crossley, D. A. II, Enok, S., Farrell, A. P., Hedrick, M. S., et al. (2014). Comparative cardiovascular physiology: future trends, opportunities and challenges. *Acta Physiol.* 210, 257–276. doi: 10.1111/apha.12170

Burggren, W. W., and Crews, D. (2014). Epigenetics in comparative biology: why we should pay attention. *Integr. Comp. Biol.* 54, 7–20. doi: 10.1093/icb/icu013

Burggren, W. W., and Elmonoufy, N. A. (2017). Critical developmental windows for morphology and hematology revealed by intermittent and continuous hypoxic incubation in embryos of quail (*Coturnix coturnix*). *PLoS One* 12:e0183649. doi: 10.1371/journal.pone.0183649

Burggren, W. W., and Mueller, C. A. (2015). Developmental critical windows and sensitive periods as three-dimensional constructs in time and space. *Physiol. Biochem Zool.* 88, 91–102. doi: 10.1086/679906

Burggren, W. W., and Reyna, K. S. (2011). Developmental trajectories, critical windows and phenotypic alteration during cardio-respiratory development. *Respir. Physiol. Neurobiol.* 178, 13–21. doi: 10.1016/j.resp.2011.05.001

Burraco, P., Valdes, A. E., and Orizaola, G. (2019). Metabolic costs of altered growth trajectories across life transitions in amphibians. *J. Anim. Ecol.* doi: 10.1111/1365-2656.13138 [Epub ahead of print].

Chan, T., and Burggren, W. (2005). Hypoxic incubation creates differential morphological effects during specific developmental critical windows in the embryo of the chicken (*Gallus gallus*). *Respir. Physiol. Neurobiol.* 145, 251–263. doi: 10.1016/j.resp.2004.09.005

Chen, X., Wang, Y., Feng, T., Yi, M., Zhang, X., and Zhou, D. (2016). The overshoot and phenotypic equilibrium in characterizing cancer dynamics of reversible phenotypic plasticity. *J. Theor. Biol.* 390, 40–49. doi: 10.1016/j.jtbi.2015.11.008

Chevin, L. M., and Hoffmann, A. A. (2017). Evolution of phenotypic plasticity in extreme environments. *Philos. Trans. R. Soc. Lond. B Biol. Sci.* 19:372.

Chevin, L. M., Lande, R., and Mace, G. M. (2010). Adaptation, plasticity, and extinction in a changing environment: towards a predictive theory. *PLoS Biol.* 8:e1000357. doi: 10.1371/journal.pbio.1000357

Cho, W. K., and Suh, B. K. (2016). Catch-up growth and catch-up fat in children born small for gestational age. *Korean J. Pediatr.* 59, 1–7. doi: 10.3345/kjp.2016.59.1.1

Cox, R. L., Calderon, de Anda, F., Mangoubi, T., and Yoshii, A. (2018). Multiple critical periods for rapamycin treatment to correct structural defects in Tsc-1-suppressed brain. *Front. Mol. Neurosci.* 11:409. doi: 10.3389/fnmol.2018.00409

Daskalakis, N. P., Bagot, R. C., Parker, K. J., Vinkers, C. H., and de Kloet, E. R. (2013). The three-hit concept of vulnerability and resilience: toward understanding adaptation to early-life adversity outcome. *Psychoneuroendocrinology* 38, 1858–1873. doi: 10.1016/j.psyneuen.2013.06.008

de Jong, M., and Leyser, O. (2012). Developmental plasticity in plants. *Cold. Spring Harb. Symp. Quant. Biol.* 77, 63–73. doi: 10.1101/sqb.2012.77.014720

Debat, V., and David, P. (2001). Mapping phenotypes: canalization, plasticity and developmental stability. *Trends Ecol. Evol.* 16, 551–561.

Dietert, R. R., Etzel, R. A., Chen, D., Halonen, M., Holladay, S. D., Jarabek, A. M., et al. (2000). Workshop to identify critical windows of exposure for children's health: immune and respiratory systems work group summary. *Environ. Health Perspect.* 108(Suppl. 3), 483–490. doi: 10.1289/ehp.00108s3483

Dobzhansky, T. (1973). Nothing in biology makes sense except in the light of evolution. *Am. Biol. Teachnol.* 35, 125–129. doi: 10.2307/4444260

Donelson, J. M., Salinas, S., Munday, P. L., and Shama, L. N. S. (2017). Transgenerational plasticity and climate change experiments: where do we go from here? *Glob. Chang. Biol.* 24, 13–34. doi: 10.1111/gcb.13903

Dubansky, B. (2018). "The interaction of environment and chronlogical and developmental time," in *Development and Environment*, ed. V. J. Inglezakis (Cham: Springer), 9–40.

Dukas, R. (1998). "Evolutionary ecology of learning," in *Cognitive Ecology: the Evolutionary Ecology of Information Processing and Decision Making*, Ed. R. Dukas (Chicago: University of Chicago Press), 129–174.

Dzialowski, E. M., von Plettenberg, D., Elmonoufy, N. A., and Burggren, W. W. (2002). Chronic hypoxia alters the physiological and morphological trajectories of developing chicken embryos. *Comp. Biochem. Physiol. A* 131, 713–724. doi: 10.1016/s1095-6433(02)00009-0

Eme, J., Mueller, C. A., Manzon, R. G., Somers, C. M., Boreham, D. R., and Wilson, J. Y. (2015). Critical windows in embryonic development: shifting incubation temperatures alter heart rate and oxygen consumption of Lake Whitefish (*Coregonus clupeaformis*) embryos and hatchlings. *Comp. Biochem. Physiol. A Mol. Integr. Physiol.* 179, 71–80. doi: 10.1016/j.cbpa.2014.09.005

Esbaugh, A. J., Ern, R., Nordi, W. M., and Johnson, A. S. (2016). Respiratory plasticity is insufficient to alleviate blood acid-base disturbances after acclimation to ocean acidification in the estuarine red drum, Sciaenops ocellatus. *J. Comp. Physiol. B* 186, 97–109. doi: 10.1007/s00360-015-0940-6

Ferner, K., and Mortola, J. P. (2009). Ventilatory response to hypoxia in chicken hatchlings: a developmental window of sensitivity to embryonic hypoxia. *Respir. Physiol. Neurobiol.* 165, 49–53. doi: 10.1016/j.resp.2008.10.004

Fischer, K., Eenhoorn, E., Bot, A. N., Brakefield, P. M., and Zwaan, B. J. (2003). Cooler butterflies lay larger eggs: developmental plasticity versus acclimation. *Proc. Biol. Sci.* 270, 2051–2056. doi: 10.1098/rspb.2003.2470

Frazier, K. S. (2017). Species differences in renal development and associated developmental nephrotoxicity. *Birth Defects Res.* 109, 1243–1256. doi: 10.1002/bdr2.1088

Gabriel, W. (2005). How stress selects for reversible phenotypic plasticity. *J. Evol. Biol.* 18, 873–883. doi: 10.1111/j.1420-9101.2005.00959.x

Gabriel, W. (2006). Selective advantage of irreversible and reversible phenotypic plasticity. *Arch. Hydrobiol.* 167, 1–4. doi: 10.1073/pnas.1408589111

Gioia, M., Michaletti, A., Scimeca, M., Marini, M., Tarantino, U., Zolla, L., et al. (2018). Simulated microgravity induces a cellular regression of the mature phenotype in human primary osteoblasts. *Cell Death Discov.* 4:59. doi: 10.1038/s41420-018-0055-4

Golovin, R. M., and Broadie, K. (2016). Developmental experience-dependent plasticity in the first synapse of the Drosophila olfactory circuit. *J. Neurophysiol.* 116, 2730–2738. doi: 10.1152/jn.00616.2016

Gomulkiewicz, R., and Kirkpatrick, M. (1992). Quantitative genetics and the evolution of reaction norms. *Evol. Dev.* 46, 390–411. doi: 10.1111/j.1558-5646.1992.tb02047.x

Grote, K., Hobler, C., Andrade, A. J., Grande, S. W., Gericke, C., Talsness, C. E., et al. (2009). Sex differences in effects on sexual development in rat offspring after pre- and postnatal exposure to triphenyltin chloride. *Toxicology* 260, 53–59. doi: 10.1016/j.tox.2009.03.006

Halldorsdottir, T., and Binder, E. B. (2017). Gene x environment interactions: from molecular mechanisms to behavior. *Annu. Rev. Psychol.* 68, 215–241. doi: 10.1146/annurev-psych-010416-044053

Hampson, S. (1991). Generalization and specialization in artificial neural networks. *Prog. Neurobiol.* 37, 383–431. doi: 10.1016/0301-0082(91)90008-o

Hector, K. L., and Nakagawa, S. (2012). Quantitative analysis of compensatory and catch-up growth in diverse taxa. *J. Anim. Ecol.* 81, 583–593. doi: 10.1111/j.1365-2656.2011.01942.x

Hempel, C. G. (1945). Studies in the logic of confirmation (I.). *Mind* 54, 1–26. doi: 10.1093/mind/liv.213.1

Hensch, T. K., and Bilimoria, P. M. (2012). Re-opening windows: manipulating critical periods for brain development. *Cerebrum* 2012:11.

Hsu, H. H., Chiu, Y. H., Coull, B. A., Kloog, I., Schwartz, J., Lee, A., et al. (2015). Prenatal particulate air pollution and asthma onset in urban children. identifying sensitive windows and sex differences. *Am. J. Respir. Crit. Care Med.* 192, 1052–1059. doi: 10.1164/rccm.201504-0658OC

Ingber, S. Z., and Pohl, H. R. (2016). Windows of sensitivity to toxic chemicals in the motor effects development. *Regul. Toxicol. Pharmacol.* 74, 93–104. doi: 10.1016/j.yrtph.2015.11.018

Jablonka, E. (2013). Epigenetic inheritance and plasticity: the responsive germline. *Prog. Biophys. Mol. Biol.* 111, 99–107. doi: 10.1016/j.pbiomolbio.2012.08.014

Jayasundara, N., and Somero, G. N. (2013). Physiological plasticity of cardiorespiratory function in a eurythermal marine teleost, the longjaw mudsucker, *Gillichthys mirabilis*. *J. Exp. Biol.* 216, 2111–2121. doi: 10.1242/jeb.083873

Josephs, E. B. (2018). Determining the evolutionary forces shaping G x E. *New Phytol.* 219, 31–36. doi: 10.1111/nph.15103

Kaji, T., and Palmer, A. R. (2017). How reversible is development? Contrast between developmentally plastic gain and loss of segments in barnacle feeding legs. *Evolution* 71, 756–765. doi: 10.1111/evo.13152

Karbowski, J. (2019). Metabolic constraints on synaptic learning and memory. *J. Neurophysiol.* 122, 1473–1490. doi: 10.1152/jn.00092.2019

Korzybski, A. (1933). *Science and Sanity: An Introduction to Non-Aristotelian Systems and General Semantics*. Oxfod: International Non-Aristotelian Libray.

Kowalski, W. J., Dur, O., Wang, Y., Patrick, M. J., Tinney, J. P., Keller, B. B., et al. (2013). Critical transitions in early embryonic aortic arch patterning and hemodynamics. *PLoS One* 8:e60271. doi: 10.1371/journal.pone.0060271

Kunes, J., and Zicha, J. (2006). Developmental windows and environment as important factors in the expression of genetic information: a cardiovascular physiologist's view. *Clin. Sci.* 111, 295–305. doi: 10.1042/cs20050271

Lage, K., Greenway, S. C., Rosenfeld, J. A., Wakimoto, H., Gorham, J. M., Segre, A. V., et al. (2012). Genetic and environmental risk factors in congenital heart disease functionally converge in protein networks driving heart development. *Proc. Natl. Acad. Sci. U.S.A.* 109, 14035–14040. doi: 10.1073/pnas.1210730109

Lande, R. (2014). Evolution of phenotypic plasticity and environmental tolerance of a labile quantitative character in a fluctuating environment. *J. Evol. Biol.* 27, 866–875. doi: 10.1111/jeb.12360

Lande, R. (2019). Developmental integration and evolution of labile plasticity in a complex quantitative character in a multiperiodic environment. *Proc. Natl. Acad. Sci. U.S.A.* 116, 11361–11369. doi: 10.1073/pnas.1900528116

Lazaro, J., Hertel, M., Muturi, M., and Dechmann, D. K. N. (2019). Seasonal reversible size changes in the braincase and mass of common shrews are flexibly modified by environmental conditions. *Sci. Rep.* 9:2489. doi: 10.1038/s41598-019-38884-1

Lenneberg, E. H. (1967). *Biological Foundations of Language*. New York, NY: John Wiley and Sons.

Ligon, D. B., Peterson, C. C., and Lovern, M. B. (2012). Acute and persistent effects of pre- and posthatching thermal environments on growth and metabolism in the red-eared slider turtle, *Trachemys scripta* elegans. *J. Exp. Zool. A Ecol. Genet. Physiol.* 317, 227–235. doi: 10.1002/jez.1716

Lisenkova, A. A., Grigorenko, A. P., Tyazhelova, T. V., Andreeva, T. V., Gusev, F. E., Manakhov, A. D., et al. (2017). Complete mitochondrial genome and evolutionary analysis of Turritopsis dohrnii, the "immortal" jellyfish with a reversible life-cycle. *Mol. Phylogenet. Evol.* 107, 232–238. doi: 10.1016/j.ympev.2016.11.007

Lloyd, C. M., and Saglani, S. (2017). Development of allergic immunity in early life. *Immunol. Rev.* 278, 101–115. doi: 10.1111/imr.12562

Manuck, S. B., and McCaffery, J. M. (2014). Gene-environment interaction. *Annu. Rev. Psychol.* 65, 41–70. doi: 10.1146/annurev-psych-010213-115100

Martin, A., Connelly, A., Bland, R. M., and Reilly, J. J. (2017). Health impact of catch-up growth in low-birth weight infants: systematic review, evidence appraisal, and meta-analysis. *Matern. Child Nutr.* 13. doi: 10.1111/mcn.12297

Matesanz, S., Gianoli, E., and Valladares, F. (2010). Global change and the evolution of phenotypic plasticity in plants. *Ann. N. Y. Acad. Sci.* 1206, 35–55. doi: 10.1111/j.1749-6632.2010.05704.x

Matesanz, S., Horgan-Kobelski, T., and Sultan, S. E. (2012). Phenotypic plasticity and population differentiation in an ongoing species invasion. *PLoS One* 7:e44955. doi: 10.1371/journal.pone.0044955

McKeown, C. R., Thompson, C. K., and Cline, H. T. (2017). Reversible developmental stasis in response to nutrient availability in the Xenopus laevis central nervous system. *J. Exp. Biol.* 220, 358–368. doi: 10.1242/jeb.151043

McVey Neufeld, K. A., Luczynski, P., Seira Oriach, C., Dinan, T. G., and Cryan, J. F. (2016). What's bugging your teen?-The microbiota and adolescent mental health. *Neurosci. Biobehav. Rev.* 70, 300–312. doi: 10.1016/j.neubiorev.2016.06.005

Mendez-Sanchez, J. F., and Burggren, W. W. (2019). Hypoxia-Induced developmental plasticity of larval growth, gill and labyrinth organ morphometrics in two anabantoid fish: the facultative air-breather Siamese fighting fish (*Betta splendens*) and the obligate air-breather the blue gourami (*Trichopodus trichopterus*). *J. Morphol.* 280, 193–204. doi: 10.1002/jmor.20931

Moffitt, T. E., Caspi, A., and Rutter, M. (2005). Strategy for investigating interactions between measured genes and measured environments. *Arch. Gen. Psychiatry* 62, 473–481.

Mueller, C. A., Willis, C., and Burggren, W. W. (2016). Salt sensitivity of the morphometry of Artemia franciscana during development: a demonstration of 3-D critical windows. *J. Exp. Biol.* 219, 571–581. doi: 10.1242/jeb.125823

Munday, P. L., Warner, R. R., Monro, K., Pandolfi, J. M., and Marshall, D. J. (2013). Predicting evolutionary responses to climate change in the sea. *Ecol. Lett.* 16, 1488–1500. doi: 10.1111/ele.12185

Noh, S., Everman, E. R., Berger, C. M., and Morgan, T. J. (2017). Seasonal variation in basal and plastic cold tolerance: adaptation is influenced by both long- and short-term phenotypic plasticity. *Ecol. Evol.* 7, 5248–5257. doi: 10.1002/ece3.3112

Okada, T., Takahashi, S., Nagano, N., Yoshikawa, K., Usukura, Y., and Hosono, S. (2015). Early postnatal alteration of body composition in preterm and small-for-gestational-age infants: implications of catch-up fat. *Pediatr. Res.* 77, 136–142. doi: 10.1038/pr.2014.164

Owens, G. K. (2007). Molecular control of vascular smooth muscle cell differentiation and phenotypic plasticity. *Novartis Found. Symp.* 283, 174–191.

Padilla, D. K., and Adolph, S. C. E. E. (1996). Plastic inducible morphologies are not always adaptive: the importance of time delays in a stochastic environment. *Evol. Ecol.* 10, 105–117. doi: 10.1007/bf01239351

Parsons, K. J., McWhinnie, K., Pilakouta, N., and Walker, L. (2019). Does phenotypic plasticity initiate developmental bias? *Evol. Dev.* 26:e12304.

Pelster, B., and Burggren, W. W. (2018). "Responses to environmental stressors in developing animals: costs and benefits of phenotypic plasticity," in *Development and Environment*, ed. V. J. Inglezakis (Cham: Springer), 97–113. doi: 10.1007/978-3-319-75935-7_5

Penfield, W., and Roberts, L. (1959). *Speech and Brain Mechanisms*. Princeton, NJ: Princeton University Press.

Pfab, F., Gabriel, W., and Utz, M. (2016). Reversible phenotypic plasticity with continuous adaptation. *J. Math. Biol.* 72, 435–466. doi: 10.1007/s00285-015-0890-3

Piersma, T., and van Gils, J. (2010). *The Flexible Phenotype: A Body-Centered Integration of Ecology, Physiology and Behaviour*. Oxford: Oxford University Press.

Pigliucci, M., Schlichting, C. D., Jones, C. S., and Schwenk, K. (1996). Developmental reaction norms: the interactions among allometry, ontogeny and plasticity. *Plant Species Biol.* 11, 69–85. doi: 10.1111/j.1442-1984.1996.tb00110.x

Pinder, A., and Burggren, W. (1983). Respiration during chronic hypoxia and hyperoxia in larval and adult bullfrogs (*Rana catesbeiana*). II. Changes in respiratory properties of whole blood. *J. Exp. Biol.* 105, 205–213.

Polo-Cavia, N., and Gomez-Mestre, I. (2017). Pigmentation plasticity enhances crypsis in larval newts: associated metabolic cost and background choice behaviour. *Sci. Rep.* 7:39739. doi: 10.1038/srep39739

Poore, K. R., Boullin, J. P., Cleal, J. K., Newman, J. P., Noakes, D. E., Hanson, M. A., et al. (2010). Sex- and age-specific effects of nutrition in early gestation and early postnatal life on hypothalamo-pituitary-adrenal axis and sympathoadrenal function in adult sheep. *J. Physiol.* 588, 2219–2237. doi: 10.1113/jphysiol.2010.187682

Popper, K. (1959). *The Logic of Scientific Discovery*. New York, NY: Routledge.

Popper, K. (1970). "A Realist View of Logic, Physics and History," in *Physics, Logic and History*, Ed. W. Yourgrau (New York, NY: Plenum Press).

Quintaneiro, C., Soares, A., Costa, D., and Monteiro, M. S. (2019). Effects of PCB-77 in adult zebrafish after exposure during early life stages. *J. Environ. Sci. Health A Tox. Hazard Subst. Environ. Eng.* 54, 478–483. doi: 10.1080/10934529.2019.1568793

Ratikainen, I. I., and Kokko, H. (2019). The coevolution of lifespan and reversible plasticity. *Nat. Commun.* 10:538. doi: 10.1038/s41467-019-08502-9

Roark, A. M., Bjorndal, K. A., and Bolten, A. B. (2009). Compensatory responses to food restriction in juvenile green turtles (*Chelonia mydas*). *Ecology* 90, 2524–2534. doi: 10.1890/08-1835.1

Russell, A. P., Lynn, S. E., Powell, G. L., and Cottle, A. (2015). The regenerated tail of juvenile leopard geckos (Gekkota: Eublepharidae: *Eublepharis macularius*) preferentially stores more fat than the original. *Zoology* 118, 183–191. doi: 10.1016/j.zool.2014.12.003

Saltz, J. B., Bell, A. M., Flint, J., Gomulkiewicz, R., Hughes, K. A., and Keagy, J. (2018). Why does the magnitude of genotype-by-environment interaction vary? *Ecol. Evol.* 8, 6342–6353. doi: 10.1002/ece3.4128

Santin, J. M., and Hartzler, L. K. (2016). Environmentally induced return to juvenile-like chemosensitivity in the respiratory control system of adult bullfrog, *Lithobates catesbeianus*. *J. Physiol.* 594, 6349–6367. doi: 10.1113/JP272777

Scheiner, S. M., and Berrigan, D. (1998). The genetics of phenotypic plasticity. VIII. The cost of plasticity in daphnia pulex. *Evolution* 52, 368–378. doi: 10.1111/j.1558-5646.1998.tb01638.x

Schmich, J., Kraus, Y., De Vito, D., Graziussi, D., Boero, F., and Piraino, S. (2007). Induction of reverse development in two marine Hydrozoans. *Int. J. Dev. Biol.* 51, 45–56. doi: 10.1387/ijdb.062152js

Senner, N. R., Conklin, J. R., and Piersma, T. (2015). An ontogenetic perspective on individual differences. *Proc. Biol. Sci.* 07:282.

Skinner, M. K. (2011). Role of epigenetics in developmental biology and transgenerational inheritance. *Birth Defects Res. C Embryo Today* 93, 51–55. doi: 10.1002/bdrc.20199

Skinner, M. K. (2015). Environmental epigenetics and a unified theory of the molecular aspects of evolution: a Neo-Lamarckian concept that facilitates Neo-Darwinian evolution. *Genome Biol. Evol.* 7, 1296–1302. doi: 10.1093/gbe/evv073

Slotsbo, S., Schou, M. F., Kristensen, T. N., Loeschcke, V., and Sorensen, J. G. (2016). Reversibility of developmental heat and cold plasticity is asymmetric and has long-lasting consequences for adult thermal tolerance. *J. Exp. Biol.* 219, 2726–2732. doi: 10.1242/jeb.143750

Snell-Rood, E. C. (2012). Selective processes in development: implications for the costs and benefits of phenotypic plasticity. *Integr. Comp. Biol.* 52, 31–42. doi: 10.1093/icb/ics067

Sommer, R. J., Dardiry, M., Lenuzzi, M., Namdeo, S., Renahan, T., Sieriebriennikov, B., et al. (2017). The genetics of phenotypic plasticity in nematode feeding structures. *Open Biol.* 7:160332. doi: 10.1098/rsob.160332

Spemann, H. (1938). *Embryonic Development and Induction*. New Haven, CT: Yale University Press.

Spicer, J. I., and Rundle, S. D. (2007). Plasticity in the timing of physiological development: physiological heterokairy–what is it, how frequent is it, and does it matter? *Comp. Biochem. Physiol. A Mol. Integr. Physiol.* 148, 712–719. doi: 10.1016/j.cbpa.2007.05.027

Sporns, O., Tononi, G., and Edelman, G. M. (2000). Connectivity and complexity: the relationship between neuroanatomy and brain dynamics. *Neural Netw.* 13, 909–922. doi: 10.1016/s0893-6080(00)00053-8

Standen, E. M., Du, T. Y., and Larsson, H. C. (2014). Developmental plasticity and the origin of tetrapods. *Nature* 513, 54–58. doi: 10.1038/nature13708

Stockard, C. R. (1921). Developmental rate and structural expression: an experimental study of twins, 'double monsters' and single deformities, and the interaction among embryonic organs during their origin and development. *Am. J. Anat.* 28, 115–275.

Sweeney, D., Lindstrom, N., and Davies, J. A. (2008). Developmental plasticity and regenerative capacity in the renal ureteric bud/collecting duct system. *Development* 135, 2505–2510. doi: 10.1242/dev.022145

Tate, K. B., Kohl, Z. F., Eme, J., Rhen, T., and Crossley, D. A. II (2015). Critical windows of cardiovascular susceptibility to developmental hypoxia in common snapping turtle (*Chelydra serpentina*) embryos. *Physiol. Biochem. Zool.* 88, 103–115. doi: 10.1086/677683

Tills, O., Spicer, J. I., and Rundle, S. D. (2010). Salinity-induced heterokairy in an upper-estuarine population of the snail *Radix balthica* (Mollusca:Pulmonata). *Aqua. Biol.* 9, 95–105. doi: 10.3354/ab00231

Toth, Z., and Hettyey, A. (2018). Egg-laying environment modulates offspring responses to predation risk in an amphibian. *J. Evol. Biol.* 31, 710–721. doi: 10.1111/jeb.13258

Uller, T. (2008). Developmental plasticity and the evolution of parental effects. *Trends Ecol. Evol.* 23, 432–438. doi: 10.1016/j.tree.2008.04.005

Uller, T., Moczek, A. P., Watson, R. A., Brakefield, P. M., and Laland, K. N. (2018). Developmental bias and evolution: a regulatory network perspective. *Genetics* 209, 949–966. doi: 10.1534/genetics.118.300995

Utz, M., Jeschke, J. M., Loeschcke, V., and Gabriel, W. (2014). Phenotypic plasticity with instantaneous but delayed switches. *J. Theor. Biol.* 340, 60–72. doi: 10.1016/j.jtbi.2013.08.038

Van Buskirk, J., and Steiner, U. K. (2009). The fitness costs of developmental canalization and plasticity. *J. Evol. Biol.* 22, 852–860. doi: 10.1111/j.1420-9101.2009.01685.x

Vickers, M. H. (2011). Developmental programming of the metabolic syndrome - critical windows for intervention. *World J. Diabetes* 2, 137–148. doi: 10.4239/wjd.v2.i9.137

Voss, P. (2013). Sensitive and critical periods in visual sensory deprivation. *Front. Psychol.* 4:664. doi: 10.3389/fpsyg.2013.00664

Wells, J. C. (2014). Adaptive variability in the duration of critical windows of plasticity: implications for the programming of obesity. *Evol. Med. Public Health* 2014, 109–121. doi: 10.1093/emph/eou019

Werner, M. S., Sieriebriennikov, B., Loschko, T., Namdeo, S., Lenuzzi, M., Dardiry, M., et al. (2017). Environmental influence on *Pristionchus pacificus* mouth form through different culture methods. *Sci. Rep.* 7:7207. doi: 10.1038/s41598-017-07455-7

West-Eberhard, M. J. (2003). *Developmental Plasticity and Evolution*. Oxford: Oxford University Press.

West-Eberhard, M. J. (2005). Developmental plasticity and the origin of species differences. *Proc. Natl. Acad. Sci. U.S.A.* 102(Suppl. 1), 6543–6549. doi: 10.1073/pnas.0501844102

Wilson, R. S., and Franklin, C. E. (2002). Testing the beneficial acclimation hypothesis. *Trends Ecol. Evol.* 17, 66–70. doi: 10.1016/s0169-5347(01)02384-9

Woods, H. A. (2014). Mosaic physiology from developmental noise: within-organism physiological diversity as an alternative to phenotypic plasticity and phenotypic flexibility. *J. Exp. Biol.* 217, 35–45. doi: 10.1242/jeb.089698

Zambonino-Infante, J. L., Mazurais, D., Dubuc, A., Queau, P., Vanderplancke, G., Servili, A., et al. (2017). An early life hypoxia event has a long-term impact on protein digestion and growth in juvenile European sea bass. *J. Exp. Biol.* 220, 1846–1851. doi: 10.1242/jeb.154922

Zhang, H., and Burggren, W. W. (2012). Hypoxic level and duration differentially affect embryonic organ system development of the chicken (*Gallus gallus*). *Poult. Sci.* 91, 3191–3201. doi: 10.3382/ps.2012-02449

Conflict of Interest: The author declares that the research was conducted in the absence of any commercial or financial relationships that could be construed as a potential conflict of interest.

Copyright © 2020 Burggren. This is an open-access article distributed under the terms of the Creative Commons Attribution License (CC BY). The use, distribution or reproduction in other forums is permitted, provided the original author(s) and the copyright owner(s) are credited and that the original publication in this journal is cited, in accordance with accepted academic practice. No use, distribution or reproduction is permitted which does not comply with these terms.

frontiers in Physiology

REVIEW
published: 31 January 2020
doi: 10.3389/fphys.2020.00035

Embryonic Temperature Programs Phenotype in Reptiles

*Sunil Kumar Singh, Debojyoti Das and Turk Rhen**

Department of Biology, University of North Dakota, Grand Forks, ND, United States

Reptiles are critically affected by temperature throughout their lifespan, but especially so during early development. Temperature-induced changes in phenotype are a specific example of a broader phenomenon called phenotypic plasticity in which a single individual is able to develop different phenotypes when exposed to different environments. With climate change occurring at an unprecedented rate, it is important to study temperature effects on reptiles. For example, the potential impact of global warming is especially pronounced in species with temperature-dependent sex determination (TSD) because temperature has a direct effect on a key phenotypic (sex) and demographic (population sex ratios) trait. Reptiles with TSD also serve as models for studying temperature effects on the development of other traits that display continuous variation. Temperature directly influences metabolic and developmental rate of embryos and can have permanent effects on phenotype that last beyond the embryonic period. For instance, incubation temperature programs post-hatching hormone production and growth physiology, which can profoundly influence fitness. Here, we review current knowledge of temperature effects on phenotypic and developmental plasticity in reptiles. First, we examine the direct effect of temperature on biophysical processes, the concept of thermal performance curves, and the process of thermal acclimation. After discussing these reversible temperature effects, we focus the bulk of the review on developmental programming of phenotype by temperature during embryogenesis (i.e., permanent developmental effects). We focus on oviparous species because eggs are especially susceptible to changes in ambient temperature. We then discuss recent work probing the role of epigenetic mechanisms in mediating temperature effects on phenotype. Based on phenotypic effects of temperature, we return to the potential impact of global warming on reptiles. Finally, we highlight key areas for future research, including the identification of temperature sensors and assessment of genetic variation for thermosensitivity.

Keywords: endocrinology, growth, sex determination, temperature, thermal acclimation

OPEN ACCESS

Edited by:
Sonnet Jonker,
Oregon Health and Science University, United States

Reviewed by:
Nicola Van Wilgen,
South African National Parks, South Africa
John Eme,
California State University San Marcos, United States

***Correspondence:**
Turk Rhen
turk.rhen@und.edu

Specialty section:
This article was submitted to Embryonic and Developmental Physiology, a section of the journal Frontiers in Physiology

Received: *18 October 2019*
Accepted: *16 January 2020*
Published: *31 January 2020*

Citation:
Singh SK, Das D and Rhen T (2020) Embryonic Temperature Programs Phenotype in Reptiles. Front. Physiol. 11:35. doi: 10.3389/fphys.2020.00035

INTRODUCTION

All species have adapted, in one way or another, to natural variation in their environment. Variation in photoperiod, temperature, precipitation, salinity of soil or water, oxygen concentration, fires, and other organisms like pathogens, predators, and prey occurs across a wide range of spatial and temporal scales. Life on Earth has also faced major challenges

during its history, including five mass extinctions caused by natural, albeit rare, events like extreme volcanic activity and the impact of very large meteors (Barnosky et al., 2011). Over the last century, humans have had a dramatic impact on the environment, causing rapid changes in climate, destroying habitat, and producing entirely new challenges that may be causing a sixth mass extinction (Barnosky et al., 2011; Scheffers et al., 2016; Waters et al., 2016). For example, human generated pollution and novel synthetic chemicals that act as endocrine disruptors are major causes of disease and death both in people and in wildlife (Gore et al., 2015; Landrigan et al., 2018). We need to understand, now more than ever, how animals and plants respond to natural and anthropogenic variation in the environment in order to predict, prevent, and/or mitigate negative impacts on our biosphere.

On one hand, organisms can maintain phenotypic stability when exposed to complex and variable environments. Physiologists refer to this as homeostasis while developmental biologists call it canalization. On the other hand, organisms may display different phenotypes in the face of environmental challenges, a phenomenon called phenotypic plasticity (Pfennig et al., 2010). Although plasticity and stability appear to be distinct strategies for dealing with environmental variation, they actually represent two ends of a continuum of potential responses. Indeed, plasticity/stability has a genetic basis with different individuals being more or less responsive to environmental influences (Via and Lande, 1985; Scheiner, 1993). Think, for instance, of people that smoke tobacco and never develop lung cancer, and others that develop lung cancer from exposure to lower levels of second-hand smoke (Warkentin et al., 2017). Such individuals have very different responses to their environment. A clear understanding of the genetic and molecular mechanisms that organisms use to maintain a stable phenotype or to change their phenotype has broad implications in areas as diverse as medicine and climate change. Here we focus on phenotypic responses to temperature, a key environmental variable that affects every living organism.

Temperature, *via* its direct effect on the rate of biochemical reactions, influences biological processes from the cellular to the organismal level (Gillooly et al., 2002; Kingsolver, 2009; Schulte et al., 2011). Within the range of body temperatures of most organisms (0–40°C), biochemical reaction rates increase with increasing temperature until a point where stability of biological molecules is compromised and reaction rates drop. This general pattern translates to higher levels of biological organization and is referred to as a thermal performance curve (**Figure 1**). In turn, temperature effects on individual organisms drive ecological processes (Stenseth et al., 2002; Brown et al., 2004).

The Intergovernmental Panel on Climate Change (IPCC, 2013) lays out unambiguous physical and biogeochemical evidence that global temperatures have been increasing since the late 1900s. Direct measurements demonstrate that land surface air temperatures, sea surface air temperatures, troposphere temperature, and ocean heat content have been increasing

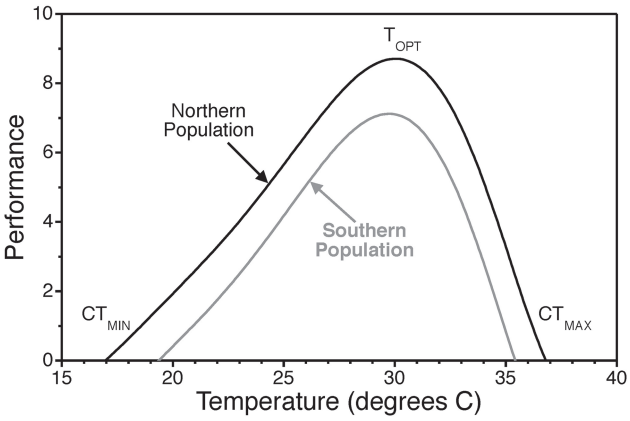

FIGURE 1 | Thermal performance curve illustrating the typical pattern of physiological performance as a function of temperature. Thermal performance curves are characterized by an optimal temperature T_{OPT} where performance is maximized. They also exhibit critical thermal minima CT_{MIN} and critical thermal maxima CT_{MAX} where performance declines to zero. Scales on the x and y axes are arbitrary and simply used to illustrate general patterns of thermal responsiveness. Optimal temperatures, the range from critical thermal minima to the critical thermal maxima, and the width of curves vary across biological scales of organization, among individuals, among populations (i.e., countergradient variation), and among species.

rapidly since 1980. During the same period, glacier mass balance and the extent of summer arctic sea ice have been declining. Even as global averages are increasing, there is spatial variation with different regions being more or less severely affected by climate change (Bellard et al., 2012).

Climate change and heterogeneity in temperature are also observed at finer spatial and temporal scales. For example, Maclean et al. (2019) estimated and analyzed hourly air temperatures at a 100-m resolution on the Lizard Peninsula, United Kingdom over nearly four decades. While there was clear warming of climate across the entire 17 square kilometer area, they found lower rates of warming on north-east facing slopes, substantial spatial variation in the number of frost-free days, and five-fold differences in the number of growing degree-days. Diurnal and seasonal patterns of temperature change normally serve as cues and as drivers of major life history events in both plants and animals (Peñuelas and Filella, 2001; Badeck et al., 2004). Body temperature, for instance, strongly influences growth rate in ectotherms (Angilletta et al., 2002). Growth rate, in turn, influences age and size at reproductive maturity (Stearns, 1992). Increasing mean temperatures and shifting patterns of thermal variance in space and time have already had a demonstrable effect on terrestrial and marine ecosystems (Parmesan and Yohe, 2003; Burrows et al., 2011).

Temperature effects on organismal phenotype are especially clear in taxonomic groups like reptiles that do not produce their own heat and have variable body temperatures (i.e., ectothermic poikilotherms). Reptiles live in a wide range of climates from tropical to sub-tropical to northern temperate zones and are susceptible to temperature effects throughout

their lifespan. Although juvenile and adult reptiles can thermoregulate *via* basking and selecting thermally distinct microhabitats and through physiological mechanisms that influence heat transfer (Adolph, 1990; Seebacher and Franklin, 2005), variation in body temperature is still substantial. Reptiles are also able to respond to temperature through the process of acclimation, which involves longer-term physiological changes that compensate for direct temperature effects on reaction rates (e.g., increases in enzyme expression to maintain the same overall rate of metabolism at a lower temperature). Acclimation is a reversible response that occurs over days or weeks in association with seasonal changes in temperature. Temperature can also have permanent developmental effects on phenotype, as observed in species with temperature-dependent sex determination. Finally, changes in thermal environment can exert selection pressure on thermal performance curves and cause evolutionary adaptation (Angilletta and Angilletta, 2009; Logan et al., 2014).

Countergradient variation in growth rate, for instance, provides strong evidence of genetic adaptation to geographic gradients in environmental variables (Conover and Schultz, 1995). In brief, countergradient variation refers to genetic differences among populations that counteract the phenotypic effects of the environmental gradient. In the case of thermal gradients with latitude in the Atlantic silverside, northern populations in cooler environments exhibit faster growth than southern populations in warmer environments when tested at the same temperatures (Conover and Present, 1990). This type of genetic adaptation would manifest as an upward shift in the thermal performance curve for growth rate such that more northern populations perform at the same level even though they live in cooler environments (**Figure 1**). It is important to note that countergradient variation is due to genetic differentiation and is not a result of physiological acclimation.

Here we briefly review the physics of temperature effects on biochemical reactions, the general pattern of thermal effects on physiology, and the process of thermal acclimation in ectotherms. However, our main focus is developmental programming of phenotype by temperature during embryogenesis (i.e., permanent developmental effects). We concentrate our review on studies of egg laying species because embryos in eggs are particularly susceptible to changes in ambient temperature and have minimal ability to thermoregulate (Telemeco et al., 2016; Cordero et al., 2018). Variation in incubation temperature in natural nests depends on the ecological conditions around the nesting area, location of the nest (shaded or open), the depth of eggs in the nest, and nesting phenology (Weisrock and Janzen, 1999; Shine and Elphick, 2001; Booth, 2006). Reptile eggs serve as an ideal model to study thermal effects because temperature can be easily manipulated. In contrast, females in live bearing lizards like *Zootoca vivipara* can behaviorally thermoregulate and alter the temperature their offspring experience (Foucart et al., 2018). Some egg-laying reptiles like prairie skinks and water pythons even brood their eggs to affect incubation temperature, which further highlights the importance of developmental temperature during embryogenesis (Lang, 1990; Shine et al., 1997).

BIOPHYSICAL EFFECTS OF TEMPERATURE

Temperature effects on biological systems can be ephemeral or they can be long-lasting. Short-lived effects are mediated by the direct, instantaneous, and reversible effect of temperature on the rate of biochemical reactions. Reaction rates increase with increasing temperatures, up until the point that elevated temperatures begin to disrupt the structure of the proteins (or other biomolecules) involved in the biological process. In addition to ephemeral effects, temperature can have lasting effects that persist well after ambient temperature changes. Persistent temperature effects on phenotype are mediated by post-translational modifications to proteins and/or changes in gene expression. These temperature-induced changes may be reversible over longer timescales (i.e., physiological acclimation) or they can be permanent and last a lifetime (i.e., developmental plasticity or polyphenism). It is therefore important to distinguish between different timescales to fully understand thermal biology (Schulte et al., 2011).

We begin our discussion of temperature at its most fundamental biophysical level. In order to quantitatively study the sensitivity of living organisms to temperature changes, it is customary to use the temperature coefficient (Q_{10}) value (Hegarty, 1973), which is a measure of the rate of change of a biological or chemical system due to temperature increase of 10°C.

$$Q_{10} = (R_2/R_1)^{10 \text{ degrees C}/(T2-T1)}$$

where R_1 is the rate of the reaction at temperature T_1, R_2 is the rate of the reaction at temperature T_2, and temperature is measured in degrees Celsius. A Q_{10} value of 1 indicates thermal independence, values above 1 indicate that reaction rates increase with increasing temperature, while values below 1 indicate that reaction rates decrease with increasing temperature. Q_{10} values for biological systems are typically between 2 ~ 3 when examined in the normal range of body temperatures for a species (i.e., the part of thermal performance curves between the critical thermal minimum and the optimal temperature). There have been few studies of metabolic rate in reptile embryos, but they also report Q_{10}'s around 2 (Angilletta, 2001; Angilletta et al., 2006).

To understand the rationale behind Q_{10} values, one needs to digress to the collision rate theory. According to this theory, the rate constants for chemical reactions are a direct function of temperature. Reactions are, at an elementary level, due to collisions of reactants with a certain threshold energy. Now, with an increase in thermal energy, the kinetic energies of the reactants increase resulting in more frequent collisions and an increase in the reaction rate. However, biochemical reactions and interactions involve proteins and other biomolecules (e.g., functional RNAs) whose three-dimensional shape depends unequivocally on non-covalent intra-molecular interactions. The stability of biomolecules is diminished at elevated operational temperatures. As these molecules start to denature at higher temperatures, reaction rates drop. This results in thermal performance curves with

an optimal temperature at which reaction rate is maximized (**Figure 1**). Critical thermal minima and maxima for thermal performance curves are defined as the temperatures where reaction rates drop to zero (**Figure 1**). Thus, Q_{10} values for biochemical processes are not a monotonic function of temperature. Several mathematical models have been developed that incorporate both the temperature dependence of reaction kinetics described by the collision rate theory (i.e., the Arrhenius equation) as well as temperature effects on enzyme stability (DeLong et al., 2017).

While this general pattern of thermal performance extends beyond simple biochemical reactions to higher levels of biological organization, the precise pattern of acute temperature effects varies because cells, tissues, organs, and organisms are complex, hierarchical systems. Performance curves at higher levels of organization vary in part because different subcomponents (e.g., biomolecules within cells) can display different thermal performance curves and the combined effect of subcomponents may be nonlinear and/or non-additive with regard to performance of the system as a whole. We refer readers to Gangloff and Telemeco (2018) for an in-depth review of thermal performance curves at higher levels of biological organization. These authors also propose a novel hypothesis, Hierarchical Mechanisms of Thermal Limitation, that integrates thermal effects on subcellular components and organ systems to better understand thermal tolerance at the whole organism level. Moreover, cells, tissues, organs, and whole organisms are dynamic systems that can sense and respond to their thermal environment through physiological acclimation (Somero, 2005; Keen et al., 2017; Rohr et al., 2018).

THERMAL ACCLIMATION IN JUVENILES AND ADULTS

Acclimation occurs when prolonged exposure to a new thermal regime, be it in nature or in a controlled laboratory setting, induces alterations in the acute response to temperature (i.e., the thermal performance curve changes). As mentioned previously, exposure to cold temperatures can induce physiological changes that compensate for the direct negative effect of low temperature on reaction rates. A well-studied example is remodeling of the heart in fish species that remain active during the cold season. Cold-induced changes in gene expression alter structural and functional properties of the heart, from the sub-cellular level (e.g., myofilaments, electrical activity, and calcium handling) to the cellular level (e.g., myocyte contraction) to the organ level (e.g., gross changes in heart size and stiffness) (reviewed by Keen et al., 2017). Together, these changes preserve whole organism performance across a broader range of temperatures than would otherwise be possible. Similar effects of cold acclimation on the cardiovascular system are observed in turtles (Risher and Claussen, 1987; Keen et al., 2016). Heat acclimation is also a well-established phenomenon in which exposure to elevated temperatures increases the critical thermal maximum of a broad range of organisms (Sinclair et al., 2016; Rohr et al., 2018), including lizards, snakes, and turtles (Murrish and Vance, 1968; Jacobson and Whitford, 1970; Williamson et al., 1989; Brown, 1996). In short, acclimation entails shift in thermal optima, critical thermal minima and maxima, and/or changes in the breadth of thermal performance curves (Rohr et al., 2018). Thermal acclimation in ectotherms is a form of phenotypic plasticity that reduces performance differences in thermally variable environments.

DEVELOPMENTAL EFFECTS OF TEMPERATURE

Temperature also has complex effects on the development of reptilian embryos. On one hand, developmental rate displays a classic thermal response. As incubation temperature increases, reptile embryos develop faster and hatch sooner (reviewed in Noble et al., 2018). This pattern is clearly seen in snapping turtle embryos, which also display evidence of countergradient variation in developmental rate (**Figure 2**; Ewert et al., 2005). Yet, hatchlings incubated at different temperatures are not simply exact replicas of each other (Rhen and Lang, 2004; Booth, 2018; Mitchell et al., 2018; Noble et al., 2018; While et al., 2018). Animals from different incubation temperatures are marked by differences in body size, body shape, amount of residual yolk, size of fat stores, locomotor performance, thermoregulatory behavior, sexual phenotype, and many other traits. In turn, incubation temperature effects on traits like critical thermal minima and maxima may have a significant impact on susceptibility of reptiles to global warming, as suggested for the velvet gecko (Dayananda et al., 2017). To understand how these differences arise, we need to examine embryogenesis in more detail.

Embryonic development can be broken down into two basic processes. First is differentiation, wherein specific cell types,

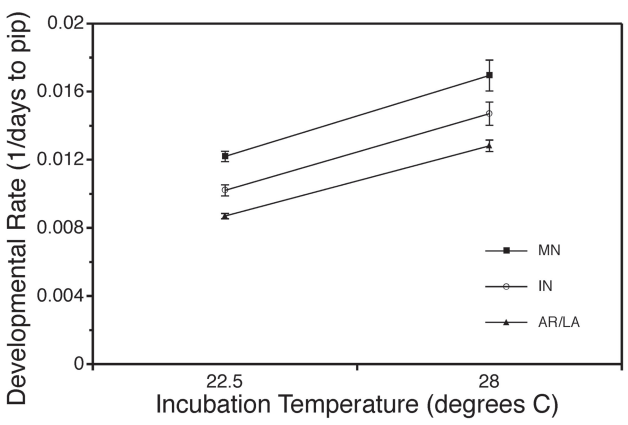

FIGURE 2 | Countergradient variation for developmental rate of embryonic common snapping turtles, *Chelydra serpentina*. Eggs from Minnesota, Indiana, and Arkansas/Louisiana were incubated at the same temperatures, 22.5 or 28°C. Incubation period was recorded as the number of days from oviposition to pipping. Developmental rate is the inverse of incubation period (1/days to pip). Data are modified from Ewert et al., 2005.

tissues, organs, and organ systems are formed. Second is growth, characterized by an increase in size of the embryo due to cell proliferation, cell hypertrophy (for certain cell types), and deposition of extracellular matrix. Another facet of embryogenesis is the simultaneous development of extraembryonic membranes that play a critical role in gas, nutrient, and waste exchange. Development in vertebrates can be further classified in terms of temporal progression of cleavage, gastrulation, neurulation, and organogenesis as well as early growth and late growth.

Given these fundamental processes, temperature most likely has its long-term effects on reptiles by influencing differentiation, growth, and/or the temporal relationships among these processes. In this context, studies in common snapping turtles and the skink *Bassiana duperreyi* have found that early to middle stages of embryogenesis are more susceptible to temperature effects than later stages of development (Yntema, 1968; Birchard and Reiber, 1995, 1996; Shine and Elphick, 2001). This suggests temperature has a greater impact on cell, tissue and organ differentiation, which occurs earlier in development, than it does on growth. The finding that the latter half of development, when embryos grow most rapidly, is less responsive to temperature suggests embryos acclimate to temperature. Studies of heart rate show that embryos in one turtle, one snake, and one lizard species, but not a second lizard species, acclimate to temperature (Du et al., 2010). We start our discussion of permanent developmental effects with an unambiguous example of temperature altering cell and organ fate decisions.

TEMPERATURE-DEPENDENT SEX DETERMINATION

Two principal mechanisms of sex determination are routinely encountered in reptiles: genotypic sex determination (GSD) and environmental sex termination (ESD). In GSD species, gonadal sex is determined by genetic factors like sex chromosomes that are inherited at fertilization. In contrast, ESD occurs when external signals determine gonadal sex well after fertilization (Bull and Vogt, 1979; Janzen, 1994). Temperature is the only external cue known to affect sex determination in reptiles (Bull and Vogt, 1979; Janzen, 1994). Even more fascinating is the fact that temperature, a continuous variable, is transduced into a binary response, with individuals normally developing either testes or ovaries (but not as intersexes). As a result, the impact of the thermal environment on sex determination is visualized as a reaction norm in which sex ratios of groups of individuals are plotted as a function of incubation temperature.

Reaction norms for TSD typically follow one of three fundamental patterns (Ewert and Nelson, 1991). In species with a male-female pattern (MF; a.k.a. pattern Ia), males are produced at low temperatures and females at high temperatures. In species with a female-male pattern (FM; a.k.a. pattern Ib), females are produced at low temperatures and males at high temperatures. The female-male-female pattern (FMF; a.k.a. pattern II) is characterized by female production at low and high temperatures with males developing at intermediate temperatures. Mixed sex ratios are produced within a transitional range between temperatures that induce exclusively one sex or the other. The term pivotal temperature refers to the temperature(s) within the transitional range(s) that produces a 1:1 sex ratio (Mrosovsky and Pieau, 1991). The FMF pattern with two pivotal temperatures has been reported in all groups of reptiles with TSD, viz., turtles, crocodilians, and lizards. Therefore, it is hypothesized that the FMF pattern is ancestral, while the FM and MF pattern are derived patterns resulting from suppression of ovary development and activation of testis development at high or low incubation temperatures (Ewert and Nelson, 1991). The common snapping turtle exhibits a dramatic latitudinal cline in TSD pattern with a gradual change from a clear FMF pattern in southern populations to a MF-like pattern in northern populations (**Figure 3**; Ewert et al., 2005). The mechanism underlying the evolutionary transition from female to male determination is uncertain because the full gene regulatory network underlying TSD is not known.

Reaction norms for TSD vary both among and within species (reviewed by Deeming, 2004; Ewert et al., 2004; Harlow, 2004; Roush and Rhen, 2018), which suggests that TSD is a threshold trait determined by a combination of genetic and environmental factors. There are differences in pivotal temperature(s) among clutches of eggs produced by different females within populations and among populations from different geographic regions (reviewed in Roush and Rhen, 2018). Variation in pivotal temperatures is correlated with latitude in some species (Ewert et al., 2005; Schroeder et al., 2016), but not others (Bodensteiner et al., 2019). In those species that exhibit geographic clines, pivotal temperatures tend to increase with an increase in latitude (Bull et al., 1982; Vogt and Flores-Villela, 1992; Ewert et al., 2005).

There are two primary hypotheses about the underlying cause of intraspecific variation in pivotal temperatures: the

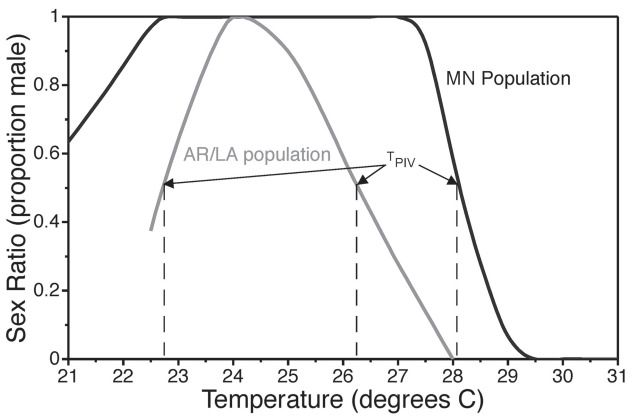

FIGURE 3 | Thermal reaction norm for sex determination in common snapping turtles, *Chelydra serpentina*, from Minnesota and the Arkansas/Louisiana border. The constant incubation temperature that produces a 1:1 sex ratio is called the pivotal temperature T_{PIV}. Data are modified from Ewert et al., 2005.

first is that there is genetic variation in temperature sensitivity of embryos and the second is that non-genetic maternal factors cause variation in sex ratio of offspring (e.g., steroid hormones deposited in egg yolk prior to oviposition). To date, few studies have rigorously addressed these hypotheses (reviewed in Roush and Rhen, 2018). We have therefore used controlled breeding studies to tease apart additive genetic effects from genetic variance due to allelic dominance and non-genetic maternal effects. We found that variation in TSD in leopard geckos and common snapping turtles is genetically based and is not due to maternal effects (Rhen et al., 2011; Schroeder et al., 2016). In these species, sex determination is clearly a classic threshold trait determined by a combination of genes and the environment.

Temperature has also been shown to have quantitative effects on sex determination in TSD species. In other words, the magnitude and duration of exposure to male (or female) producing temperatures during the critical sex-determining period influences the likelihood of embryos developing testes or ovaries (Yntema, 1979; Mrosovsky and Pieau, 1991; Wibbels et al., 1991; Lang and Andrews, 1994; Merchant-Larios et al., 2010; Rhen et al., 2015). For example, 31°C has a more potent feminizing effect on snapping turtle embryos than does 29.5°C, which is closer to the pivotal temperature of 28.2°C in the focal population from Minnesota (**Figure 3**; Rhen et al., 2015). Conversely, 24°C is a more potent masculinizing temperature than 25°C, which in turn is more masculinizing than 26.5°C (Rhen et al., 2015). These observations imply that temperature is influencing production of some biochemical factor (or factors) in a quantitative way and that this signal is translated into a binary developmental response *via* a threshold-like mechanism (**Figure 4**). Aromatase, a steroidogenic enzyme that converts androgens into estrogens, is likely to be a key factor. If estrogen concentration in embryonic gonads is below a critical threshold, gonads develop into testes. If they are above this threshold, gonads develop into ovaries (**Figure 4**).

Indeed, ovary determination in TSD species is estrogen dependent in virtually all turtle, lizard, and crocodilian species that have been examined to date. Applying estrogens to embryos at male temperatures drives ovary formation, while aromatase inhibitors, which block estrogen synthesis, obstruct ovary development and induce testis development at temperatures that normally produce females or mixed sex ratios (Crews et al., 1994; Dorizzi et al., 1994; Rhen and Lang, 1994; Pieau et al., 1999; Pieau and Dorizzi, 2004; Freedberg et al., 2006; Lance, 2009; Rhen and Schroeder, 2010). In accord with these experimental manipulations, aromatase expression at female temperatures is higher than at male temperatures in several reptile species with TSD (Desvages and Pieau, 1992; Desvages et al., 1993; Lance, 2009; Rhen and Schroeder, 2010).

The specific mechanisms that regulate aromatase expression in embryonic gonads are unknown. We hypothesize that one or more genes encode sensors that are activated when temperature is in a particular range (**Figure 5**). The sensor (or sensors) then triggers the bipotential gonads to develop as ovaries. Recent studies suggest that epigenetic regulators of histone H3 methylation on lysine 27 (H3K27) may be involved in mediating temperature effects on expression of various sex-determining

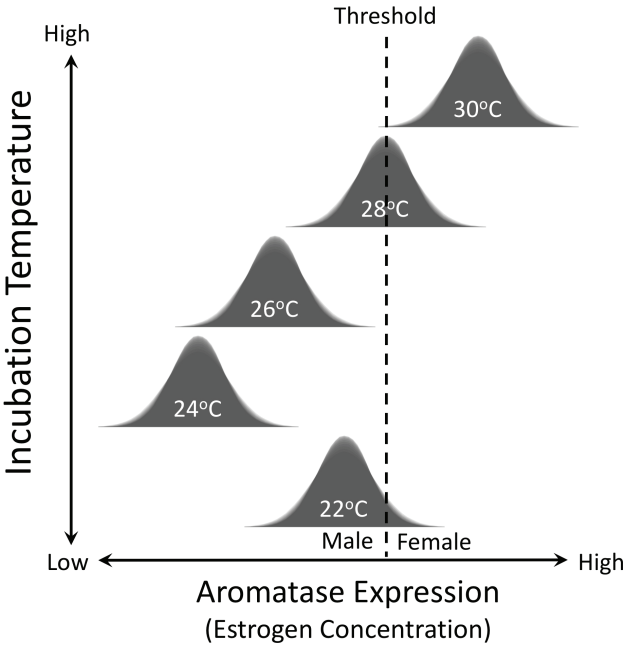

FIGURE 4 | Threshold model for temperature-dependent sex determination. Incubation temperature during development influences expression of the aromatase enzyme, which synthesizes estrogens. Variation in expression of aromatase enzyme and the concentration of estrogen is normally distributed at each incubation temperature. If estrogen concentration in embryonic gonads is below a critical threshold, gonads develop into testes. If they are above this threshold, gonads develop into ovaries.

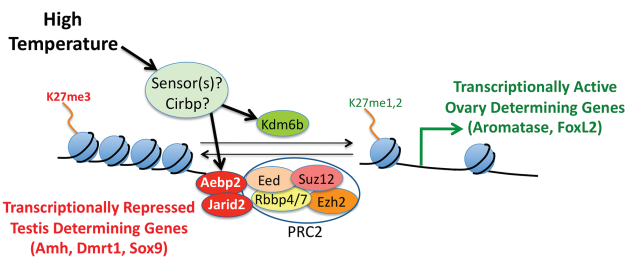

FIGURE 5 | A conceptual model of the molecular mechanisms underlying temperature-dependent sex determination. Hypothetical temperature sensors influence expression and/or splicing of epigenetic regulators like Jarid2, Aebp2, and Kdm6b. In turn, these proteins influence methylation levels of histone H3 on lysine 27. Tri-methylation of H3K27 results in silencing of target genes, while mono- or di-methylation of H3K27 results in activation of target genes.

genes (**Figure 5**). In other vertebrates, Jumonji and AT-Rich Interaction Domain Containing 2 (Jarid2) helps recruit Polycomb Repressive Complex 2 (PRC2) to specific genomic locations (Healy et al., 2019). In turn, PRC2 methylates H3K27, which results in transcriptional silencing of target genes (**Figure 5**). In contrast, Lysine Demethylase 6B (Kdm6b) removes methyl groups from H3K27, thereby relieving repression (**Figure 5**).

In a study of bearded dragons (*Pogona vitticeps*), Deveson et al. (2017) found that Jarid2 and Kdm6b retain introns in

temperature-induced ZZ females unlike ZZ males or ZW females. Similarly, differentially retained introns were detected at male- and female-producing temperatures in *Alligator mississippiensis* and *Trachemys scripta*, which are known to exhibit TSD. In yet another study, expression of Kdm6b (Ge et al., 2018) regulates Doublesex and Mab-3 Related Transcription Factor 1 (Dmrt1) expression. In turn, Dmrt1 acts as a transcription factor that is important for testis determination at male-producing temperatures in *Trachemys scripta*.

There is strong evidence that Cold-inducible RNA Binding Protein (Cirbp) plays a role in TSD in the snapping turtle (Schroeder et al., 2016). This gene displays temperature-dependent, allele specific expression. One allele is induced by exposure to a female producing temperature, while expression of the other allele is not affected by this thermal treatment. There is a strong genetic association between Cirbp genotype and the sex of hatchlings. When exposed to a female temperature for just 2.5 days, homozygotes for the temperature sensitive allele are four times more likely to develop ovaries than are heterozygotes, which are in turn four times more likely to develop ovaries than homozygotes for the temperature in-sensitive allele. This association extends to the family and population level and provides another mechanistic link between genes and the environment.

Despite evidence that aromatase, Jarid2, Kdm6b, and Cirbp are factors involved in mediating temperature effects on sex determination, the actual temperature sensors have yet to be identified in TSD species (Georges and Holleley, 2018). It will also be important to carry out mechanistic studies to understand how these genes interact with each other to determine sex.

TEMPERATURE EFFECTS ON QUANTITATIVE TRAITS

While sex ratios provide a clear, albeit course, measure of temperature effects on cell, tissue, and organ differentiation, there are many other examples of persistent thermal effects on quantitative phenotypes in reptiles. Others have reviewed temperature effects on a wide range of traits (Rhen and Lang, 2004; Booth, 2018; Mitchell et al., 2018; Noble et al., 2018; While et al., 2018). Thus, we discuss just a few interesting examples of long-lasting effects on physiology and behavior.

Incubation Temperature May Program Metabolism

Incubation has been shown to influence thyroid hormone physiology and metabolic rate. Resting metabolic rate and circulating thyroid hormone concentration decreased with increasing incubation temperature in hatchling snapping turtles that had been incubated across a wide range of temperatures (O'Steen and Janzen, 1999). Measurements were conducted in hatchlings held at the same ambient temperatures, which indicates that prior incubation temperature had a persistent effect on metabolic physiology. In another experiment in the same paper, eggs were incubated at two temperatures, one that produces males and one that produces females, and treated with triiodothyronine. Thyroid hormone treatment during embryogenesis had no effect on sex determination but increased developmental rate (treated turtles hatched sooner than controls), decreased hatchling mass, and raised the resting metabolic rate of hatchlings. Given that snapping turtles were studied a few days after hatching, longer-term studies will be required to distinguish whether these effects are simply due to thermal acclimation or are the result of developmental programming of metabolic phenotype. Nevertheless, studies of American alligators do suggest that disruption of thyroid hormone signaling during embryogenesis can program functioning of the hypothalamic-pituitary-thyroid axis as long as 10 months after hatching (Boggs et al., 2013).

Incubation Temperature Programs Endocrine Phenotype

Incubation temperature influences steroid hormone synthesis during embryonic development. Exposure to different hormonal environments may in turn program physiological and behavioral traits. For instance, incubation temperature during embryonic development has been shown to affect circulating levels of estradiol-17β, progesterone and testosterone in juvenile red-eared slider turtles (Rhen et al., 1999). The circulating concentration of estradiol-17β, progesterone, testosterone, and dihydrotestosterone also differs among juvenile leopard geckos that were incubated at different temperatures (Rhen et al., 2005). Importantly, these effects on steroid levels persist into adulthood in the leopard gecko (Crews et al., 1998; Rhen et al., 2000). This strongly suggests that temperature during embryonic development directly or indirectly (*via* its effect on steroidogenesis) programs the hypothalamic-pituitary-gonad axis (Rhen and Crews, 2002). In accord with this inference, incubation temperature alters patterns of metabolic capacity in specific hypothalamic nuclei of leopard geckos in adulthood (Sakata et al., 2000; Sakata and Crews, 2003, 2004).

Incubation Temperature Programs Growth Physiology

Incubation temperature has been shown to influence both embryonic and post-hatching growth rate in a number of reptiles (Noble et al., 2018; While et al., 2018). Thermal effects on embryonic growth rate can be attributed to a direct Q_{10} effect, whereas persistent effects on hatchlings and juveniles show thermal acclimation or permanent developmental effects on growth physiology. Cooler incubation temperatures produced hatchlings that grow significantly faster than hatchlings from the hottest incubation temperatures in the green anole (Goodman, 2008), the broad-snouted caiman (Pina et al., 2007), and the Murray River turtle (Micheli-Campbell et al., 2011). Incubation temperature has also been shown to influence post-hatching growth rate in numerous studies of the snapping turtle (Bobyn and Brooks, 1994; Rhen and Lang, 1995, 1999; O'Steen, 1998).

Rhen and Lang (1995) used experimental manipulations to decouple temperature and sex effects, revealing that incubation temperature programmed growth physiology independently of its effect on sex determination. In snapping turtles, temperatures

that normally yield males produce faster growing turtles than temperatures that produce females. These studies examined growth in common gardens over several months to a year after hatching. Thermal acclimation normally occurs over a period of days or weeks so these incubation temperature effects on growth physiology are likely to be permanent. Indeed, incubation temperature affects adult body size in leopard geckos (Tousignant and Crews, 1995). Again, it is likely that temperature is altering neuroendocrine phenotype (i.e., the hypothalamus, pituitary, and growth hormone signaling). However, incubation temperature effects on subsequent growth do not always translate into differences in adult body size: incubation temperature has a temporary effect on body size in juvenile Australian jacky dragons (*Amphibolurus muricatus*) (Warner and Shine, 2005).

Incubation Temperature Programs the Brain and Behavior

Several of the physiological traits discussed above are regulated by neuroendocrine mechanisms, so it is not surprising that temperature has persistent effects on the behavior of reptiles. An assortment of behaviors has been studied, including thermoregulation, righting and swimming performance, as well as sociosexual behaviors. Most of these studies have examined behavior in hatchlings or juveniles, but a few have shown embryonic programming of adult behaviors.

Thermoregulatory behavior of snapping turtles, for instance, is programmed by incubation temperature (O'Steen, 1998; Rhen and Lang, 1999). Both studies report a negative correlation between incubation temperature and the thermal environment selected by juvenile turtles. O'Steen (1998) measured mean preferred temperatures ranging from 24.5 to 28°C. In other studies of snapping turtles, mean temperatures selected in aquatic thermal gradients were 28 and 30°C for hatchlings (Williamson et al., 1989; Knight et al., 1990) and 28°C for adults (Schuett and Gatten, 1980). Selection of particular ambient temperatures is likely to influence growth rate because body temperature has a profound effect on growth. Williamson et al. (1989) found that hatchlings held at 15°C did not grow at all, while those held at 25°C grew seven-fold in mass over 1 year. Rhen and Lang (1999) similarly reported that snapping turtles held at 19°C grew very slowly or not at all while those held at 28°C grew rapidly. Turtles that had been incubated at cool and intermediate temperatures (24 and 26.5°C) were able to grow at 19°C, but turtles from a warm incubation temperature (29°C) did not grow at 19°C. These observations suggest incubation temperature programs the critical thermal minimum for growth. Further studies will be required to determine whether critical thermal maxima also differ and if preferred body temperatures match optimal temperatures for growth in snapping turtles from different incubation temperatures.

Micheli-Campbell et al. (2011) report that swimming behavior and performance in the turtle *Elusor macrurus* are altered by incubation temperature. Hatchling turtles from cool and intermediate temperatures swim more and have a stronger mean stroke force than turtles from the highest incubation temperature. Turtles from cool and intermediate temperatures are also able to right themselves more quickly when turned on their back. In contrast, yearling turtles from a warm temperature righted themselves faster than turtles from a cooler temperature in two other species *Graptemys ouachitensis* and *Trachemys scripta* (Freedberg et al., 2004). Extreme embryonic temperatures increased righting time relative to intermediate temperatures in *Caretta caretta* (Fisher et al., 2014). The mechanism underlying these differences in locomotor performance is unknown. However, these effects can last as long as 1 year.

The impact of incubation temperature on behavior in adult leopard geckos of both sexes has been studied extensively (reviewed in Crews et al., 1998; Rhen and Crews, 2002; Sakata and Crews, 2004). Both embryonic temperature and gonadal sex affect sexual and aggressive behavior, sex steroid levels in the circulation, and the metabolic activity of several brain regions, including hypothalamic nuclei critical for the display of sociosexual behaviors (**Figure 6**). Sexual dimorphism in sociosexual behavior in leopard geckos follows the basic pattern found in mammals (Rhen and Crews, 1999, 2000). Females do not display male-typical scent marking or sexual behavior when treated with androgens that activate these behaviors in males. This indicates that sexual dimorphism in hormone responsiveness in adulthood is programmed at some point during ontogeny, presumably by sex differences in secretion of steroid hormones (Rhen et al., 2005).

In addition to pronounced sex differences, there is substantial intrasexual variation in sexual and aggressive behavior that is

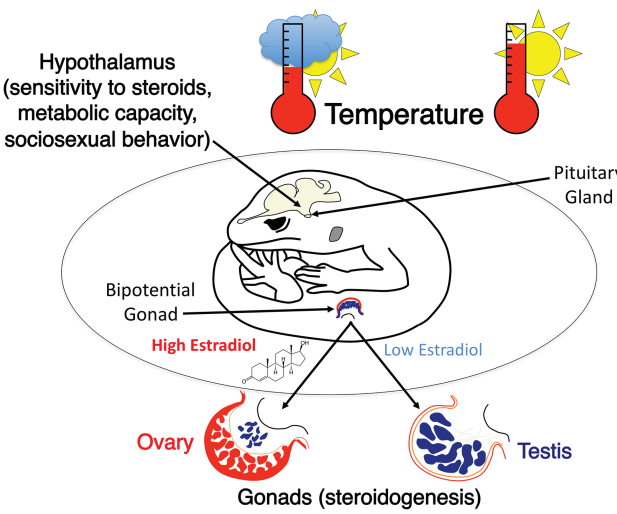

FIGURE 6 | A graphical illustration of temperature effects on neural and gonad development in the leopard gecko. Incubation temperature determines sex and causes intrasexual variation in sociosexual behaviors. These differences in behavior are correlated with significant differences in metabolic capacity within specific hypothalamic nuclei as well as differences in sensitivity to sex steroids that activate sociosexual behaviors.

programmed by embryonic temperature. Male leopard geckos from a temperature that produces a female-biased sex ratio are more sexually active and less aggressive towards females than are males from a temperature that produces a male-biased sex ratio (Flores et al., 1994). Yet, temperature also affects endocrine physiology in adult males: males from a female-biased temperature have a lower ratio of androgens to estrogens when compared to males from a male-biased temperature (Tousignant and Crews, 1995; Crews et al., 1996).

To test whether the persistent effects of incubation temperature on behavior in adults were simply due to differences in hormone profiles in adulthood or to programming during early development, male leopard geckos from different temperatures were castrated and treated with the same levels of testosterone or dihydrotestosterone in adulthood. Males from the male-biased and the female-biased incubation temperatures behaved very differently even though they had the same levels of circulating hormones: males from the male-biased temperature scent marked more than males from the female-biased temperature (Rhen and Crews, 1999). Conversely, males from the female-biased incubation temperature were more sexually active (i.e., courted and mounted females more) than males from the male-biased temperature. Taken together, these findings demonstrate that embryonic temperature programs the male leopard gecko brain to respond differently to sex steroids in adulthood (i.e., classic organizational effects).

Incubation temperature effects on behavior in leopard geckos are correlated with physiological differences in the brain. More sexually active males from the female-biased temperature have greater metabolic capacity (i.e., cytochrome oxidase) in several brain regions than less sexually active males from the male-biased temperature. Incubation temperature effects on metabolic capacity in the preoptic area of the hypothalamus make sense because this region of the brain is essential for the display of male sexual behavior in all vertebrates, including leopard geckos (Edwards et al., 2004). Developmental temperature also influences metabolic capacity in brain nuclei that regulate agonistic behavior (Crews et al., 1996; Coomber et al., 1997). In summary, embryonic temperature clearly programs endocrine physiology, neurological phenotype, and behavior and may program metabolic physiology and some aspects of locomotor performance in a various reptilian species.

CURRENT RESEARCH ON EPIGENETIC MECHANISMS

The specific molecular factors that transduce temperature into a biological signal are largely unknown. However, there is increasing evidence that these hypothetical factors target epigenetic mechanisms, which provide a link to cell, tissue, and organ differentiation. Epigenetic mechanisms have been shown to play a role in environmental regulation of several traits in animals. In recent years, attempts have been made to survey epigenetic mechanisms to understand how temperature programs phenotype including studies of DNA methylation and histone modifications in several reptiles with TSD (Navarro-Martin et al., 2011; Matsumoto et al., 2013, 2016; Czerwinski et al., 2016; Yatsu et al., 2016; Fan et al., 2017; Radhakrishnan et al., 2017, 2018; Ge et al., 2018; Martín-del-Campo et al., 2019).

Whether genetically or environmentally programmed, developmental events like cell fate determination and cellular differentiation involve permanent changes in gene expression (Barsi et al., 2014). Post-translational modifications of histones and DNA methylation are key epigenetic marks that play a part in development by regulating cell-type and tissue-specific patterns of gene expression (Cedar and Bergman, 2009; Greer and Shi, 2012). Cytosine methylation (i.e., 5-methylcytosine) in particular is associated with gene silencing and is stably passed from mother to daughter cells during mitosis. In mammals, DNA methylation has context dependent effects on gene expression, depending on whether 5-methylcytosines are found at transcription start sites, in gene bodies, in repetitive DNA, or in enhancers and silencers (Jones, 2012).

Changes in DNA methylation mediate various environmental effects on phenotype. Temperature affects DNA methylation at the genome-wide level in many animals (Anastasiadi et al., 2017; Metzger and Schulte, 2017). A correlation between body temperature and overall DNA methylation level has been previously shown in vertebrates (Jabbari et al., 1997) and reptiles (Varriale and Bernardi, 2006). Differential DNA methylation at sex-determining genes may be a critical factor for sex determination in animals (Gorelick, 2003). In some TSD species, the promoter region of the aromatase gene shows tissue specific, sexually dimorphic DNA methylation, which is affected by temperature exposure during the sex-determining period. More specifically, higher methylation of particular cytosines is associated with lower aromatase expression in gonads of embryos at male-producing temperatures when compared to embryos at female-producing temperatures in two fish and one turtle species (Navarro-Martin et al., 2011; Matsumoto et al., 2013; Fan et al., 2017).

Differentially methylated regions have been reported in genome-wide studies of hatchling testes and ovaries in the painted turtle, *Chrysemys picta* (Radhakrishnan et al., 2017). Methylated DNA immunoprecipitation combined with next generation sequencing of the DNA (MeDIP-Seq) and analysis of CpG content in the genome shows sexually dimorphic DNA methylation at promoter, exon, intron, and inter-genic regions in the painted turtle genome. The study identified a total of 5,647 differentially methylated regions between male and female gonads including several genes reported to be involved in gonadal development. However, the observation of differential DNA methylation in hatchling gonads may reflect a role in maintenance of cell and organ fate rather than a role in sex determination in embryos incubated at male and female producing temperatures. Future studies should examine temperature effects on DNA methylation in embryos during the temperature sensitive period.

Radhakrishnan et al. (2018) tried to correlate temperature with epigenetic mechanisms by studying differences in expression of genes known to be involved in DNA methylation and

histone modification along with some small RNAs in TSD (*Chrysemys picta*) and GSD (*Apalone spinifera*) turtle species. Several genes involved in DNA methylation (Dnmt3b) and histone methylation (Nsd1, Setd1a, Carm1, Prmt1, Ash1l, and Prdm2) were found to be differentially regulated between male and female producing temperatures in *Chrysemys picta* (Radhakrishnan et al., 2018). These results together underscore the importance of studying mechanisms involved in epigenetic regulation of gene expression and TSD.

Along with DNA methylation, histone modifications have been shown to play a crucial role in early embryonic development in reptiles (Feiner et al., 2018). Kdm6b is differentially expressed between gonadal transcriptomes from embryos incubated at male and female producing temperatures in TSD species *Alligator mississippiensis* (Yatsu et al., 2016) and *Trachemys scripta elegans* (Czerwinski et al., 2016). Ge et al. (2018) showed the sexually dimorphic expression of Kdm6b during the sex-determining period in *Trachemys scripta* embryos favors testis development. Another epigenetic regulator (Jarid2) shows temperature-dependent intron retention and differential expression of isoforms in male and female gonads in bearded dragons (Deveson et al., 2017). Jarid2 is currently being investigated as a potential TSD gene (Georges and Holleley, 2018).

TEMPERATURE EFFECTS ON DEVELOPMENT PLASTICITY IN LIGHT OF GLOBAL WARMING

In summary, incubation temperature during embryogenesis has significant effects on numerous hatchling phenotypes in reptiles. Many of the phenotypic differences examined are not simply due to direct temperature effects on rates of biochemical reactions (i.e., the Q_{10} effect). Neither are they the result of reversible physiological changes (i.e., thermal acclimation). Rather, they appear to be permanent developmental effects (i.e., fetal programming of phenotype). Indeed, some studies demonstrate temperature effects lasting into adulthood. Recent work suggests that epigenetic marks like DNA methylation and histone modifications may mediate the persistent effects of temperature in reptiles. In other organisms, such marks are involved in conferring cellular "memory" of environmental signals during early development (Bird, 2002; Ringrose and Paro, 2004; Hansen et al., 2008; Jones, 2012).

It is imperative to determine whether (1) these temperature effects translate to nature and (2) global warming is likely to have an impact on reptiles (and other ectotherms) in the wild. Studies of TSD species suggest the answer to both questions is yes. Variation in sex ratio is correlated with nest or water temperatures in nature in crocodilians, lizards, turtles, and fish (Janzen, 1994; Weisrock and Janzen, 1999; Wapstra et al., 2009; Simoncini et al., 2014; Pezaro et al., 2016; Jensen et al., 2018; Patricio et al., 2018; Honeycutt et al., 2019; Mitchell and Janzen, 2019; Tilley et al., 2019). These studies indicate that TSD is operative in nature. Moreover, warming temperatures over the last couple of decades are correlated with extremely female biased sex ratios in sea turtles from some rookeries, but not others (Hays et al., 2017). However, some laboratory studies that mimic fluctuating nest temperatures produce results that are not simply predicted by amount of time embryos spend above or below pivotal temperatures (Escobedo-Galván, 2013).

More research is clearly needed to assess the impact of temperature in natural nests on other traits in reptiles, but we expect that patterns observed at constant temperatures in laboratory studies will generally correlate with thermal effects in nature. If so, we can begin to predict the long-term impact of global warming. In the case of biased primary sex ratios in TSD species, there are several behavioral, physiological, and evolutionary changes that could mitigate the effects of climate change. Adult females may respond *via* changes in nesting phenology or selection of different thermal microenvironments for their nests (Hays et al., 2017; Jensen et al., 2018; Patricio et al., 2018). Genetic variation in thermosensitivity of embryos will also play a critical role in evolutionary responses. In snapping turtles, for instance, there is evidence of standing genetic variation for embryonic developmental rate (i.e., significant counter gradient variation) and for TSD (i.e., sex determination is heritable).

Research on the epigenetic mechanisms that mediate temperature effects in reptiles may more broadly inform our understanding of thermal biology. For example, PRC2 regulates histone methylation at the floral repressor gene and temperature-dependent vernalization in the model plant *Arabidopsis thaliana* (Coustham et al., 2012). Given that temperature has such a pervasive effect on living organisms, our hypothetical "temperature sensors" might also be highly conserved.

FUTURE RESEARCH DIRECTIONS

While epigenetic mechanisms are likely to be important for understanding the pleiotropic effects of temperature on phenotype, we appear to be missing those specific factors that actually sense and transduce thermal variation into a biological signal. In other words, we are still in search of the physical link between the kinetic energy of molecules in living organisms and the specific molecular, cellular, and developmental mechanisms that produce distinct phenotypes. Therefore, one key area for future research is the identification of temperature sensors that induce specific phenotypes. One approach would be to work upstream from known mediators of thermal effects, like the aromatase gene in TSD species. Another approach would be to use random mutagenesis to identify loci that influence thermal reaction norms, but this would be limited to a handful of model organisms suitable for forward genetics. Once these hypothetical temperature sensors are found, an important set of questions will center on how temperature alters their molecular structure and function. Such studies will reveal how these sensors interact with and regulate epigenetic mechanisms.

A second vital area for research is the assessment of genetic variation for thermosensitivity and the identification of the specific DNA variants that cause this variation. Phenotypic and genotypic variation in thermosensitivity is necessary for evolutionary responses

to a changing climate (Hoffmann and Sgrò, 2011). We only briefly discussed countergradient variation, but this pattern of genetic adaptation to thermal clines provides a good model for classical and molecular genetic analyses of thermosensitivity. Genetic variation in TSD is also a fertile area for study. The snapping turtle is an excellent model given the extent of variation in TSD both within and among populations. Ultimately, identification of temperature sensors and natural genetic variation in thermosensitivity will help us understand how life on Earth has adapted to thermal variation in the past and how it is likely to adapt to climate change now and in the future.

AUTHOR CONTRIBUTIONS

SS, DD, and TR prepared the draft and revised the manuscript.

FUNDING

This work was supported by the National Science Foundation of the United States (grant numbers IOS-0923300, IOS-1558034, and IOS-1755282). This work was also supported by the Pilot Postdoctoral Program at the University of North Dakota.

REFERENCES

Adolph, S. C. (1990). Influence of behavioral thermoregulation on microhabitat use by two Sceloporus lizards. *Ecology* 71, 315–327. doi: 10.2307/1940271

Anastasiadi, D., Díaz, N., and Piferrer, F. (2017). Small ocean temperature increases elicit stage-dependent changes in DNA methylation and gene expression in a fish, the European sea bass. *Sci. Rep.* 7:12401. doi: 10.1038/s41598-017-10861-6

Angilletta, M. J. (2001). Variation in metabolic rate between populations of a geographically widespread lizard. *Physiol. Biochem. Zool.* 74, 11–21. doi: 10.1086/319312

Angilletta, M. J. Jr., and Angilletta, M. J. (2009). *Thermal adaptation: A theoretical and empirical synthesis*. New York, NY: Oxford University Press.

Angilletta, M. J., Lee, V., and Silva, A. C. (2006). Energetics of lizard embryos are not canalized by thermal acclimation. *Physiol. Biochem. Zool.* 79, 573–580. doi: 10.1086/501062

Angilletta, M. J., Niewiarowski, P. H., and Navas, C. A. (2002). The evolution of thermal physiology in ectotherms. *J. Therm. Biol.* 27, 249–268. doi: 10.1016/S0306-4565(01)00094-8

Badeck, F. W., Bondeau, A., Bottcher, K., Doktor, D., Lucht, W., Schaber, J., et al. (2004). Responses of spring phenology to climate change. *New Phytol.* 162, 295–309. doi: 10.1111/j.1469-8137.2004.01059.x

Barnosky, A. D., Matzke, N., Tomiya, S., Wogan, G. O. U., Swartz, B., Quental, T. B., et al. (2011). Has the Earth's sixth mass extinction already arrived? *Nature* 471, 51–57. doi: 10.1038/nature09678

Barsi, J. C., Tu, Q., and Davidson, E. H. (2014). General approach for in vivo recovery of cell type specific effector gene sets. *Genome Res.* 24, 860–868. doi: 10.1101/gr.167668.113

Bellard, C., Bertelsmeier, C., Leadley, P., Thuiller, W., and Courchamp, F. (2012). Impacts of climate change on the future of biodiversity. *Ecol. Lett.* 15, 365–377. doi: 10.1111/j.1461-0248.2011.01736.x

Birchard, G. F., and Reiber, C. L. (1995). Growth, metabolism, and chorioallantoic vascular density of developing snapping turtles (*Chelydra serpentina*): influence of temperature. *Physiol. Zool.* 68, 799–811. doi: 10.1086/physzool.68.5.30163932

Birchard, G. F., and Reiber, C. L. (1996). Heart rate during development in the turtle embryo: effect of temperature. *J. Comp. Physiol. B* 166, 461–466. doi: 10.1007/BF02338288

Bird, A. (2002). DNA methylation patterns and epigenetic memory. *Genes Dev.* 16, 6–21. doi: 10.1101/gad.947102

Bobyn, M. L., and Brooks, R. J. (1994). Interclutch and interpoplulation variation in the effects of incubation conditions on sex, survival, and growth of hatchling turtles (*Chelydra serpentina*). *J. Zool.* 233, 233–257. doi: 10.1111/j.1469-7998.1994.tb08586.x

Bodensteiner, B. L., Warner, D. A., Iverson, J. B., Milne-Zelman, C. L., Mitchell, T. S., Refsnider, J. M., et al. (2019). Geographic variation in thermal sensitivity of early life traits in a widespread reptile. *Ecol. Evol.* 9, 2791–2802. doi: 10.1002/ece3.4956

Boggs, A. S. P., Lowers, R. H., Cloy-McCoy, J. A., and Guillette, L. J. Jr. (2013). Organizational changes to thyroid regulation in *Alligator mississippiensis*: evidence for predictive adaptive responses. *PLoS One* 8:e55515. doi: 10.1371/journal.pone.0055515

Booth, D. T. (2006). Influence of incubation temperature on hatchling phenotype in reptiles. *Physiol. Biochem. Zool.* 79, 274–281. doi: 10.1086/499988

Booth, D. T. (2018). Incubation temperature induced phenotypic plasticity in oviparous reptiles: where to next? *J. Exp. Zool. A Ecol. Integr. Physiol.* 329, 343–350. doi: 10.1002/jez.2195

Brown, R. P. (1996). Thermal biology of the gecko *Tarentola boettgeri*: comparisons among populations from different elevations within gran Canaria. *Herpetologica* 52, 396–405.

Brown, J. H., Gillooly, J. F., Allen, A. P., Savage, V. M., and West, G. B. (2004). Toward a metabolic theory of ecology. *Ecology* 85, 1771–1789. doi: 10.1890/03-9000

Bull, J. J., and Vogt, R. C. (1979). Temperature-dependent sex determination in turtles. *Science* 206, 1186–1188. doi: 10.1126/science.505003

Bull, J. J., Vogt, R. C., and McCoy, C. J. (1982). Sex determining temperatures in turtles: a geographic comparison. *Evolution* 36, 326–332. doi: 10.1111/j.1558-5646.1982.tb05048.x

Burrows, M. T., Schoeman, D. S., Buckley, L. B., Moore, P., Poloczanska, E. S., Brander, K. M., et al. (2011). The pace of shifting climate in marine and terrestrial ecosystems. *Science* 334, 652–655. doi: 10.1126/science.1210288

Cedar, H., and Bergman, Y. (2009). Linking DNA methylation and histone modification: patterns and paradigms. *Nat. Rev. Genet.* 10, 295–304. doi: 10.1038/nrg2540

Conover, D. O., and Present, T. M. (1990). Countergradient variation in growth rate: compensation for length of the growing season among Atlantic silversides from different latitudes. *Oecologia* 83, 316–324. doi: 10.1007/BF00317554

Conover, D. O., and Schultz, E. T. (1995). Phenotypic similarity and the evolutionary significance of countergradient variation. *Trends Ecol. Evol.* 10, 248–252. doi: 10.1016/S0169-5347(00)89081-3

Coomber, P., Crews, D., and Gonzalez-Lima, F. (1997). Independent effects of incubation temperature and gonadal sex on the volume and metabolic capacity of brain nuclei in the leopard gecko (*Eublepharis macularius*), a lizard with temperature-dependent sex determination. *J. Comp. Neurol.* 380, 409–421. doi: 10.1002/(SICI)1096-9861(19970414)380:3<409::AID-CNE9>3.0.CO;2-6

Cordero, G. A., Telemeco, R. S., and Gangloff, E. J. (2018). Reptile embryos are not capable of behavioral thermoregulation in the egg. *Evol. Dev.* 20, 40–47. doi: 10.1111/ede.12244

Coustham, V., Li, P., Strange, A., Lister, C., Song, J., and Dean, C. (2012). Quantitative modulation of polycomb silencing underlies natural variation in vernalization. *Science* 337, 584–587. doi: 10.1126/science.1221881

Crews, D., Bergeron, J. M., Bull, J. J., Flores, D., Tousignant, A., Skipper, J. K., et al. (1994). Temperature-dependent sex determination in reptiles: proximate mechanisms, ultimate outcomes, and practical applications. *Dev. Genet.* 15, 297–312. doi: 10.1002/dvg.1020150310

Crews, D., Coomber, P., Baldwin, R., Azad, N., and Gonzalez-Lima, F. (1996). Effects of gonadectomy and hormone treatment on the morphology and metabolic capacity of brain nuclei in the leopard gecko (*Eublepharis macularius*) a lizard with temperature-dependent sex determination. *Horm. Behav.* 30, 474–486. doi: 10.1006/hbeh.1996.0051

Crews, D., Sakata, J., and Rhen, T. (1998). Developmental effects on intersexual and intrasexual variation in growth and reproduction in a lizard with temperature-dependent sex determination. *Comp. Biochem. Physiol. C* 119, 229–241. doi: 10.1016/s0742-8413(98)00012-7

Czerwinski, M., Natarajan, A., Barske, L., Looger, L. L., and Capel, B. (2016). A time-course analysis of systemic and gonadal effects of temperature on sexual development of the red-eared slider turtle *Trachemys scripta elegans*. *Dev. Biol.* 420, 166–177. doi: 10.1016/j.ydbio.2016.09.018

Dayananda, B., Murray, B. R., and Webb, J. K. (2017). Hotter nests produce hatchling lizards with lower thermal tolerance. *J. Exp. Biol.* 220, 2159–2165. doi: 10.1242/jeb.152272

Deeming, D. C. (2004). "Prevalence of TSD in crocodilians" in *Temperature-dependent sex determination in vertebrates*. eds. N. Valenzuela and V. Lance (Washington, DC: Smithsonian Institution), 33–41.

DeLong, J. P., Gibert, J. P., Luhring, T. M., Bachman, G., Reed, B., Neyer, A., et al. (2017). The combined effects of reactant kinetics and enzyme stability explain the temperature dependence of metabolic rates. *Ecol. Evol.* 7, 3940–3950. doi: 10.1002/ece3.2955

Desvages, G., Girondot, M., and Pieau, C. (1993). Sensitive stages for the effects of temperature on gonadal aromatase activity in embryos of the marine turtle *Dermochelys coriacea*. *Gen. Comp. Endocrinol.* 92, 54–61. doi: 10.1006/gcen.1993.1142

Desvages, G., and Pieau, C. (1992). Aromatase activity in gonads of turtle embryos as a function of the incubation temperature of eggs. *J. Steroid Biochem. Mol. Biol.* 41, 851–853. doi: 10.1016/0960-0760(92)90437-N

Deveson, I. W., Holleley, C. E., Blackburn, J., Graves, J. A. M., Mattick, J. S., Waters, P. D., et al. (2017). Differential intron retention in Jumonji chromatin modifier genes is implicated in reptile temperature-dependent sex determination. *Sci. Adv.* 3:e1700731. doi: 10.1126/sciadv.1700731

Dorizzi, M., Richard-Mercier, N., Desvages, G., Girondot, M., and Pieau, C. (1994). Masculinization of gonads by aromatase inhibitors in a turtle with temperature-dependent sex determination. *Differentiation* 58, 1–8. doi: 10.1046/j.1432-0436.1994.5810001.x

Du, W. G., Ye, H., Zhao, B., Warner, D. A., and Shine, R. (2010). Thermal acclimation of heart rates in reptilian embryos. *PLoS One* 5:e15308. doi: 10.1371/journal.pone.0015308

Edwards, N., Kriegsfeld, L., and Crews, D. (2004). Neural substrates for sexual and thermoregulatory behavior in the male leopard gecko. *Eublepharis macularius*. *Brain Res.* 1029, 77–83.

Escobedo-Galván, A. H. (2013). Temperature-dependent sex determination in an uncertain world: advances and perspectives. *Rev. Mex. Biodivers.* 84, 727–730. doi: 10.7550/rmb.32441

Ewert, M. A., Etchberger, C. R., and Nelson, C. E. (2004). "Turtle sex-determining modes and TSD patterns, and some TSD pattern correlates" in *Temperature-dependent sex determination in vertebrates*. eds. N. Valenzuela and V. Lance (Washington, DC: Smithsonian Books), 21–32.

Ewert, M. A., Lang, J. W., and Nelson, C. E. (2005). Geographic variation in the pattern of temperature-dependent sex determination in the American snapping turtle (*Chelydra serpentina*). *J. Zool.* 265, 81–95. doi: 10.1017/S0952836904006120

Ewert, M. A., and Nelson, C. E. (1991). Sex determination in turtles: diverse patterns and some possible adaptive values. *Copeia* 1991, 50–69. doi: 10.2307/1446248

Fan, Z., Zou, Y., Jiao, S., Tan, X., Wu, Z., Liang, D., et al. (2017). Significant association of cyp19a promoter methylation with environmental factors and gonadal differentiation in olive flounder *Paralichthys olivaceus*. *Comp. Biochem. Physiol. A Mol. Integr. Physiol.* 208, 70–79. doi: 10.1016/j.cbpa.2017.02.017

Feiner, N., Rago, A., While, G. M., and Uller, T. (2018). Developmental plasticity in reptiles: insights from temperature-dependent gene expression in wall lizard embryos. *J. Exp. Zool. A Ecol. Integr. Physiol.* 329, 351–361. doi: 10.1002/jez.2175

Fisher, L. R., Godfrey, M. H., and Owens, D. W. (2014). Incubation temperature effects on hatchlign performance in the loggerhead sea turtle (*Caretta caretta*). *PLoS One* 9:2114880. doi: 10.1371/journal.pone.0114880

Flores, D., Tousignant, A., and Crews, D. (1994). Incubation temperature affects the behavior of adult leopard geckos (*Eublepharis macularius*). *Physiol. Behav.* 55, 1067–1072. doi: 10.1016/0031-9384(94)90389-1

Foucart, T., Heulin, B., and Lourdais, O. (2018). Small changes, big benefits: testing the significance of maternal thermoregulation in a lizard with extended egg retention. *Biol. J. Linn. Soc.* 125, 280–291. doi: 10.1093/biolinnean/bly105

Freedberg, S., Nelson, C. E., and Ewert, M. A. (2006). Estradiol-β induces lasting sex reversal at male-producing temperatures in kinostemid turtles. *J. Herpetol.* 40, 95–98. doi: 10.1670/139-05N.1

Freedberg, S., Stumpf, A. L., Ewert, M. A., and Nelson, C. E. (2004). Developmental environment has long-lasting effects on behavioral performance in two turtles with environmental sex determination. *Evol. Ecol. Res.* 6, 739–747.

Gangloff, E. J., and Telemeco, R. S. (2018). High temperature, oxygen, and performance: insights from reptiles and amphibians. *Integr. Comp. Biol.* 58, 9–24. doi: 10.1093/icb/icy005

Ge, C., Ye, J., Weber, C., Sun, W., Zhang, H., Zhou, Y., et al. (2018). The histone demethylase KDM6B regulates temperature-dependent sex determination in a turtle species. *Science* 360, 645–648. doi: 10.1126/science.aap8328

Georges, A., and Holleley, C. E. (2018). How does temperature determine sex? *Science* 360, 601–602. doi: 10.1126/science.aat5993

Gillooly, J. F., Charnov, E. L., West, G. B., Savage, V. M., and Brown, J. H. (2002). Effects of size and temperature on developmental time. *Nature* 417, 70–73. doi: 10.1038/417070a

Goodman, R. M. (2008). Latent effects of egg incubation temperature on growth in the lizard *Anolis carolinensis*. *J. Exp. Zool. A Ecol. Genet. Physiol.* 309, 525–533. doi: 10.1002/jez.483

Gore, A. C., Chappell, V. A., Fenton, S. E., Flaws, J. A., Nadal, A., Prins, G. S., et al. (2015). EDC-2: the Endocrine Society's second scientific statement on endocrine-disrupting chemicals. *Endocr. Rev.* 36, E1–E150. doi: 10.1210/er.2015-1010

Gorelick, R. (2003). Evolution of dioecy and sex chromosomes *via* methylation driving Muller's ratchet. *Biol. J. Linn. Soc.* 80, 353–368. doi: 10.1046/j.1095-8312.2003.00244.x

Greer, E. L., and Shi, Y. (2012). Histone methylation: a dynamic mark in health, disease and inheritance. *Nat. Rev. Genet.* 13, 343–357. doi: 10.1038/nrg3173

Hansen, K. H., Bracken, A. P., Pasini, D., Dietrich, N., Gehani, S. S., Monrad, A., et al. (2008). A model for transmission of the H3K27me3 epigenetic mark. *Nat. Cell Biol.* 10, 1291–1300. doi: 10.1038/ncb1787

Harlow, P. S. (2004). "Temperature-dependent sex determination in lizards" in *Temperature dependent sex determination in vertebrates*. eds. N. Valenzuela and V. Lance (Washington, DC: Smithsonian Institution), 42–52.

Hays, G. C., Mazaris, A. D., Schofield, G., and Laloe, J.-O. (2017). Population viability at extreme sex-ratio skews produced by temperature-dependent sex determination. *Proc. R. Soc. B* 284:20162576. doi: 10.1098/rspb.2016.2576

Healy, E., Mucha, M., Glancy, E., Fitzpatrick, D. J., Conway, E., Neikes, H. K., et al. (2019). PRC2.1 and PRC2.2 synergize to coordinate H3K27 trimethylation. *Mol. Cell* 76, 437–452. doi: 10.1016/j.molcel.2019.08.012

Hegarty, T. W. (1973). Temperature coefficient (Q10), seed germination and other biological processes. *Nature* 243, 305–306. doi: 10.1038/243305a0

Hoffmann, A. A., and Sgrò, C. M. (2011). Climate change and evolutionary adaptation. *Nature* 470, 479–485. doi: 10.1038/nature09670

Honeycutt, J. L., Deck, C. A., Miller, S. C., Severance, M. E., Atkins, E. B., Luckenbach, J. A., et al. (2019). Warmer waters masculinize wild populations of a fish with temperature-dependent sex determination. *Sci. Rep.* 9:6527. doi: 10.1038/s41598-019-42944-x

IPCC (2013). "Climate change 2013: the physical science basis" in *Contribution of working group I to the fifth assessment report of the intergovernmental panel on climate change*. eds. T. F. Stocker, D. Qin, G.-K. Plattner, M. Tignor, S. K. Allen and J. Boschunget al. (Cambridge, United Kingdom and New York, NY, USA: Cambridge University Press), 1535.

Jabbari, K., Caccio, S., de Barros, J. P. P., Desgres, J., and Bernardi, G. (1997). Evolutionary changes in CpG and methylation levels in the genome of vertebrates. *Gene* 205, 109–118. doi: 10.1016/S0378-1119(97)00475-7

Jacobson, E. R., and Whitford, W. G. (1970). The effect of acclimation on physiological responses to temperature in the snakes, *Thamnophis proximus* and *Natrix rhombifera*. *Comp. Biochem. Physiol.* 35, 439–449. doi: 10.1016/0010-406X(70)90607-9

Janzen, F. J. (1994). Climate change and temperature-dependent sex determination in reptiles. *Proc. Natl. Acad. Sci. USA* 91, 7487–7490. doi: 10.1073/pnas.91.16.7487

Jensen, M. P., Allen, C. D., Eguchi, T., Bell, I. P., LaCasella, E. L., Hilton, W. A., et al. (2018). Environmental warming and feminization of one of the largest sea turtle populations in the world. *Curr. Biol.* 28, 154–159. doi: 10.1016/j.cub.2017.11.057

Jones, P. A. (2012). Functions of DNA methylation: islands, start sites, gene bodies and beyond. *Nat. Rev. Genet.* 13, 484–492. doi: 10.1038/nrg3230

Keen, A. N., Klaiman, J. M., Shiels, H. A., and Gillis, T. E. (2017). Temperature-induced cardiac remodeling in fish. *J. Exp. Biol.* 220, 147–160. doi: 10.1242/jeb.128496

Keen, A. N., Shiels, H. A., and Crossley, D. A. (2016). Cardiovascular function, compliance, and connective tissue remodeling in the turtle, *Trachemys scripta*, following thermal acclimation. *Am. J. Physiol. Regul. Integr. Comp. Physiol.* 311, R133–R143. doi: 10.1152/ajpregu.00510.2015

Kingsolver, J. G. (2009). The well-temperatured biologist (American society of naturalists presidential address). *Am. Nat.* 174, 755–768. doi: 10.1086/648310

Knight, T. W., Layfield, J. A., and Brooks, R. J. (1990). Nutritional status and mean selected temperature of hatchling snapping turtles (*Chelydra serpentina*): is there a thermophilic response to feeding? *Copeia* 4, 1067–1072.

Lance, V. A. (2009). Is regulation of aromatase expression in reptiles the key to understanding temperature-dependent sex determination? *J. Exp. Zool. A Ecol. Genet. Physiol.* 311, 314–322. doi: 10.1002/jez.465

Landrigan, P. J., Fuller, R., Acosta, N. J., Adeyi, O., Arnold, R., Baldé, A. B., et al. (2018). The lancet commission on pollution and health. *Lancet* 391, 462–512. doi: 10.1016/S0140-6736(17)32345-0

Lang, J. W. (1990). Behavioral thermoregulation of eggs by prairie skinks. *Am. Zool.* 30:A108.

Lang, J. W., and Andrews, H. V. (1994). Temperature-dependent sex determination in crocodilians. *J. Exp. Zool.* 270, 28–44. doi: 10.1002/jez.1402700105

Logan, M. L., Cox, R. M., and Calsbeek, R. (2014). Natural selection on thermal performance in a novel thermal environment. *Proc. Natl. Acad. Sci. USA* 111, 14165–14169. doi: 10.1073/pnas.1404885111

Maclean, I. M., Mosedale, J. R., and Bennie, J. J. (2019). Microclima: an R package for modelling meso- and microclimate. *Methods Ecol. Evol.* 10, 280–290. doi: 10.1111/2041-210X.13093

Martín-del-Campo, R., Sifuentes-Romero, I., and García-Gasca, A. (2019). Hox genes in reptile development, epigenetic regulation, and teratogenesis. *Cytogenet. Genome Res.* 157, 34–45. doi: 10.1159/000495712

Matsumoto, Y., Buemio, A., Chu, R., Vafaee, M., and Crews, D. (2013). Epigenetic control of gonadal aromatase (cyp19a1) in temperature-dependent sex determination of red-eared slider turtles. *PLoS One* 8:e63599. doi: 10.1371/journal.pone.0063599

Matsumoto, Y., Hannigan, B., and Crews, D. (2016). Temperature shift alters DNA methylation and histone modification patterns in gonadal aromatase (cyp19a1) gene in species with temperature-dependent sex determination. *PLoS One* 11:e0167362. doi: 10.1371/journal.pone.0167362

Merchant-Larios, H., Díaz-Hernández, V., and Marmolejo-Valencia, A. (2010). Gonadal morphogenesis and gene expression in reptiles with temperature-dependent sex determination. *Sex. Dev.* 4, 50–61. doi: 10.1159/000276768

Metzger, D. C., and Schulte, P. M. (2017). Persistent and plastic effects of temperature on DNA methylation across the genome of three spine stickleback (*Gasterosteus aculeatus*). *Proc. R. Soc. B Biol. Sci.* 284:20171667. doi: 10.1098/rspb.2017.1667

Micheli-Campbell, M. A., Campbell, H. A., Cramp, R. L., Booth, D. T., and Franklin, C. E. (2011). Staying cool, keeping strong: incubation temperature affects performance in a freshwater turtle. *J. Zool.* 285, 266–273. doi: 10.1111/j.1469-7998.2011.00840.x

Mitchell, T. S., and Janzen, F. J. (2019). Substrate influences turtle nest temperature, incubation period, and offspring sex ratio in the field. *Herpetologica* 75, 57–62. doi: 10.1655/D-18-00001

Mitchell, T. S., Janzen, F. J., and Warner, D. A. (2018). Quantifying the effects of embryonic phenotypic plasticity on adult phenotypes in reptiles: a review of current knowledge and major gaps. *J. Exp. Zool. A Ecol. Integr. Physiol.* 329, 203–214. doi: 10.1002/jez.2187

Mrosovsky, N., and Pieau, C. (1991). Transitional range of temperature, pivotal temperatures and thermosensitive stages for sex determination in reptiles. *Amphibia-Reptilia* 12, 169–179.

Murrish, D. E., and Vance, V. J. (1968). Physiological responses to temperature acclimation in the lizard *Uta mearnsi*. *Comp. Biochem. Physiol.* 27, 329–337. doi: 10.1016/0010-406X(68)90775-5

Navarro-Martin, L., Vinas, J., Ribas, L., Diaz, N., Gutierrez, A., Di Croce, L., et al. (2011). DNA methylation of the gonadal aromatase (cyp19a) promoter is involved in temperature-dependent sex ratio shifts in the European sea bass. *PLoS Genet.* 7:e1002447. doi: 10.1371/journal.pgen.1002447

Noble, D. W., Stenhouse, V., Riley, J. L., Warner, D. A., While, G. M., Du, W. G., et al. (2018). A comprehensive database of thermal developmental plasticity in reptiles. *Sci. Data* 5:180138. doi: 10.1038/sdata.2018.138

O'Steen, S. (1998). Embryonic temperature influence juvenile temperature choice and growth rate in snapping turtles *Chelydra serpentina*. *J. Exp. Zool.* 201, 439–449.

O'Steen, S., and Janzen, F. J. (1999). Embryonic temperature affects metabolic compensation and thyroid hormones in hatchling snapping turtles. *Physiol. Biochem. Zool.* 72, 520–533. doi: 10.1086/316690

Parmesan, C., and Yohe, G. (2003). A globally coherent fingerprint of climate change impacts across natural ecosystems. *Nature* 421, 37–42. doi: 10.1038/nature01286

Patricio, A. R., Varela, M. R., Barbosa, C., Broderick, A. C., Catry, P., Hawkes, L. A., et al. (2018). Climate change resilience of a globally important sea turtle nesting population. *Glob. Chang. Biol.* 25, 522–535. doi: 10.1111/gcb.14520

Peñuelas, J., and Filella, I. (2001). Phenology: responses to a warming world. *Science* 294, 793–795. doi: 10.1126/science.1066860

Pezaro, N., Thompson, M. B., and Doody, J. S. (2016). Seasonal sex ratios and the evolution of temperature-dependent sex determination in oviparous lizards. *Evol. Ecol.* 30, 551–565. doi: 10.1007/s10682-016-9820-0

Pfennig, D. W., Wund, M. A., Snell-Rood, E. C., Cruickshank, T., Schlichting, C. D., and Moczek, A. P. (2010). Phenotypic plasticity's impacts on diversification and speciation. *Trends Ecol. Evol.* 25, 459–467. doi: 10.1016/j.tree.2010.05.006

Pieau, C., and Dorizzi, M. (2004). Oestrogens and temperature-dependent sex determination in reptiles: all is in the gonads. *J. Endocrinol.* 181, 367–377. doi: 10.1677/joe.0.1810367

Pieau, C., Dorizzi, M., and Richard-Mercier, N. (1999). Temperature-dependent sex determination and gonadal differentiation in reptiles. *Cell. Mol. Life Sci.* 55, 887–900. doi: 10.1007/s000180050342

Pina, C. I., Larriera, A., Medina, M., and Webb, G. J. W. (2007). Effects of incubation temperature on the size of *Caiman latirostris* (Crocodylia: Alligatoridae) at hatching and after one year. *J. Herpetol.* 41, 205–210. doi: 10.1670/0022-1511(2007)41[205:EOITOT]2.0.CO;2

Radhakrishnan, S., Literman, R., Mizoguchi, B., and Valenzuela, N. (2017). MeDIP-seq and nCpG analyses illuminate sexually dimorphic methylation of gonadal development genes with high historic methylation in turtle hatchlings with temperature-dependent sex determination. *Epigenetics Chromatin* 10:28. doi: 10.1186/s13072-017-0136-2

Radhakrishnan, S., Literman, R., Neuwald, J. L., and Valenzuela, N. (2018). Thermal response of epigenetic genes informs turtle sex determination with and without sex chromosomes. *Sex. Dev.* 12, 308–319. doi: 10.1159/000492188

Rhen, T., and Crews, D. (1999). Embryonic temperature and gonadal sex organize male-typical sexual and aggressive behavior in a lizard with temperature-dependent sex determination. *Endocrinology* 140, 4501–4508. doi: 10.1210/endo.140.10.7083

Rhen, T., and Crews, D. (2000). Organization and activation of sexual and agonistic behavior in the leopard gecko, *Eublepharis macularius*. *Neuroendocrinology* 71, 252–261. doi: 10.1159/000054543

Rhen, T., and Crews, D. (2002). Variation in reproductive behavior within a sex: neural systems and endocrine activation. *J. Neuroendocrinol.* 14, 517–531. doi: 10.1046/j.1365-2826.2002.00820.x

Rhen, T., Fagerlie, R., Schroeder, A., Crossley, D. A. II, and Lang, J. W. (2015). Molecular and morphological differentiation of testes and ovaries in relation to the thermosensitive period of gonad development in the snapping turtle, *Chelydra serpentina*. *Differentiation* 89, 31–41. doi: 10.1016/j.diff.2014.12.007

Rhen, T., and Lang, J. W. (1994). Temperature-dependent sex determination in the snapping turtle: manipulation of the embryonic sex steroid environment. *Gen. Comp. Endocrinol.* 96, 243–254. doi: 10.1006/gcen.1994.1179

Rhen, T., and Lang, J. W. (1995). Phenotypic plasticity for growth in the common snapping turtle: effects of incubation temperature, clutch, and their interaction. *Am. Nat.* 146, 726–747. doi: 10.1086/285822

Rhen, T., and Lang, J. W. (1999). Temperature during embryonic and juvenile development influences growth in hatchling snapping turtles, *Chelydra serpentina*. *J. Therm. Biol.* 24, 33–41. doi: 10.1016/S0306-4565(98)00035-7

Rhen, T., and Lang, J. W. (2004). "Phenotypic effects of incubation temperature" in *Temperature-dependent sex determination*. eds. N. Valenzuela and V. Lance (Washington, DC: Smithsonian Institution Press), 90–98.

Rhen, T., Sakata, J. T., and Crews, D. (2005). Effects of gonadal sex and incubation temperature on the ontogeny of gonadal steroid concentrations and secondary sex structures in leopard geckos, *Eublepharis macularius*. *Gen. Comp. Endocrinol.* 142, 289–296. doi: 10.1016/j.ygcen.2005.01.018

Rhen, T., Sakata, J. T., Zeller, M., and Crews, D. (2000). Sex steroid levels across the reproductive cycle of female leopard geckos, *Eublepharis macularius*, from different incubation temperatures. *Gen. Comp. Endocrinol.* 118, 322–331. doi: 10.1006/gcen.2000.7477

Rhen, T., and Schroeder, A. (2010). Molecular mechanisms of sex determination in reptiles. *Sex. Dev.* 4, 16–28. doi: 10.1159/000282495

Rhen, T., Schroeder, A., Sakata, J. T., Huang, V., and Crews, D. (2011). Segregating variation for temperature-dependent sex determination in a lizard. *Heredity* 106, 649–660. doi: 10.1038/hdy.2010.102

Rhen, T., Willingham, E., Sakata, J. T., and Crews, D. (1999). Incubation temperature influences sex-steroid levels in juvenile red-eared slider turtles, *Trachemys scripta*, a species with temperature-dependent sex determination. *Biol. Reprod.* 61, 1275–1280. doi: 10.1095/biolreprod61.5.1275

Ringrose, L., and Paro, R. (2004). Epigenetic regulation of cellular memory by the polycomb and trithorax group proteins. *Annu. Rev. Genet.* 38, 413–443. doi: 10.1146/annurev.genet.38.072902.091907

Risher, J. F., and Claussen, D. L. (1987). The effects of cold acclimation on electrocardiogram parameters in five species of turtles. *Comp. Biochem. Physiol. A* 87, 73–80. doi: 10.1016/0300-9629(87)90428-2

Rohr, J. R., Civitello, D. J., Cohen, J. M., Roznik, E. A., Sinervo, B., and Dell, A. I. (2018). The complex drivers of thermal acclimation and breadth in ectotherms. *Ecol. Lett.* 21, 1425–1439. doi: 10.1111/ele.13107

Roush, D., and Rhen, T. (2018). Developmental plasticity in reptiles: critical evaluation of the evidence for genetic and maternal effects on temperature-dependent sex determination. *J. Exp. Zool. A Ecol. Integr. Physiol.* 329, 287–297. doi: 10.1002/jez.2194

Sakata, J. T., Coomber, P., Gonzalez-Lima, F., and Crews, D. (2000). Functional connectivity among limbic brain areas: differential effects of incubation temperature and gonadal sex in the leopard gecko, *Eublepharis macularius*. *Brain Behav. Evol.* 55, 139–151. doi: 10.1159/000006648

Sakata, J. T., and Crews, D. (2003). Embryonic temperature shapes behavioral change following social experience in male leopard geckos, *Eublepharis macularius*. *Anim. Behav.* 66, 839–846. doi: 10.1006/anbe.2003.2294

Sakata, J. T., and Crews, D. (2004). Developmental sculpting of social phenotype and plasticity. *Neurosci. Biobehav. Rev.* 28, 95–112. doi: 10.1016/j.neubiorev.2004.01.001

Scheffers, B. R., De Meester, L., Bridge, T. C., Hoffmann, A. A., Pandolfi, J. M., Corlett, R. T., et al. (2016). The broad footprint of climate change from genes to biomes to people. *Science* 354:aaf7671. doi: 10.1126/science.aaf7671

Scheiner, S. (1993). Genetics and evolution of phenotypic plasticity. *Annu. Rev. Ecol. Syst.* 24, 35–68. doi: 10.1146/annurev.es.24.110193.000343

Schroeder, A. L., Metzger, K. J., Miller, A., and Rhen, T. (2016). A novel candidate gene for temperature-dependent sex determination in the common snapping turtle. *Genetics* 203, 557–571. doi: 10.1534/genetics.115.182840

Schuett, G. W., and Gatten, R. E. (1980). Thermal preference in snapping turtles (*Chelydra serpentina*). *Copeia* 1980, 149–152. doi: 10.2307/1444147

Schulte, P. M., Healy, T. M., and Fangue, N. A. (2011). Thermal performance curves, phenotypic plasticity, and the time scales of temperature exposure. *Integr. Comp. Biol.* 51, 691–702. doi: 10.1093/icb/icr097

Seebacher, F., and Franklin, C. E. (2005). Physiological mechanisms of thermoregulation in reptiles: a review. *J. Comp. Physiol. B* 175, 533–541. doi: 10.1007/s00360-005-0007-1

Shine, R., and Elphick, M. J. (2001). The effect of short-term weather fluctuations on temperatures inside lizard nests, and on the phenotypic traits of hatchling lizards. *Biol. J. Linn. Soc.* 72, 555–565. doi: 10.1111/j.1095-8312.2001.tb01338.x

Shine, R., Madsen, T. R. L., Elphick, M. J., and Harlow, P. S. (1997). The influence of nest temperatures and maternal brooding on hatchling phenotypes in water pythons. *Ecology* 78, 1713–1721. doi: 10.1890/0012-9658(1997)078[1713:TIONTA]2.0.CO;2

Simoncini, M. S., Cruz, F. B., Larriera, A., and Pina, C. I. (2014). Effects of climatic conditions on sex ratios in nests of broad-snouted caiman. *J. Zool.* 293, 243–251. doi: 10.1111/jzo.12140

Sinclair, B. J., Marshall, K. E., Sewell, M. A., Levesque, D. L., Willett, C. S., Slotsbo, S., et al. (2016). Can we predict ectotherm responses to climate change using thermal performance curves and body temperatures? *Ecol. Lett.* 19, 1372–1385. doi: 10.1111/ele.12686

Somero, G. N. (2005). Linking biogeography to physiology: evolutionary and acclamatory adjustments of thermal limits. *Front. Zool.* 2:1. doi: 10.1186/1742-9994-2-1

Stearns, S. C. (1992). *The evolution of life histories*. New York: Oxford University Press.

Stenseth, N. C., Mysterud, A., Ottersen, G., Hurrell, J. W., Chan, K. S., and Lima, M. (2002). Ecological effects of climate fluctuations. *Science* 297, 1292–1296. doi: 10.1126/science.1071281

Telemeco, R. S., Gangloff, E. J., Cordero, G. A., Mitchell, T. S., Bodensteiner, B. L., Holden, K. G., et al. (2016). Reptile embryos lack the opportunity to thermoregulate by moving within the egg. *Am. Nat.* 188, E13–E27. doi: 10.1086/686628

Tilley, D., Ball, S., Ellick, J., Godley, B. J., Weber, N., Weber, S. B., et al. (2019). No evidence of fine scale thermal adaptation in green turtles. *J. Exp. Mar. Biol. Ecol.* 514–515, 110–117. doi: 10.1016/j.jembe.2019.04.001

Tousignant, A., and Crews, D. (1995). Incubation temperature and gonadal sex affect growth and physiology in the leopard gecko (*Eublepharis macularius*), a lizard with temperature-dependent sex determination. *J. Morphol.* 224, 159–170. doi: 10.1002/jmor.1052240205

Varriale, A., and Bernardi, G. (2006). DNA methylation in reptiles. *Gene* 385, 122–127. doi: 10.1016/j.gene.2006.05.034

Via, S., and Lande, R. (1985). Genotype-environment interaction and the evolution of phenotypic plasticity. *Evolution* 39, 505–522. doi: 10.1111/j.1558-5646.1985.tb00391.x

Vogt, R. C., and Flores-Villela, O. (1992). Effects of incubation temperature on sex determination in a community of neotropical freshwater turtles in southern Mexico. *Herpetologica* 1992, 265–270.

Wapstra, E., Uller, T., Sinn, D. L., Olsson, M., Mazurek, K., Joss, J., et al. (2009). Climate effects on offspring sex ratio in a viviparous lizard. *J. Anim. Ecol.* 78, 84–90. doi: 10.1111/j.1365-2656.2008.01470.x

Warkentin, M. T., Morris, D., Bebb, G., and Brenner, D. R. (2017). The role of DNA repair capacity in lung cancer risk among never-smokers: a systematic review of epidemiologic studies. *Cancer Treat. Res. Commun.* 13, 13–24. doi: 10.1016/j.ctarc.2017.08.001

Warner, D. A., and Shine, R. (2005). The adaptive significance of temperature-dependent sex determination: experimental tests with a short-lived lizard. *Evolution* 59, 2209–2221. doi: 10.1111/j.0014-3820.2005.tb00929.x

Waters, C. N., Zalasiewicz, J., Summerhayes, C., Barnosky, A. D., Poirier, C., Gałuszka, A., et al. (2016). The Anthropocene is functionally and stratigraphically distinct from the Holocene. *Science* 351:aad2622. doi: 10.1126/science.aad2622

Weisrock, D. W., and Janzen, F. J. (1999). Thermal and fitness-related consequences of nest location in painted turtles (*Chrysemys picta*). *Funct. Ecol.* 13, 94–101. doi: 10.1046/j.1365-2435.1999.00288.x

While, G. M., Noble, D. W., Uller, T., Warner, D. A., Riley, J. L., Du, W. G., et al. (2018). Patterns of developmental plasticity in response to incubation temperature in reptiles. *J. Exp. Zool. A Ecol. Integr. Physiol.* 329, 162–176. doi: 10.1002/jez.2181

Wibbels, T., Bull, J. J., and Crews, D. (1991). Chronology and morphology of temperature-dependent sex determination. *J. Exp. Zool.* 260, 371–381. doi: 10.1002/jez.1402600311

Williamson, L. U., Spotila, J. R., and Standora, E. A. (1989). Growth selected temperature and CTM of young snapping turtles, *Chelydra serpentina*. *J. Therm. Biol.* 14, 33–39. doi: 10.1016/0306-4565(89)90027-2

Yatsu, R., Miyagawa, S., Kohno, S., Parrott, B. B., Yamaguchi, K., Ogino, Y., et al. (2016). RNA-seq analysis of the gonadal transcriptome during *Alligator mississippiensis* temperature-dependent sex determination and differentiation. *BMC Genomics* 17:77. doi: 10.1186/s12864-016-2396-9

Yntema, C. L. (1968). A series of stages in the embryonic development of *Chelydra serpentina*. *J. Morphol.* 125, 219–251. doi: 10.1002/jmor.1051250207

Yntema, C. L. (1979). Temperature levels and periods of sex determination during incubation of eggs of *Chelydra serpentina*. *J. Morphol.* 159, 17–27. doi: 10.1002/jmor.1051590103

Conflict of Interest: The authors declare that the research was conducted in the absence of any commercial or financial relationships that could be construed as a potential conflict of interest.

Copyright © 2020 Singh, Das and Rhen. This is an open-access article distributed under the terms of the Creative Commons Attribution License (CC BY). The use, distribution or reproduction in other forums is permitted, provided the original author(s) and the copyright owner(s) are credited and that the original publication in this journal is cited, in accordance with accepted academic practice. No use, distribution or reproduction is permitted which does not comply with these terms.

frontiers in Physiology

ORIGINAL RESEARCH
published: 10 June 2020
doi: 10.3389/fphys.2020.00614

Identification of Novel miRNAs Involved in Cardiac Repair Following Infarction in Fetal and Adolescent Sheep Hearts

*Mitchell C. Lock[1], Ross L. Tellam[1], Jack R. T. Darby[1], Jia Yin Soo[1], Doug A. Brooks[1,2], Mike Seed[3], Joseph B. Selvanayagam[4] and Janna L. Morrison[1]**

[1] Early Origins of Adult Health Research Group, University of South Australia, Adelaide, SA, Australia, [2] Mechanisms in Cell Biology and Disease Research Group, School of Pharmacy and Medical Sciences, University of South Australia, Adelaide, SA, Australia, [3] Division of Cardiology, The Hospital for Sick Children, Toronto, ON, Canada, [4] Cardiac Imaging Research, Department of Heart Health, South Australian Health & Medical Research Institute, Flinders University, Adelaide, SA, Australia

OPEN ACCESS

Edited by:
Sonnet Jonker, Oregon Health & Science University, United States

Reviewed by:
Hieu D. Hoang, Columbia University, United States
Adam John Watkins, University of Nottingham, United Kingdom

***Correspondence:**
Janna L. Morrison
Janna.Morrison@unisa.edu.au

Specialty section:
This article was submitted to Embryonic and Developmental Physiology, a section of the journal Frontiers in Physiology

Received: *26 March 2020*
Accepted: *15 May 2020*
Published: *10 June 2020*

Citation:
Lock MC, Tellam RL, Darby JRT, Soo JY, Brooks DA, Seed M, Selvanayagam JB and Morrison JL (2020) Identification of Novel miRNAs Involved in Cardiac Repair Following Infarction in Fetal and Adolescent Sheep Hearts. Front. Physiol. 11:614. doi: 10.3389/fphys.2020.00614

Aims: Animal models have been used to show that there are critical molecular mechanisms that can be activated to induce myocardial repair at specific times in development. For example, specific miRNAs are critical for regulating the response to myocardial infarction (MI) and improving the response to injury. Manipulating these miRNAs in small animal models provides beneficial effects post-MI; however it is not known if these miRNAs are regulated similarly in large mammals. Studying a large animal where the timing of heart development in relation to birth is similar to humans may provide insights to better understand the capacity to repair a developing mammalian heart and its application to the adult heart.

Methods: We used a sheep model of MI that included permanent ligation of the left anterior descending (LAD) coronary artery. Surgery was performed on fetuses (at 105 days gestation when all cardiomyocytes are mononucleated and proliferative) and adolescent sheep (at 6 months of age when all cardiomyocytes contribute to heart growth by hypertrophy). A microarray was utilized to determine the expression of known miRNAs within the damaged and undamaged tissue regions in fetal and adolescent hearts after MI.

Results: 73 miRNAs were up-regulated and 58 miRNAs were down-regulated significantly within the fetal infarct compared to remote cardiac samples. From adolescent hearts 69 non-redundant miRNAs were up-regulated and 63 miRNAs were down-regulated significantly in the infarct area compared to remote samples. Opposite differential expression profiles of 10 miRNAs within tissue regions (Infarct area, Border zone and Remote area of the left ventricle) occurred between the fetuses and adolescent sheep. These included miR-558 and miR-1538, which when suppressed using LNA anti-miRNAs in cell culture, increased cardiomyoblast proliferation.

Conclusion: There were significant differences in miRNA responses in fetal and adolescent sheep hearts following a MI, suggesting that the modulation of novel miRNA expression may have therapeutic potential, by promoting proliferation or repair in a damaged heart.

Keywords: cardiac, regeneration, fetus, myocardial infarction, miRNA

INTRODUCTION

Cardiovascular disease is one of the largest causes of morbidity and mortality worldwide, and is due to the limited capacity to repair human adult heart tissue after myocardial damage (Wong et al., 2012; Benjamin et al., 2017; Wilkins et al., 2017). The lack of regenerative potential is presumed to be the result of cardiomyocyte quiescence, and although there is some evidence for cardiomyocyte proliferation in adult humans, this is insufficient for regeneration or repair (Bergmann et al., 2009; Barnett and van den Hoff, 2011). Current treatments after acute coronary syndromes address the ongoing symptoms and attempt to prevent re-infarction (Dalal et al., 2015). The current lack of effective treatments for repairing heart tissue damage necessitate new approaches to promote the regeneration of adult human heart tissue.

The adult zebrafish, neonatal mouse and fetal sheep have a remarkable ability to regenerate heart tissue after myocardial infarction (MI) (Herdrich et al., 2010; Jopling et al., 2010; Porrello et al., 2011). By studying the transitional period of cardiomyocyte proliferation to quiescence in zebrafish and mouse models, several promising target miRNAs are associated with regeneration For example, the inhibition of miR-15 family members leads to increased mitosis of cardiomyocytes in neonatal mice, promotes adult mouse cardiomyocyte proliferation, improves cardiac function after MI and improves contractile function after ischemia/reperfusion injury (Hullinger et al., 2012; Porrello et al., 2012). miR-133 is down-regulated during the period of cardiomyocyte regeneration and proliferation in injured zebrafish myocardium, implicating it in the regulation of cell cycle progression (Yin et al., 2012). The inhibition of miR-34 family members has shown therapeutic potential, where cardiac remodeling was attenuated and improved cardiac function in mouse models of both pressure overload and MI with up-regulation of growth factor target genes including *Vegf, Vcl, Sirt1, Notch1,* and *Pofut1* (Bernardo et al., 2012; Boon et al., 2013). Lastly, inhibition of target genes of miR-590 and miR-199a, such as *Clic5, Hopx,* and *Homer1*, using short interfering RNAs, results in approximately double the number of cardiomyocytes undergoing DNA synthesis and significantly increased cytokinesis (Eulalio et al., 2012). Studying a model organism for heart regeneration that closely reflects the cardiac developmental timing of humans, such as sheep (Botting et al., 2012; Lock et al., 2017, 2018; Morrison et al., 2018), may reveal additional miRNAs that regulate cardiomyocyte proliferation, and which may potentially have clinical relevance. We therefore utilized a sheep model of MI to investigate the differential miRNA expression in regenerative fetal hearts and non-regenerative adolescent hearts.

MATERIALS AND METHODS

Animal Ethics and Housing

Experimental protocols for animal research were approved by the South Australian Health and Medical Research Institute (SAHMRI) Animal Ethics Committee (SAM046). Experiments were designed and reported with reference to the ARRIVE guidelines (Kilkenny et al., 2010). The experiments comply with the policies and regulations of the European Convention for the Protection of Vertebrate Animals used for Experimental and other Scientific Purposes (Grundy, 2015). In total, 10 Merino ewes and their fetuses and 12 adolescent sheep (∼6 months old) were used in this study (supplied by South Australian Medical Science Research Institute). Each ewe or adolescent sheep was housed in an individual pen in an indoor housing facility (Preclinical Imaging and Research Laboratories, SAHMRI) that was maintained at a constant ambient temperature of between 20 and 22°C with a 12 h light/dark cycle.

Surgical Procedure to Ligate the Left Anterior Descending (LAD) Coronary Artery

At 102 days gestation (term, 150 days), ewes underwent surgery under aseptic conditions using general anaesthesia induced by the intravenous infusion of diazepam (0.3 mg/kg) and ketamine (7 mg/kg), and maintained with inhalation of isoflurane (1–2%) in oxygen. Briefly, vascular catheters (Critchley Electrical Products, Silverwater, Australia) were inserted as previously described (Danielson et al., 2005; Duan et al., 2017; Lock et al., 2020) in the maternal jugular vein, the amniotic cavity and the fetal carotid artery and jugular vein.

Animals underwent thoracotomy and were randomly allocated to Sham surgery (fetus, $n = 5$; adolescent sheep, $n = 5$) or ligation of the left anterior descending (LAD) coronary artery (fetus, $n = 5$; adolescent sheep, $n = 5$) to induce infarction. Lignocaine was administered intravenously to all fetuses (0.2 mL bolus) and adolescents (100 mg/500 mL) prior to incising the pericardial sac. For animals in the infarction group, a silk suture was placed around the second diagonal of the LAD coronary artery and tied off, while observing blanching of the heart tissue. The thoracotomy incision was tightly sutured in layers (ribs, muscle and skin). The fetus was then returned to the ewe's uterus and the uterus was sutured closed.

Fetal catheters were exteriorized through a small incision in the ewe's flank. At surgery, antibiotics were administered to the ewe (154 mg of Procaine penicillin, 393 mg of benzathine penicillin, 500 mg of dihydrostreptomycin; Lyppards, Adelaide, Australia) and fetuses (150 mg of Procaine penicillin,

112 mg of benzathine penicillin, 250 mg of dihydrostreptomycin; Lyppards). When the ewes and adolescent sheep recovered from anesthesia, they were given analgesia (20 μg/kg, Xylazil, Troy Laboratories, Australia). Antibiotics were administered intramuscularly to each ewe or adolescent sheep for 3 days after surgery and to each fetus intra-amniotically (500 mg of ampicillin; Lyppards).

Post-mortem and Tissue Collection

On the 3rd day after ligation of the LAD coronary artery ewes and adolescent sheep were humanely killed via overdose of sodium pentobarbitone (8 g; Vibrac Australia, Peakhurst, Australia). The ewes' uterus was removed by hysterotomy, and the fetus was removed and weighed. The heart was quickly dissected, weighed and reverse perfused through the aorta with heparin sulfate (5 mL; to prevent clotting and flush blood from the heart) and a saturated KCl solution (5 mL; to arrest the heart in diastole). The heart was photographed, cut into sections and the infarct visualized using 2,3,5-triphenyltetrazolium chloride (TTC) staining (as previously published; Duan et al., 2017; Lock et al., 2019). A total of 10 fetuses [Sham, $n = 5$ (3 female, 2 male); MI, $n = 5$ (3 male, 2 female)] and 10 adolescent sheep (Sham, $n = 5$; MI, $n = 5$ all male) underwent post-mortem and were used for molecular analyses. Ventricle tissue was collected from the infarct area, the border zone (salvageable tissue immediately surrounding the Infarct area) and a remote area of the left ventricle, as well as the corresponding areas from Sham animals. Tissue was either frozen in liquid nitrogen for miRNA microarray and qRT-PCR analyses or fixed in 4% paraformaldehyde for histological and immunohistochemistry analyses.

miRNA Microarray Analysis

A custom designed miRNA microarray was employed using a service provider (LC Sciences, United States; Morrison et al., 2015). It contained multiple (3–8) replicates of 3,098 probes and multiple replicates (8–80) of 56 control probes. The former probes were for identified ovine miRNA and additional mammalian miRNA sequences downloaded from miRBase[1], as previously described (Morrison et al., 2015). The available miRBase entries for ovine species are limited; however, since many miRNAs are highly conserved amongst species, the microarray was supplemented with miRNAs from other species. The multispecies probes on the microarray caused redundancy by design. The experimental design included three biological replicates from each treatment group and age.

Background subtracted raw data from the manufacturer (LC Sciences, United States; Casella and Berger, 2001; Bolstad, 2004) was analyzed using a 2-factor ANOVA (factors: age (Fetus and Adolescent) and region (Remote, Border and Infarct); 6 groups) (Eisen et al., 1998). Data was filtered at $P < 0.05$ for each factor and the interaction. For miRNA probes identified as significant for an interaction, one-way ANOVA was used to determine significantly deregulated probes within each age group. *P*-values for this analysis were not corrected for multiple testing, as although there were 1894 expressed probes, many of these were for 808 unique miRNAs, with some probes likely to also cross hybridize or reflect highly related miRNA families. Thus, many of the probes on the microarray were not independent. For each factor and interaction, the mean value of all probes was taken for the six groupings (Fetal and Adolescent, Remote, Border, and Infarct). Probes with overall mean signal less than 500 (unreliable signal) as well as any probes with a signal of zero in one or more sample (unreliable probes) were then removed. K-means clustering was performed using the CLCBIO Genomics Workbench program suite[2] using the mean probe values from each group. Data reported in the clustering analysis are represented as untransformed raw signal. Euclidean distance and $K = 10$ were selected for k-means clustering as this revealed profile stability with the addition of further clusters not creating any substantially different patterns. Unsupervised principal component analysis (PCA) and hierarchical clustering analyses of sample data used the default options in ClustVis[3].

miRNA Target Prediction

Significantly deregulated probes were separated into groups based on their expression profiles across tissue regions at both ages. miRNA target predictions for the significantly up-regulated or down-regulated probes in the Infarct samples compared to the Remote samples was performed using miRWalk 3 (University of Heidelberg[4]). miRNA target prediction involves high rates of false positive targets and hence conservative strategies were utilized (Pinzon et al., 2017). MiRWalk used a consensus approach based on the intersection of at least three different methods and utilized target mRNA information from the human, bovine, and mouse genomes.

Predicted Target Term Enrichments

Gene Ontology (GO) term enrichments and KEGG pathway functional enrichments were performed using miRWalk 3 by hypergeometric tests (Fisher-exact-test). Redundant terms generated by the multiple species background were removed. Only enriched terms with an FDR corrected $P < 0.05$ were used.

Real-Time PCR for miRNA and Target Genes

All essential information regarding the qRT-PCR procedure is included as per the MIQE guidelines (Bustin et al., 2009). Total RNA was extracted from frozen heart tissue for each fetus and adolescent sheep using QIAzol Lysis Reagent solution and QIAgen miRNeasy purification columns, as per manufacturer guidelines (Qiagen, Germany). Total RNA was quantified by spectrophotometric measurements at 260 and 280 nm in a NanoDrop Lite Spectrophotometer (Thermo Fisher Scientific) and the 260/280 nm ratio. RNA samples were checked for integrity, as well as protein and DNA contamination using spectrophotometer results and agarose gel stained using ethidium bromide. cDNA was synthesized using Superscript III First Strand Synthesis System (Invitrogen, United States)

[1]http://www.mirbase.org/

[2]http://www.clcbio.com/

[3]https://biit.cs.ut.ee/clustvis/

[4]http://mirwalk.umm.uni-heidelberg.de/

using 1 μg of total RNA, random hexamers, dNTP, DTT and Superscript III in a final volume of 20 μL, as per the manufacturer's guidelines in a MJ Mini personal thermocycler (Biorad, United States). Controls containing either no RNA transcript or no Superscript III were used to test for reagent contamination and genomic DNA contamination, respectively. miRNA cDNA was synthesized using the miScript II RT Kit (Qiagen, Germany) according to the manufacturer's guidelines. Each sample contained 4 μL 5x miScript Hiflex buffer, 2 μL 10x Nucleics mix, 2 μL miScript Reverse Transcriptase mix and 1 μg extracted RNA. The no amplification control (NAC) negative control samples replaced the miScript Reverse Transcriptase mix with 2 μL of molecular grade water. The geNorm component of qbaseplus 2.0 software (Biogazelle, Belgium) was used to determine the most stable reference genes from a panel of candidate reference genes (Vandesompele et al., 2002) and the minimum number of reference genes required to calculate a stable normalization factor, as previously described (Soo et al., 2012; McGillick et al., 2013). For qRT-PCR data output normalization, three stable reference genes *RPLP0* (NM_001012682.1), *HPRT1* (NM_001034035.1) and *YWHAZ* (AY970970) (Passmore et al., 2009) were run in parallel with all target genes, as previously described. For miRNA qRT-PCR, target miRNAs were normalized against miR-208 (MI0000251); miR-92-1 (MS00006594) and SNORD61-1 (MS00033705, QIAGEN, Australia). Relative expression of target genes (*BIRC5*, NM_001001855.2; *SPAG5*, XM_004012500.1; *CHEK1*, XM_004019518.1; *CDK1*, NM_001142509.1; *GJA1*, XM_004011159.1; *CTGF*, NM_001164714.1; *PGAM1*, NM_001034054; *SRF*, XM_004019222.1; *CLIC5*, XM_004018860.1; *HOPX*, NM_174097.2, and *HOMER1*, NM_001076052.1) and miRNAs (miR-15a, MS00008785; miR-15b, MS00008799; miR-16, MS00031493; miR-195, MS00008953; miR497, MS00031906; miR-199a, MS00007602; and miR-590, MS00010269; QIAGEN, Australia) were measured by qRT-PCR using KiCqStart SYBR Green qPCR ReadyMix (Sigma Aldrich, United States) or miScript SYBR Green PCR Kit (QIAGEN, Australia) in a final volume of 6 μL on a ViiA7 Fast Real-time PCR system (Applied Biosystems, United States) as previously described. Each qRT-PCR well contained 3 μL SYBR Green Master Mix (2X), 2 μL of forward and reverse primer mixed with H_2O to obtain final primer concentrations and 1 μL of diluted relevant cDNA. Each sample was run in triplicate for target genes and reference genes. The abundance of each transcript relative to the abundance of stable reference genes (Hellemans et al., 2007) was calculated using DataAssist 3.0 analysis software (Applied Biosystems, United States) and expressed as mRNA mean normalized expression (MNE) ± SEM. Outliers were identified using the ROUT method with a false discovery rate Q = 1% (GraphPad Prism 8, United States) and were removed from the analysis.

H9c2 Cell Culture Experiments

H9c2 cells derived from rat embryonic ventricular cardiomyoblasts were cultured in Glutamax DMEM (Gibco, United States) media that contained 10% (v/v) fetal bovine serum and 1% v/v penicillin/streptomycin at 37°C in an atmosphere of 95% air and 5% CO_2. Hypoxia was induced by incubation in sealed hypoxia chambers containing 94% N_2, 5% CO_2, and 1% O_2 to simulate tissue hypoxia during ischemia (Yao et al., 2017). Since miRNAs are generally conserved between species, we first checked that the sequences of the chosen miRNAs were not different between species using miRbase (University of Manchester[1]) and used the HSA version of the miRNA for the remainder of the experiments to improve interspecies translation. Cells were seeded into 6-well-plates at a density of 100,000 cells per well and 96-well-plates at 5000 cells per well. 100 nmol miRNA-inhibitors [hsa-miR-558, hsa-miR-1538, hsa-miR-150 or the manufacturer negative control 5 (NC5) miRNA (IDT, United States)] were each diluted in 125 μL OPTIMEM media (Gibco, United States) and combined with Lipofectamine 2000 (Thermo Fisher Scientific, United States) before further dilution in culture media. Cells were treated with either normal media Glucose/Normoxia, No-Glucose/Normoxia, Glucose/Hypoxia or No-Glucose/Hypoxia culture conditions for 48 h to simulate lack of oxygen and glucose supply during an infarction. Cells in 6-well-plates were either lysed in Qiazol (Qiagen, United States) for qRT-PCR or fixed in 4% formaldehyde (Sigma Aldrich, United States) for subsequent immunohistochemistry analysis. 96-well-plates were aspirated of culture media after treatment and 100 μL fresh media was added to each well. Twenty microliter of MTS Proliferation assay reagent (Promega, United States) was then added to each well and incubated for 2 h at 37°C. Thereafter the absorption of each well was measured at the wavelength of 490 nm by a spectrophotometer. Potential target genes of novel miRNAs were determined using miRWalk 3 (University of Heidelberg[4]). Target genes were selected based on how significantly likely they were to be modulated by the miRNAs of interest and are expressed in cardiac tissue. The expression of target genes *PAPPA, JAG, NF2, MYOC1,* and *SOX4* act as markers to ensure that miRNA inhibition is effectively associated an upregulation of target gene expression.

Immunohistochemistry

Rehydrated cardiomyoblasts were blocked for endogenous peroxidase activity with 3% hydrogen peroxide (Sigma-Aldrich, United States), followed by heat-induced antigen retrieval in sodium-citrate buffer (pH 6.0). Slides were incubated overnight with the primary antibody (Aurora-B, ab2254, Abcam, United States) at 4°C following incubation with non-immune serum (serum-blocking solution; Histostain-Plus Kit; Invitrogen, United States) to prevent non-specific binding. Negative control slides with the primary antibody omitted were used to demonstrate the absence of non-specific binding of the secondary antibody or reagent contamination. In addition, negative control slides, where primary antibody was substituted by rabbit serum (Sigma-Aldrich, United States) were carried out at the same protein concentration as the diluted primary antibodies (Hewitt et al., 2014). Negative controls were incubated overnight at 4°C in parallel with test slides under the same experimental conditions. A Histostain-Plus kit (Invitrogen, United States) was used with horseradish peroxidase and Histostain-Plus broad spectrum 3,3'-diaminobenzidine (DAB) chromagen for visualization of positive cells. All sections were counterstained with Mayer's hematoxylin

(Sigma-Aldrich, United States). Following optimization, the substrate-chromagen reaction was allowed to occur for the same time for all slides. Images of stained slides were taken using a NanoZoomer-XR (Hamamatsu, Japan) and quantified using the VIS software package (Visiopharm, Denmark), as previously described (Lock et al., 2015).

Statistical Analysis

Statistical analyses for qRT-PCR and immunohistochemistry were performed within the STATA 12 program (StataCorp, United States). Analyses between tissue regions (Infarct vs. Border vs. Remote) at each age were assessed using a nested Analysis of Variance (ANOVA). A Bonferroni *post hoc* test was performed with multiple comparisons for each tissue region against the Sham tissue.

RESULTS

Two strategies were employed to assess the expression of miRNAs after MI in the fetus and adolescent sheep heart samples. qRT-PCR was used to evaluate changes in the expression of key miRNAs and their target genes, which have been identified as playing important roles in cardiac regeneration in zebrafish and mouse models. miRNA microarray analysis provided a more comprehensive analysis to profile 3,098 probes representing miRNAs from several mammalian species, to then identify differentially expressed probes, and to predict mRNA targets and enriched functions associated with clustered unique miRNAs.

Profiling of Zebrafish and Mouse miRNAs Implicated in Cardiac Regeneration in Sheep

A number of miRNAs have been identified as possible therapeutic targets in small animals, which retain heart regenerative capacity for a period of time after birth. The most promising of these candidate miRNAs were investigated in our large animal model to determine if the changes in miRNA expression are consistent across species.

miR-15 Family

The miR-15 family contains five miRNA, miR-15a, miR-15b, miR-16, miR-195, and miR-497. In the ventricular tissue from adolescent animals there was a significant increase in expression of miR-15a in the Infarct sample compared to the Remote samples and Sham controls (**Figure 1A**; $P = 0.017$, 0.0017, respectively). miR-15b was decreased in the Border and Infarct samples compared to both the Remote samples and Sham controls in the fetuses (**Figure 1B**; $P \leq 0.05$, < 0.001, respectively). In the adolescent sheep, there was an increase in miR-15b expression in the Infarct samples compared to Sham controls, as well as Remote and Border samples (**Figure 1B**; $P = 0.007$, $P < 0.001$, respectively). The expression of miR-16 was decreased in the fetal Border and Infarct samples compared with the Remote sample ($P < 0.05$) and was increased in the Infarct sample compared with Remote samples ($P < 0.05$) in the adolescent sheep (**Figure 1C**). miR-195 expression was increased in the fetal Border and Infarct samples compared to Remote samples (**Figure 1D**; $P < 0.05$). In the adolescent animals there was an increase in expression of miR-195 in the Infarct samples compared to Remote and Sham samples (**Figure 1D**; $P < 0.05$, $P < 0.001$ respectively). The expression of miR-497 was significantly decreased in the fetal Infarct samples compared to Border samples (**Figure 1E**; $P < 0.05$). In the adolescent sheep there was an increase in miR-497 expression in the Infarct samples compared to Remote and Sham samples (**Figure 1E**, $P < 0.05$, $P = 0.007$ respectively). miR-15 family target genes demonstrated similar expression profiles (**Figure 2**).

miR-133a

The expression of miR-133a was significantly down-regulated in fetal Infarct compared to Border samples (**Figure 3A**; $P < 0.05$). In adolescent sheep, there was a significant decrease in Infarct compared to Remote, Border and Sham samples (**Figure 3A**; $P < 0.001$, $P < 0.05$, $P < 0.001$, respectively). The higher expression of this miRNA in adolescent sheep is consistent with increased expression of miR-133a with age in multiple species (Liu et al., 2008; Morrison et al., 2015); but, the decreased expression in the Infarct samples within adolescent sheep was unexpected. miR-133a target gene expression did not mirror the expression of miR-133a (**Figures 3B–E**).

miR-34 Family

miR-34a expression was significantly higher in the adolescent sheep heart samples compared to the fetuses ($P < 0.0001$, **Supplementary Files**). There was no significant difference in the expression of miR-34a in the fetal Infarct samples after MI; but, miR-34awas down-regulated in the adolescent Infarct samples compared to Remote samples ($P = 0.018$, **Supplementary Files**). miR-34b expression was not significantly different at either age.

miR-25

miR-25 is another miRNA that has a reported role in cardio-protection after infarction. Interestingly, in the current investigation miR-25 was not significantly changed in the fetal heart in response to MI, but this miRNA was up-regulated in the Infarct samples in the adolescent animals compared to Remote samples ($P < 0.004$, **Supplementary Files**).

miR-199a

miR-199a and miR-590 have cardioprotective roles after infarction in mice (Eulalio et al., 2012; Ali, 2013; Wang and Martin, 2014). miR-199a was significantly up-regulated in the Infarct samples compared to the Remote samples in both fetuses and adolescent sheep ($P = 0.009$, $P = 0.007$, respectively, **Supplementary Files**). However, their target genes were up-regulated in the infarct area compared to Remote and Sham samples, indicating that these miRNAs have a smaller role in sheep cardiac regeneration (**Supplementary Figure 1**).

miR-17∼miR-92 Cluster

The miR-17∼miR-92 cluster of miRNAs are also potential promoters of cell cycle in mice and sheep that are down-regulated

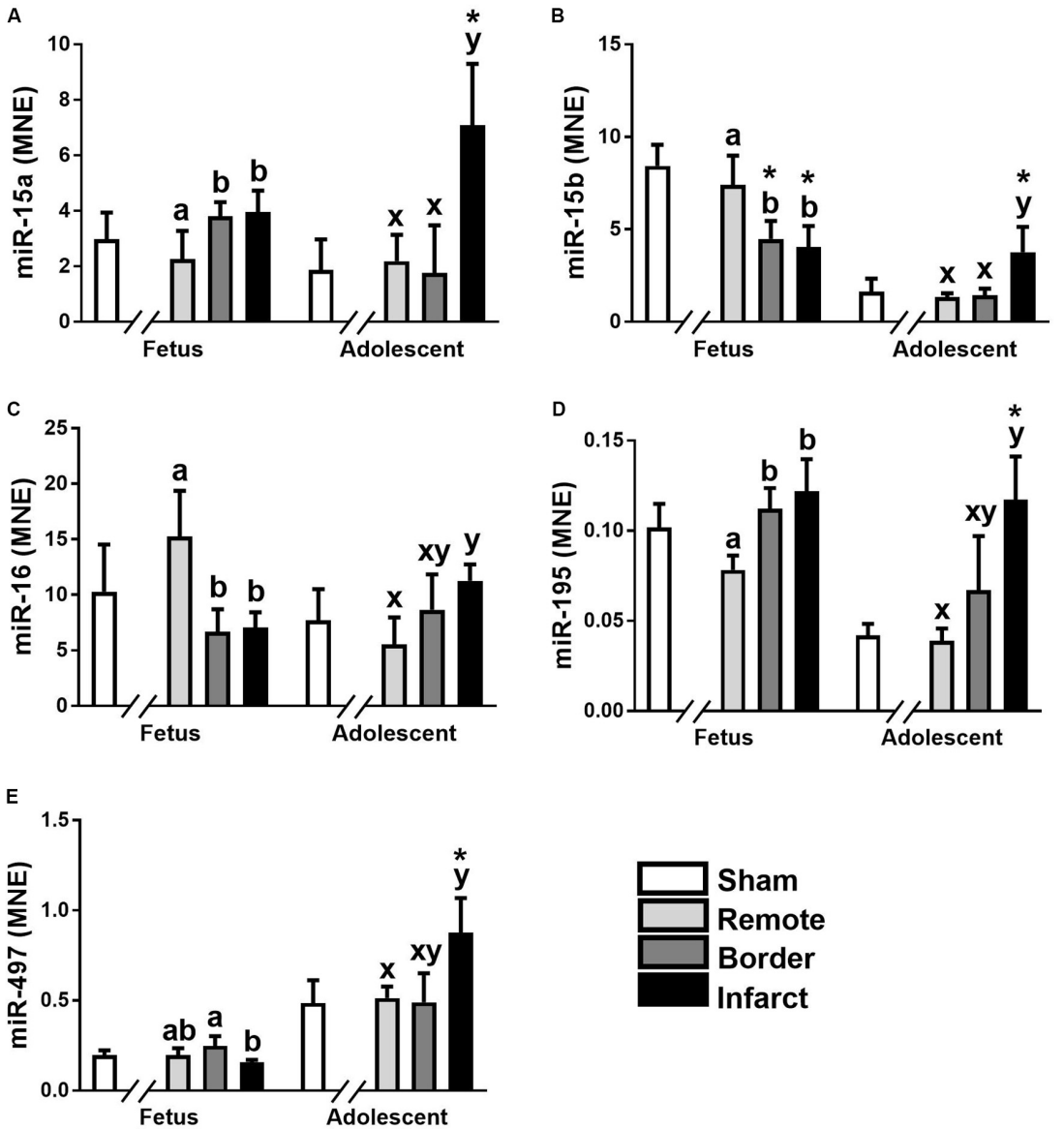

FIGURE 1 | Expression of the miR-15 family in sheep 3 days post-MI. Mean normalized expression (MNE) of miR-15a **(A)**, miR-15b **(B)**, miR-16 **(C)**, miR-195 **(D),** and miR-497 **(E)** in Sham, Remote, Border zone, and Infarct Tissue. Superscript letters (Fetal Sheep; a, b and Adolescent Sheep; x, y) represent significance between tissue regions (Remote, Border and Infarct) at each age ($P < 0.05$). *Represents significantly different data from the sham animals at each age ($P < 0.05$). Analyses between tissue regions (Infarct vs. Border vs. Remote) at each age were assessed using a nested Analysis of variance (ANOVA). A Bonferroni *post hoc* test was performed with multiple comparisons for each tissue region against the Sham tissue. $n = 5$ per treatment group per age.

at birth (Chen et al., 2013; Morrison et al., 2015). miR-17, miR-18a and miR-92a expression were significantly higher in the fetuses compared to adolescent sheep ($P = 0.01$, 0.004, 0.02, respectively, **Supplementary Files**); however, there was no effect of MI on expression at either age. Expression of miR-19a was too low for statistical analysis, but miR-19b was highly expressed in fetuses, although expression remained unchanged between the MI tissue regions. However, miR-19b was significantly up-regulated in the adolescent sheep in the Infarct samples compared to Remote samples ($P = 0.03$, **Supplementary Files**). Expression of miR-20a and miR-20b expression were higher in the fetuses compared to the adolescent animals ($P = 0.03$, $P = 0.007$, respectively, **Supplementary Files**), but were unchanged at both ages in response to MI.

miRNA Microarray Analysis

miRNA Probe PCA Analysis and Clustering

miRNA microarrays were used to investigate the immediate miRNA response to infarction [$n = 3$ per tissue region (Infarct, Border, Remote) and at each age (Fetal, Adolescent)]. This approach complements the qRT-PCR targeted miRNA approach and has the potential to identify additional miRNAs and broad

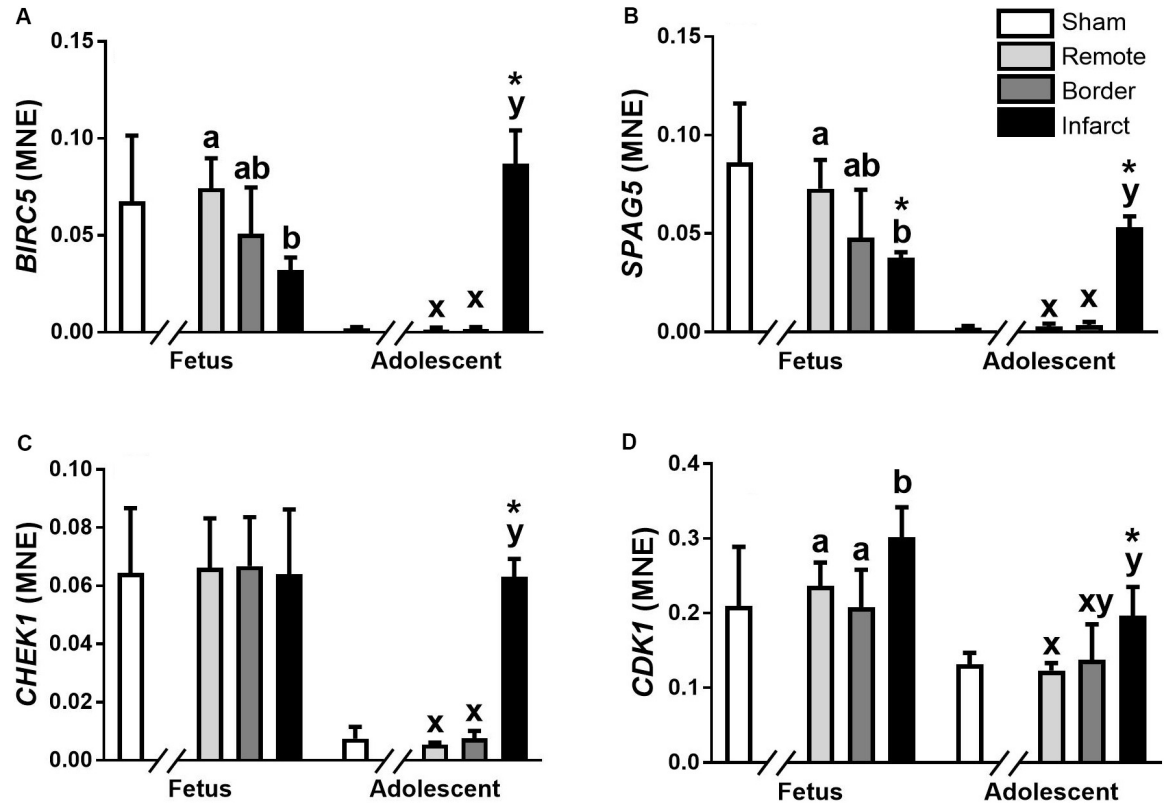

FIGURE 2 | qRT-PCR validation of miR-15 family target mRNA expression in sheep 3 days post-MI. Mean normalized expression (MNE) of *BIRC5* **(A)**, *SPAG5* **(B)**, *CHEK1* **(C),** and *CDK1* **(D)** in Sham, Remote, Border zone, and Infarct Tissue. Superscript letters (Fetal Sheep; a, b and Adolescent Sheep; x, y) represent significance between tissue regions (Remote, Border and Infarct) at each age ($P < 0.05$). *Represents significantly different data from the sham animals at each age ($P < 0.05$). Analyses between tissue regions (Infarct vs. Border vs. Remote) at each age were assessed using a nested Analysis of Variance (ANOVA). A Bonferroni *post hoc* test was performed with multiple comparisons for each tissue region against the Sham tissue. $n = 5$ per treatment group per age.

functional themes associated with cardiac regeneration in sheep. A PCA analysis of the microarray data shows separation of the two age groups and three treatment groups as well as clustering of the biological replicates within each of the groups (**Figure 4**). The PC2 dimension separated the groups on the basis of age, while separation of groups along PC1 highlighted the infarction response for both ages. The fetal Remote and Border samples were nearly superimposable. Overall, the fetal response to infarction was more constrained than the adolescent response. The adolescent Border sample showed considerable variance along PC1. The analysis demonstrates that multiple miRNAs have altered expression in the response to cardiac damage in the sheep; this suggests substantial complexity in the miRNA regulation of the heart regenerative response.

K-means clustering ($k = 10$) of the significant differentially expressed (DE) probes was undertaken separately at each age. This analysis clusters together miRNAs with similar expression changes in response to MI (**Table 1** and **Supplementary Figures 2**, **3**). Clusters 7, 8, and 9 in the adolescent animals were combined for mRNA target prediction as they contained multispecies probes for the same miRNAs. Cluster 1 in the fetal samples had insufficient mRNA targets for gene ontology analysis. Clusters 3 and 6 in the fetuses and Cluster 5 in adolescent sheep were the largest, containing 41, 46, and 58 probes respectively. Cluster 3 in the fetal samples showed an overall increase in expression in Infarct compared to Remote samples, while Cluster 6 showed an overall decline in miRNA expression in the Infarct samples compared to the Remote samples. In the fetal samples, Clusters 1, 2, 3, 4, and 5 were all increasing expression in the Infarct samples compared with Remote samples. Clusters 6, 7, 9, and 10 all had declining expression in the Infarct samples compared with Remote samples. In the adolescent sheep Clusters 1, 3, 4, 6, 7, 9, and 10 all had increased expression in the Infarct samples compared with Remote samples. Clusters 2, 5, and 8 were all declining expression in the Infarct samples compared with Remote samples.

miRNA qRT-PCR Expression Validation

By design, a single miRNA could be separated into multiple clusters due to the array featuring multiple species probes for the same miRNA or probes identifying miRNA family variants. The miRNA expression patterns measured using qRT-PCR were generally consistent with the expression measured by the miRNA microarray. Probes for miR-15a and miR-16 were present in Clusters 3 and 5 in the fetuses and Clusters 1 and 6 in the adolescent sheep. These clusters had increased expression in

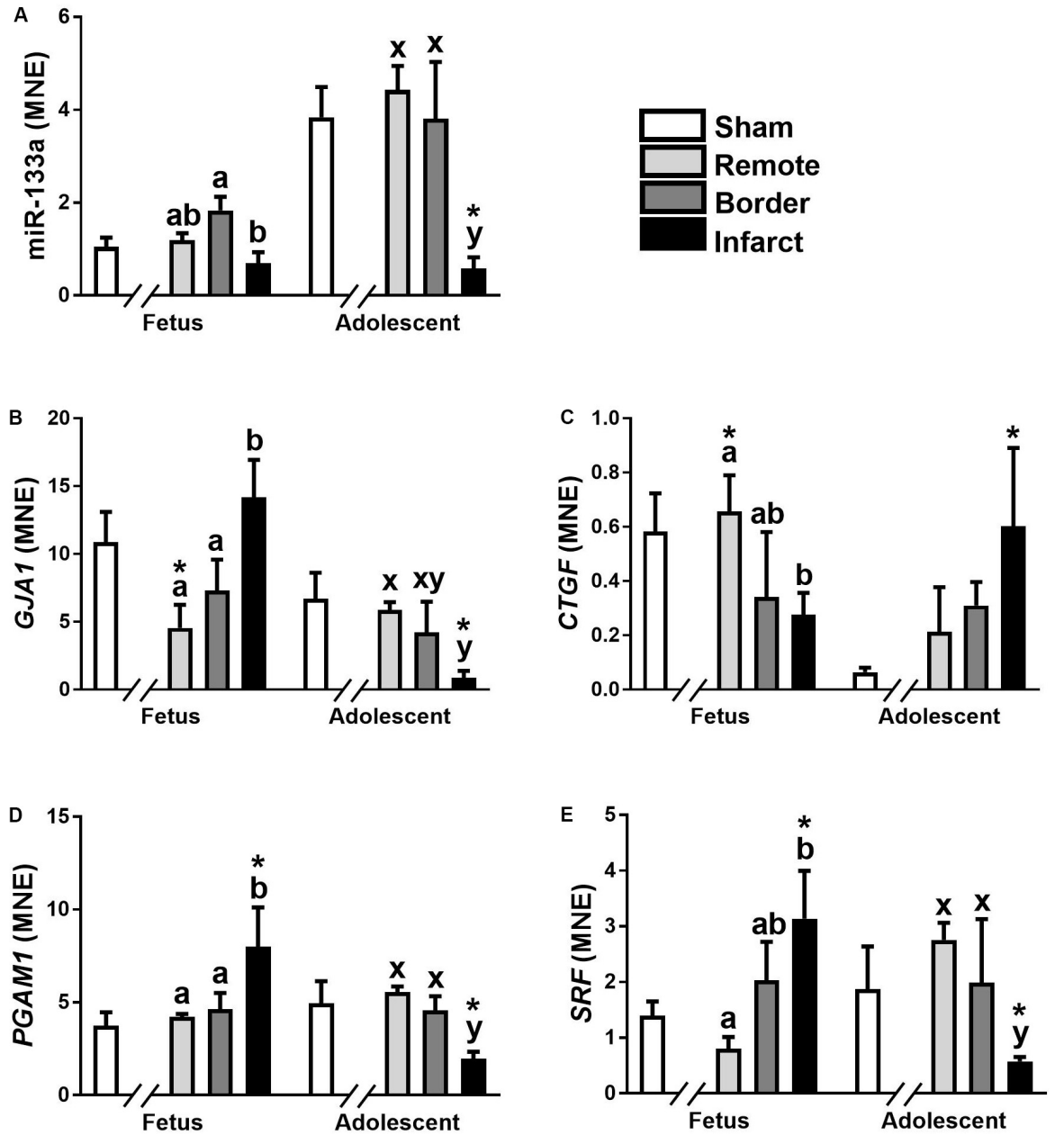

FIGURE 3 | qRT-PCR validation of miR-133a and mRNA target expression in sheep 3 days post-MI. Mean normalized expression (MNE) of miR-133a **(A)**, *GJA1* **(B)**, *CTGF* **(C)**, *PGAM1* **(D)**, and *SRF* **(E)** in Sham, Remote, Border zone, and Infarct Tissue. Superscript letters (Fetal Sheep; a, b and Adolescent Sheep; x, y) represent significance between tissue regions (Remote, Border, and Infarct) at each age ($P < 0.05$). *Represents significantly different data from the sham animals at each age ($P < 0.05$). Analyses between tissue regions (Infarct vs. Border vs. Remote) at each age were assessed using a nested Analysis of variance (ANOVA). A Bonferroni *post hoc* test was performed with multiple comparisons for each tissue region against the Sham tissue. $n = 5$ per treatment group per age.

the Infarct samples compared to Remote samples, which was consistent with qRT-PCR miR-15a expression, whereas miR-16 was down-regulated in fetal Infarct samples in the qRT-PCR data but increased in the microarray data. This latter difference may be explained because the clustered probes for miR-16 were for the miR-16a and miR-16c-5p variants, which were not specifically measured in qRT-PCR. Probes for miR-133a were present in Clusters 6 and 7 in the fetus and Clusters 2, 5, and 8 in the adolescent sheep. These clusters all had decreasing expression profiles that mirrors the qRT-PCR data for miR-133a where there was decreased expression in the Infarct compared with Border samples in the fetal samples and decreased expression in the Infarct compared with the Border and Remote samples in the adolescent sheep. Fold change comparisons (Infarct/Remote) of miRNAs using both methods at each age showed strong correlations with $r^2 = 0.91$, 0.84, 0.93 and 0.90 ($P < 0.0001$,

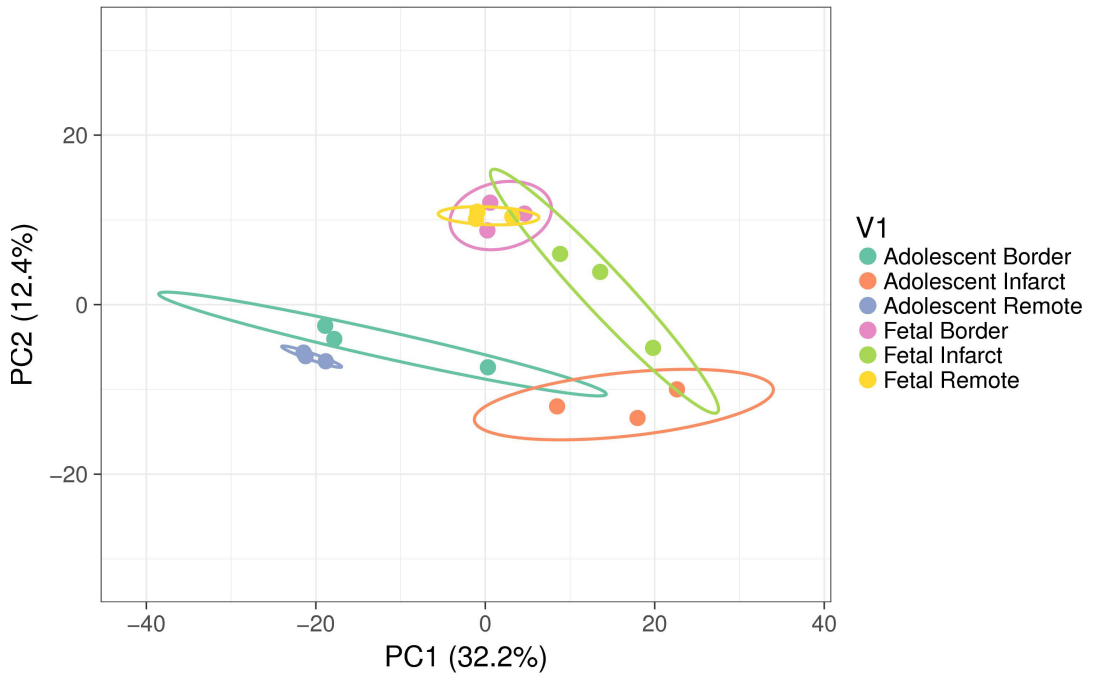

FIGURE 4 | Principal component analysis (PCA) of miRNA expression using all samples. The ellipses show the 95% confidence level for each group. Each group consisted of samples from three animals. The variance explained in each principal component (PC) is shown in brackets. The PC2 dimension separated the groups on the basis of age while separation of groups along PC1 highlighted the infarction response for both ages. The fetal Remote and Border samples were near superimposable. The adolescent Border sample showed considerable variance along PC1.

$P < 0.0001$) for fetus and adolescent samples, respectively (**Supplementary Figure 4**).

miRNA Target Prediction and Pathway Enrichment

Microarray probes that were significantly differentially regulated in the Infarct compared to Remote samples were grouped based on expression profile (higher or lower in the Infarct compared to Remote samples at each age group). Since miRNAs have a large number of target mRNAs, and these targets often overlap, there was a high level of consistency between pathways of predicted targets of miRNAs between fetal and adolescent sheep (**Supplementary File 2**). The most enriched KEGG pathway terms at both ages for the mRNA targets predicted from the significantly deregulated miRNAs included: *Pathways in cancer (map05200)*, *MAPK signaling pathway (map04010)*, *Axon guidance (map04360)*, *Proteoglycans in cancer (map05205)*, *cAMP signaling pathway (map04024)*, *Ras signaling pathway (map04014)*, *Signaling pathways regulating pluripotency of stem cells (map04550)*, *Wnt signaling pathway (map04310)*, *Leukocyte transendothelial migration (map04670)*, *Endocytosis (map04144)* (**Supplementary File 2**). The most enriched gene ontology terms using Biological Process for the significantly deregulated miRNAs at both ages included: *Canonical Wnt signaling pathway (GO:0060070)*, *Wnt signaling pathway (GO:0016055)*, *Angiogenesis (GO:0001525)*, *Protein ubiquitination (GO:0016567)*, *Positive regulation of GTPase activity (GO:0043547)*, *Nervous system development (GO:0007399)*, *Regulation of transcription from RNA polymerase II promoter (GO:0006357)*, *Covalent chromatin modification (GO:0016569)*.

Due to the high level of similarity in pathways of predicted target mRNAs at both ages, target genes were also predicted for the uniquely up-regulated and uniquely down-regulated miRNAs at each age. To do this, miRNAs with the same direction of change between fetuses and adolescent sheep were removed and gene target prediction was repeated. This method was used to identify pathways that were differentially regulated as a function of age in response to infarction (**Tables 2**, **3**). Predicted mRNAs of the uniquely deregulated miRNAs that were oppositely expressed in fetuses and adolescent sheep were significantly enriched for *FoxO signaling pathway (map04068)*, *Proteoglycans in cancer (map05205)* and *Neurotrophin signaling pathway (map04722)* KEGG terms (**Table 2**). *Insulin signaling pathway (map04910)* and *Sphingolipid signaling pathway (map04071)* were uniquely enriched for the predicted target genes of up-regulated and down-regulated miRNAs, respectively, in the fetuses (**Table 2**). *Rap1 signaling pathway (map04015)* and *Fc gamma R (map04666)* were both uniquely enriched for the predicted target genes of up-regulated miRNAs whereas *Wnt signaling pathway (map04310)* was enriched for the predicted target genes of down-regulated miRNAs in the adolescent Infarct samples (**Table 2**). Uniquely enriched gene ontology terms for Biological Processes included *Canonical Wnt signaling*

TABLE 1 | miRNA expression k-means clusters.

Fetal cluster number	Direction of change	miRNA
1	Increased in infarct	miR-21, miR-21a-5p, miR-451, miR-7641
2	Increased in infarct	let-7j, miR-1273e, miR-1285, miR-155, miR-199a-3p, miR-21, miR-222a-3p, miR-223-3p, miR-2478, miR-25, miR-25-3p, miR-29a, miR-376c-3p, miR-381, miR-381-5p, miR-3957-3p, miR-451, miR-451b, miR-5100, miR-6236, miR-6240, miR-7977
3	Increased in infarct	miR-106a, miR-1224-5p, miR-1246, miR-125b, miR-125b-5p, miR-1260, miR-1260a, miR-1260b, miR-1285, miR-1357, miR-1386, miR-142-3p, **miR-15a**, **miR-16a**, miR-1895, miR-199b, miR-19b, miR-20a, miR-20b, miR-21, miR-223, miR-2311, miR-2478, miR-2887, miR-2888, miR-29a-3p, miR-29d-3p, miR-30b-3p, miR-339b, miR-379-5p, miR-3968, miR-4454, miR-4792, miR-486-5p, miR-5100, miR-6119-5p, miR-6240, miR-6412, miR-716a, miR-716b, miR-7641
4	Increased in infarct	let-7i, miR-1246, miR-1254, miR-127, miR-1273e, miR-1285, miR-140, **miR-16c-5p**, miR-199a-3p, miR-199a-5p, miR-199c, miR-21, miR-2137, miR-214, miR-221, miR-222, miR-30c, miR-451, miR-5126, miR-6323, miR-6236-p5
5	Increased in infarct	miR-451, miR-7641, miR-21
6	Decreased in infarct	let-7e-5p, miR-1, miR-100, miR-1285, **miR-133a-5p**, miR-1386, miR-139, miR-1-3p, miR-150, miR-151-5p, miR-151b, miR-181a, miR-1973, miR-224, miR-23b, miR-23b-3p, miR-24, miR-28c, miR-29a, miR-30a-3p, miR-30c, miR-30d, miR-30d-5p, miR-30e-3p, miR-30f, miR-331-3p, miR-339b, miR-3431, miR-374b, miR-378, miR-378a, miR-378b, miR-378c, miR-378d, miR-378e, miR-378f, miR-378g, miR-378i, miR-4454, miR-452-3p, miR-558, miR-574, miR-6240, miR-669e, miR-7641, miR-99a
7	Decreased in infarct	miR-1, **miR-133**, **miR-133a**, **miR-133a-3p**, miR-133b, miR-133b-3p, miR-374a, miR-499, miR-499-5p, miR-499b-5p
9	Decreased in infarct	miR-133c, miR-145, miR-30a-5p, miR-30b, miR-30b-5p, miR-30c, miR-30c-5p, miR-30d, miR-30e-5p, miR-30f, miR-499
10	Decreased in infarct	miR-125a, miR-125a-5p, miR-1386, miR-1538-p3, miR-181a-5p, miR-181c, miR-2487-p5, miR-30d, miR-4448, miR-4454, miR-5100, miR-6240-p3, miR-716a-p5, miR-716b
Adolescent cluster number	**Direction of change**	
1	Increased in infarct	let-7j, miR-1260b, miR-1285, mir-1538, **miR-16c-5p**, miR-21, miR-223, miR-30c-1-3p, miR-3957-3p, miR-4454, miR-5100, miR-5126, mir-6236, mir-6240, mir-716a, miR-716b, miR-7977
2	Decreased in infarct	miR-34a, miR-125b, miR-125b-5p, **miR-133a**, miR-133b-3p, miR-133c, miR-185, miR-197, miR-22-3p, miR-22-5p, miR-23b, miR-24, miR-27b, miR-30a-5p, miR-30b, miR-30b-5p, miR-30c, miR-30c-5p, miR-30d, miR-30d-5p, miR-30e-5p, miR-30f, miR-99a.
3	Increased in infarct	let-7i, miR-106a, miR-106b, miR-1224-5p, miR-1260b, miR-127, miR-1386, miR-150, miR-155, **miR-15a**, miR-1895, miR-199a-3p, miR-199b, miR-19b, miR-20a, miR-20b, miR-2478, miR-25, miR-25-3p, miR-2887, miR-2888, miR-29a, miR-30b-3p, miR-339b, miR-376c-3p, miR-376e-3p, miR-379-5p, miR-3968, miR-409-3p, miR-4454, miR-4792, miR-487b-3p, miR-5100, miR-558, miR-6119-5p, miR-7641
4	Increased in infarct	miR-106a, miR-1246, miR-1260, miR-1260a, miR-1260b, miR-1285, miR-1357, miR-142-3p, **miR-15a-5p**, miR-199a-3p, miR-199a-5p, miR-199c, miR-2137, miR-214, miR-2313-5p, miR-2311, miR-2478, miR-2487, miR-381-5p, miR-4454, miR-4484, miR-451b, miR-5100, miR-6236-5p, miR-6240, miR-6323, miR-6412, miR-716a, miR-716b, miR-7641
5	Decreased in infarct	miR-1, miR-100, miR-103-3p, miR-125a, miR-125a-5p, **miR-133a-5p**, miR-139, miR-1-3p, miR-148b, miR-151-5p, miR-151b, miR-181a, miR-181a-5p, miR-181c, miR-1973, miR-23a-3p, miR-221, miR-222, miR-222a-3p, miR-224, miR-23b-3p, miR-23b, miR-26-5p, miR-28c, miR-29a, miR-29a-3p, miR-29b, miR-29d-3p, miR-2284x, miR-30a-3p, miR-30a-5p, miR-30b, miR-30c, miR-30c-5p, miR-30d-5p, miR-30e-3p, miR-30f, miR-331-3p, miR-339b, miR-3431, miR-361, miR-374b, miR-378, miR-378a, miR-378b, miR-378c, miR-378d, miR-378e, miR-378f, miR-378i, miR-424-5p, miR-452-3p, miR-486, miR-486-5p, miR-4306, miR-574, miR-669e, miR-99a
6	Increased in infarct	miR-1246, miR-1254, miR-1273e, miR-1285, **miR-16a**, miR-21, miR-223-3p, miR-451
7	Increased in infarct	miR-7641
8	Decreased in infarct	miR-1, **miR-133**, **miR-133a**, **miR-133a-3p**, **miR-133a-p5**, miR-133b, miR-499, miR-499-5p, miR-499b-5p, miR-193b
9	Increased in infarct	miR-1273e, miR-21, miR-451, miR-7641
10	Increased in infarct	miR-21, miR-21a-5p, miR-7641

Differentially expressed microarray probes were first identified and subjected to k-means clustering. All species identifiers were then removed and a non-redundant list of miRNAs was obtained. Anonymous probes beginning with the designation "PC" were excluded. A full list of probes with species identifiers can be found in ***Supplementary File 1****. miRNAs that were included in the targeted analysis of previously implicated miRNAs in mouse and zebrafish studies using qRT-PCR analyses are highlighted in bold.*

pathway (GO:0060070) and *Endocytosis (GO:0006897),* which were oppositely regulated at each age (**Table 3**). *Wnt signaling pathway (GO:0016055)* was uniquely enriched for the predicted target genes of up-regulated miRNAs in the fetuses (**Table 3**). Whereas *Collagen fibril organization (GO:0030199), Intracellular protein transport (GO:0006886),* and *Protein localization to*

TABLE 2 | Top 10 KEGG pathway enrichment terms for predicted targets of uniquely deregulated miRNAs in the infarct compared to remote samples.

Treatment group	KEGG pathway terms	Term accession	Pathway hits	P^{adj}
Predicted targets of fetal up-regulated miRNAs	Axon guidance	map04360	98	0.000
	Pathways in cancer	map05200	180	0.000
	FoxO signaling pathway	map04068	73	0.0091
	Proteoglycans in cancer	map05205	101	0.0091
	MAPK signaling pathway	map04010	119	0.0091
	Insulin signaling pathway	map04910	75	0.0091
	ErbB signaling pathway	map04012	51	0.0102
	Ras signaling pathway	map04014	109	0.0102
	AMPK signaling pathway	map04152	68	0.0109
	Regulation of actin cytoskeleton	map04810	103	0.0109
Predicted targets of fetal down-regulated miRNAs	Axon guidance	map04360	119	0.000
	Ras signaling pathway	map04014	142	0.000
	Pathways in cancer	map05200	229	0.000
	AMPK signaling pathway	map04152	87	0.007
	Oxytocin signaling pathway	map04921	101	0.0081
	ErbB signaling pathway	map04012	64	0.0081
	Neurotrophin signaling pathway	map04722	82	0.0081
	cAMP signaling pathway	map04024	119	0.0106
	MAPK signaling pathway	map04010	145	0.0113
	Sphingolipid signaling pathway	map04071	82	0.0113
Predicted targets of adolescent up-regulated miRNAs	Endocytosis	map04144	123	0.000
	Axon guidance	map04360	81	0.0055
	Ras signaling pathway	map04014	98	0.0055
	Regulation of actin cytoskeleton	map04810	95	0.0055
	Neurotrophin signaling pathway	map04722	62	0.0055
	AMPK signaling pathway	map04152	62	0.0069
	Rap1 signaling pathway	map04015	91	0.0069
	Fc gamma R	map04666	47	0.0069
	Pathways in cancer	map05200	150	0.0082
	cAMP signaling pathway	map04024	85	0.0082
Predicted targets of adolescent down-regulated miRNAs	MAPK signaling pathway	map04010	169	0.000
	Axon guidance	map04360	127	0.000
	Wnt signaling pathway	map04310	106	0.000
	Pathways in cancer	map05200	258	0.000
	Proteoglycans in cancer	map05205	136	0.0041
	FoxO signaling pathway	map04068	98	0.0041
	Ras signaling pathway	map04014	152	0.0041
	cAMP signaling pathway	map04024	130	0.0072
	Oxytocin signaling pathway	map04921	107	0.0078
	ErbB signaling pathway	map04012	67	0.0078

P-values were corrected for multiple testing using Benjamini-Hochberg method. P^{adj} is the FDR q-value. All enrichments were performed through miRWalk.

plasma membrane (GO:0072659) were uniquely enriched in the adolescent sheep.

Identification of Potential miRNA Targets for Treatment of Cardiac Disease

miRNA responses to infarction at one age, but not the other may potentially contribute to the differing physiological responses to infarction at the fetal and adolescent ages, and therefore are of particular interest. These specific miRNA responses may underpin the differing repair capacities of fetal and adolescent sheep heart tissues. Several miRNAs were detected that had opposite expression profiles in fetus compared with adolescent sheep (**Figure 5**). miR-140 was uniquely up-regulated in fetal Infarct compared to Remote samples. This miRNA has a role in cardiac muscle hypertrophy (Joshi et al., 2016) as well as mitochondrial fission and apoptosis through mitofusin 1 (Mfn1) in rat hearts (Li et al., 2014). Five miRNAs were significantly down-regulated in the fetal Infarct compared to the Remote samples (let-7e, miR-145, miR-374a, miR-378g, and miR-4448; **Figure 5**). Some of these miRNAs were previously investigated including miR-145, which protects the heart from autophagy after infarction in rabbits (Higashi et al., 2015), but hypoxia downregulates the expression of this miRNA in

TABLE 3 | Top 10 gene ontology biological process terms for predicted mRNA targets of uniquely deregulated miRNAs.

Treatment group	Biological processes	Term accession	Pathway hits	P^{adj}
Predicted targets of fetal up-regulated miRNAs	Protein ubiquitination	GO:0016567	153	0.0001
	Response to ATP	GO:0033198	38	0.0003
	Peptidyl-serine phosphorylation	GO:0018105	114	0.0007
	Adenosine catabolic process	GO:0006154	23	0.0007
	Intracellular signal transduction	GO:0035556	213	0.0007
	Protein dephosphorylation	GO:0006470	98	0.0011
	Cellular response to heat	GO:0034605	39	0.0013
	Positive regulation of NF-kappaB transcription factor activity	GO:0051092	88	0.0014
	Canonical Wnt signaling pathway	GO:0060070	111	0.0015
	Wnt signaling pathway	GO:0016055	127	0.0017
Predicted targets of fetal down-regulated miRNAs	Water transport	GO:0006833	44	0.0008
	Positive regulation of MAPK cascade	GO:0043410	83	0.0011
	Peptidyl-serine phosphorylation	GO:0018105	139	0.0014
	Intracellular signal transduction	GO:0035556	262	0.0016
	Endocytosis	GO:0006897	131	0.0035
	Protein ubiquitination	GO:0016567	174	0.0037
	Peptidyl-tyrosine dephosphorylation	GO:0035335	44	0.0039
	Response to ATP	GO:0033198	40	0.0041
	Protein polyubiquitination	GO:0000209	89	0.0045
	Actin cytoskeleton organization	GO:0030036	104	0.0052
Predicted targets of adolescent up-regulated miRNAs	Nervous system development	GO:0007399	192	0.0001
	Intracellular signal transduction	GO:0035556	193	0.0002
	Sensory perception of sound	GO:0007605	107	0.0006
	Neuron migration	GO:0001764	90	0.0008
	Collagen fibril organization	GO:0030199	44	0.001
	Endocytosis	GO:0006897	97	0.0011
	Intracellular protein transport	GO:0006886	107	0.0012
	Positive regulation of I-kappaB kinase/NF-kappaB signaling	GO:0043123	83	0.0015
	Memory	GO:0007613	54	0.0016
	Peptidyl-serine phosphorylation	GO:0018105	98	0.0018
Predicted targets of adolescent down-regulated miRNAs	Neuron migration	GO:0001764	141	0.0001
	Peptidyl-serine phosphorylation	GO:0018105	153	0.0004
	Intracellular signal transduction	GO:0035556	288	0.0004
	Protein autophosphorylation	GO:0046777	175	0.0011
	Protein localization to plasma membrane	GO:0072659	117	0.0012
	Canonical Wnt signaling pathway	GO:0060070	147	0.0015
	Nervous system development	GO:0007399	134	0.0015
	cAMP catabolic process	GO:0006198	21	0.0015
	Protein ubiquitination	GO:0016567	189	0.0019
	Actin cytoskeleton organization	GO:0030036	59	0.0025

P-values were corrected for multiple testing using Benjamini-Hochberg method. P^{adj} is the FDR q-value. All enrichments were performed through miRWalk.

mouse cardiac fibroblasts (Wang et al., 2014). miR-374 regulates vascular endothelial growth factor receptor-1 signaling in rats and modulates the inflammatory process in humans (Lee et al., 2017; Doumatey et al., 2018). 14 miRNAs were uniquely down-regulated in the adolescent Infarct compared to Remote samples (**Figure 5**) and included some miRNAs known to be involved in rodent cardiac regeneration, including miR-34a (a miRNA associated with cardiac repair in mice; Yang et al., 2015) and miR-26, which plays a major role in regulating cardiac collagen I expression in rats (Zheng et al., 2018). Inhibition of the miR-34 family has been shown to have therapeutic potential for human cardiac pressure overload and MI (Bernardo et al., 2012; Boon et al., 2013; Lock et al., 2017). The expression of the miR-34 family is increased in the mouse heart after MI (Lin et al., 2010) and in cardiac tissue from patients with heart disease (Thum et al., 2007; Greco et al., 2012). In sheep heart tissue we observed the opposite expression profile, with down-regulation of miR-34a in Infarct compared to Remote samples in adolescent sheep and no change in fetal expression. This result indicates that the miR-34 family may have a less prominent role in sheep heart responses to infarction compared to other mammals. One miRNA (miR-2313) was uniquely up-regulated in the adolescent

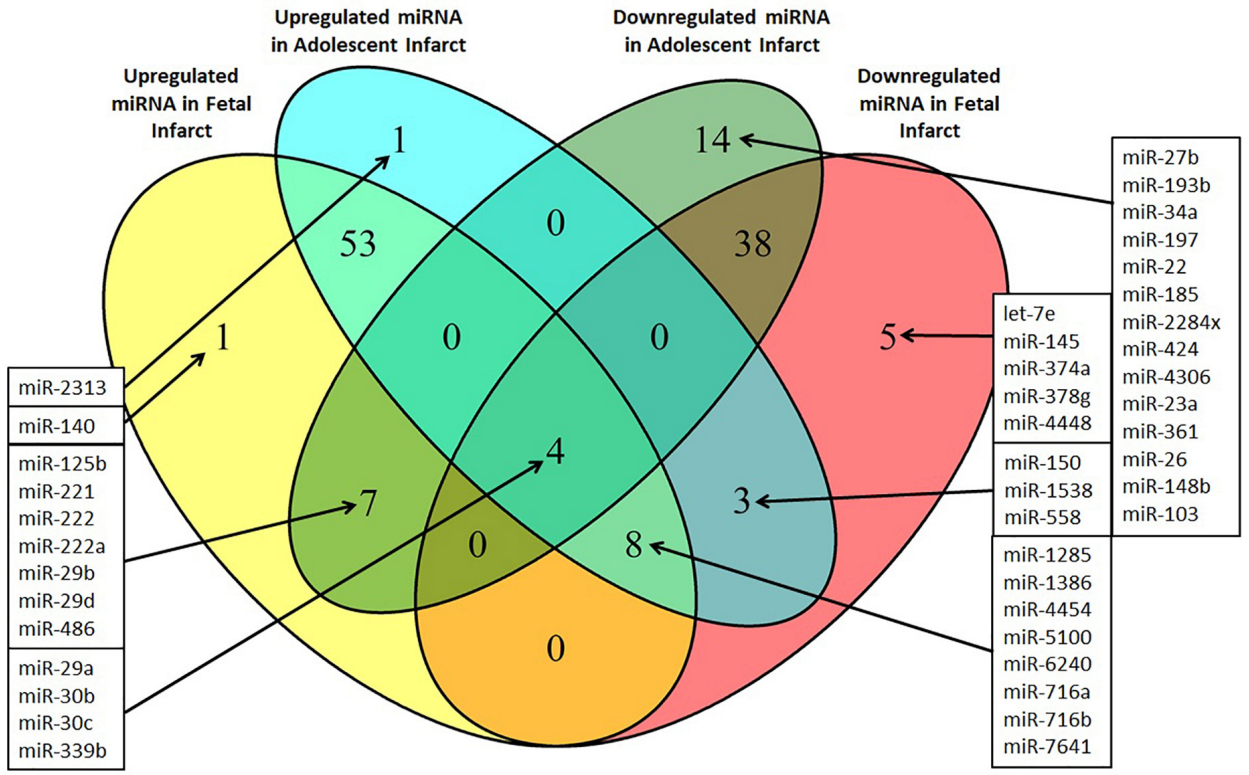

FIGURE 5 | Venn diagram of differentially expressed miRNAs in the Infarct samples compared to Remote samples and Border samples in fetal and adolescent sheep. $n = 3$ per age group. Only miRNAs that were significantly upregulated or downregulated are shown ($P < 0.05$).

Infarct samples compared to Remote samples. This miRNA was discovered in the bovine genome, and possible human homologs, which may represent a potential target for inhibition after infarction. Since the microarray contained probes from multiple species for the same miRNA, four miRNAs appeared to be both up-regulated and down-regulated in both the fetuses and lambs, this was an artifact of the multispecies redundancy likely due to slightly different seed sequences between species leading to inconsistent binding of the miRNAs to the probes. Since the direction of change was inconclusive, these miRNAs were not investigated further. Several miRNAs were oppositely regulated in each age group. Of particular interest were three miRNAs that were significantly up-regulated in the adolescent Infarct, but were down-regulated in the fetal Infarct (miR-1538, miR-558, and miR-150). miR-150 was previously investigated for its role in cancer metastasis (Wang et al., 2015; Li et al., 2016; Sun et al., 2016), pulmonary hypertension (Li et al., 2019) and B cell development (Zhou et al., 2007). mRNA targets of these three miRNAs (miR-150, miR-558, and miR-1538) were predicted using miRWalk, and gene ontology was performed to determine if the miRNAs may be involved in regulating functions that could be important in cardiac repair. Given that miRNAs have hundreds of potential target genes, identifying target pathways rather than specific genes allows a better overview of the potential role of miRNAs. KEGG pathway terms for predicted target mRNAs of miR-558 included *AMPK Signaling pathway* ($P = 4.5E-07$), *Axon guidance* ($P = 3.97E-06$), *Pathways in cancer* ($P = 8.93E-05$), *PI3K-Akt signaling pathway* ($P = 0.0014$) and *HIF-1 Signaling pathway* ($P = 0.004$). KEGG pathway terms for predicted target mRNAs of miR-1538 included *Circadian entrainment* ($P = 7.63E-08$), *ErbB signaling pathway* ($P = 6.60E-08$), *VEGF signaling pathway* ($P = 1.30E-04$), and several "Cancer" pathways synonymous with cell proliferation.

H9c2 Cell Culture Analysis

Novel miRNA targets for treatment of cardiovascular disease were identified from the microarray data; these included miR-150, miR-558, and miR-1538, which were investigated further by their inhibition in cell culture. H9c2 cardiomyoblasts were cultured with anti-miRNAs for three miRNAs of interest (miR-558, miR-1538, and miR-150) as well as a negative control for a miRNA sequence not expressed in mammals (NC5; Integrated DNA Technologies, United States). Cell proliferation was measured in live and fixed cells using a colorimetric MTS assay and anti-Aurora-B (a marker of cells entering cytokinesis) immunohistochemistry staining, respectively. miR-558 inhibition caused an increase ($P < 0.05$) in cardiomyoblast proliferation under the "Normoxia," "Normoxia, Low Glucose," and "Hypoxia" conditions using both the MTS assay and Aurora-B staining (**Figures 6**, **7**). miR-1538 inhibition caused an increase ($P < 0.05$) in cell proliferation under "Normoxia,"

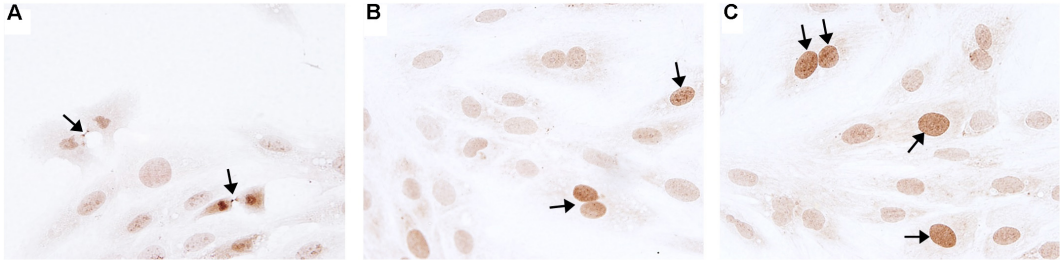

FIGURE 6 | Aurora B immunohistochemistry staining. Representative micrographs of Aurora B immunohistochemistry staining (marker of cells entering cytokinesis) of H9c2 cardiomyoblasts after treatment with Hypoxia (1% O_2). **(A)** Example of midbody staining in cells undergoing cytokinesis. **(B)** Negative control miRNA. **(C)** miR-558 inhibitor. Arrows indicate positive staining.

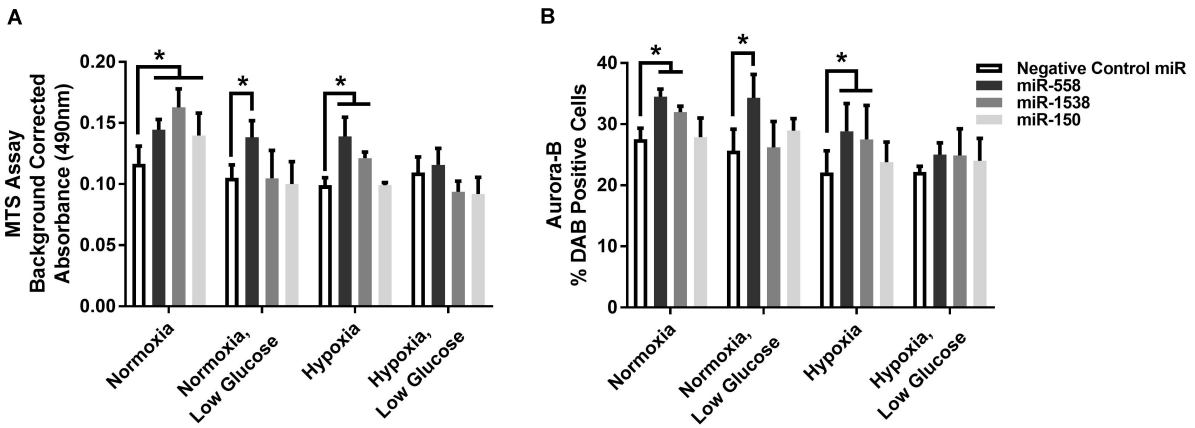

FIGURE 7 | Cell proliferation measures. **(A)** MTS cell proliferation assay. Background corrected proliferation assay absorbance of test anti-miRNAs. **(B)** % DAB Positive cells stained using an anti-Aurora-B antibody in 80 counting frames (Negative Control anti-miRNA, anti-miR-558, anti-miR-1538, anti-miR-150) on H9c2 cardiomyoblasts under Normoxia/Hypoxia or Glucose/Low Glucose conditions. *Represents significantly different data from the Negative Control miR group ($P < 0.05$). Nx, normoxia; LG, low glucose; Hx, hypoxia. Mean ± Standard Deviation.

and "Hypoxia" conditions using both MTS assay and Aurora-B staining. miR-150 inhibition was least effective in promoting proliferation, only increasing cell proliferation ($P < 0.05$) using the MTS assay in "Normoxia." The expression of predicted target mRNAs for miR-558 and miR-1538 included *PAPPA, JAG, NF2, MYOC1,* and *SOX4. NF2* was unchanged in response to miRNA inhibition (**Figure 8**). This could be due to a false-positive in the mRNA target prediction. miR-558 inhibition resulted in an increase in expression of *PAPPA* in "Normoxia, Low Glucose," *MYOC1* in "Normoxia" and "Hypoxia," *JAG* in "Normoxia, Low Glucose," and *SOX4* in the "Hypoxia" and "Hypoxia, Low Glucose" conditions (**Figures 8**, **9**; $P < 0.05$). miR-1538 inhibition resulted in an increase in expression of *PAPPA* in "Normoxia," *MYOC1* in "Normoxia" and "Hypoxia," *JAG* in "Normoxia, Low Glucose," and *SOX4* in the "Hypoxia" and "Hypoxia, Low Glucose" conditions (**Figures 8**, **9**; $P < 0.05$). miR-150 inhibition increased the expression of only *MYOC1* in "Normoxia" and "Hypoxia" conditions (**Figures 8**, **9**; $P < 0.05$). Overall, inhibition miR-558 and miR-1538 were effective for promoting cell proliferation *in vitro* and effectively modulating the expression of their predicted target mRNAs. Further mRNA targets may be identified from the differentially regulated miRNAs identified in the current investigation, and additional testing of these miRNAs on adult differentiated primary cardiomyocytes may provide evidence supporting enhanced cardiomyocyte proliferation in large animals at this age.

DISCUSSION

The predicted target mRNA term enrichments for miRNAs that were up-regulated or down-regulated in Infarct compared to Remote samples included a number of biological themes that could be associated with cardiac repair and regeneration. Common themes comprised cancer-related terms (may reflect increased cell proliferation), inflammatory cell/leukocyte migration (inflammation), protein transport and ubiquitination, MAPK signaling, and WNT signaling. Since it was not possible to perform target prediction against a cardiac-only background in miRWalk, there was an absence of muscle related enrichment terms. A number of these themes were present at both ages in response to infarction, indicating that a large number of pathways are similarly regulated in the regenerative and quiescent heart. Recent evidence by our group and others demonstrated a

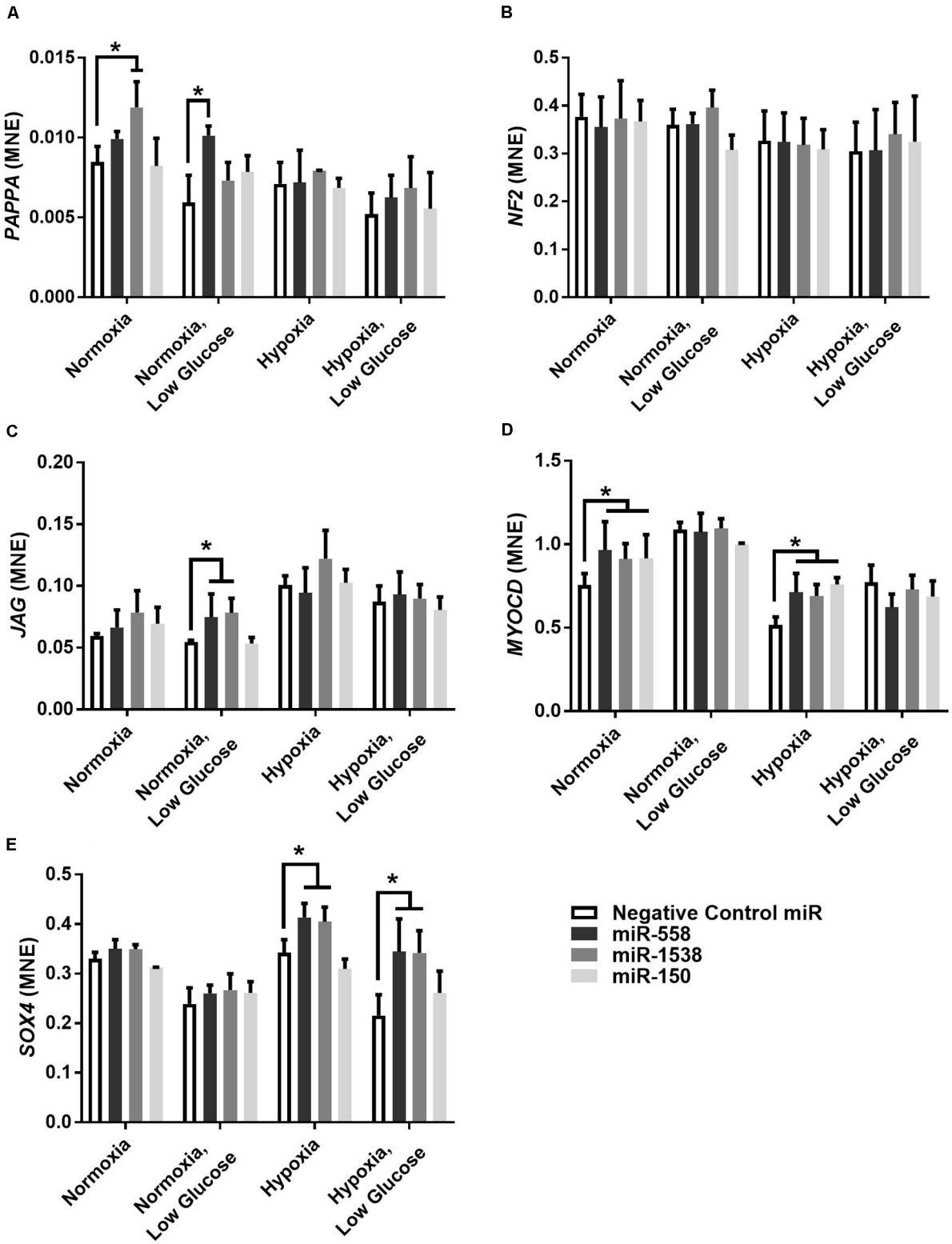

FIGURE 8 | Target gene expression of anti-miRNAs. Mean normalized expression (MNE) of predicted target genes of anti-miRNAs, *PAPPA* **(A)**, *NF2* **(B)**, *JAG* **(C)**, *MYOC1* **(D)**, and *SOX4* **(E)** demonstrating successful inhibition of miRNA resulting in decreased inhibition of target mRNAs. *Represents significantly different data from the negative control group ($P < 0.05$). $n = 4$ per treatment group.

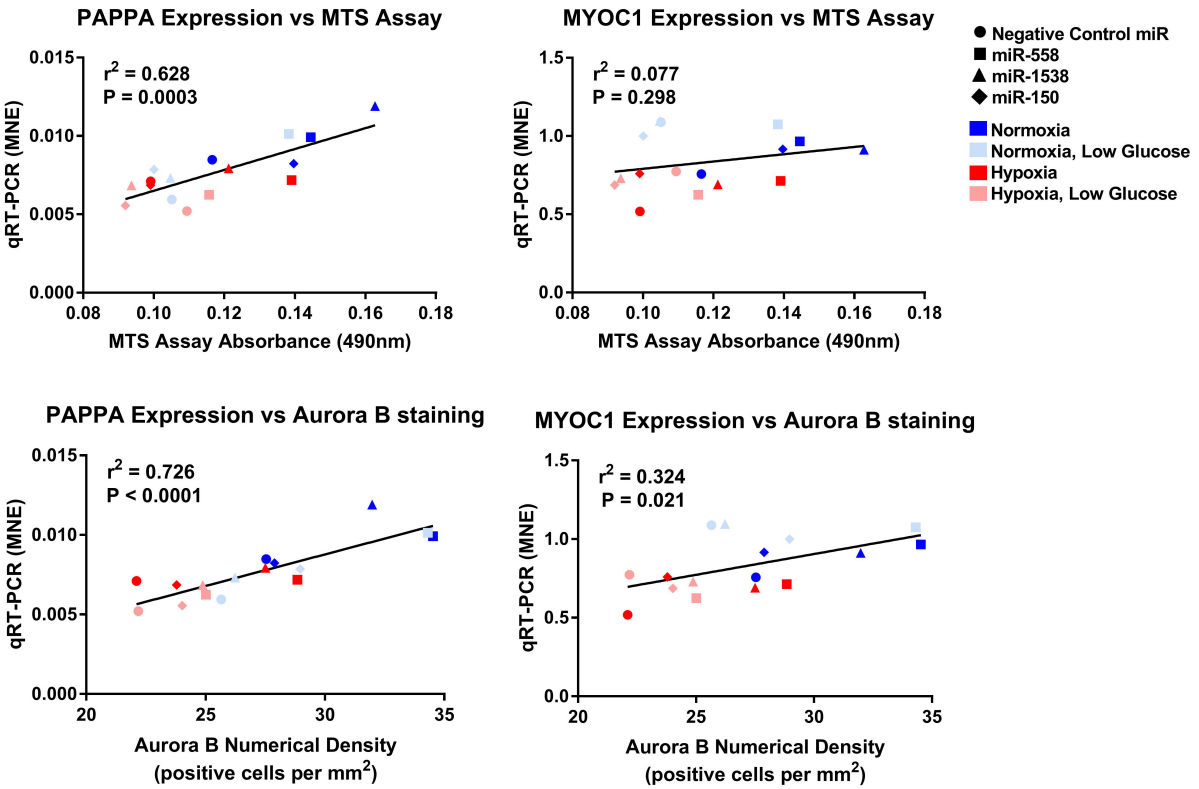

FIGURE 9 | Linear regression of *PAPPA* and *MYOC1* expression against measures of proliferation. Mean normalized expression of predicted target genes of anti-miRNAs against MTS and Aurora B proliferation measures demonstrating effectiveness of miRNA treatments within each oxygen environment.

largely similar but highly attenuated gene expression response to infarction in the regenerative heart compared to the quiescent heart (Zgheib et al., 2014; Mills et al., 2017; Quaife-Ryan et al., 2017; Lock et al., 2019). This response indicates a "resistance" to damage in the regenerative heart and is supported by the similar enrichment terms of predicted targets from deregulated miRNAs after infarction, as demonstrated in this study (**Supplementary File 2**). In addition, some similar themes between fetal and adolescent sheep may be due to the nature of miRNAs targeting a number of mRNAs, false positives in the mRNA target prediction method, as well as gene pathway enrichments including both promotors and repressors of pathways. These factors may lead to a large number of similar pathway enrichments at both ages. Limiting the term enrichments to miRNAs that were exclusively up-regulated or down-regulated at each age helped tease apart the molecular mechanisms underpinning the proliferative capacity or lack thereof in fetuses and adolescent hearts, respectively. Some of the pathways that are targeted by the identified uniquely deregulated miRNAs within this study are discussed below and how they may be exploited to improve cardiac regeneration.

Uniquely Deregulated Term Enrichments

FoxO Signaling

Forkhead box (Fox) family transcription factors have been implicated in cardiomyocyte cell cycle control as well as adult cardiovascular disease (Ronnebaum and Patterson, 2010). FoxO signaling was predicted to be oppositely regulated in the fetuses and adolescent sheep based on the miRNA target genes. miRNAs that suppress *FoxO* mRNA were up-regulated in the fetuses resulting in a decrease in FoxO expression in response to infarction, compared with an opposing decrease in miRNA expression in the adolescent sheep consistent with an increase in FoxO expression. Decreased FoxO activity in the proliferative fetal heart is a logical outcome given that FoxO is a major negative regulator of cardiomyocyte proliferation in fetal life. Forced expression of FoxO inhibits rat cardiomyocyte cell proliferation and induces expression of cell cycle inhibitors p21 and p27 (Sengupta et al., 2013). In the adult rat heart, activation of FoxO promotes cardiomyocyte survival under conditions of oxidative stress and is linked to AMPK and IGF signaling (Ronnebaum and Patterson, 2010), as well as many other pathways that were also significantly enriched in this study (*endoplasmic reticulum stress, autophagy, mitochondrial fission*, and *cell cycle*). FoxO therefore represents an interesting intermediary target pathway for miRNA inhibition to improve the repair response after infarction. However, there are a number of challenges associated with targeting specific isoforms of FoxO (FOXO1 and FOXO3) as well as differing effects within different cell types of the heart (Sengupta et al., 2013; Li et al., 2016). This would likely be an ongoing issue when utilizing miRNAs to target expression of this pathway as there would be probable cross-over suppression of both isoforms of FOXO as indicated by the

predicted target mRNAs (from the fetal up-regulated miRNAs; miR-6337, miR-1197, miR-125b, miR-24, miR-1, miR-1285, miR-140, miR-221, miR-222, and miR-411b all have predicted targets in the FoxO pathway).

Wnt Signaling Pathway

In the current investigation, the Wnt Signaling and Canonical Wnt signaling pathways were both consistently regulated pathways by a large number of the differentially regulated miRNAs. The Wnt pathway has been an area of interest in recent years for cardiac disease due to its demonstrated role in the regeneration of cardiac tissue (and other organs such as bone marrow, intestines and skin) in small animal models (Lock et al., 2018). The data from the current investigation and other data suggests that this may be one of the pivotal pathways being regulated during cardiac repair and regeneration (Mills et al., 2017; Quaife-Ryan et al., 2017). Three Wnt signaling pathways have been characterized: (i) the canonical Wnt pathway, (ii) the non-canonical planar cell polarity (PCP) pathway, and (iii) the non-canonical Wnt/calcium pathway. These pathways each have differing transcription factors and target genes but are linked by the binding of a Wnt-protein ligand to a Frizzled family receptor on the plasma membrane, which interacts with the intracellular Disheveled protein. Wnt target genes are modulated through a number of mechanisms, with the central Wnt signaling proteins linking multiple important molecular pathways in cardiomyocyte proliferation and survival such as the Hippo and MAPK pathways (Lock et al., 2018). Of particular interest were miR-6337, miR-1197, miR-24, miR-25, miR-125b, miR-29b, miR-1285, miR-486, and miR-222, all of which were up-regulated in the fetal Infarct compared to Remote samples and had predicted targets in the Wnt signaling pathways. Further investigation of the specific deregulated miRNAs that target this pathway could cause transient modulation of this powerful signaling cascade and potentially alter the proliferative ability of cardiomyocytes after infarction.

Sphingolipid Signaling

Sphingolipid signaling pathway was significantly enriched for a number of the deregulated miRNAs. Sphingolipids are derivatives of the amino alcohol sphingosine and are active components of the cardiomyocytes cell membrane, which play an important role in intracellular signal transduction and regulate diverse cellular processes such as proliferation, maturation, apoptosis and the cellular stress response (Borodzicz et al., 2015). The most important sphingolipids include ceramide (CER), sphingosine (SPH), and sphingosine-1-phosphate (S1P). Some proteins such as tumor necrosis factor-α [TNF-α; which was down-regulated in the fetal Infarct samples compared to Remote samples and up-regulated in the adolescent Infarct samples compared to Remote and Sham samples (Lock et al., 2019)] induce synthesis of CER from sphingomyelin via sphingomyelinase. CER can then act as a second messenger, promoting the apoptosis of cardiomyocytes (Borodzicz et al., 2015). On the other hand, sphingosine-1-phosphate is cardioprotective (Jin et al., 2002; Knapp et al., 2012a; Karliner, 2013). The ratio of CER and S1P is particularly important for control of apoptosis of cardiomyocytes in the remote area of the myocardium after MI (Knapp et al., 2012b). miRNA regulation of the proteins involved in the synthesis and signaling cascade of sphingolipids appears to be important for their regulation following MI. In particular, let-7e, miR-6391, miR-378g, miR-4454, miR-671, miR-145, miR-574, miR-2411, miR-558, and miR-1538 were all down-regulated in the fetal Infarct compared to Remote samples and contained predicted mRNA targets within the sphingolipid signaling pathway. Further investigation of this signaling pathway may therefore allow for control of apoptosis in the non-infarcted areas of the heart after heart attack, mitigating cardiomyocyte loss and subsequent pathological hypertrophy.

Neurotrophin Signaling

The neurotrophin pathway was also significantly enriched for predicted mRNA targets of oppositely regulated miRNAs at both ages. Interestingly, brain derived neurotrophic factor (BDNF) has a cardioprotective role in the heart after infarction by preventing adverse remodeling, and acts on endothelial cells to promote neovascularization in response to hypoxic stimuli via the Akt pathway (Okada et al., 2012). From the miRNAs that were down-regulated in the fetus and were up-regulated in the adolescent sheep; let-7e and miR-6391 were of particular interest in the regulation of the neurotrophin signaling pathway as they had a large number of predicted target genes within this pathway (**Supplementary File 2**). Inhibition of these miRNAs may therefore help prevent adverse tissue remodeling after heart attack.

Cardiac Fibrosis

Regulation of cardiac fibrosis and extracellular matrix deposition following infarction is crucial to maintain contractile function of the ventricles and prevent ventricular rupture (Sattler and Rosenthal, 2016). We previously reported increased percentage of staining of picrosirius red in the Infarcted samples compared with Sham samples for both age groups (Lock et al., 2019), but that the localization of the staining was different between the two age groups (the fetal sheep had larger deposition of collagen in the Border-zone than the Infarct area). *COL1A1* is the major component of type 1 collagen forming a large portion of the extracellular matrix (Pauschinger et al., 1998). We have also previously reported that there was an opposite expression profile between fetuses and adolescent sheep for both the collagen genes *COL1A1* and *COL3A1* between the individual tissue regions, indicating a reciprocal relationship between the two collagen types in response to infarction (Lock et al., 2019). This difference of collagen type following infarction is important as these collagen fibers maintain different elasticity, stiffness and capacity for degradation by metalloproteinases (MMPs) and is therefore likely one of the aspects of the fetal heart that allows for its regeneration. Although this scar formation allows for higher survival rates after infarction, the diminished contractile ability of the scar tissue has detrimental effects on long term heart function leading to chronic heart disease (AIHW, 2015). Interestingly, there was an up-regulation of miRNAs in the adolescent Infarct samples that had predicted mRNA targets involved in collagen fibril organization (miR-25, miR-3535, miR-6391) indicating a

down-regulation of collagen organization within the adolescent Infarct samples. Another miRNA of interest was miR-26, which was down-regulated in the adolescent Infarct samples and plays a major role in the regulation of cardiac collagen I expression (Zheng et al., 2018). The observed decrease in miR-26 expression may help explain the increased expression of *COL1A1* in the adolescent Infarct samples and represents a valuable molecular target for up-regulation to prevent adverse cardiac fibrosis and reduce infarct size post-infarct setting in adults.

Potential Targets for miRNA Therapeutic Inhibition

The current investigation identified 10 miRNAs that were oppositely regulated in fetuses and adolescent sheep and the effect of inhibition of these miRNAs on cardiomyocyte proliferation was then assessed *in vitro*. Inhibiting miR-558 and miR-1538 was effective for increasing the expression of their target mRNAs and increasing the number of cells within the cell cycle in H9c2 cultured cells. SOX4 was only increased in the hypoxia anti-miRNA treatment groups, which is likely due to hypoxia-inducible factors (*HIF1A* and *HIF3A*) being amongst the predicted targets for miR-558 and miR-1538. SOX4 most likely has a hypoxia response element within its promotor region, resulting in an up-regulation in gene expression only in the hypoxia anti-miRNA treatment groups (Yeh et al., 2013). One limitation of this cell culture approach is that the anti-miRNA treatments were tested in an immortal cardiomyoblast cell line, which already has a high rate of proliferation. Through this study, we identified unique miRNAs in sheep and were able to successfully inhibit these miRNAs in rat cardiomyoblasts, thereby demonstrating the potential translational capacity of miRNAs as a treatment between species. Further studies inhibiting these miRNAs *in vivo* will determine if this treatment has the capacity to improve the cardiovascular outcomes and reduce scar tissue formation after myocardial infarction, and may prove to be a powerful clinical intervention for transient changes in gene expression helping prevent the onset of chronic heart disease.

CONCLUSION

Through investigating cardiac regeneration in fetal sheep, we have identified potential miRNA therapeutics for cardiovascular disease. Though the translational capacity and high throughput benefits of small animal experiments is clear, further investigation of therapeutics using large animal models, such as sheep and pigs, will help bridge the physiological gap, and allows for identification of additional unique targets for investigation. Delivery of miRNAs specifically to the heart remains a significant challenge for translation to clinical use, some studies have demonstrated success with intravenous delivery; however, to avoid potential off-target effects, intracardiac delivery is the current preferred *in vivo* delivery method. Although it was not possible to assess subtle sex specific effects within this study, our data suggests no effect of sex. This is apparent in the PCA plot where the fetal Remote samples were virtually super-imposable and contained two male and one female sample. In addition, our previous studies using this model demonstrated no significant difference between sex for sham or remote samples using gene array (Lock et al., 2020). However, we recognize that evaluating the response to infarction in both sexes is clinically important and will be assessed in future studies. A powerful tool in the study was the inclusion of the salvageable border zone tissue. This tissue is the first site in which cardiomyocyte proliferation begins in mammals capable of regeneration (Herdrich et al., 2010; Porrello et al., 2011; Zgheib et al., 2014), and thus important changes within this region may be missed in studies measuring expression on only the infarct and healthy tissue regions. Predicted mRNA targets of deregulated miRNAs were most significantly enriched for *FoxO, Wnt,* and *Cardiac Fibrosis* signaling after infarction in the sheep heart. miRNAs and their targets are often conserved between species, hence targeting these pathways through modulation of identified uniquely deregulated miRNAs may improve repair of the adult human heart. miR-558 and miR-1538 were oppositely regulated in the fetal and adolescent hearts in response to MI. When inhibited in H9c2 cells these miRNAs were both effective targets for increasing cell proliferation and target gene expression and therefore represent strong prospective therapeutics to improve cardiac outcomes post-MI. The next step is to interrogate the efficacy of these two miRNAs using the same MI sheep model. These miRNAs may also be useful targets for cardiovascular diseases outside of MI where an increase in cardiomyocyte proliferation would be beneficial. One such example is fetuses with intrauterine growth restriction (IUGR) that have a lower cardiomyocyte endowment than normally grown fetuses (Botting et al., 2014). The lower number of cardiomyocytes in IUGR infants leads to pathological hypertrophy and an increased risk of cardiovascular disease in later life (Wang et al., 2011; Lock et al., 2017). Modulating the expression of these miRNAs in damaged hearts allows for a short-term change in gene expression and may aid in prevention of the lasting development of chronic heart disease.

DATA AVAILABILITY STATEMENT

The microarray data in this study has been deposited into Figshare (https://figshare.com/s/27972b2c60aeb4cac853).

ETHICS STATEMENT

The animal study was reviewed and approved by the South Australian Health and Medical Research Institute (SAHMRI) Animal Ethics Committee.

AUTHOR CONTRIBUTIONS

ML, DB, and JM were responsible for the conception and design of the experiments. ML, JYS, JD, MS, JBS, and JM were involved in experimentation and sample and data acquisition. ML and

JM drafted the manuscript. All authors were involved in analysis, interpretation of the data, and contributed to the final version.

FUNDING

The animal component of the project was funded by a Research Themes Investment Scheme grant from the University of South Australia. JM was funded by National Health and Medical Research Council Career Development Fellowship (APP1066916) and Australian Research Council Future Fellowship (FT170100431, Level 3). ML, JD, and JYS were funded by an Australian Government Research Training Program scholarship.

ACKNOWLEDGMENTS

We thank Stacey Holman and Erin McGillick for assisting with performing surgical procedures and post-surgical care of ewes and their fetuses. We acknowledge advice on experimental design and critical comment of the manuscript by Dr. Enzo Porrello at Murdoch Children's Research Institute.

SUPPLEMENTARY MATERIAL

The Supplementary Material for this article can be found online at: https://www.frontiersin.org/articles/10.3389/fphys.2020.00614/full#supplementary-material

REFERENCES

AIHW (2015). *Cardiovascular Disease, Diabetes and Chronic Kidney Disease—Australian Facts: Risk Factors. Cardiovascular, Diabetes and Chronic Kidney Disease Series no. 4*. Canberra, ACT: Australian Institute of Health and Welfare.

Ali, Z. A. (2013). The next regeneration: identifying cardiac regeneration-inducing microRNAs using functional screening. *Circ. Cardiovasc. Genet.* 6, 135–136.

Barnett, P., and van den Hoff, M. J. (2011). Cardiac regeneration: different cells same goal. *Med. Biol. Eng. Comput.* 49, 723–732.

Benjamin, E. J., Blaha, M. J., Chiuve, S. E., Cushman, M., Das, S. R., Deo, R., et al. (2017). Heart disease and stroke statistics-2017 update: a report from the american heart association. *Circulation* 135, e146–e603.

Bergmann, O., Bhardwaj, R. D., Bernard, S., Zdunek, S., Barnabé-Heider, F., Walsh, S., et al. (2009). Evidence for cardiomyocyte renewal in humans. *Science* 324, 98–102.

Bernardo, B. C., Gao, X. M., Winbanks, C. E., Boey, E. J., Tham, Y. K., Kiriazis, H., et al. (2012). Therapeutic inhibition of the miR-34 family attenuates pathological cardiac remodeling and improves heart function. *Proc. Natl. Acad. Sci. U.S.A.* 109, 17615–17620.

Bolstad, B. M. (2004). *Low Level Analysis of High density Oligonucleotide Array Data: Background, Normalization and Summarization*. Oakland, CA: University of California.

Boon, R. A., Iekushi, K., Lechner, S., Seeger, T., Fischer, A., Heydt, S., et al. (2013). MicroRNA-34a regulates cardiac ageing and function. *Nature* 495, 107–110.

Borodzicz, S., Czarzasta, K., Kuch, M., and Cudnoch-Jedrzejewska, A. (2015). Sphingolipids in cardiovascular diseases and metabolic disorders. *Lipids Health Dis.* 14:55.

Botting, K. J., Mcmillen, I. C., Forbes, H., Nyengaard, J. R., and Morrison, J. L. (2014). Chronic hypoxemia in late gestation decreases cardiomyocyte number but does not change expression of hypoxia-responsive genes. *J. Am. Heart Assoc.* 3:e000531.

Botting, K. J., Wang, K. C., Padhee, M., Mcmillen, I. C., Summers-Pearce, B., Rattanatray, L., et al. (2012). Early origins of heart disease: low birth weight and determinants of cardiomyocyte endowment. *Clin. Exp. Pharmacol. Physiol.* 39, 814–823.

Bustin, S. A., Benes, V., Garson, J. A., Hellemans, J., Huggett, J., Kubista, M., et al. (2009). The MIQE guidelines: minimum information for publication of quantitative real-time PCR experiments. *Clin. Chem.* 55, 611–622.

Casella, G., and Berger, R. L. (2001). *Statistical Inference*, 2nd Edn. Pacific Grove, CA: Duxbury Press.

Chen, J., Huang, Z. P., Seok, H. Y., Ding, J., Kataoka, M., Zhang, Z., et al. (2013). mir-17-92 cluster is required for and sufficient to induce cardiomyocyte proliferation in postnatal and adult hearts. *Circ. Res.* 112, 1557–1566.

Dalal, H. M., Doherty, P., and Taylor, R. S. (2015). Cardiac rehabilitation. *BMJ* 351:h5000.

Danielson, L., Mcmillen, I. C., Dyer, J. L., and Morrison, J. L. (2005). Restriction of placental growth results in greater hypotensive response to alpha-adrenergic blockade in fetal sheep during late gestation. *J. Physiol.* 563, 611–620.

Doumatey, A. P., He, W. J., Gaye, A., Lei, L., Zhou, J., Gibbons, G. H., et al. (2018). Circulating MiR-374a-5p is a potential modulator of the inflammatory process in obesity. *Sci. Rep.* 8:680.

Duan, A. Q., Lock, M. C., Perumal, S. R., Darby, J. R., Soo, J. Y., Selvanayagam, J. B., et al. (2017). Feasibility of detecting myocardial infarction in the sheep fetus using late gadolinium enhancement CMR imaging. *J. Cardiovasc. Magn. Reson.* 19:69.

Eisen, M. B., Spellman, P. T., Brown, P. O., and Botstein, D. (1998). Cluster analysis and display of genome-wide expression patterns. *Proc. Natl. Acad. Sci. U.S.A.* 95:14863.

Eulalio, A., Mano, M., Dal Ferro, M., Zentilin, L., Sinagra, G., Zacchigna, S., et al. (2012). Functional screening identifies miRNAs inducing cardiac regeneration. *Nature* 492, 376–381.

Greco, S., Fasanaro, P., Castelvecchio, S., D'alessandra, Y., Arcelli, D., Di Donato, M., et al. (2012). MicroRNA dysregulation in diabetic ischemic heart failure patients. *Diabetes* 61, 1633–1641.

Grundy, D. (2015). Principles and standards for reporting animal experiments in the journal of physiology and experimental physiology. *J. Physiol.* 593, 2547–2549.

Hellemans, J., Mortier, G., De Paepe, A., Speleman, F., and Vandesompele, J. (2007). qBase relative quantification framework and software for management and automated analysis of real-time quantitative PCR data. *Genome Biol.* 8:R19.

Herdrich, B. J., Danzer, E., Davey, M. G., Allukian, M., Englefield, V., Gorman, J. H. III, et al. (2010). Regenerative healing following foetal myocardial infarction. *Eur. J. Cardiothorac. Surg.* 38, 691–698.

Hewitt, S. M., Baskin, D. G., Frevert, C. W., Stahl, W. L., and Rosa-Molinar, E. (2014). Controls for immunohistochemistry: the histochemical society's standards of practice for validation of immunohistochemical assays. *J. Histochem. Cytochem.* 62, 693–697.

Higashi, K., Yamada, Y., Minatoguchi, S., Baba, S., Iwasa, M., Kanamori, H., et al. (2015). MicroRNA-145 repairs infarcted myocardium by accelerating cardiomyocyte autophagy. *Am. J. Physiol. Heart Circ. Physiol.* 309, H1813–H1826.

Hullinger, T. G., Montgomery, R. L., Seto, A. G., Dickinson, B. A., Semus, H. M., Lynch, J. M., et al. (2012). Inhibition of miR-15 protects against cardiac ischemic injury. *Circ. Res.* 110, 71–81.

Jin, Z. Q., Zhou, H. Z., Zhu, P., Honbo, N., Mochly-Rosen, D., Messing, R. O., et al. (2002). Cardioprotection mediated by sphingosine-1-phosphate and ganglioside GM-1 in wild-type and PKC epsilon knockout mouse hearts. *Am. J. Physiol. Heart Circ. Physiol.* 282, H1970–H1977.

Jopling, C., Sleep, E., Raya, M., Marti, M., Raya, A., and Izpisua Belmonte, J. C. (2010). Zebrafish heart regeneration occurs by cardiomyocyte dedifferentiation and proliferation. *Nature* 464, 606–609.

Joshi, S. R., Dhagia, V., Gairhe, S., Edwards, J. G., Mcmurtry, I. F., and Gupte, S. A. (2016). MicroRNA-140 is elevated and mitofusin-1 is downregulated in the right ventricle of the Sugen5416/hypoxia/normoxia model of pulmonary arterial hypertension. *Am. J. Physiol. Heart Circ. Physiol.* 311, H689–H698.

Karliner, J. S. (2013). Sphingosine kinase and sphingosine 1-phosphate in the heart: a decade of progress. *Biochim. Biophys. Acta* 1831, 203–212.

Kilkenny, C., Browne, W. J., Cuthill, I. C., Emerson, M., and Altman, D. G. (2010). Improving bioscience research reporting: the ARRIVE guidelines for reporting animal research. *PLoS Biol.* 8:e1000412. doi: 10.1371/journal.pbio.1000412

Knapp, M., Zendzian-Piotrowska, M., Blachnio-Zabielska, A., Zabielski, P., Kurek, K., and Gorski, J. (2012a). Myocardial infarction differentially alters sphingolipid levels in plasma, erythrocytes and platelets of the rat. *Basic Res. Cardiol.* 107:294.

Knapp, M., Zendzian-Piotrowska, M., Kurek, K., and Blachnio-Zabielska, A. (2012b). Myocardial infarction changes sphingolipid metabolism in the uninfarcted ventricular wall of the rat. *Lipids* 47, 847–853.

Lee, J. S., Song, D. W., Park, J. H., Kim, J. O., Cho, C., and Kim, D. H. (2017). miR-374 promotes myocardial hypertrophy by negatively regulating vascular endothelial growth factor receptor-1 signaling. *BMB Rep.* 50, 208–213.

Li, H., Ouyang, R., Wang, Z., Zhou, W., Chen, H., Jiang, Y., et al. (2016). MiR-150 promotes cellular metastasis in non-small cell lung cancer by targeting FOXO4. *Sci. Rep.* 6:39001.

Li, J., Li, Y., Jiao, J., Wang, J., Li, Y., Qin, D., et al. (2014). Mitofusin 1 is negatively regulated by microRNA 140 in cardiomyocyte apoptosis. *Mol. Cell. Biol.* 34, 1788–1799.

Li, Y., Ren, W., Wang, X., Yu, X., Cui, L., Li, X., et al. (2019). MicroRNA-150 relieves vascular remodeling and fibrosis in hypoxia-induced pulmonary hypertension. *Biomed Pharmacother.* 109, 1740–1749.

Lin, R. C., Weeks, K. L., Gao, X. M., Williams, R. B., Bernardo, B. C., Kiriazis, H., et al. (2010). PI3K(p110 alpha) protects against myocardial infarction-induced heart failure: identification of PI3K-regulated miRNA and mRNA. *Arterioscler Thromb. Vasc. Biol.* 30, 724–732.

Liu, N., Bezprozvannaya, S., Williams, A. H., Qi, X., Richardson, J. A., Bassel-Duby, R., et al. (2008). microRNA-133a regulates cardiomyocyte proliferation and suppresses smooth muscle gene expression in the heart. *Genes Dev.* 22, 3242–3254.

Lock, M. C., Botting, K. J., Tellam, R. L., Brooks, D., and Morrison, J. L. (2017). Adverse intrauterine environment and cardiac miRNA expression. *Int. J. Mol. Sci.* 18:2628.

Lock, M. C., Darby, J. R. T., Soo, J. Y., Brooks, D. A., Perumal, S. R., Selvanayagam, J. B., et al. (2019). Differential response to injury in fetal and adolescent sheep hearts in the immediate post-myocardial infarction period. *Front. Physiol.* 10:208. doi: 10.3389/fphys.2019.00208

Lock, M. C., Mcgillick, E. V., Orgeig, S., Zhang, S., Mcmillen, I. C., and Morrison, J. L. (2015). Mature surfactant protein-B expression by immunohistochemistry as a marker for surfactant system development in the fetal sheep lung. *J. Histochem. Cytochem.* 63, 866–878.

Lock, M. C., Tellam, R. L., Botting, K. J., Wang, K. C. W., Selvanayagam, J. B., Brooks, D. A., et al. (2018). The role of miRNA regulation in fetal cardiomyocytes, cardiac maturation and the risk of heart disease in adults. *J. Physiol.* 596, 5625–5640.

Lock, M. C., Tellam, R. L., Darby, J. R. T., Soo, J. Y., Brooks, D. A., Macgowan, C. K., et al. (2020). Differential gene responses 3 days following infarction in the fetal and adolescent sheep heart. *Physiol. Genomics* 52, 143–159.

McGillick, E. V., Orgeig, S., Mcmillen, I. C., and Morrison, J. L. (2013). The fetal sheep lung does not respond to cortisol infusion during the late canalicular phase of development. *Physiol. Rep.* 1, 1–15.

Mills, R. J., Titmarsh, D. M., Koenig, X., Parker, B. L., Ryall, J. G., Quaife-Ryan, G. A., et al. (2017). Functional screening in human cardiac organoids reveals a metabolic mechanism for cardiomyocyte cell cycle arrest. *Proc. Natl. Acad. Sci. U.S.A.* 114, E8372–E8381.

Morrison, J. L., Berry, M. J., Botting, K. J., Darby, J. R. T., Frasch, M. G., Gatford, K. L., et al. (2018). Improving pregnancy outcomes in humans through studies in sheep. *Am. J. Physiol. Regul. Integr. Comp. Physiol* 315, R1123–R1153.

Morrison, J. L., Zhang, S., Tellam, R. L., Brooks, D. A., Mcmillen, I. C., Porrello, E. R., et al. (2015). Regulation of microRNA during cardiomyocyte maturation in sheep. *BMC Genomics* 16:541. doi: 10.1186/s12864-015-1693-z

Okada, S., Yokoyama, M., Toko, H., Tateno, K., Moriya, J., Shimizu, I., et al. (2012). Brain-derived neurotrophic factor protects against cardiac dysfunction after myocardial infarction via a central nervous system-mediated pathway. *Arterioscler Thromb. Vasc. Biol.* 32, 1902–1909.

Passmore, M., Nataatmadja, M., and Fraser, J. (2009). Selection of reference genes for normalisation of real-time RT-PCR in brain-stem death injury in Ovis aries. *BMC Mol. Biol.* 10:72. doi: 10.1186/1471-2199-10-72

Pauschinger, M., Doerner, A., Remppis, A., Tannhauser, R., Kuhl, U., and Schultheiss, H. P. (1998). Differential myocardial abundance of collagen type I and type III mRNA in dilated cardiomyopathy: effects of myocardial inflammation. *Cardiovasc. Res.* 37, 123–129.

Pinzon, N., Li, B., Martinez, L., Sergeeva, A., Presumey, J., Apparailly, F., et al. (2017). microRNA target prediction programs predict many false positives. *Genome Res.* 27, 234–245.

Porrello, E. R., Mahmoud, A. I., Simpson, E., Hill, J. A., Richardson, J. A., Olson, E. N., et al. (2011). Transient regenerative potential of the neonatal mouse heart. *Science* 331, 1078–1080.

Porrello, E. R., Mahmoud, A. I., Simpson, E., Johnson, B. A., Grinsfelder, D., Canseco, D., et al. (2012). Regulation of neonatal and adult mammalian heart regeneration by the miR-15 family. *Proc. Natl. Acad. Sci. U.S.A.* 110, 187–192.

Quaife-Ryan, G. A., Sim, C. B., Ziemann, M., Kaspi, A., Rafehi, H., Ramialison, M., et al. (2017). Multicellular transcriptional analysis of mammalian heart regeneration. *Circulation* 136, 1123–1139.

Ronnebaum, S. M., and Patterson, C. (2010). The FoxO family in cardiac function and dysfunction. *Annu. Rev. Physiol.* 72, 81–94.

Sattler, S., and Rosenthal, N. (2016). The neonate versus adult mammalian immune system in cardiac repair and regeneration. *Biochim. Biophys. Acta* 1863, 1813–1821.

Sengupta, A., Kalinichenko, V. V., and Yutzey, K. E. (2013). FoxO1 and FoxM1 transcription factors have antagonistic functions in neonatal cardiomyocyte cell-cycle withdrawal and IGF1 gene regulation. *Circ. Res.* 112, 267–277.

Soo, P. S., Hiscock, J., Botting, K. J., Roberts, C. T., Davey, A. K., and Morrison, J. L. (2012). Maternal undernutrition reduces P-glycoprotein in guinea pig placenta and developing brain in late gestation. *Reprod. Toxicol.* 33, 374–381.

Sun, W., Zhang, Z., Wang, J., Shang, R., Zhou, L., Wang, X., et al. (2016). MicroRNA-150 suppresses cell proliferation and metastasis in hepatocellular carcinoma by inhibiting the GAB1-ERK axis. *Oncotarget* 7, 11595–11608.

Thum, T., Galuppo, P., Wolf, C., Fiedler, J., Kneitz, S., Van Laake, L. W., et al. (2007). MicroRNAs in the human heart: a clue to fetal gene reprogramming in heart failure. *Circulation* 116, 258–267.

Vandesompele, J., De Preter, K., Pattyn, F., Poppe, B., Van Roy, N., De Paepe, A., et al. (2002). Accurate normalization of real-time quantitative RT-PCR data by geometric averaging of multiple internal control genes. *Genome Biol.* 3:RESEARCH0034.

Wang, F., Ren, X., and Zhang, X. (2015). Role of microRNA-150 in solid tumors. *Oncol. Lett.* 10, 11–16.

Wang, J., and Martin, J. F. (2014). Macro advances in microRNAs and myocardial regeneration. *Curr. Opin. Cardiol.* 29, 207–213.

Wang, K. C., Zhang, L., Mcmillen, I. C., Botting, K. J., Duffield, J. A., Zhang, S., et al. (2011). Fetal growth restriction and the programming of heart growth and cardiac insulin-like growth factor 2 expression in the lamb. *J. Physiol.* 589, 4709–4722.

Wang, Y. S., Li, S. H., Guo, J., Mihic, A., Wu, J., Sun, L., et al. (2014). Role of miR-145 in cardiac myofibroblast differentiation. *J. Mol. Cell. Cardiol.* 66, 94–105.

Wilkins, E., Wilson, L., Wickramasinghe, K., Bhatnagar, P., Leal, J., Luengo-Fernandez, R., et al. (2017). *European Cardiovascular Disease Statistics 2017*. Brussels: European Heart Network.

Wong, C. X., Brooks, A. G., Leong, D. P., Roberts-Thomson, K. C., and Sanders, P. (2012). The increasing burden of atrial fibrillation compared with heart failure and myocardial infarction: a 15-year study of all hospitalizations in australia. *Arch. Int. Med.* 172, 739–741.

Yang, Y., Cheng, H. W., Qiu, Y., Dupee, D., Noonan, M., Lin, Y. D., et al. (2015). MicroRNA-34a plays a key role in cardiac repair and regeneration following myocardial infarction. *Circ. Res.* 117, 450–459.

Yao, L., Zhou, Q., Wang, L., and Hou, G. (2017). MicroRNA-182-5p protects H9c2 cardiomyocytes from hypoxia-induced apoptosis by down-regulation of PTEN. *Int. J. Clin. Exp. Pathol.* 10, 5220–5226.

Yeh, Y. M., Chuang, C. M., Chao, K. C., and Wang, L. H. (2013). MicroRNA-138 suppresses ovarian cancer cell invasion and metastasis by targeting SOX4 and HIF-1alpha. *Int. J. Cancer* 133, 867–878.

Yin, V. P., Lepilina, A., Smith, A., and Poss, K. D. (2012). Regulation of zebrafish heart regeneration by miR-133. *Dev. Biol.* 365, 319–327.

Zgheib, C., Allukian, M. W., Xu, J., Morris, M. W. Jr., Caskey, R. C., Herdrich, B. J., et al. (2014). Mammalian fetal cardiac regeneration after myocardial infarction is associated with differential gene expression compared with the adult. *Ann. Thorac. Surg.* 97, 1643–1650.

Zheng, L., Lin, S., and Lv, C. (2018). MiR-26a-5p regulates cardiac fibroblasts collagen expression by targeting ULK1. *Sci. Rep*. 8:2104.

Zhou, B., Wang, S., Mayr, C., Bartel, D. P., and Lodish, H. F. (2007). miR-150, a microRNA expressed in mature B and T cells, blocks early B cell development when expressed prematurely. *Proc. Natl. Acad. Sci. U.S.A.* 104, 7080–7085.

Conflict of Interest: The authors declare that the research was conducted in the absence of any commercial or financial relationships that could be construed as a potential conflict of interest.

Copyright © 2020 Lock, Tellam, Darby, Soo, Brooks, Seed, Selvanayagam and Morrison. This is an open-access article distributed under the terms of the Creative Commons Attribution License (CC BY). The use, distribution or reproduction in other forums is permitted, provided the original author(s) and the copyright owner(s) are credited and that the original publication in this journal is cited, in accordance with accepted academic practice. No use, distribution or reproduction is permitted which does not comply with these terms.

frontiers in Physiology

ORIGINAL RESEARCH
published: 23 June 2020
doi: 10.3389/fphys.2020.00601

Interleukin 1 Receptor 1 Knockout and Maternal High Fat Diet Exposure Induces Sex-Specific Effects on Adipose Tissue Adipogenic and Inflammatory Gene Expression in Adult Mouse Offspring

*Pania E. Bridge-Comer[1], Jasmine F. Plows[1,2], Farha Ramzan[1], Rachna Patel[1], Thashma P. Ganapathy[1], Joanna L. Stanley[1], Mark H. Vickers[1] and Clare M. Reynolds[1,3,4]**

[1]Developmental Programming Research Group, The Liggins Institute, The University of Auckland, Auckland, New Zealand, [2]Saban Research Institute, Children's Hospital Los Angeles, Los Angeles, CA, United States, [3]UCD School of Public Health, Physiotherapy and Sports Science, University College Dublin, Dublin, Ireland, [4]Conway Institute/Institute of Food and Health, University College Dublin, Dublin, Ireland

OPEN ACCESS

Edited by:
Gina Galli,
The University of Manchester,
United Kingdom

Reviewed by:
Jonatan Dereke,
Lund University, Sweden
Emily Camm,
University of Cambridge,
United Kingdom

***Correspondence:**
Clare M. Reynolds
c.reynolds@auckland.ac.nz

Specialty section:
This article was submitted to Embryonic and Developmental Physiology, a section of the journal Frontiers in Physiology

Received: 25 March 2020
Accepted: 14 May 2020
Published: 23 June 2020

Citation:
Bridge-Comer PE, Plows JF, Ramzan F, Patel R, Ganapathy TP, Stanley JL, Vickers MH and Reynolds CM (2020) Interleukin 1 Receptor 1 Knockout and Maternal High Fat Diet Exposure Induces Sex-Specific Effects on Adipose Tissue Adipogenic and Inflammatory Gene Expression in Adult Mouse Offspring. Front. Physiol. 11:601. doi: 10.3389/fphys.2020.00601

Background: The global incidence of obesity continues to rise, increasing the prevalence of metabolic diseases such as insulin resistance, dyslipidemia, and type 2 diabetes mellitus. Low-grade chronic inflammation, associated with the obese state, also contributes to the development of these metabolic comorbidities. Interleukin-1-receptor-1 (IL-1R1), a pro-inflammatory mediator, bridges the metabolic and inflammatory systems. In young male mice, deficiency of IL-1R1 (IL-1R1$^{-/-}$) paired with a high-fat diet (HFD) offered beneficial metabolic effects, however in female mice, the same pairing led to metabolic dysfunction. Therefore, we examined the contribution of maternal HFD in combination with IL1R1$^{-/-}$ to metabolic health in adult offspring.

Methods: Female C57BL/6 and IL-1R1$^{-/-}$ mice were randomly assigned to a control diet (10% kcal from fat) or HFD (45% kcal from fat) 10 days prior to mating and throughout gestation and lactation. Male and female offspring were housed in same-sex pairs post-weaning and maintained on control diets until 16 weeks old. At 15 weeks, an oral glucose tolerance test (OGTT) was performed to assess glucose tolerance. Histological analysis was carried out to assess adipocyte size and gene expression of adipogenic and inflammatory markers were examined.

Results: IL-1R1$^{-/-}$ contributed to increased body weight in male and female adult offspring, irrespective of maternal diet. IL-1R1$^{-/-}$ and maternal HFD increased adipocyte size in the gonadal fat depot of female, but not male offspring. In female offspring, there was reduced expression of genes involved in adipogenesis and lipid metabolism in response to IL1R1$^{-/-}$ and maternal HFD. While there was an increase in inflammatory gene expression in response to maternal HFD, this appeared to be reversed in IL1R1$^{-/-}$ female offspring.

In male offspring, there was no significant impact on adipogenic or lipid metabolism pathways. There was an increase in inflammatory gene expression in IL1R1$^{-/-}$ male offspring from HFD-fed mothers.

Conclusion: This study suggests that IL-1R1 plays a complex and important role in the metabolic health of offspring, impacting adipogenesis, lipogenesis, and inflammation in a sex-specific manner.

Keywords: developmental programming, adipose tissue, inflammation, IL-1R1, high fat diet, maternal diet

INTRODUCTION

Obesity is quickly becoming the most common chronic health condition globally and is instrumental in the development of co-morbidities such as dyslipidemia, insulin resistance (IR), and type 2 diabetes (Blüher, 2019). Low-grade chronic inflammation is strongly associated with obesity and is thought to be one of the major contributory factors in progression to overt metabolic disease (Saltiel and Olefsky, 2017). There is now clear evidence that exposure to maternal dietary, emotional, and environmental stressors during gestation can predispose offspring to obesity and metabolic dysfunction in later life (Reynolds et al., 2017; McGowan and Matthews, 2018). However, there is limited knowledge around the impact of metabolic inflammation during pregnancy and its effects on the next generation (Segovia et al., 2017).

There has been a robust effort over recent years to understand the molecular mediators involved in metabolic inflammation. Interleukin (IL)-1β has been continuously implicated as a major driving force in the pathogenesis of metabolic disease (Jager et al., 2007; Koenen et al., 2011). Previous studies have demonstrated that deletion of IL-1R1 signaling prevents the onset of IR in a mouse model of diet-induced obesity (McGillicuddy et al., 2011; Finucane et al., 2015). It is notable that this protection is reserved exclusively to younger male mice with detrimental metabolic effects of IL-1R1 depletion observed in older male mice (García et al., 2006; McGillicuddy et al., 2013).

IL-1 signaling during pregnancy has been associated with deleterious effects including increased activation and expression observed in woman with gestational diabetes mellitus [GDM; Katra et al. (2016)] and pre-eclampsia (Siljee et al., 2013). While IL-1 signaling has a functional role during normal pregnancy, particularly in the induction of labor, increased concentrations as a result of infection or obesity-induced meta-inflammation can alter the hormonal balance which is required for maintenance of normal pregnancy (Allport et al., 2001; Terzidou et al., 2006). Additionally, several groups have identified an association between single nucleotide polymorphisms in genes related to IL-1 signaling and increased risk for pregnancy complications (Li et al., 2014; Nair et al., 2014). However, a recent study by our group has identified that IL-1 signaling may be important for maintaining metabolic health in female mice, with depletion resulting in increased adipocyte size and metabolic dysregulation pre, during, and post pregnancy (Plows et al., 2019). A fine balance exists between the inflammatory milieu and metabolic health and is likely altered in response to factors such as age and sex.

Early life-exposure to inflammatory agents such as bacterial lipotoxin results in programming of immune function (Mandal et al., 2013). However, the effect of maternal "meta-inflammation" resulting from obesity and high fat (HF) consumption has not been comprehensively examined within the developmental programming of obesity and metabolic disease paradigm. This study therefore examined the effect of a maternal HF diet during pregnancy and the potential contribution of IL-1 signaling to metabolic programming in adult offspring with a focus on adipose tissue effects.

MATERIALS AND METHODS

Animal Procedures

All animal procedures were approved by the AgResearch Animal Ethics Committee in accordance with the New Zealand Animal Welfare Act, 1999. IL1R1$^{-/-}$ (B6.129S7-IL1R1tm1lmx/J) and C57BL/6J breeding pairs were imported from the Jackson Laboratory, USA, and housed in a animal containment facility at AgResearch, Ruakura, Waikato, New Zealand (22°C, lights on at 06:00 h, off at 18:00 h, humidity at 40–45%, and woodchip bedding). Third-generation female pups were given free access to standard laboratory chow until 10 weeks of age, at which time they were randomly assigned to receive either purified control diet (CD; Research Diets Inc., New Brunswick, USA; #D12450H, 20% kcal from protein, 70% kcal carbohydrate, and 10% kcal fat) or matched (for protein and micronutrient content) HF diet (HFD, Research Diets Inc.; #D12451, 20% kcal from protein, 35% kcal carbohydrate, and 45% kcal fat). This generated four groups (n = 8/group) in a balanced experimental design: (1) C57CD (C57BL/6J fed a CD), (2) C57HF (C57BL/6J fed a HFD), (3) IL1CD (IL1R1$^{-/-}$ fed a CD), and (4) IL1HF (IL1R1$^{-/-}$ fed a HFD). Mice began diets 10 days before mating and throughout pregnancy and lactation. At postnatal day 2 (PD2), litters were weighed and sexed using anogenital distance and were reduced to three males and three females to ensure standardized nutrition until weaning. Weaning occurred at PD21 (n = 6–8 litters/group). Offspring were housed in same-sex sibling groups and weighed weekly from week 3 to week 16. An oral glucose tolerance test (OGTT) was carried out 1 week prior to cull.

Oral Glucose Tolerance Test (OGTT)

Offspring were fasted for 6 h and then weighed. The tip of the tail (<1 mm) was cut and the resulting blood was read

by glucometer (Optimum Freestyle Neo, Abbott Laboratories, Alameda, CA, USA). Two grams per kilogram of D-glucose (Sigma-Aldrich, NZ) was orally gavaged, and blood glucose concentrations were measured at 0, 15, 30, 60, 90, and 120 min.

Tissue Collection

Mice were fasted for 6 h and culled by cervical dislocation. A cardiac puncture was performed immediately following death and blood was collected in an EDTA coated tube and centrifuged at 2,000 rpm for 10 min at 4°C. Resulting plasma was stored at −20°C. Organs were dissected, weighed, and snap-frozen in liquid nitrogen and then stored at −80°C or fixed in neutral-buffered formalin for histological analysis.

Plasma Analysis

Fasting plasma insulin, leptin, and testosterone concentrations were analyzed using commercial mouse-specific ELISAs (UltraSensitive Mouse Insulin ELISA #90080; Mouse Leptin ELISA #90030; Mouse Testosterone ELISA 80552; Crystal Chem., Chicago, IL, USA), according to manufacturers' instructions.

Histological Analysis

Gonadal adipose tissue samples were fixed in 10% NBF and were paraffin embedded and sectioned (10 μm) using a Leica RM 2135 rotary microtome (Leica Instruments, Nussloch, Germany). Hematoxylin and eosin (H&E) staining was performed, and sections were mounted using DPX mountant. Slides were visualized under a light microscope, and images captured with NIS Elements-D software (Nikon 800, Tokyo, Japan). Four representative images were taken from each section by an individual blinded to the study groups. A minimum of 100 adipocytes per animal were analyzed. Any cells that were not fully visible were not included in the analysis. Cells that were 150 μm or under were excluded to ensure that stromal vascular cells were not analyzed. Images were analyzed using ImageJ to determine average adipocyte size and adipocyte size distribution per sample.

Gene Expression Analysis

RNA was extracted from gonadal adipose tissue using TRI Reagent and stored at −80°C. Single-stranded cDNA was prepared using RT^2 First Strand Kit (SABioscience; Qiagen, Hilden, Germany). The expression of 84 genes relevant to IR was analyzed using the Mouse Insulin Resistance RT^2 Profiler PCR Array (SABioscience). mRNA expression was quantified by real-time PCR (RT-PCR) on a LightCycler® 480 SYBR Green I Master (Roche Diagnostics, Auckland, New Zealand). To control between-sample variability, mRNA levels were normalized to the geometric mean of a panel of housekeeping genes for each sample by subtracting the Cycle threshold (Ct) of controls from the Ct for the gene of interest producing a ΔCt value. The ΔCt for each treatment sample was compared to the mean ΔCt for control samples using the relative quantification 2-(ΔΔCt) method to determine fold change (Livak and Schmittgen, 2001).

Statistical Analysis

Statistical analysis was performed using SPSS 24 (IBM, Armonk, NY, USA). Repeated measure ANOVA was performed for the OGTT and weight trajectory data. All other data were analyzed by two-way factorial ANOVA, with genotype and maternal diet as factors. Outliers were assessed as any value greater than 1.5 box-lengths from the edge of each group's boxplot, and were subsequently winsorized. The Shapiro–Wilk's test was then performed to assess normality of the data, and Levene's test was used to assess homogeneity of variances. In the event that one or more groups were not normally distributed and/or homogenous, the data were suitably transformed. Bonferroni *post hoc* tests were performed for multiple comparisons testing between groups when ANOVA found a significant effect. Differences between groups were considered significant at $p < 0.05$. Data are presented as mean ± SEM and graphed using Prism 6 software (GraphPad Software Inc., La Jolla, USA).

RESULTS

IL-1R1$^{-/-}$ Increased Glucose Concentrations and Body Weight Irrespective of Maternal Diet in Female and Male Offspring

IL-1R1$^{-/-}$ induced an increase in the body weight of female and male offspring by 16 weeks of age irrespective of maternal diet. This was associated with a significant increase in fasting plasma glucose and gonadal fat mass (**Table 1**). There was a reduction in OGTT area under the curve (AUC) in female IL-1HF offspring compared to C57CD and C57HF groups creating an overall genotype effect (**Figures 1A,B**). In male offspring, there was a significant increase in OGTT AUC in IL-1R1$^{-/-}$ compared to C57BL/6 groups (**Figures 1D,E**). Maternal diet did not have an effect on weight, fasting glucose, OGTT, or fat mass in male and female offspring. However, there was a maternal diet effect on insulin concentrations in both female and male offspring. In females, C57HF had significantly increased insulin compared to all other groups (**Figure 1C**). Testosterone concentrations followed a similar pattern with significantly increased concentrations in C57HF compared to all other groups (**Table 1**). In male offspring, there was a significant increase in insulin concentrations in C57HF compared to C57CD and IL1HF groups and an interaction effect with an increase in IL1CD compared to C57CD and a decrease in IL1HF compared to C57HF (**Figure 1F**). There was a significant increase in IL1CD testosterone concentrations compared to all other groups (**Table 1**). There was no significant effect on leptin concentrations between groups (**Table 1**).

Adipose Tissue Morphology and Adipogenic Gene Expression in Response to Maternal Diet and IL-1R1$^{-/-}$ Genotype

Maternal diet and IL-1R1$^{-/-}$ resulted in increased average adipocyte size in the gonadal fat pad of female offspring. All groups were significantly increased compared to C57CD. Further, there was a reduction in average adipocyte size

between IL1CD and IL1HF groups (**Figures 2A,B**). When adipocyte size was delineated by size distribution, there was a clear shift to the right in the distribution curve in C57HF, IL1CD, and IL1HF groups compared to C57CD, with a reduction in smaller adipocytes and increased numbers of hypertrophic adipocytes (**Figure 2C**).

There was a clear effect of maternal diet on adipocyte size in the gonadal fat pad of male offspring although there was no genotype effect (**Figures 2D,E**). The distribution of adipocyte size showed that C57HF and IL1HF had an increased percentage of adipocytes in the hypertrophic size category (**Figure 2F**).

In line with increased adipocyte size in female offspring, there was a reduction in the gene expression of a number of markers related to adipogenesis. While significance was not reached, there was a trend towards decreased peroxisome profilerator activated receptor gamma (*Pparg*) and resistin (*Retn*) expression in relation to maternal diet and genotype (**Figures 3A,C**). PPAR co-activator 1 alpha (*Ppargc1*) was significantly reduced with maternal diet with expression reduced in all groups compared to C57CD (**Figure 3B**). Insulin-like growth factor (*Igf1*) was increased with maternal diet (**Figure 3D**). There was a significant reduction in hormone sensitive lipase (*Lipe*) in IL-1R1$^{-/-}$ groups irrespective of maternal diet (**Figure 3E**). Stearoyl Co-A desaturase (*Scd1*) expression was significantly increased in C57HF compared to all other groups (**Figure 3F**).

In the male offspring, IL1CD had increased *Pparg* expression compared to other groups creating an interaction effect (**Figure 3A**). *Retn* expression was increased in all groups compared to C57CD (**Figure 3C**). There was no significant difference between groups with *Ppargc1*, *Igf1*, *Lipe*, or *Scd1* (**Figures 3B,D–F**).

IL-1R1$^{-/-}$ Genotype Alters Lipid Metabolism Gene Expression in Gonadal Adipose Tissue of Female but not Male Offspring

In the female offspring, there was a significant reduction in acetyl co-A carboxylase 2 (*Acacb*) gene expression in IL1CD compared to C57CD creating an overall genotype effect (**Figure 4A**). Long chain fatty acid Co-A ligase 1 (*Acsl1*) expression was reduced in IL-1R1$^{-/-}$ groups irrespective of maternal diet (**Figure 4B**). There was a significant increase in the leptin receptor (*Lepr*) expression in IL1CD group creating an overall genotype effect (**Figure 4E**). Oxidized low-density lipoprotein receptor 1 (*Olr1*) was reduced in IL1CD and IL1HF compared to C57CD, creating an overall genotype effect (**Figure 4G**).

There were no significant effects of either maternal diet or genotype on lipid metabolism markers in the male offspring (**Figures 4B,D,F,H**).

Differential Inflammatory Gene Expression Profiles in Female and Male Offspring in Response to Maternal Diet and Genotype

In the female offspring, there was a significant increase in the monocyte chemotactic protein 5 gene (*Ccl12*) and CC chemokine receptor (*Ccr4*) in C57HF compared to all other groups (**Figures 5A,C**). There was a reduction in tumor necrosis factor (*Tnf*) expression in IL-1R1$^{-/-}$ groups irrespective of maternal diet (**Figure 5E**). There was no difference between groups for mammalian target of rapamycin (*mTor*), toll-like receptor 4 (*Tlr4*), and *Tnf* receptor 2 (*Tnfrsf1b*) (**Figures 5G,I,K**).

In the male offspring, there was no difference between groups for *Ccl12*, *Ccr4*, and *Tnf* (**Figures 5B,D,F**). *mTor* and *Tnfrsf1b* expressions were significantly increased in the IL1HF group contributing to an overall maternal diet effect. There was a decrease in IL1CD compared to all other groups creating an interaction effect (**Figure 5H**), however, this only reached significance with *mTor* (**Figures 5H,L**). *Tlr4* was increased in the C57HF group compared to C57CD. This was partially normalized in the IL1HF group contributing to an interaction effect (**Figure 5J**).

DISCUSSION

It is now well-accepted that maternal dietary stressors during pregnancy can have a marked impact on the risk of obesity and cardiometabolic disease in offspring during later life (Reynolds et al., 2017; Chang et al., 2019). Furthermore, the

TABLE 1 | Physiological outcomes in female and male offspring.

	C57CD	IL1CD	C57HF	IL1HF	Diet	Genotype	DxG
Females							
Weight (g)	21.4 ± 0.2	23.4 ± 0.3*	22.2 ± 0.4	23.1 ± 0.4*	NS	0.0004	NS
Glucose (mmol/L)	7.4 ± 0.4	8.1 ± 0.2	7.4 ± 0.3	8.5 ± 0.4	NS	0.009	NS
Leptin (ng/ml)	1.13 ± 0.3	1.2 ± 0.3	1.11 ± 0.2	0.9 ± 0.3	NS	NS	NS
Testosterone (ng/ml)	0.04 ± 0.01	0.05 ± 0.02	0.18 ± 0.04*	0.05 ± 0.01^{+}	0.03	0.057	0.043
GF%BW	1.02 ± 0.07	1.46 ± 0.1*	1.06 ± 0.07$^{\wedge}$	1.23 ± 0.11	NS	0.017	0.059
Males							
Weight (g)	27.8 ± 0.4	31.1 ± 0.7*	28.6 ± 0.4$^{\wedge}$	28.6 ± 0.6$^{\wedge}$	0.004	NS	0.003
Glucose (mmol/l)	7.5 ± 0.2	8.3 ± 0.3	7.5 ± 0.3	9.1 ± 0.4*$^{+}$	NS	<0.001	NS
Leptin (ng/ml)	1.1 ± 0.3	0.8 ± 0.2	0.8 ± 0.2	0.8 ± 0.1	NS	NS	NS
Testosterone (ng/ml)	0.6 ± 0.2	2.9 ± 0.6*	0.7 ± 0.4$^{\wedge}$	1.1 ± 0.4$^{\wedge}$	0.0503	0.005	0.024
GF%BW	1.1 ± 0.1	1.5 ± 0.2	1.3 ± 0.1	1.9 ± 0.2*	0.04	0.0006	NS

$p < 0.05$ with respect to C57CD; $^{+}p < 0.05$ with respect to C57HF; $^{\wedge}p < 0.05$ with respect to IL1CD. GF%BW, gonadal fat expressed as a percentage of body weight; DxIL1, interaction between diet and genotype derived from 2-way ANOVA.

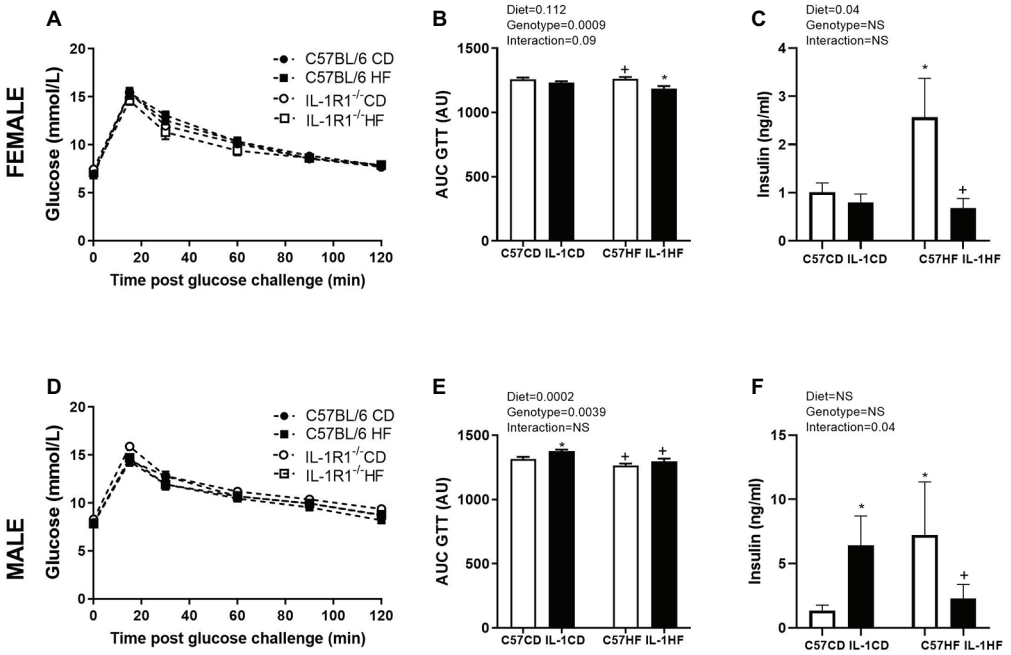

FIGURE 1 | Impact of IL-1R1$^{-/-}$ and maternal high-fat diet (HFD) on offspring glucose tolerance and plasma insulin concentrations. Oral glucose tolerance test (OGTT) (2 g/kg) at 12 weeks in 6 h fasted female **(A)** and male **(D)** offspring. Area under the OGTT curve in female **(B)** and male **(E)** offspring. Insulin concentrations as measured by ELISA in female **(C)** and male offspring **(F)**. Data are expressed as mean ± SEM. N = 6–8 litters/group. $^{*}p < 0.05$ with respect to C57CD. $^{+}p < 0.05$ with respect to C57HF.

critical windows where early life nutrition and environment influence later metabolic health coincide with the development of the immune system. The IL-1 signaling pathway represents a point of intersection between metabolic and inflammatory systems, with previous work demonstrating a protective metabolic effect of IL-1R1 depletion in young male mice exposed to diet-induced obesity (McGillicuddy et al., 2011). However, it is clear that the role of this pathway in metabolic processes is complex, with evidence that older male mice become spontaneously obese and insulin resistant (García et al., 2006; McGillicuddy et al., 2013). A recent study from our group has also highlighted the detrimental effect of IL-1R1 depletion in nulliparous, pregnant, and postpartum female mice (Plows et al., 2019). Here, we demonstrated a reduction in weight gain and decreased kilocalorie consumption over pregnancy in IL-1R1$^{-/-}$ mice where there was no change in glucose tolerance and an increase in adipocyte size resulting in decreased adipose tissue insulin sensitivity. Given the complexity of this pathway in terms of metabolic regulation, we examined its impact in relation to metabolic programming of offspring adiposity and glucose tolerance. There were minimal changes in glucose tolerance, with protective effects of IL-1R1$^{-/-}$ on maternal HFD-induced programming of insulin concentration in both sexes. Both IL-1R1$^{-/-}$ and maternal HFD had a considerable negative impact on adipocyte size as well as lipid metabolism and adipogenic gene expression in female but not male offspring despite beneficial effects of IL-1R1$^{-/-}$ in inflammatory pathways.

In the current study, female offspring on an IL-1R1$^{-/-}$ genetic background remained heavier and had an increased fat mass. Despite this, maternal HFD-induced increases in insulin secretion were prevented with IL-1R1 depletion, accompanied by a moderate improvement in glucose tolerance. Following a similar trend to insulin, IL-1R1 depletion prevented elevation of maternal-HFD induced testosterone concentrations in female offspring. To our knowledge, there are no data examining the impact of IL-1R1 signaling on testosterone production. However, it is possible that elevated testosterone concentrations in the maternal HFD diet fed control animals may contribute to adverse metabolic outcomes such as hyperinsulinemia. Not only is there evidence implicating testosterone in the pathogenesis of insulin resistance in females (Corbould, 2008) but there are also studies which have demonstrated a developmental origin for polycystic ovary syndrome, characterized by increased testosterone and metabolic dysfunction (Franks, 2012).

There was no effect of maternal HFD on glucose tolerance, weight gain, or testosterone concentrations in male offspring. However, there was a programming effect on insulin concentrations. Despite preventing hyperinsulinemia, male offspring with an IL-1R1$^{-/-}$ background had increased, albeit modestly, glucose intolerance. This was accompanied by a significant increase in weight and fat mass. There is evidence that IL-1R1$^{-/-}$ mice become spontaneously obese and glucose intolerant as they age (García et al., 2006; McGillicuddy et al., 2013). These animals were culled at 16 weeks of age, this may represent a time-point at which this transition to a detrimental metabolic phenotype begins. Given the increase in fat mass in the IL1HF group, it is unlikely that IL-1R1 signaling represents a valid target for the effects of maternal HFD diet on developmental programming of obesity.

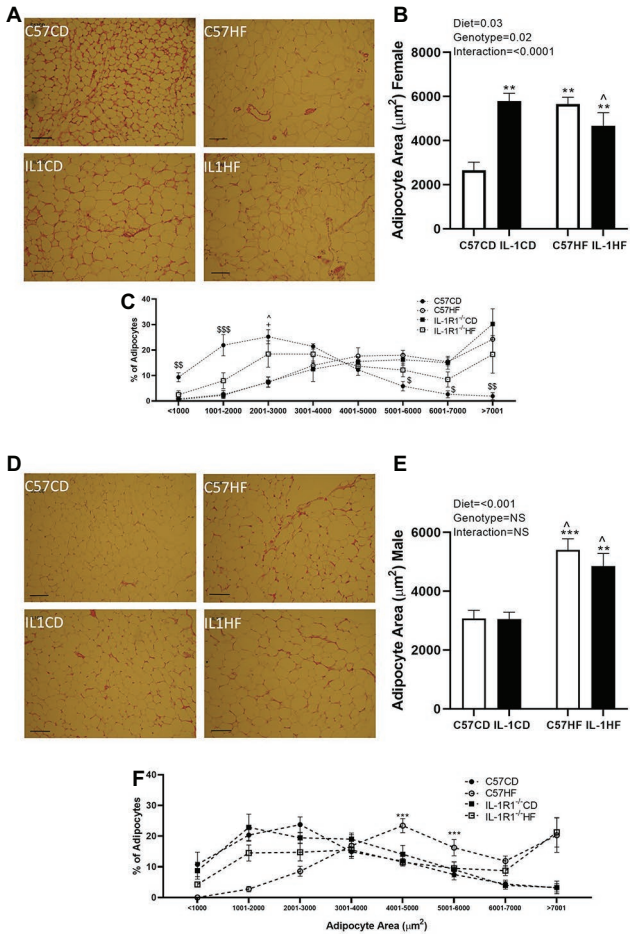

FIGURE 2 | The effect of IL-1R1$^{-/-}$ and maternal HFD on offspring adipocyte size and distribution. Representative gonadal adipose tissue sections stained by hematoxylin and eosin (scale represents 200 μm) in female **(A)** and male **(D)** offspring. Mean adipocyte area analyzed by ImageJ. Four representative images were blindly analyzed per animal in female **(B)** and male **(E)** offspring. Adipocyte area distribution in female **(C)** and male **(F)** offspring. Data are expressed as mean ± SEM. N = 6–8 litters/group. $^{**}p < 0.01$, $^{***}p < 0.001$ with respect to C57CD. $^{+}p < 0.05$ with respect to C57HF. $^{\wedge}p < 0.05$ with respect to IL1CD. $^{\$}p < 0.05$, $^{\$\$}p < 0.01$, $^{\$\$\$}p < 0.01$, C57CD compared to all other groups.

In line with overall increases in weight and fat mass, it is unsurprising to see an overall increase in adipocyte size in response to both maternal HFD and IL-1R1$^{-/-}$ background in female offspring. Maternal HFD preempted an increase in adipocyte size irrespective of genotype in male offspring. There is significant evidence showing that adipose tissue dysfunction is related to the enlargement of adipocytes. The ability of adipocytes to differentiate from preadipocytes has a huge impact on the health and function of the adipose tissue. When these adipogenic processes are disrupted, adipocyte hypertrophy occurs. This reduces the capacity of the adipose tissue to respond to insulin contributing to systemic metabolic dysfunction. There are a number of studies which demonstrate that adipocyte hypertrophy in the absence of obesity can predict later type 2 diabetes (Weyer et al., 2000; Hammarstedt et al., 2012). The converse of this is also true where severely obese individuals with smaller adipocytes remain insulin sensitive (Klöting et al., 2010).

A panel of genes relating to adipogenic processes were examined to determine the relationship between adiposity and metabolic health in response to maternal HFD and IL1R1$^{-/-}$. There was a significant reduction of *Ppargc1*, which encodes PGC-1alpha, a master regulator of mitochondrial biogenesis, in response to both IL-1R1$^{-/-}$ genotype and maternal HFD in female but not male offspring. PGC-1alpha acts as a co-activator for PPARγ and is critical for adipogenesis and the regulation of fatty acid oxidation pathways (Liang and Ward, 2006). Reduction of *Ppargc1* in both morbidly obese patients (Semple et al., 2004) and rodents fed a HFD (Kleiner et al., 2012) is associated with significant metabolic dysregulation. It is therefore likely that reduction in this co-activator prevents adipocyte expansion resulting in hypertrophy, thus limiting the capacity to both store and efficiently process fatty acids. In the current study, we also see a negative correlation between *Ppargc1* and *Igf1* in the female offspring. While IGF1 is a known regulator of growth and differentiation, there is evidence that as adipocytes undergo hypertrophy, there is a reduction in IGF1 resulting in recruitment of macrophages to the adipose tissue, and these immune cells then produce IGF1 to compensate for the reduction in adipocytes (Chang et al., 2016).

Hormone sensitive lipase (HSL) is encoded by the gene *Lipe* and is involved in the mobilization of fat stores through the hydrolysis of lipids to fatty acids. There is evidence that knockout of HSL results in increased adipocyte size in rodents (Osuga et al., 2000) and a loss of function mutation in humans was associated with increased risk for metabolic dysfunction (Albert et al., 2014). These studies underscore the importance of HSL in adipocyte function. The current study demonstrates a significant reduction in *Lipe* in female IL1R1$^{-/-}$ mice irrespective of genotype. There is also a decrease in *Acacb*, which encodes the protein ACC2, a rate limiting step in fatty acid uptake and oxidation in the mitochondria, in female IL1R1$^{-/-}$ groups irrespective of maternal diet. Depletion of this protein improves overall metabolic health in mice fed a HFD (Takagi et al., 2018). Furthermore, there was a decrease in expression of *Acsl1*, which encodes a protein which mediates the conversion of long-chain fatty acids to fatty acyl-CoA esters producing important substrates for mitochondrial fatty acid biosynthesis, in IL1R1$^{-/-}$ groups irrespective of genotype. Recent reports have demonstrated that *Acsl1* depletion dampens insulin stimulated glucose uptake and fatty acid efflux in 3t3-L1 adipocytes (Lobo et al., 2009). Overall, these changes in lipid metabolism may inhibit the efficiency of the adipose tissue to mobilize and efficiently utilize lipids which in the short term may reduce the flux of fatty acids to peripheral tissues but may have long term effect *via* the enlargement of adipocytes and overall lipid metabolic health.

Female offspring also exhibited alterations in the expression of several genes involved in immune cell chemotaxis. *Ccl12* encodes MCP-5, which promotes macrophage recruitment to the adipose tissue and promotes IR in response to HFD (Kim et al., 2014). The current study demonstrated an increase in *Ccl12* gene expression in response to maternal HFD, and

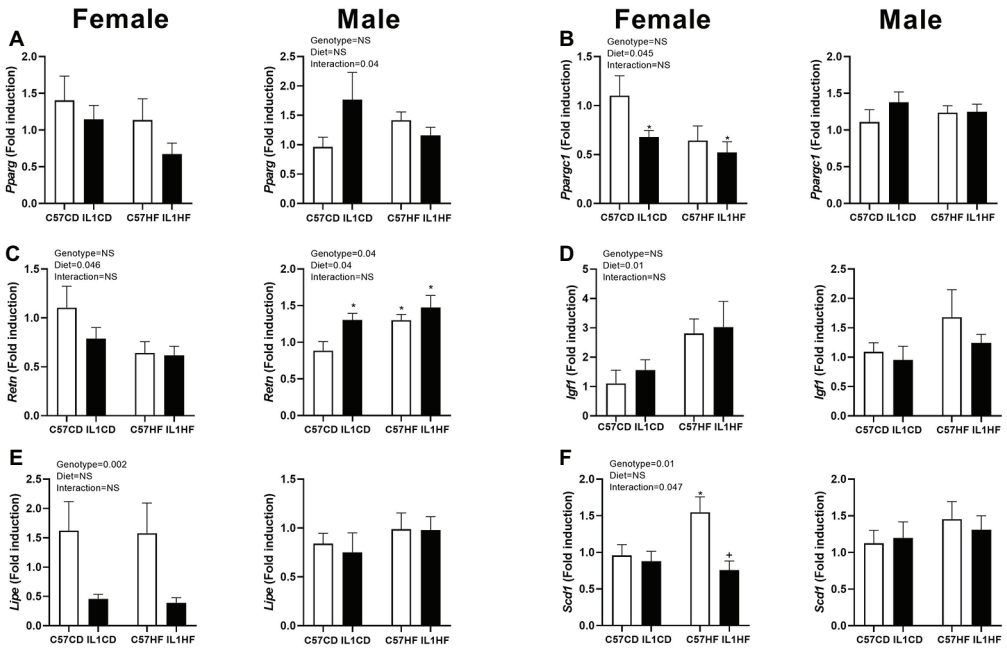

FIGURE 3 | Gene expression of adipogenic markers in adipose tissue. Adipose tissue gene expression of markers related to adipogenesis. **(A)** *Pparg*, **(B)** *Ppargc1*, **(C)** *Retn*, **(D)** *Igf1*, **(E)** *Lipe*, and **(F)** *Scd1*. Data are expressed as mean ± SEM. N = 6–8 litters/group. $^{*}p < 0.05$ with respect to C57CD. $^{+}p < 0.05$ with respect to C57HF.

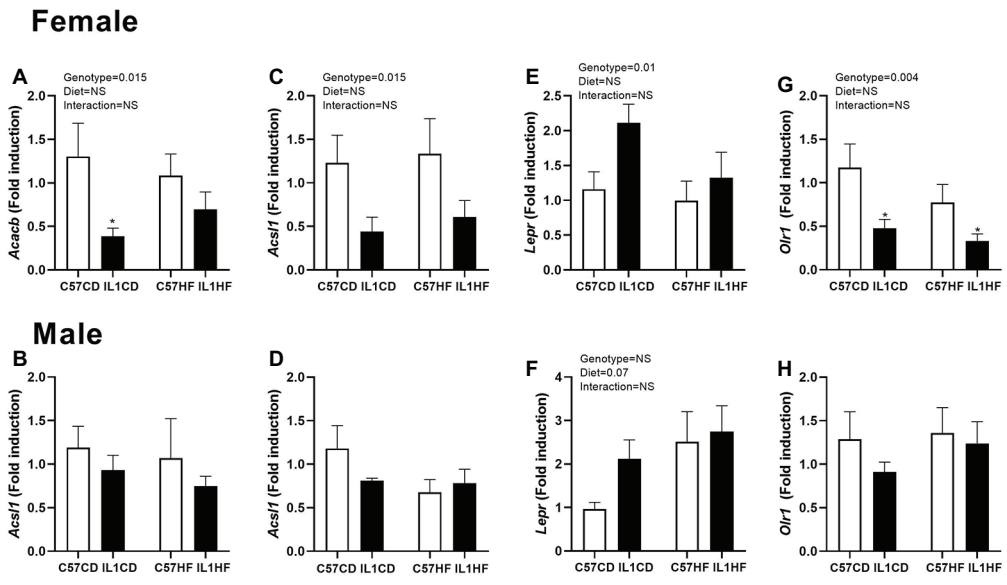

FIGURE 4 | Gene expression of lipid metabolism markers in adipose tissue. Adipose tissue gene expression of markers related to adipogenesis. *Acacb* in female **(A)** and male **(B)** offspring, *Acsl1* in female **(C)** and male **(D)** offspring, *Lepr* in female **(E)** and male **(F)** offspring, and *Olr1* in female **(G)** and male **(H)** offspring. Data are expressed as mean ± SEM. N = 6–8 litters/group. $^{*}p < 0.05$ with respect to C57CD.

IL1R1$^{-/-}$ prevented this increase. There is some evidence that *Ccl12* is increased in response to prenatal exposure to HFD. However, these studies focus on behavioral changes in the offspring and there appears to be a paucity of information on *Ccl12* in relation to metabolic health in the offspring. We also see an increase in the expression chemokine receptor *Ccr4* in response to maternal HFD in C57BL/6 but not IL1R1$^{-/-}$ mice. This receptor binds MCP-1, a key protein in the recruitment of macrophages to the adipose tissue, and subsequent IR in response to diet-induced obesity (Kanda et al., 2006). Our results are perhaps not surprising given that MCP-1 is involved in the regulation of the IL-1 pathway (Gavrilin et al., 2000).

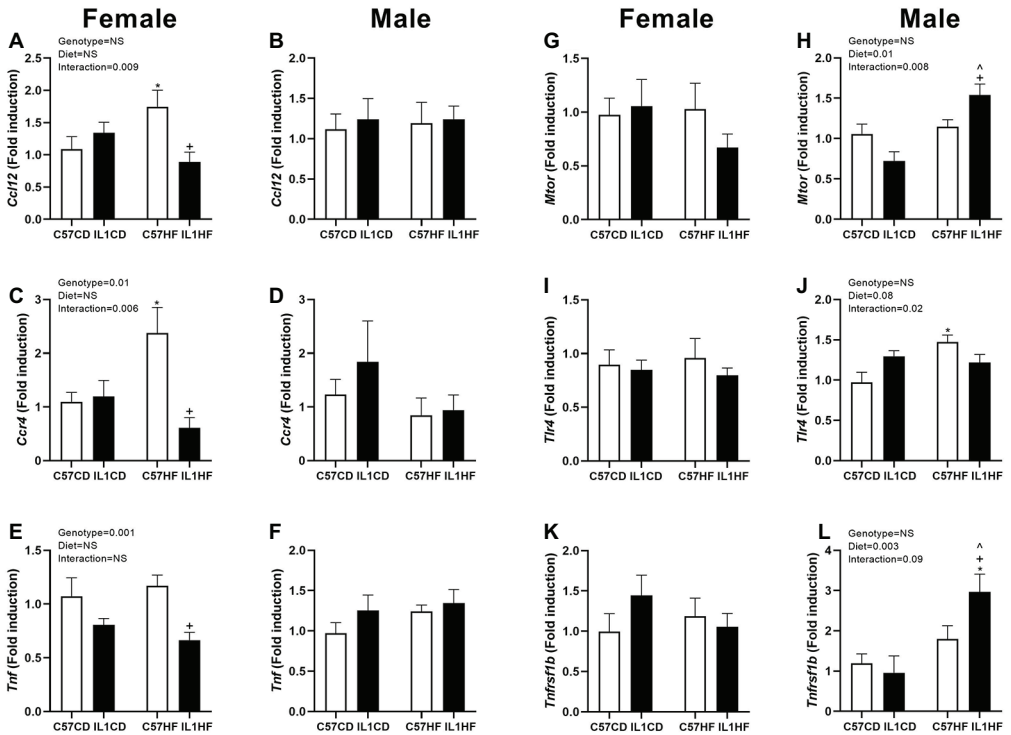

FIGURE 5 | Adipose tissue gene expression of inflammatory markers in female and male offspring. Adipose tissue gene expression of markers related to inflammation. *Ccl12* in female **(A)** and male **(B)** offspring, *Ccr4* in female **(C)** and male **(D)** offspring, *Tnf* in female **(E)** and male **(F)** offspring, *mTor* in female **(G)** and male **(H)** offspring, *Tlr4* in female **(I)** and male **(J)** offspring, and *Tnfrsf1b* in female **(K)** and male **(L)** offspring. Data are expressed as mean ± SEM. N = 6–8 litters/group. $^{*}p < 0.05$ with respect to C57CD. $^{+}p < 0.05$ with respect to C57HF. $^{\wedge}p < 0.05$ with respect to IL1CD.

Furthermore, a role for this protein has been shown in response to maternal HFD, where offspring from mothers fed a HFD had increased MCP-1 which was associated with improved glucose tolerance (Murabayashi et al., 2013). There is also evidence of an IL1R1$^{-/-}$ mediated reduction in the gene expression of *Tnf*, a potent cytokine known to have a negative influence on metabolic health (Hotamisligil, 1999). It is possible that the moderate benefits in glucose tolerance observed in female offspring, despite adipocyte hypertrophy, may be mediated by alterations in immune signaling.

While the impact of maternal diet and IL1R1$^{-/-}$ on lipid metabolism and chemokine expression is limited in males, there is evidence of alterations in several genes which influence metabolic inflammatory processes. mTOR is a critical regulator of cellular metabolism and plays an important role in adipogenesis, lipid metabolism, and inflammatory processes (Mao and Zhang, 2018). Hyper-activation of mTOR signaling has the capacity to increase fat mass and reduce glucose tolerance in mice (Robitaille et al., 2013). It is therefore possible that the increase in adipocyte size in male offspring from HFD-fed mothers may be linked to increased mTOR expression. We also observed a significant increase in *Tnfrsfb*, a receptor for TNF, in the adipose tissue of male offspring exposed to prenatal HFD, independent of genotype. Given the important role of TNF in metabolic dysfunction and adipose tissue biology, it is possible that increases in this receptor may compensate for the lack of IL-1 signaling and thereby influence the glucose intolerance observed in male offspring.

There are several limitations to this current study. Firstly, the knockout model used represents a whole body knockout of the IL1R1 receptor. This may be problematic when interpreting results in specific tissues as the overall phenotype observed may be due to a complex interplay of different organ systems. It would therefore be useful to develop an adipose tissue specific IL1R1$^{-/-}$ to examine the specific contribution of adipose tissue inflammation in the developmental programming paradigm. Another limitation is the lack of littermate controls. While animals came from the same source and IL1R1$^{-/-}$ were maintained on a C57Bl/6 background, there is the possibility that artifactual variation might be introduced between the C57Bl/6 control group and the IL1R1$^{-/-}$ group. This may result from factors such as differences in microbiome composition, and genetic drift etc. and may ultimately skew the results of the study. It is possible that some of the detrimental effects observed in the IL1R1$^{-/-}$ group are due to compensation in other inflammatory mediators such as TNF. We had a limited capacity to conduct comprehensive analysis of circulating plasma proteins. This limited our capacity to uncover any changes in inflammatory profile of these animals. We did examine the inflammatory profile in adipose tissue *via* PCR analysis, a high correlation between RNA and protein concentrations in key inflammatory proteins.

CONCLUSION

Previous work from our group demonstrated that IL-1R1$^{-/-}$ resulted in metabolic dysregulation during pregnancy and demonstrated features associated with gestational diabetes including significant adipocyte hypertrophy and evidence of adipose tissue IR (Plows et al., 2019). We sought to expand this work by examining whether IL-1 signaling impacts long-term outcomes in offspring exposed to a HFD *in utero*. Our results show that while there was little impact on glucose tolerance between groups, both IL1R1 knockout and maternal HFD resulted in adipocyte hypertrophy and altered gene expression in pathways relating to adipogenesis, lipid metabolism, and inflammation in a sex-specific manner. This furthers the understanding of diet-induced metabolic inflammation in relation to *in utero* exposures and lends support to the importance of studying both male and female subjects. There are clear beneficial effects of depletion of the IL-1 signaling pathway in females, particularly in relation to inflammation which are not seen in males. This may in part explain why males are more susceptible to metabolic dysregulation following *in utero* exposure to HFD. This work highlights the complexity of IL-1 signaling in terms of metabolic health and the importance of cardiometabolic outcomes in response to *in utero* exposures.

DATA AVAILABILITY STATEMENT

The raw data supporting the conclusions of this article will be made available by the authors, without undue reservation, to any qualified researcher.

ETHICS STATEMENT

The animal study was reviewed and approved by AgResearch Animal Ethics Committee in accordance with the New Zealand Animal Welfare Act, 1999.

AUTHOR CONTRIBUTIONS

PBC collected data, performed analysis, and contributed to the writing of the manuscript. JP and FR performed analysis and edited the manuscript. RP and TG collected data. JS and MV reviewed the manuscript. CR designed the study, collected data, and wrote the manuscript. All authors have read and approved the manuscript.

FUNDING

This work was funded by the Health Research Council of New Zealand (Emerging Researcher grant). CR is supported by an HRC Sir Charles Hercus Health Research Fellowship.

ACKNOWLEDGMENTS

The authors would like to thank Robert Smith and Ric Broadhurst from AgResearch for their expert animal assistance. They would also like to thank Satya Amirapu, who prepared the histological samples for visualizing.

REFERENCES

Albert, J. S., Yerges-Armstrong, L. M., Horenstein, R. B., Pollin, T. I., Sreenivasan, U. T., Chai, S., et al. (2014). Null mutation in hormone-sensitive lipase gene and risk of type 2 diabetes. *N. Engl. J. Med.* 370, 2307–2315. doi: 10.1056/NEJMoa1315496

Allport, V. C., Pieber, D., Slater, D. M., Newton, R., White, J. O., and Bennett, P. R. (2001). Human labour is associated with nuclear factor-κB activity which mediates cyclo-oxygenase-2 expression and is involved with the 'functional progesterone withdrawal'. *Mol. Hum. Reprod.* 7, 581–586. doi: 10.1093/molehr/7.6.581

Blüher, M. (2019). Obesity: global epidemiology and pathogenesis. *Nat. Rev. Endocrinol.* 15, 288–298. doi: 10.1038/s41574-019-0176-8

Chang, E., Hafner, H., Varghese, M., Griffin, C., Clemente, J., Islam, M., et al. (2019). Programming effects of maternal and gestational obesity on offspring metabolism and metabolic inflammation. *Sci. Rep.* 9, 1–15. doi: 10.1038/s41598-019-52583-x

Chang, H. R., Kim, H. J., Xu, X., and Ferrante, A. W. (2016). Macrophage and adipocyte IGF1 maintain adipose tissue homeostasis during metabolic stresses. *Obesity* 24, 172–183. doi: 10.1002/oby.21354

Corbould, A. (2008). Effects of androgens on insulin action in women: is androgen excess a component of female metabolic syndrome? *Diabetes Metab. Res. Rev.* 24, 520–532. doi: 10.1002/dmrr.872

Finucane, O. M., Lyons, C. L., Murphy, A. M., Reynolds, C. M., Klinger, R., Healy, N. P., et al. (2015). Monounsaturated fatty acid–enriched high-fat diets impede adipose NLRP3 inflammasome–mediated IL-1β secretion and insulin resistance despite obesity. *Diabetes* 64, 2116–2128. doi: 10.2337/db14-1098

Franks, S. (2012). Animal models and the developmental origins of polycystic ovary syndrome: increasing evidence for the role of and rogens in programming reproductive and metabolic dysfunction. *Endocrinology* 153, 2536–2538. doi: 10.1210/en.2012-1366

García, M. C., Wernstedt, I., Berndtsson, A., Enge, M., Bell, M., Hultgren, O., et al. (2006). Mature-onset obesity in interleukin-1 receptor I knockout mice. *Diabetes* 55, 1205–1213. doi: 10.2337/db05-1304

Gavrilin, M. A., Deucher, M. F., Boeckman, F., and Kolattukudy, P. E. (2000). Monocyte chemotactic protein 1 upregulates IL-1beta expression in human monocytes. *Biochem. Biophys. Res. Commun.* 277, 37–42. doi: 10.1006/bbrc.2000.3619

Hammarstedt, A., Graham, T. E., and Kahn, B. B. (2012). Adipose tissue dysregulation and reduced insulin sensitivity in non-obese individuals with enlarged abdominal adipose cells. *Diabetol. Metab. Syndr.* 4:42. doi: 10.1186/1758-5996-4-42

Hotamisligil, G. S. (1999). The role of TNFalpha and TNF receptors in obesity and insulin resistance. *J. Intern. Med.* 245, 621–625. doi: 10.1046/j.1365-2796.1999.00490.x

Jager, J., Grémeaux, T., Cormont, M., Le Marchand-Brustel, Y., and Tanti, J. -F. (2007). Interleukin-1β-induced insulin resistance in adipocytes through down-regulation of insulin receptor substrate-1 expression. *Endocrinology* 148, 241–251. doi: 10.1210/en.2006-0692

Kanda, H., Tateya, S., Tamori, Y., Kotani, K., Hiasa, K., Kitazawa, R., et al. (2006). MCP-1 contributes to macrophage infiltration into adipose tissue, insulin resistance, and hepatic steatosis in obesity. *J. Clin. Invest.* 116, 1494–1505. doi: 10.1172/JCI26498

Katra, P., Dereke, J., Nilsson, C., and Hillman, M. (2016). Plasma levels of the interleukin-1-receptor antagonist are lower in women with gestational diabetes mellitus and are particularly associated with postpartum development of type 2 diabetes. *PLoS One* 11:e0155701. doi: 10.1371/journal.pone.0155701

Kim, D., Kim, J., Yoon, J. H., Ghim, J., Yea, K., Song, P., et al. (2014). CXCL12 secreted from adipose tissue recruits macrophages and induces insulin resistance in mice. *Diabetologia* 57, 1456–1465. doi: 10.1007/s00125-014-3237-5

Kleiner, S., Mepani, R. J., Laznik, D., Ye, L., Jurczak, M. J., Jornayvaz, F. R., et al. (2012). Development of insulin resistance in mice lacking PGC-1α in adipose tissues. *Proc. Natl. Acad. Sci. U. S. A.* 109, 9635–9640. doi: 10.1073/pnas.1207287109

Klöting, N., Fasshauer, M., Dietrich, A., Kovacs, P., Schön, M. R., Kern, M., et al. (2010). Insulin-sensitive obesity. *Am. J. Physiol. Endocrinol. Metab.* 299, E506–E515. doi: 10.1152/ajpendo.00586.2009

Koenen, T. B., Stienstra, R., van Tits, L. J., de Graaf, J., Stalenhoef, A. F. H., Joosten, L. A. B., et al. (2011). Hyperglycemia activates caspase-1 and TXNIP-mediated IL-1β transcription in human adipose tissue. *Diabetes* 60, 517–524. doi: 10.2337/db10-0266

Li, J., Liu, M., Zong, J., Tan, P., Wang, J., Wang, X., et al. (2014). Genetic variations in IL1A and IL1RN are associated with the risk of preeclampsia in Chinese Han population. *Sci. Rep.* 4:5250. doi: 10.1038/srep05250

Liang, H., and Ward, W. F. (2006). PGC-1α: a key regulator of energy metabolism. *Adv. Physiol. Educ.* 30, 145–151. doi: 10.1152/advan.00052.2006

Livak, K. J., and Schmittgen, T. D. (2001). Analysis of relative gene expression data using real-time quantitative PCR and the 2(−Delta Delta C(T)) method. *Methods* 25, 402–408. doi: 10.1006/meth.2001.1262

Lobo, S., Wiczer, B. M., and Bernlohr, D. A. (2009). Functional analysis of long-chain acyl-CoA synthetase 1 in 3T3-L1 adipocytes. *J. Biol. Chem.* 284, 18347–18356. doi: 10.1074/jbc.M109.017244

Mandal, M., Donnelly, R., Elkabes, S., Zhang, P., Davini, D., David, B. T., et al. (2013). Maternal immune stimulation during pregnancy shapes the immunological phenotype of offspring. *Brain Behav. Immun.* 33, 33–45. doi: 10.1016/j.bbi.2013.04.012

Mao, Z., and Zhang, W. (2018). Role of mTOR in glucose and lipid metabolism. *Int. J. Mol. Sci.* 19:E2043. doi: 10.3390/ijms19072043

McGillicuddy, F. C., Harford, K. A., Reynolds, C. M., Oliver, E., Claessens, M., Mills, K. H. G., et al. (2011). Lack of interleukin-1 receptor I (IL-1RI) protects mice from high-fat diet–induced adipose tissue inflammation coincident with improved glucose homeostasis. *Diabetes* 60, 1688–1698. doi: 10.2337/db10-1278

McGillicuddy, F. C., Reynolds, C. M., Finucane, O., Coleman, E., Harford, K. A., Grant, C., et al. (2013). Long-term exposure to a high-fat diet results in the development of glucose intolerance and insulin resistance in interleukin-1 receptor I-deficient mice. *Am. J. Physiol. Endocrinol. Metab.* 305, E834–E844. doi: 10.1152/ajpendo.00297.2013

McGowan, P. O., and Matthews, S. G. (2018). Prenatal stress, glucocorticoids, and developmental programming of the stress response. *Endocrinology* 159, 69–82. doi: 10.1210/en.2017-00896

Murabayashi, N., Sugiyama, T., Zhang, L., Kamimoto, Y., Umekawa, T., Ma, N., et al. (2013). Maternal high-fat diets cause insulin resistance through inflammatory changes in fetal adipose tissue. *Eur. J. Obstet. Gynecol. Reprod. Biol.* 169, 39–44. doi: 10.1016/j.ejogrb.2013.02.003

Nair, R. R., Khanna, A., and Singh, K. (2014). Association of interleukin 1 receptor antagonist (IL1RN) gene polymorphism with recurrent pregnancy loss risk in the North Indian population and a meta-analysis. *Mol. Biol. Rep.* 41, 5719–5727. doi: 10.1007/s11033-014-3443-8

Osuga, J., Ishibashi, S., Oka, T., Yagyu, H., Tozawa, R., Fujimoto, A., et al. (2000). Targeted disruption of hormone-sensitive lipase results in male sterility and adipocyte hypertrophy, but not in obesity. *Proc. Natl. Acad. Sci. U. S. A.* 97, 787–792. doi: 10.1073/pnas.97.2.787

Plows, J. F., Vickers, M. H., Ganapathy, T. P., Bridge-Comer, P. E., Stanley, J. L., and Reynolds, C. M. (2019). Interleukin-1 receptor-1 deficiency impairs metabolic function in pregnant and non-pregnant female mice. *Mol. Nutr. Food Res.* e1900770. doi: 10.1002/mnfr.201900770 [Epub ahead of print]

Reynolds, C. M., Segovia, S. A., and Vickers, M. H. (2017). Experimental models of maternal obesity and neuroendocrine programming of metabolic disorders in offspring. *Front. Endocrinol.* 8:245. doi: 10.3389/fendo.2017.00245

Robitaille, A. M., Christen, S., Shimobayashi, M., Cornu, M., Fava, L. L., Moes, S., et al. (2013). Quantitative phosphoproteomics reveal mTORC1 activates de novo pyrimidine synthesis. *Science* 339, 1320–1323. doi: 10.1126/science.1228771

Saltiel, A. R., and Olefsky, J. M. (2017). Inflammatory mechanisms linking obesity and metabolic disease. *J. Clin. Invest.* 127, 1–4. doi: 10.1172/JCI92035

Segovia, S. A., Vickers, M. H., and Reynolds, C. M. (2017). The impact of maternal obesity on inflammatory processes and consequences for later offspring health outcomes. *J. Dev. Orig. Health Dis.* 8, 529–540. doi: 10.1017/S2040174417000204

Semple, R. K., Crowley, V. C., Sewter, C. P., Laudes, M., Christodoulides, C., Considine, R. V., et al. (2004). Expression of the thermogenic nuclear hormone receptor coactivator PGC-1alpha is reduced in the adipose tissue of morbidly obese subjects. *Int. J. Obes. Relat. Metab. Disord.* 28, 176–179. doi: 10.1038/sj.ijo.0802482

Siljee, J. E., Wortelboer, E. J., Koster, M. P. H., Imholz, S., Rodenburg, W., Visser, G. H. A., et al. (2013). Identification of interleukin-1 beta, but no other inflammatory proteins, as an early onset pre-eclampsia biomarker in first trimester serum by bead-based multiplexed immunoassays. *Prenat. Diagn.* 33, 1183–1188. doi: 10.1002/pd.4219

Takagi, H., Ikehara, T., Kashiwagi, Y., Hashimoto, K., Nanchi, I., Shimazaki, A., et al. (2018). ACC2 deletion enhances IMCL reduction along with acetyl-CoA metabolism and improves insulin sensitivity in male mice. *Endocrinology* 159, 3007–3019. doi: 10.1210/en.2018-00338

Terzidou, V., Lee, Y., Lindström, T., Johnson, M., Thornton, S., and Bennett, P. R. (2006). Regulation of the human oxytocin receptor by nuclear factor-κB and CCAAT/enhancer-binding protein-β. *J. Clin. Endocrinol. Metab.* 91, 2317–2326. doi: 10.1210/jc.2005-2649

Weyer, C., Foley, J. E., Bogardus, C., Tataranni, P. A., and Pratley, R. E. (2000). Enlarged subcutaneous abdominal adipocyte size, but not obesity itself, predicts type II diabetes independent of insulin resistance. *Diabetologia* 43, 1498–1506. doi: 10.1007/s001250051560

Conflict of Interest: The authors declare that the research was conducted in the absence of any commercial or financial relationships that could be construed as a potential conflict of interest.

Copyright © 2020 Bridge-Comer, Plows, Ramzan, Patel, Ganapathy, Stanley, Vickers and Reynolds. This is an open-access article distributed under the terms of the Creative Commons Attribution License (CC BY). The use, distribution or reproduction in other forums is permitted, provided the original author(s) and the copyright owner(s) are credited and that the original publication in this journal is cited, in accordance with accepted academic practice. No use, distribution or reproduction is permitted which does not comply with these terms.

frontiers in Physiology

REVIEW
published: 16 July 2020
doi: 10.3389/fphys.2020.00757

Programming of Renal Development and Chronic Disease in Adult Life

Eugenie R. Lumbers[1,2], Yoga Kandasamy[1,2,3], Sarah J. Delforce[1,2], Amanda C. Boyce[4], Karen J. Gibson[4] and Kirsty G. Pringle[1,2]*

[1] School of Biomedical Sciences and Pharmacy, Faculty of Health and Medicine, The University of Newcastle, Callaghan, NSW, Australia, [2] Hunter Medical Research Institute, Newcastle, NSW, Australia, [3] Department of Neonatology, Townsville University Hospital, Douglas, QLD, Australia, [4] School of Medical Sciences, University of New South Wales, Sydney, NSW, Australia

OPEN ACCESS

Edited by:
Gina Galli,
The University of Manchester, United Kingdom

Reviewed by:
Chenbei Chang,
The University of Alabama at Birmingham, United States
Dean A. Myers,
The University of Oklahoma Health Sciences Center, United States

***Correspondence:**
Eugenie R. Lumbers
eugenie.lumbers@newcastle.edu.au

Specialty section:
This article was submitted to Embryonic and Developmental Physiology, a section of the journal Frontiers in Physiology

Received: *11 March 2020*
Accepted: *11 June 2020*
Published: *16 July 2020*

Citation:
Lumbers ER, Kandasamy Y, Delforce SJ, Boyce AC, Gibson KJ and Pringle KG (2020) Programming of Renal Development and Chronic Disease in Adult Life. Front. Physiol. 11:757. doi: 10.3389/fphys.2020.00757

Chronic kidney disease (CKD) can have an insidious onset because there is a gradual decline in nephron number throughout life. There may be no overt symptoms of renal dysfunction until about two thirds or more of the nephrons have been destroyed and glomerular filtration rate (GFR) falls to below 25% of normal (often in mid-late life) (Martinez-Maldonaldo et al., 1992). Once End Stage Renal Disease (ESRD) has been reached, survival depends on renal replacement therapy (RRT). CKD causes hypertension and cardiovascular disease; and hypertension causes CKD. Albuminuria is also a risk factor for cardiovascular disease. The age of onset of CKD is partly determined during fetal life. This review describes the mechanisms underlying the development of CKD in adult life that results from abnormal renal development caused by an adverse intrauterine environment. The basis of this form of CKD is thought to be mainly due to a reduction in the number of nephrons formed *in utero* which impacts on the age dependent decline in glomerular function. Factors that affect the risk of reduced nephron formation during intrauterine life are discussed and include maternal nutrition (malnutrition and obesity, micronutrients), smoking and alcohol, use of drugs that block the maternal renin-angiotensin system, glucocorticoid excess and maternal renal dysfunction and prematurity. Since CKD, hypertension and cardiovascular disease add to the disease burden in the community we recommend that kidney size at birth should be recorded using ultrasound and those individuals who are born premature or who have small kidneys at this time should be monitored regularly by determining GFR and albumin:creatinine clearance ratio. Furthermore, public health measures aimed at limiting the prevalence of obesity and diabetes mellitus as well as providing advice on limiting the amount of protein ingested during a single meal, because they are all associated with increased glomerular hyperfiltration and subsequent glomerulosclerosis would be beneficial.

Keywords: renal, development, oligonephropathy, glomerular hypertension, renin, nutrition

INTRODUCTION

Renal disease can have an insidious onset. Apart from congenital causes of chronic kidney disease (CKD) and syndromes that result in renal failure (Acute Kidney Injury, IgA nephropathy, glomerulonephritis, renal infections, and tumors), there may be no overt symptoms of renal dysfunction until about two thirds or more of the nephrons have been destroyed and glomerular filtration rate (GFR) falls to below 25% of normal (often in mid-late life) (Martinez-Maldonaldo et al., 1992). Once End Stage Renal Disease (ESRD) has been reached, survival depends on renal replacement therapy (RRT).

Chronic kidney disease causes hypertension and cardiovascular disease; and hypertension causes CKD. Albuminuria is also a risk factor for cardiovascular disease. Therefore, a stronger emphasis on assessing renal function by estimated glomerular filtration rate (eGFR) and albuminuria should be included in risk assessment tables for heart disease and hypertension, a conclusion drawn from a meta-analysis carried out in 2015 (Matsushita et al., 2015).

The early onset of CKD has its origins in fetal life. This review describes the mechanisms underlying development of CKD in adult life that result from abnormal renal development caused by an adverse intrauterine environment. The basis of this form of CKD is thought to be mainly due to a reduction in the number of nephrons formed *in utero*. However, as described below, renal programming of tubular function may also result in renal dysfunction. The effects of programming on renal development can also be sex specific (Gingery et al., 2009; Lankadeva et al., 2014).

Although the number of nephrons in adults varies widely (Hoy et al., 2003), it is useful to consider that each kidney has about 1,000,000 nephrons. Each nephron is composed of a large number of different cells, each with unique properties to carry out different functions. The correct assembly of these cells in terms of their location has to occur for normal renal function. It is for these reasons that neonephrogenesis cannot occur once nephrogenesis is complete, even though renal progenitor cells persist which are able to repair injured portions of existing nephrons (Romagnani et al., 2013, **Figure 1**). Since nephrogenesis in the human fetus is complete by term, no new nephrons can be formed after birth. Consequently, at this time and throughout childhood, the number of nephrons is greatly in excess of the number required to serve the metabolic mass of the individual until adult size is reached. A sufficient number and function of filtering nephrons underpins the successful regulation of fluid and electrolyte balance and blood pressure while rapidly eliminating unwanted toxins and by-products of metabolism. The kidney is the most complex structural organ in the body, so it is not surprising therefore that it is susceptible to alterations in its pattern of development.

David Barker's seminal research on the relationship between maternal health and programming of cardiovascular disease in offspring resulted in the development of a body of knowledge that exposed the potential long-term consequences of adverse intrauterine development on the predisposition to chronic disease in adult life, or the discipline now known as the Developmental Origins of Health and Disease (DOHaD) (Barker et al., 1989). This field of research examines the impact of the intrauterine and early life environment on offspring development and programming, particularly through epigenetic events. While it has been known for many years that ingestion by the mother of drugs like thalidomide (Taussig, 1962) or exposure to chemicals such as mercury, which caused Minimata disease (Matsumoto et al., 1965), were teratogens, there had been little appreciation that some chronic diseases that occur in adult life also have their origins *in utero*. Barker used birthweight as a measure of the degree to which maternal health had impacted on fetal development. He was the first to show that infants born with a low birth weight had a greater risk of developing hypertension, cardiovascular disease and diabetes mellitus in middle age (Zanetti et al., 2018).

Brenner and Chertow (1994) postulated that low birth weight infants also have fewer nephrons and this predisposes them, as adults, to systemic and glomerular hypertension as well as CKD. They based their hypothesis on three findings: (1) the association between birth weight and nephron number; (2) the inverse relationship between birth weight and hypertension in adult life; and (3) the inverse relationship between blood pressure and nephron number (Brenner and Chertow, 1994). These observations showed that abnormal renal development plays a pivotal role in the pathogenesis of the developmental origins of hypertension and cardiovascular disease.

The human fetus completes nephrogenesis before term [at 36 weeks of gestation (Osathanondh and Potter, 1963)]. Therefore, renal development in preterm infants born before 36 weeks is likely to be altered and may be affected by the adverse milieu of neonatal intensive care (e.g., hypotension, hypoxia and exposure to nephrotoxic antibiotics) (Keijzer-Veen et al., 2010; Sutherland et al., 2011). In females, the reduction in kidney volume effect persists into adult life (Keijzer-Veen et al., 2010).

In postnatal life an individual can be exposed to a variety of stressors that cause damage to nephrons. These include renal infections, diabetes mellitus and autoimmune diseases, e.g., streptococcal glomerulonephritis and IgA nephropathy. If an individual is born with fewer nephrons these conditions are more likely to cause an early onset of CKD compared with their impact on the renal health of individuals who are endowed with a full complement of nephrons at birth. This 'second-hit' therefore exacerbates the prevalence of renal disease (Hoy et al., 2006).

The question also arises as to whether maternal oligonephropathy can cause transgenerational changes in renal development and predispose her offspring to CKD, cardiovascular disease and hypertension in adult life. Does abnormal maternal renal function (occurring as a result of oligonephropathy) impact on fetal kidney development and renal function in her young offspring?

This review describes how an adverse intrauterine environment can alter nephrogenesis, cause oligonephropathy and possibly tubular dysfunction, so predisposing to CKD (**Figure 2**). It does not discuss the genetic defects that cause congenital abnormalities in the kidney and urinary tract (CAKUT). These are, however, relatively common accounting

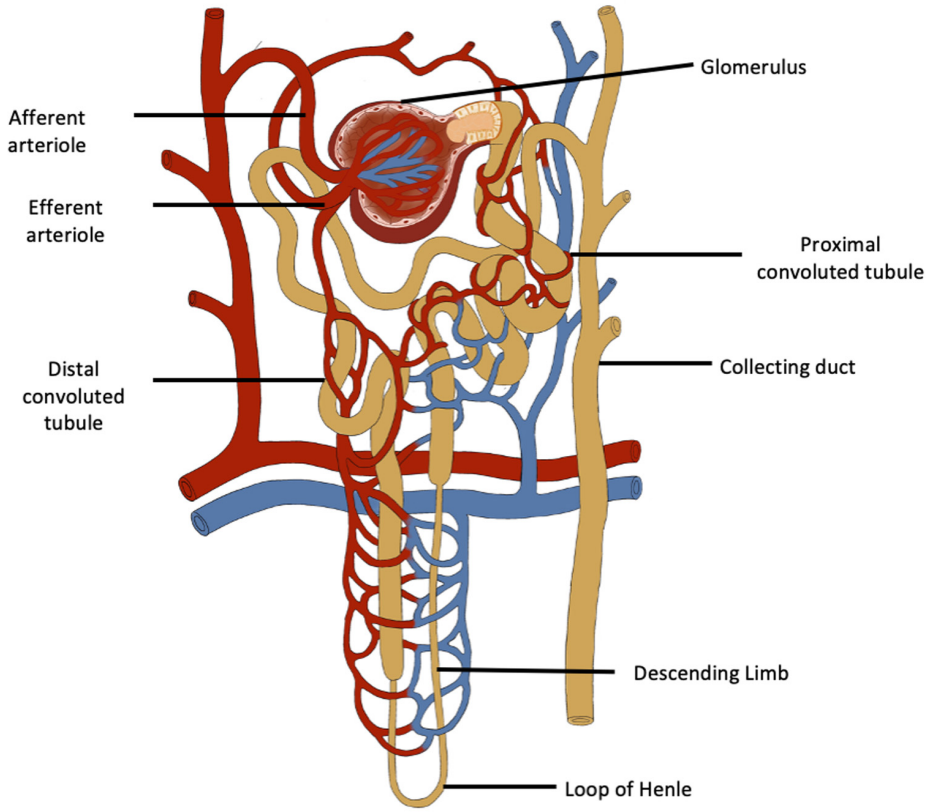

FIGURE 1 | The functional unit of the kidney is the nephron which has a complex structure and a complex variety of cells. Neonephrogenesis cannot occur although there are renal progenitor cells, podocyte progenitor cells and tubular progenitor cells that can repair existing nephrons.

for about 40% of cases of ESRD in patients younger than 30 years (van der Ven et al., 2018).

Before addressing those factors that limit the intrauterine acquisition of nephrons, this review examines the physiological reasons behind why this predisposes individuals to an earlier onset of CKD in adult life, which is the necessity to maintain GFR regardless of the number of nephrons available to contribute to the formation of urine. It should be noted that throughout life there is a progressive loss of normal glomeruli and an increase in sclerotic glomeruli. It seems that glomeruli also disappear because the decrease in non-sclerotic glomeruli is not quantitatively matched to the increase in sclerotic glomeruli (**Figure 3**, Denic et al., 2017). Therefore, an individual who starts life with fewer nephrons will develop CKD at an earlier age than an individual endowed with a larger number of nephrons.

THE CONFLICT BETWEEN GLOMERULAR FILTRATION RATE (GFR) AND THE NUMBER OF NEPHRONS AVAILABLE TO FILTER THE BLOOD

The first step in the formation of urine is the production of an ultrafiltrate of plasma generated by the pumping action of the heart, which forces fluid from the glomerular capillaries across the glomerular basement membrane (GBM) into the blind ending of the renal tubule known as Bowman's capsule. The major force opposing the production of the plasma ultrafiltrate is the colloid osmotic pressure of the plasma proteins, which are not filtered. The GBM consists of endothelial cells, the glomerular membrane, and podocytes that wrap around the membrane. Podocytes have foot processes that are comprised of a functioning slit diaphragm in between a network of proteins. The outer surface of the foot processes have a negatively charged glycocalyx that faces into the urinary space and maintains the cytoarchitecture of the podocytes through charge repulsion. Thus this three layered barrier to filtration results in size and charge selective filtration (Reiser and Altintas, 2016). In the mammalian kidney the glomerular filtration rate (GFR) is high, with a GFR between 90 and 120 mL/min/1.73 m^2 body surface area.

Metabolism is the sum of all the reactions occurring within the cells of the body. As a fundamental process it needs the cardiovascular system to supply sufficient nutrients to all metabolizing tissues and systems to efficiently eliminate the waste products of metabolism (lungs and kidneys). Each element within the system is interdependent and influenced by metabolic rate. Therefore, GFR, as the first step in the elimination of products of metabolism by the kidney, is set by the metabolic rate (Singer, 2001). In small animals like the shrew, which has a very high

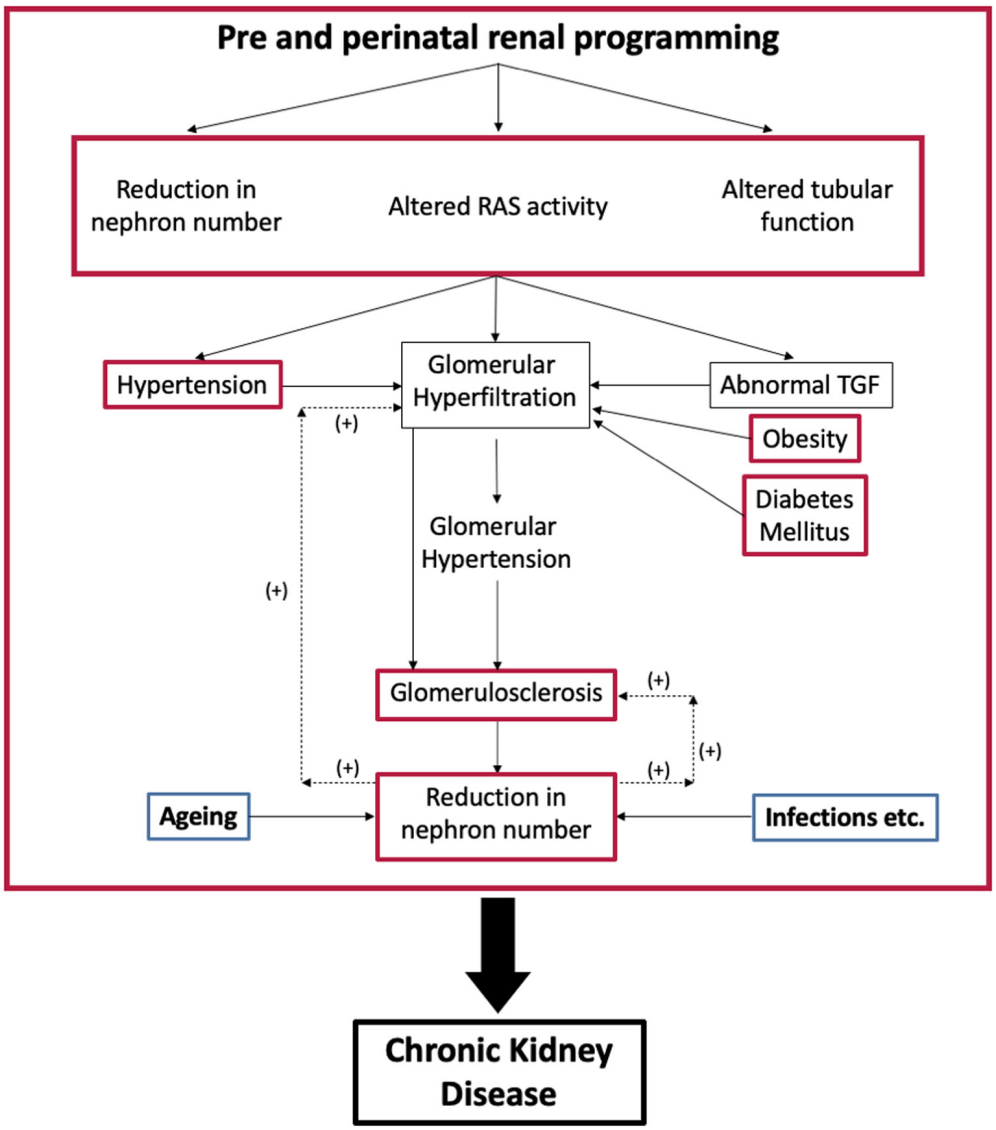

FIGURE 2 | Interaction between programmed changes in renal development [oligonephropathy, tubular function and activity of the renin-angiotensin system (RAS); red] and postnatal health. Postnatal conditions like hypertension, diabetes mellitus, and obesity (red) cause glomerular hyperfiltration that can lead to glomerulosclerosis and a further reduction in nephron number. Aging and infection also affect nephron numbers (blue). TGF, tubuloglomerular feedback.

metabolic rate (oxygen consumption is 3–4 times higher than expected), the kidneys are 1.91% of the body weight (2.8 times greater than expected) (Singer, 2001).

By convention, GFR is normalized to body surface area (BSA) because metabolic rate is related to BSA and it was assumed that this would be more accurate as it eliminated changes in mass due to obesity. In adults of normal body weight, GFR/BSA and GFR not corrected for BSA are similar. In obese subjects, however, the calculation of GFR/BSA results in a value that is inappropriately low because BSA is calculated from height and weight. **Table 1** compares the effects of indexing GFR (measured using [Cr^{51}] EDTA) to BSA within female patients in a hospital nephrology unit who had low BMIs, with the effects of indexing GFR to BSA in females in the hospital metabolic disorders unit who had high BMIs. It can be seen that the difference between the mean absolute GFR and mean indexed GFR increases as BMI increases, i.e., the mean indexed GFR is inappropriately reduced because the greater weight of individuals used in the calculation of BSA. Since the number of nephrons does not increase after birth and they are not related to an individual's fat mass, in obese subjects each individual nephron must form a greater volume of glomerular ultrafiltrate: this is masked by calculating eGFR. This possibly explains why obesity is a risk factor in patients with nephropathies (Geddes et al., 2008). In infants there are also a number of issues that complicate estimation of GFR indexed to BSA/1.73 m^2 (Delanaye et al., 2005; Geddes et al., 2008).

The overall absolute GFR is the result of filtration of plasma by about 1 million nephrons in each kidney. If the

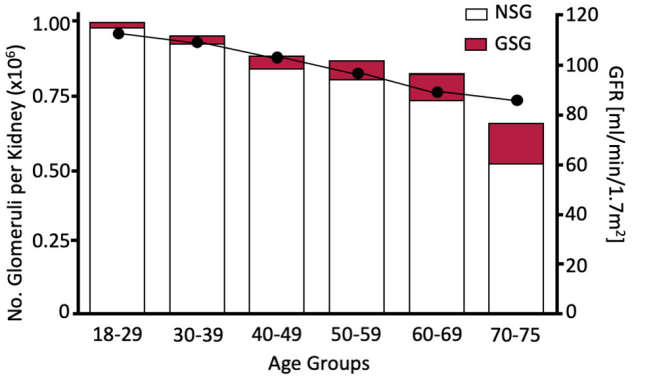

FIGURE 3 | Age dependent increase in glomerulosclerotic nephrons (GSG) and decrease in non-sclerotic nephrons (left axis) and GFR. Since the total nephron population declines to <80% of the population measured in the 18–29 age group nephrons must have disappeared as well as becoming sclerotic. Redrawn from Denic et al. (2017).

TABLE 1 | Mean difference between absolute (ml/min) and indexed (ml/min/1.73 m^2) GFR and body mass index (BMI).

BMI) (kg/m2)	*n*	Mean absolute GFR	Mean indexed) GFR (Dubois)	Mean difference between indexed and absolute GFR
18.5–25	40	44.47	43.38	−1.09
>30	81	81.73	70.94	−18.2*
>40	33	110.17	87.76	−24.85*

*$P < 0.0001$ (Delanaye et al., 2005).

number of nephrons is reduced, GFR does not fall to a similar extent. For example, removal of 2/3 of the total renal mass (and therefore nephron number) in an animal model is associated with only a small 17% reduction in renal blood flow/g kidney weight and 16.5% reduction in GFR/g kidney weight. Since the number of nephrons was reduced to about 1/3 of the original population it follows that the remaining nephrons have to filter more (Gibson et al., 2006). This phenomenon is known as glomerular hyperfiltration. Glomerular hyperfiltration occurs in individuals with fewer than the normal complement of nephrons, for example after unilateral nephrectomy, especially early in life (Godron-Dubrasquet et al., 2017). Thus, individuals with a solitary kidney from early life onwards should have their renal function regularly monitored throughout life.

Occurring in 'normal' healthy individuals, glomerular hyperfiltration is said to be present if the GFR is greater than the 95% confidence limits for the patient's age group. With aging, GFR declines so an apparently normal GFR in an elderly person can mask glomerular hyperfiltration. Hyperfiltration is often associated with albuminuria, possibly due to leakage across the glomerular barrier or failure of tubular protein reabsorption. Thus, albuminuria is a robust measure of renal dysfunction (Hoy and McDonald, 2004). In individuals with oligonephropathy, a so-called 'normal estimated GFR' (eGFR) (calculated from the serum creatinine) has to be the result of hyperfiltration.

Any form of proteinuria and glomerular hyperfiltration leads to secondary focal segmental glomerulosclerosis and the loss of nephrons (Rosenberg and Kopp, 2017). Glomerular hyperfiltration causes glomerular damage if there is raised intraglomerular hydrostatic pressure known as intraglomerular hypertension. This can be the result of hypertension, afferent arteriolar dilation or increased efferent arteriolar tone. Tubular sodium reabsorption also corrects GFR via tubuloglomerular feedback (TGF), so failure of TGF can cause glomerular hyperfiltration (Vallon, 2003).

In pregnancy, the increase in renal blood flow (RBF) is greater than the increase in GFR and there is no intraglomerular hypertension, so this physiological glomerular hyperfiltration probably does not result in long term renal damage (Helal et al., 2012). Furthermore, it is comparatively short-term. In conditions like obesity, where GFR increases to cope with increased metabolic demand, hypertension, and diabetes mellitus, there is intraglomerular hypertension (Helal et al., 2012).

HOW DOES GLOMERULAR HYPERFILTRATION DAMAGE THE NEPHRON?

High intra-glomerular capillary pressures exert shear forces on the endothelial cells lining the capillary wall. The mechanical stresses caused by the consequent rise in filtration rate, cause the GBM to increase and therefore impose stress on the podocyte foot processes. Although the podocytes hypertrophy, mismatching of the increase in GBM area and the extent to which it is covered by podocytes can occur. The podocytes detach, leading to denuded areas of GBM. The result is segmental sclerosis. The high rate of filtration also causes mechanical stresses that dilate the urinary space and proximal tubules. In early diabetes mellitus the increase in sodium reabsorption is linked to increased glucose reabsorption with a reduction in tubuloglomerular feedback (TGF; Vallon, 2003) and release of inflammatory mediators that cause inflammation. The destruction of podocytes and glomerular inflammation leads to fibrosis and destruction of the glomerular capillary complex essential for filtration. This process is known as glomerulosclerosis. It is exacerbated when the pro-inflammatory arm of the renin-angiotensin system (RAS), the Angiotensin II/AT_1R axis is activated either to maintain efferent arteriolar tone and hence GFR (**Figure 4**) as occurs in hypertension (Simons et al., 1994; Keller et al., 2003) or by activation of the renal G-coupled protein receptor, GRP91, by high glucose levels as occurs in diabetes mellitus (Peti-Peterdi, 2010). Alternatively, loss of the anti-inflammatory arm of the RAS [ACE2-Ang(1–7)-MasR], as occurs in COVID-19 infection, results in high levels of Ang II and loss of the anti-inflammatory peptide Ang-(1–7) causing acute renal failure (Cheng et al., 2020). Limiting these consequences of hyperfiltration by blocking the formation of Ang II or blocking its interaction with the AT_1R are mainstays in the treatment of hypertension and diabetes.

Since nephrogenesis is complete by about 36 weeks of gestation, all the nephrons an individual will ever have are present at term. Thus, oligonephropathy caused by fetal growth

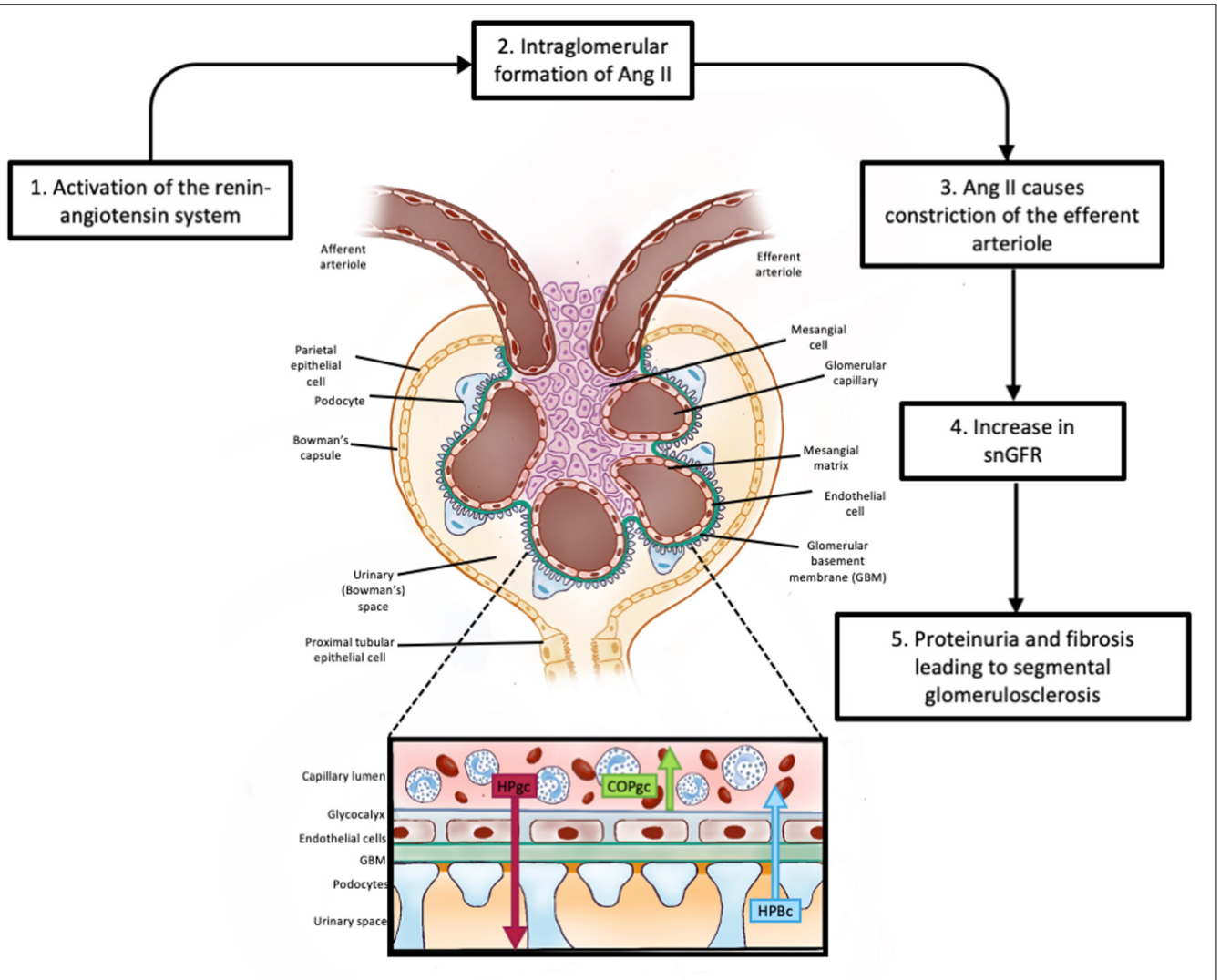

FIGURE 4 | Glomerular filtration. This figure shows the basic cellular structure of the glomerulus; an enlargement of the filtration barrier (Kf) to ultrafiltration showing the two major forces involved in the formation of the glomerular ultrafiltrate (HPgc; the hydrostatic pressure within the glomerular capillaries). COPgc; the colloid osmotic pressure exerted by plasma proteins retained within the glomerular capillary. Other pressures affecting ultrafiltration include the hydrostatic pressure of the ultrafiltrate within Bowman's capsule and the colloid osmotic pressure of any proteins that may have undergone ultrafiltration. Filtration equilibrium is reached when pressures favoring filtration are equal to pressures opposing filtration. The hydrostatic pressure within the glomerular capillary is influence by arterial pressure and by the degree of constriction of the efferent arteriole. Release of renin from the myoepitheliod cells lining the afferent arteriole generates angiotensin I which is converted to angiotensin II (Ang II) as it transits the glomerular capillaries. Ang II causes constriction of the efferent arteriole, raising HPgc and increasing filtration rate. SnGFR: is the single nephron glomerular filtration rate.

restriction or in the early postnatal life of the preterm infant, may itself be associated with glomerular hyperfiltration (GH) because single nephron filtration rate (SNGFR) is increased. This can even occur *in utero* (Gibson et al., 2007; Turner et al., 2015). A high SNGFR at birth predisposes to an early onset of CKD. This is especially the case if the kidney is exposed to a second hit from those postnatal factors that also cause glomerular hyperfiltration (e.g., hypertension, diabetes mellitus, and obesity). The early onset of GH in individuals born with a fewer number of nephrons or who lose nephrons is, in early postnatal life undetected, as the eGFR will appear to be 'normal.' There is also strong evidence (Keller et al., 2003) that individuals with fewer nephrons are more likely to suffer from essential hypertension, which in turn causes glomerular hyperfiltration and glomerulosclerosis.

Intrauterine growth restriction is not only associated with a reduction in nephron number and hence CKD (Brenner and Chertow, 1994) but also with cardiovascular disease and diabetes mellitus. This triad or syndrome is inextricably linked through the adverse effects of poor renal function on cardiovascular health and the adverse effects of diabetes mellitus on renal health.

The long-term impact of pregnancy-induced hyperfiltration on the development of CKD is unknown. It can be assumed however, that conditions like hypertension, diabetes mellitus, and obesity occurring in pregnancy are likely to exacerbate any

effects of pregnancy-induced hyperfiltration on glomerular and tubular integrity. Moreover, if the mother has oligonephropathy, any effects of pregnancy-induced hyperfiltration exacerbated by glomerular hypertension associated with obesity, the onset of hypertension, or gestational diabetes will predispose these women to an early onset of CKD.

Pregnancy induced hyperfiltration is not the only form of hyperfiltration occurring in response to physiological events. High protein meals/infusions of amino acids also cause hyperfiltration, probably as an evolutionary adaptation resulting in increased renal perfusion and glomerular filtration (Meyer et al., 1983a,b). Interestingly, glomerular hyperfiltration in response to amino acid infusions can be demonstrated in the fetus; it is associated with increased expression of angiotensinogen, the substrate for renin (Boyce et al., 2005). Human volunteers fed 50–70 g of protein had a 50% increase in GFR and patients maintained on total parenteral nutrition also had a 50% increase in GFR during the 12 h of amino acid infusion (Meyer et al., 1983b). The amount of protein in the diet influences renal health in remnant kidney animal models (Kleinknecht et al., 1979; Salusky et al., 1981). Thus, it can be assumed that when there is a severe reduction in nephron number at birth, a high dietary protein intake could hasten the rate of progression toward CKD in adult life.

DEVELOPMENT OF THE KIDNEY

Each nephron is composed of a large variety of cells, each with unique properties and functions. The correct assembly of these cells is required for normal renal function. The kidney is an extraordinarily complex organ. Briefly, three successive sets of kidneys develop during embryogenesis. These are the pronephros, the mesonephros and the metanephros; they are derived from the intermediate mesoderm. The pronephros begins to develop during the fourth week of gestation and deteriorates by the end of that week. The metanephros matures into the fully functional kidney. Only the metanephric mesenchyme can form renal tubules (Gilbert, 2000). The ureteric bud, which arises from the mesonephric duct (Wolffian duct), invades the mesoderm laterally. This epithelial mesenchymal interaction is driven by factors secreted by the condensing mesenchyme [notably *GDNF/c-RET/Wnt11* (Yosypiv, 2008) and hepatocyte growth factor (HGF)] and leads to budding and the formation of the collecting tubules, calyces, the renal pelvis and ureters.

Conversely, the ureteric buds stimulate differentiation of the adjacent mesoderm into the metanephric blastema, which forms the glomerulus, capsule and tubules of the nephron. The structural differentiation of the condensed mesenchyme around the ureteric vesicle is driven by the transcription factor (WT1) and a host of factors secreted by the ureteric bud including fibroblast growth factor 2 (FGF2), which maintains WT1 transcription, and bone morphogenetic protein (BMP7). Leukocyte Inhibitory factor (LIF) begins epithelial transformation of aggregated mesenchymal cells that is induced by FGF2 and stimulates secretion of Wnt4 (found in S-shaped tubules), which completes the transition to epithelial renal tubules. For a detailed and excellent description of nephrogenesis see Gilbert (2000). The S-shaped body, which forms the glomerular cleft (Bowmans capsule), is lined by podocyte progenitor cells while renal progenitor cells and tubular progenitor cells line the tubules. Capillaries invaginate the blind ending Bowman's capsule and form the glomerular tuft. Further differentiation occurs as gestation continues.

Ureteric budding determines how many nephrons are formed. This process is known as branching morphogenesis as the ureteric bud divides into two buds, which each divide into two buds and so forth. The arterial tree undergoes a similar form of fractal branching directed by renin precursor cells. A new arteriolar branch is formed by the coalescence of renin cells around the site at which a new vessel will sprout. The elongating vessel is covered by renin containing cells which, like smooth muscle and juxtaglomerular cells, are driven to differentiate by the transcription factor, *Foxd1* (Gomez, 2017).

The formation of nephrons occurs radially so that the outermost nephrons are the most immature. This means that renal blood flow is lower in outer nephrons and the amount of oxyhaemoglobin reaching the outer cortical nephrons is lowest. In preterm infants, some outer glomeruli are often seriously damaged making it unlikely that they will ever filter plasma (Black et al., 2013).

ABNORMAL RENAL DEVELOPMENT

Abnormal renal development can occur as a result of congenital anomalies, effects of the intrauterine environment, or as a result of prematurity (**Figure 5**).

Genetic

The various genetic defects that are associated with CAKUT are not discussed further. Suffice to say that CAKUT represents 20–30% of all prenatally detected congenital anomalies (Queisser-Luft et al., 2002).

At a less clinically definable level Zhang et al. (2008) showed that a common polymorphism in the *RET* gene (RET^{1476A}) was associated with about a 10% decrease in kidney volume and a 9% increase in Cystatin C (a measure of GFR) in newborns. Interestingly, the correlation between the hypomorphic RET^{1476A} with another hypomorphic SNP (PAX^{AAA}) was associated with a 23% reduction in kidney volume compared with homozygotes carrying RET^{1476G} and PAX^{GGG}. *RET* and *PAX* mutations act synergistically to affect branching morphogenesis. Zhang et al. (2008) showed that disrupting branching morphogenesis affects nephron number. Kidney volume and nephron number are strongly associated in the neonate (Zhang et al., 2008).

Some of the effects of blockade of the renin-angiotensin-aldosterone system (RAS) on renal development are similar to those seen in some congenital renal abnormalities. In particular, RAS blockade is associated with oligonephropathy and abnormal vascular development (Tufro-McReddie et al., 1995). Chen et al. (2004) have reviewed the effects of blockade of the RAS on

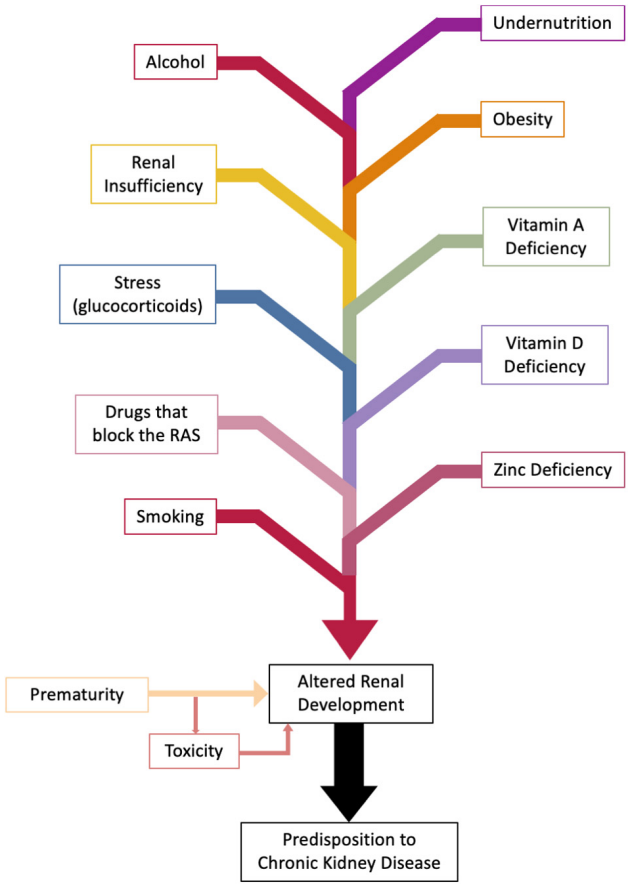

FIGURE 5 | Factors altering fetal and perinatal renal development. Nephrogenesis is complete at 36 weeks of gestation. Effects on kidney development can be wide ranging from oligonephropathy, glomerular hypertrophy, tubular defects (Chen et al., 2004), and altered activity of the fetal renin-angiotensin system (RAS). Genetic factors are excluded.

renal tubular function. Furthermore, Angiotensin (Ang) II acting via the Ang II type 1 receptor (AT_1R) stimulates ureteric bud branching by blocking *Spry 1*, releasing the *GDNF/c- RET/Wnt 11* pathway, the major stimulator of ureteric budding. Acting via the Ang II type 2 receptor (AT_2R), Ang II upregulates *Pax2* and stimulates ureteric branching (Yosypiv, 2008).

The (pro)renin receptor (*ATP6AP2*, (P)RR) probably plays a role in renal development (Song and Yosypiv, 2011), however, deletion of the gene is lethal to the embryo, so it is more difficult to generate viable knockout models. Yosypiv et al. (2019) showed that while kidney stromal cell (P)RR was not necessary for ureteric branching, in conditional knockouts the lack of (P)RR affected arterial development and glomerular number. Since these knockouts had fewer renin containing cells the authors concluded that stromal (P)RR has an essential role in development of renin-expressing cells required for the proper development of the renal arterial tree. Abnormal expression of the renal RAS has been found in a number of animal models in which renal programming has been studied (Woods et al., 2001; Moritz et al., 2002).

Environmental

The Barker hypothesis was based on epidemiological evidence showing that individuals who were small at birth were more likely to develop hypertension, cardiovascular disease and type II diabetes in later life. Events like the Dutch famine (Painter et al., 2005) and famine in China (Wang et al., 2018) also showed an association between malnutrition during pregnancy and birth weight. In both cases, low birth weight was associated with proteinuria or albuminuria, signs of renal dysfunction in adult life. Hinchliffe et al. (1992) also showed that nephron number was reduced in infants that were small at birth.

It is very difficult to measure nephron numbers in human populations because the kidneys have to be removed to count nephrons. Zhang et al. (2008) showed that in infants who died prior to 3 months of age, there was a strong correlation ($P = 0.019$) between kidney weight and the number of glomeruli. Regression analysis showed that there were 23,549 additional glomeruli/g kidney tissue (95% confidence interval of 4,590–42,238 glomeruli/g). A surrogate marker of kidney weight is the measurement of kidney volume using ultrasound. Ultrasound measurement of kidney volume before birth therefore provides a very useful surrogate measure of nephron number. Zhang et al. (2008) measured total renal volume by ultrasound and confirmed that there was a relationship between renal volume and glomerular number in a study that looked at the associations between common genetic variants and kidney size.

Since nephrogenesis is complete before birth, kidney volume at birth provides the best estimate of nephron number because postnatal renal growth is due to growth of the individual nephrons, in particular the renal tubules. There is a consensus that small for gestational age babies have smaller kidney volumes (Mishra et al., 2014). Therefore, it was logical that animal models, developed to study the developmental origins of chronic disease, first investigated the effects of reduced intrauterine growth due to undernutrition on nephrogenesis. Studies in animal models have shown that maternal health has a strong impact on the number of nephrons that her offspring develop (**Figure 5**). Specific factors that have been shown to be involved are:

(1) Maternal malnutrition/obesity;
(2) Maternal micronutrient deficiency (Vitamins A and D, zinc);
(3) Maternal smoking and alcohol intake;
(4) Administration of RAS blocking drugs;
(5) Maternal glucocorticoids; and
(6) Maternal renal dysfunction.

Some of these associations share a common pathway via which they influence fetal renal growth. For example, RAS blocking drugs (Lumbers et al., 1993; Barr, 1994; Woods et al., 2001; Lasaitiene et al., 2003), maternal undernutrition (Woods et al., 2001), Vitamin D deficiency (Boyce et al., 2013) or treatment with glucocorticoids in early gestation (Peers et al., 2001; Moritz et al., 2011), are all associated with altered activity of the RAS in the developing kidney and may exert their programming effects by altering early renal RAS expression or activity. On the other hand, oxidative stress and inflammation have been

implicated in the etiology of oligonephropathy associated with maternal obesity, zinc deficiency and smoking (Tomat et al., 2011; Jackson et al., 2012; Flynn et al., 2013). Maternal alcohol and Vitamin A deficiency are associated with reduced expression of key genes involved in branching morphogenesis but oxidative stress may also play a key role (Gray et al., 2010). Furthermore, factors that restrict fetal growth are associated with smaller kidney volumes at birth and therefore are associated with oligonephropathy. As there is often catch-up growth after birth they will go through life with fewer nephrons and one can predict that they will when coupled with the age dependent decline in nephrons that occurs in healthy people develop CKD earlier than infants who appropriately grown for their gestational age (Kandasamy et al., 2014).

Prematurity also adversely affects kidney development because nephrogenesis is not complete at birth and therapeutic interventions can be toxic for the developing kidney.

Maternal Diet

Malnutrition

The effects of maternal global nutrient restriction (GNR) on the development of the kidneys using animal models has been extensively reviewed by Lee et al. (2019a). Lee et al. (2019a) concluded that maternal global nutrient restriction during pregnancy had a detrimental effect on kidney structure and function, that is, the kidneys were smaller, there was oligonephropathy and GFR was lower.

Pregnant rats fed a low-protein diet have small offspring. These animals have small kidneys and, in a number of studies, the offspring develop hypertension in adult life (Woods et al., 2001). They have also been shown to have fewer nephrons. Interestingly, the level of expression of renin in the kidneys of these animals is depressed. This reduced level of expression of renin, which is essential for both normal glomerulogenesis (Tufro-McReddie et al., 1995) and tubular development (Yosypiv, 2008) could be due to a deficiency in amino acids in the developing embryo, as a sustained supply of amino acids during intrauterine life stimulates the renal RAS (Boyce et al., 2005). Langley-Evans et al. (2003) cite data showing that supplementation of a low protein diet with glycine, alanine, or urea restored renal morphology and glomerular number but only glycine supplementation in the maternal diet prevented hypertension in offspring. This suggests that there is a dissociation between oligonephropathy and hypertension in rat offspring fed a low protein diet. This finding may be restricted to this model of oligonephropathy, as unilateral nephrectomy of the ovine fetus in mid-gestation is associated with hypertension at 6 months postnatal age (Singh et al., 2009). Sheep, like humans, complete nephrogenesis before birth.

Obesity

Although malnutrition is endemic in the developing world, in first world countries there is an epidemic of obesity. In animal studies a high-fat maternal diet (lard) resulted in offspring developing a syndrome similar to metabolic syndrome with obesity and hypertension. In these animals a high-fat diet did not affect kidney weight and glomerular number in offspring, but renal renin activity and renal Na-K-ATPase activity was suppressed (Armitage et al., 2005).

Studies by Jackson and Flyn clearly demonstrated that both pre- and postnatal exposure to a high fat/fructose diet caused changes in the kidney that were characteristic of long-standing inflammation and there was a synergistic effect of maternal obesity and a high-fat diet after birth (Jackson et al., 2012; Flynn et al., 2013). These changes (including an increase in glomerulosclerosis index), which were attributed to oxidative stress, were most severe in offspring exposed to a high-fat/fructose diet throughout the whole of gestation and in the early postnatal period (Jackson et al., 2012; Flynn et al., 2013). Glastras et al. (2016) also found that maternal obesity due to a high fat/fructose diet was associated with oxidative stress in offspring. They concluded, however, that postnatal exposure to this diet induced an overwhelming effect compared with diet-induced maternal obesity.

Lee et al. (2019b) found that fetuses of obese Indigenous women had smaller kidney volumes relative to their estimated body weights. This was because the fetuses were bigger than fetuses carried by Indigenous women with lower body weights. Since GFR is linked to metabolic rate and BSA it follows that these fetuses were born hyperfiltering. Coupled with their propensity to have higher body weights during childhood it is likely that in these children obesity will contribute to an increased risk of CKD in adult life (Lee et al., 2019b).

Micronutrients: Vitamins A, D and Zinc

Vitamin A deficiency

Vitamin A is essential for normal cell growth and development, so it is not surprising that severe Vitamin A deficiency leads to fetal death or congenital abnormalities (Wilson et al., 1953). Mild vitamin A deficiency is, however, relatively common (Merlet-Benichou et al., 1999). Lelievre-Pegorier et al. (1998) carried out an elegant study in pregnant rats who were exposed to vitamin A deficiency throughout gestation and showed that there was a strong correlation between the number of glomeruli in offspring and fetal retinol levels ($r = 0.83$, $P < 0.001$). Metanephroi from vitamin A deficient embryos grew less effectively *in vitro* but they could be rescued by supplementation with retinol (Lelievre-Pegorier et al., 1998). Retinol levels determined levels of expression of c-ret, a key pathway in nephrogenesis (see above). In an exciting study it was shown by Makrakis et al. (2007) that administration of retinoic acid to pregnant rats on a low protein diet offset the effects of protein deficiency on glomerular number.

Although these animal studies conclusively show a role for vitamin A deficiency in determining nephron number there are no definitive studies in human populations. Since mild vitamin A deficiency is common when there is poverty, these studies need to be carried out because mild vitamin A deficiency could account for smaller kidneys in these populations (Goodyer et al., 2007).

Vitamin D deficiency

A deficiency of vitamin D in pregnant women is quite common (Lips, 2010). Since the major source of vitamin D is from the action of ultraviolet light on the skin, it follows that the fetus can only obtain adequate levels of vitamin D from its mother.

Formation of active vitamin D or 1,25 dihydroxycholecalciferol ($1,25(OH)_2D_3$) from $25(OH)D_3$ (the precursor to Vitamin D, which is formed in the liver from cholecalciferol produced in the skin) occurs in the kidney.

The effects of vitamin D on kidney development is confusing. On the one hand, vitamin D appears to increase glomerular development (Rogers et al., 2004), yet maternal vitamin D deficiency also increases nephron number (Maka et al., 2008; Nascimento et al., 2012). For these reasons the effects of both maternal Vit D deficiency and excess on offspring nephron endowment were studied and it was found that there were more glomeruli per milligram of kidney at PND20 in offspring of deficient mothers (78.09 ± 2.63 Nglom/mg) than in both replete and high vitamin D mothers (55.42 ± 2.83 and 58.26 ± 3.69, $P = 0.001$) (Burkitt et al., 2014). Although offspring nephron number was increased by maternal vitamin D deficiency, these additional nephrons could be abnormal. Boyce et al. (2013) found that adult male offspring of vitamin D deficient dams who ate normal chow from weaning had a reduced creatinine clearance and others have reported high blood pressure and ventricular hypertrophy in young offspring maintained on a vitamin D deficient diet (Gezmish et al., 2010; Tare et al., 2011).

Vitamin D acts via the vitamin D receptor (VDR), a nuclear receptor that regulates the transcription of a large number of genes. Since the VDR interacts with a cAMP response element (CRE) in the REN gene to suppress renin gene expression (Li et al., 2002), a deficiency of Vitamin D in the fetus could upregulate renin expression. Boyce et al. (2013) showed that offspring of pregnant rats subjected to a diet low in maternal vitamin D had increased renal renin expression at E20 (during nephrogenesis) and in adult life. This suggests that vitamin D deficiency could increase nephron number via RAS stimulation.

In contrast to the findings of Boyce et al. (2013) at E20 and adulthood, at PND20 it was subsequently found that several RAS genes, including renin, were downregulated (Burkitt et al., 2014). While downregulation at this stage (when nephrogenesis has been completed) does not negate the hypothesis that vitamin D deficiency stimulates nephrogenesis via upregulation of the RAS, it is does raise the possibility that there may be an alternative mechanism. In many tissues vitamin D inhibits cell proliferation and stimulates differentiation (Brown et al., 1999). Thus, vitamin D deficiency might stimulate proliferation and inhibit maturation of nephrons. Given that the increase in nephron number was associated with reduced renal function in adulthood, it is possible that the initial stages of nephrogenesis were stimulated but maturation was impaired resulting in poor renal function.

Notably, the effects of Vitamin D deficiency were sex specific. In both sexes during fetal life *REN* expression was increased and the kidney to body weight ratio was reduced at PND3 and PND20 but they were not different at 22 weeks. In males from Vit D deficient pregnancies, the renin levels were two times control levels. Adult males also had a reduced creatinine clearance, solute excretion and suppressed urinary Na/K ratio suggestive of increased aldosterone secretion. In females, the GFR was normal and the urine dilute because they drank more.

It is also interesting to note that even though glomerular number was increased in Vit D deficient offspring, kidney to body weight ratios were reduced despite the overall reduction in body weight, which further suggests abnormal tubular development (Boyce et al., 2013).

Zinc deficiency

Marginal or moderate zinc deficiency is common. Zinc plays an essential role in gene expression and organ development because it is present in over 300 enzymes where it plays a role in catalysis. Its levels affect the activity of NO producing enzymes (NOS synthase), antioxidants such as glutathione and enzymes involved in free radical scavenging such as glutathione peroxidase and catalase. As well zinc inhibits the activity of NADPH oxidases that catalyze the production of superoxide anion from oxygen. Free radicals activate inflammatory pathways leading to cell death (Tomat et al., 2011).

Therefore, it is not surprising that low maternal intake of zinc has marked effects on renal development and blood pressure in male offspring (Tomat et al., 2007). Male rats had oligonephropathy associated with a reduced GFR (Tomat et al., 2008), proteinuria and renal fibrosis, increased evidence of renal apoptosis and higher lipid peroxidation products. Catalase and glutathione peroxidase activities were reduced as were glutathione levels (Tomat et al., 2008). In male offspring of rats fed a low zinc diet and sacrificed at 6 days of age, the activity of the renal RAS was significantly altered; in particular the pro-inflammatory Ang II/AT_1R axis was activated, ACE abundance was greater and the Ang II/ANG (1–7) ratio greater than in male rats fed a normal zinc diet (Gobetto et al., 2020). These effects were sex specific. Although both male and female zinc deficient rats had a greater abundance of AT_1R, the Ang II/AT1R axis was not activated in female rats but Ang (1–7) levels were increased as was the abundance of the AT_2R (Gobetto et al., 2020). Thus, the anti-inflammatory arms of the RAS were more active in females and probably protected them from the effects of the dysfunctional RAS and its associated inflammatory effects on oligonephropathy and renal artery modeling seen in male offspring.

Maternal Smoking and Alcohol

The adverse effects of smoking and alcohol on fetal growth, development and postnatal health are well known. Alcohol in high doses is a teratogen (Caputo et al., 2016), smoking reduces fetal growth (Diehm et al., 2017) but do either/both have specific effects on renal development that could contribute to the early onset of CKD? The answer is yes.

Smoking

Smoking during pregnancy leads to intrauterine growth restriction. We showed in an Indigenous cohort that smoking during pregnancy was associated with a reduction in birth weight of 327 g and smaller kidney volumes (Diehm et al., 2017); these infants therefore had oligonephropathy and were hyperfiltering from birth.

There were fewer nephrons as adults in the offspring of Balb/C mice exposed to cigarette smoke during pregnancy and lactation and the albumin/creatinine ratio was increased (Al-Odat et al., 2014). The renal expression of a pro-inflammatory

marker, macrophage chemoattractant protein 1 (MCP1) was also increased. The authors point out that there are 4,000 chemicals in cigarette smoke that could impact on renal development. They showed an altered pattern of expression of key growth factors involved in nephrogenesis such as GDNF1, Pax 2 and Wnt II, all of which were increased at postnatal day (PND) 1 and a reduction in FGF 7 and 10. These patterns of expression were different at PND20 and similar to controls at week 13. It is suggested that oxidative stress plays a key role (Kabuto et al., 2004).

Taal et al. (2011) studied over 1,000 children from smoking and non-smoking mothers from 30 weeks of gestation to 2 years of age and concluded that consumption of >10 cigarettes/day was associated with a smaller kidney volume at this age.

Alcohol

Fetal alcohol syndrome (FAS) is best known for its effects on cognition, learning, and emotional and social development but it has widespread effects on growth and organogenesis (Caputo et al., 2016). The effects on the kidney are subtle. Moore et al. (1997) reported that light drinking (<3 glasses per week) was not associated with renal anomalies while moderate drinking (3–13 glasses per week) was associated with an increased risk of renal agenesis (odds ratio, 2.5; 95% confidence interval, 1.2–5.1).

Animal studies do, however, show a convincing effect of alcohol on renal development. In the sheep, a moderate to high intake [0.75 g/kg i.v. given daily from 95 to 133 days of gestation, maternal peak blood ethanol level (BEC) was 0.12g/dL] over the last third of gestation caused oligonephropathy [about 46,000 fewer nephrons (Gray et al., 2008)] and rats gavaged with 1 g/kg body weight ethanol on days 13.5 and 14.5 gestation had reduced nephron numbers and impaired branching morphogenesis (Gray et al., 2010). In both studies alcohol intake was high (BEC was 0.107 g/dl, 1 h after dosing rats). Alcohol caused a reduction in body weight so that kidney:body weight ratios appeared higher in female offspring of treated rats at PN30 than controls, but they were the same as controls in adult life. However, both male and female offspring of treated dams had 10–20% fewer nephrons. The relative expression of key genes involved in branching morphogenesis, GDNF, FGF7, Wnt11, TGFβ2, and TGFβ3 was reduced in E15.5 kidneys of ethanol-exposed fetuses (Gray et al., 2010). Metanephroi cultured in ethanol for 5 days had reduced ureteric budding (Gray et al., 2010).

Inhibition of RAS Activity During Development

The role of the RAS, including its (pro)renin receptor, in renal development has been described above. It is not surprising therefore, that it was reported some time ago that oligohydramnios due to fetal anuria occurred when drugs that block the activity of the RAS were used to treat maternal hypertension (Lumbers et al., 1993; Barr, 1994). Earlier in renal development their administration causes renal papillary necrosis, lack of tubular development and hydronephrosis (Lasaitiene et al., 2003). It is important to appreciate these deleterious effects of RAS blockade on renal development because these drugs continue to be used to treat maternal hypertension. Nadeem et al. (2015) found that exposure even in the first trimester resulted in the early requirement for renal replacement therapy (RRT). They recommended that women who are on RAS blocking drugs and who are sexually active should have pregnancy testing if not using contraception (Cragan et al., 2015; Nadeem et al., 2015).

Conditional knockout of the (pro)renin receptor also causes abnormal renal development (Song and Yosypiv, 2011). The (pro)renin receptor not only activates prorenin, it also stimulates a number of signaling pathways including Wnt/β-catenin, ERK1/2 and PLZF pathways. These effects of (P)RR are independent from Ang II and are likely mediated by the receptor's function as part of the vacuolar ATPase. Therefore, drugs that inhibit vacuolar ATPase may also affect renal development. These include bafilomycin and proton pump inhibitors (PPIs). PPIs have been suggested as a potential treatment for preeclampsia (Hastie et al., 2019) and have been used to treat pregnant women. They seem safe but it is also possible that they have subtle effects on fetal kidney development that do not manifest clinically for years.

Maternal Glucocorticoids

A Cochrane review Roberts et al. (2017) found that administration of corticosteroids to women at risk of preterm birth reduced neonatal mortality because they advanced maturation of the lung so improving postnatal respiratory function. Corticosteroids are also administered in pregnancy to treat a number of conditions (e.g., asthma and autoimmune disease). Glucocorticoids can, however, have unwanted effects on blood pressure and kidney function of offspring. Dodic et al. (1998) showed that a 48h infusion of dexamethasone (DEX) into pregnant ewes at 26–28 days of gestation (term 150 days) resulted in lambs that had higher blood pressures after birth compared with control animals (Dodic et al., 1998) and fewer bigger nephrons (Wintour et al., 2003). To see if tubuloglomerular feedback (TGF) was involved in the development of hypertension in young sheep whose mothers were treated with DEX at 26–27 days gestation, TGF was measured in both DEX treated fetuses and lambs. There was an increase in TGF sensitivity that persisted after birth and therefore could play a role in development of hypertension later in life (Turner et al., 2017). Since this difference in TGF sensitivity was no longer seen after inhibition of nitric oxide production it was concluded that there was lower tonic production of NO, which attenuates TGF sensitivity (Turner et al., 2017). The significance of this work is that similar changes in TGF sensitivity are seen in spontaneously hypertensive strains of rats [Milan and SHR (Persson et al., 1985; Boberg and Persson, 1986; Brannstrom and Arendshorst, 1999)]. It is worth noting that this change in TGF sensitivity occurred before there was any change in blood pressure.

Ortiz et al. (2001) showed in rats, that maternal dexamethasone (0.2 mg) given on days 15–16 and 17–18 of gestation reduced glomerular numbers of 2 months old male and female offspring. They later showed that only male offspring were hypertensive at 6 months of age (Ortiz et al., 2003). Both male and female offspring had significant glomerulosclerosis, although it was more severe in males. This work shows that a number of factors influence kidney development and the future health of offspring whose mothers were treated with synthetic

steroids on the development of the kidney, including time of administration, sex and effects on blood pressure.

Significantly, Moritz et al. (2011) showed that naturally occurring steroids had effects similar to those of synthetic steroids on blood pressure (although the mechanisms underlying hypertension were different) and on the kidney. That is, naturally occurring steroids administered to the mother reduced glomerular number, altered the activity of the renal renin-angiotensin system and increased the expression of the epithelial sodium channel (α, β, and γ subunit) and the Na-K-ATPase (Moritz et al., 2011). This work is significant as it implies that anything resulting in severe maternal stress, which elevates maternal cortisol levels, could affect renal development.

Maternal Renal Insufficiency

It is known that renal disease in pregnant women is associated with adverse pregnancy outcomes (Blom et al., 2017) but does mild maternal renal insufficiency alter the development of the kidneys of her offspring?

The effects of mild maternal renal insufficiency on fetal renal function was studied in ewes who had one kidney removed and a branch of the renal artery in the remaining kidney occluded (subtotal nephrectomy; STNx) so that 30–50% of the remaining kidney became ischaemic (Gibson et al., 2006) before they were mated about 2–6 months after surgery. Ewes and fetuses were studied in the last fifth of gestation. The ewes had a raised serum creatinine and maternal GFR/kg bodyweight was only 54% that of intact pregnant ewes (Intact) (Gibson et al., 2006). Fetal GFR of STNx ewes was higher (about 1 ml/min) than the GFR of fetuses from Intact ewes. Both total and proximal tubular sodium reabsorption were reduced in fetuses of STNx ewes (Gibson et al., 2007). Moreover, infusion of amino acids known to stimulate ovine fetal RBF and GFR (Boyce et al., 2005) did not increase either RBF or GFR in fetuses of STNx ewes although it did cause an increase in both parameters in Intact fetuses (Gibson et al., 2007). Two weeks after birth, lambs from STNx (STNxL) and Intact (IntactL) ewes had a similar number of nephrons and their kidney weights were similar. However, STNxL had glomerular hypertrophy (glomeruli were about 30% larger) and there was a positive relationship between glomerular volume and urinary protein excretion. Therefore, exposure of the fetus to maternal renal insufficiency caused long-term changes in glomerular morphology (Brandon et al., 2008).

STNxL also had higher blood pressures at 26–27 days of age and there was abnormal programming of their RASs, in that the increase plasma renin levels in response to acute hemorrhage (1.6 ml/min/kg for 10 min) was attenuated (Brandon et al., 2011). Nor was the RAS in female STNxL as sensitive to altered salt intake as in IntactL (Brandon et al., 2009, 2011). In these 6-month old STNxL females, GFR was related to blood pressure and their plasma renin levels did not decrease, although plasma aldosterone levels did in response to a high salt intake. These animals had increased plasma sodium levels and reduced hematocrits; thus, they were volume expanded, probably because Ang II production was sustained in the presence of a high salt diet (Brandon et al., 2009).

To find out if these changes were related to dysregulation of tubuloglomerular feedback (TGF), studies were carried out in STNxF (Turner et al., 2015). In fact TGF was not different between STNxF and IntactF and it was concluded that the increase in GFR in STNx was related to an increase in filtration coefficient (Kf) (Turner et al., 2015). This fits with the glomerular hypertrophy described previously in STNxL. This finding is in contrast to the programming of TGF by maternal dexamethasone treatment given to the ewe in early gestation, which reduces glomerular number and causes hypertension in offspring (described above).

In conclusion, maternal renal dysfunction so mild that it does not interfere with normal fertility has profound effects on offspring kidney development, with glomerulomegaly and hyperfiltration predisposing to glomerulosclerosis in adult life and a blunted renin response to a high salt intake also contributing glomerulosclerosis and possibly causing hypertension.

PREMATURITY

In the human, nephrogenesis is not complete until about 36 weeks of gestation. Therefore, the more premature the infant the greater the impact of prematurity on nephrogenesis.

Studies have shown that prematurely born infants have smaller kidneys (Kandasamy et al., 2013) and in premature infants total kidney volume almost doubled from 28 to 37 weeks, although they were still smaller than kidney weights of term neonates. Since the eGFRs were similar, prematurely born infants must have higher SNGFRs, which suggests that they are already hyperfiltering (Kandasamy et al., 2018). Sutherland et al. (2011) showed that glomerulogenesis was accelerated in preterm human infants after birth; these glomeruli were also larger and there was a significantly greater percentage of abnormal glomeruli. Li et al. (2020) using ultrasound, came to a similar conclusion; the renal cortical region underwent accelerated growth after birth, but postnatal growth of the medulla was retarded. In the premature baboon (independent of steroid exposure) there was a high proportion of abnormal glomeruli (ranging from 0.2 to 18%) (Gubhaju et al., 2009).

The postnatal environment for the preterm infant is an environment in which hypoxia, hypotension, and infection are likely and antibiotics and other drugs that may be nephrotoxic are used. Thus, there are potentially a number of causes of disrupted kidney development in the preterm infant and its impact on adult renal function and cardiovascular health is largely unknown.

Keijzer-Veen et al. (2007) assessed renal function and kidney size in a cohort of 29 young adults (20 years old) who were born preterm (<32 weeks gestation) (Keijzer-Veen et al., 2007) and did not find any difference in renal function or kidney size between the preterm and control groups. However, a more recent study by South et al. (2019) published follow up data from a cohort of 96 adolescents (14 years) who were born preterm (<28 weeks) and showed that these children had elevated blood pressures and lower eGFRs compared with their peers were who were born at term (South et al., 2019).

TRANSGENERATIONAL MODIFICATION OF RENAL DEVELOPMENT AND RENAL DISEASE

A multiplicity of factors account for the high prevalence of CKD/ESRD in adult Indigenous Australians (Hoy et al., 1998b) but an underlying factor is oligonephropathy associated with low birth weight. Hoy et al. (1998a) first showed an association in Indigenous Australians between low birth weight and renal disease and in particular between low birth weight and a high albumin/creatinine ratio. Indigenous Australians have fewer nephrons; i.e., there are about 200,000 fewer nephrons or only 75% of those found in non-Indigenous Australians (Hoy et al., 2006). This means that there is probably pre-existing glomerular hyperfiltration and, since both obesity and diabetes mellitus also cause glomerular hyperfiltration (see above), they, together with the lower nephron number accelerate progression to CKD.

In Indigenous Australians the prevalence of ESRD and RRT is 6–8 times non-Indigenous Australians (age adjusted) and the median age at which they developed ESRD is about 30 years younger than non-Indigenous Australians. It is highly likely that many Indigenous Australian women have mild renal dysfunction (Hughes et al., 2018; Hoy et al., 2020) as evidenced by albuminuria, which is a robust measure of risk of future development of renal and cardiovascular disease (Hoy and McDonald, 2004).

Pringle et al. (2018) have shown that urinary protein/creatinine ratios were higher in Indigenous pregnant women than in non-Indigenous pregnant women, all of whom had uncomplicated pregnancy outcomes (Pringle et al., 2018). Indigenous Australians also have a high prevalence of small for gestational age babies and premature birth (Gingery et al., 2009) and an increased incidence of obesity and diabetes mellitus (Pringle et al., 2019). Kandasamy et al. (2014) found that Indigenous Australian infants had smaller kidney volumes than non-Indigenous infants. Since there was no difference in GFR (expressed ml.min.1.73 m^2), it follows that single nephron GFR (SNGFR) must have been increased in Indigenous neonates.

While there are genetic polymorphisms that contribute to this epidemic of CKD (Duffy et al., 2016), some of those SNPs commonly associated with hypertension and CKD in other populations have a very low prevalence in Indigenous Central Australians (Grimson et al., 2016). Conversely, the prevalence of the DD genotype in the ACE gene is higher in Indigenous Australians requiring dialysis than it is in healthy controls, suggesting that overactivity of the RAS exacerbates chronic renal disease (Lester et al., 1999).

The impact of the sheep data showing the impact of maternal subtotal nephrectomy prior to conception on renal function of offspring both prenatally and postnatally clearly demonstrates that maternal renal health is a determinant of offspring renal health. That is, there is a transgenerational effect on renal health as well as a genetic contribution Duffy et al. (2016) the ACE I/D polymorphism and p53 polymorphisms account for 15% of the heritability of a high albumin/creatinine and blood pressure.

CONCLUSION

A lower nephron number and larger glomerular volume as a result of hyperfiltration is therefore the transgenerational substrate for the continuing high risk of ESRD and RRT, particularly in Indigenous communities. However, throughout life, a progressive reduction in nephron number due to nephrosclerosis occurs (**Figure 3**). Thus, a low nephron number at birth, the imposition of obesity, diabetes mellitus and (to a lesser extent these days) post-streptococcal glomerulonephritis accelerates this glomerular loss so CKD occurs at a younger age. Since nephron number has been determined by the time of birth, considerable attention should be given to those maternal lifestyle factors that affect nephrogenesis (such as alcohol, smoking, obesity, adequate nutrition, and micronutrients). However, the effects of maternal renal health on the risk of early onset of CKD in their offspring will only be eliminated when the prevalence of renal dysfunction in pregnant women is reduced. As emphasized at the beginning of this review, CKD (as measured by albumin/creatinine) is a significant a risk factor for hypertension and cardiovascular disease. Therefore, any progress in reducing the prevalence of CKD also brings further benefit by reducing cardiovascular disease.

We recommend that kidney volumes should be measured at birth and infants with small kidney volumes or those who are premature be monitored throughout life by measuring eGFR and albumin/creatinine ratio. Particular attention should be paid to their level of nutrition and programs that prevent obesity and type II diabetes mellitus introduced into the routine delivery of primary health care. Hypertension requires treatment and continuous surveillance. Finally, it is tempting to suggest that ingestion of large amounts of protein should be advised against.

AUTHOR CONTRIBUTIONS

EL wrote the first draft of the manuscript. KP, YK, SD, AB, and KG contributed to manuscript revision. All authors approved the final submission.

REFERENCES

Al-Odat, I., Chen, H., Chan, Y. L., Amgad, S., Wong, M. G., Gill, A., et al. (2014). The impact of maternal cigarette smoke exposure in a rodent model on renal development in the offspring. *PLoS One* 9:e103443. doi: 10.1371/journal.pone.0103443

Armitage, J. A., Lakasing, L., Taylor, P. D., Balachandran, A. A., Jensen, R. I., Dekou, V., et al. (2005). Developmental programming of aortic and renal structure in offspring of rats fed fat-rich diets in pregnancy. *J. Physiol.* 565(Pt 1), 171–184. doi: 10.1113/jphysiol.2005.084947

Barker, D. J., Osmond, C., Golding, J., Kuh, D., and Wadsworth, M. E. (1989). Growth in utero, blood pressure in childhood and adult life, and mortality

from cardiovascular disease. *BMJ* 298, 564–567. doi: 10.1136/bmj.298.6673.564

Barr, M. (1994). Teratogen update: angiotensin-converting enzyme inhibitors. *Teratology* 50, 399–409. doi: 10.1002/tera.1420500606

Black, M. J., Sutherland, M. R., Gubhaju, L., Kent, A. L., Dahlstrom, J. E., and Moore, L. (2013). When birth comes early: effects on nephrogenesis. *Nephrology* 18, 180–182. doi: 10.1111/nep.12028

Blom, K., Odutayo, A., Bramham, K., and Hladunewich, M. A. (2017). Pregnancy and glomerular disease: a systematic review of the literature with management guidelines. *Clin. J. Am. Soc. Nephrol.* 12, 1862–1872. doi: 10.2215/cjn.00130117

Boberg, U., and Persson, A. E. (1986). Increased tubuloglomerular feedback activity in Milan hypertensive rats. *Am. J. Physiol.* 250(6 Pt 2), F967–F974.

Boyce, A. C., Gibson, K. J., Wintour, E. M., Koukoulas, I., and Lumbers, E. R. (2005). Effects of 7-day amino acid infusion on renal growth, function, and renin-angiotensin system in fetal sheep. *Am. J. Physiol. Regul. Integr. Comp. Physiol.* 289, R1099–R1106.

Boyce, A. C., Palmer-Aronsten, B. J., Kim, M. Y., and Gibson, K. J. (2013). Maternal vitamin D deficiency programmes adult renal renin gene expression and renal function. *J. Dev. Orig. Health Dis.* 4, 368–376. doi: 10.1017/s2040174413000342

Brandon, A. E., Boyce, A. C., Lumbers, E. R., and Gibson, K. J. (2009). Maternal renal dysfunction in sheep is associated with salt insensitivity in female offspring. *J. Physiol.* 587, 261–270. doi: 10.1113/jphysiol.2008.158808

Brandon, A. E., Boyce, A. C., Lumbers, E. R., Kumarasamy, V., and Gibson, K. J. (2011). Programming of the renin response to haemorrhage by mild maternal renal impairment in sheep. *Clin. Exp. Pharmacol. Physiol.* 38, 102–108. doi: 10.1111/j.1440-1681.2010.05473.x

Brandon, A. E., Boyce, A. C., Lumbers, E. R., Zimanyi, M. A., Bertram, J. F., and Gibson, K. J. (2008). Glomerular hypertrophy in offspring of subtotally nephrectomized ewes. *Anat. Rec.* 291, 318–324. doi: 10.1002/ar.20651

Brannstrom, K., and Arendshorst, W. J. (1999). Resetting of exaggerated tubuloglomerular feedback activity in acutely volume-expanded young SHR. *Am. J. Physiol.* 276, F409–F416.

Brenner, B. M., and Chertow, G. M. (1994). Congenital oligonephropathy and the etiology of adult hypertension and progressive renal injury. *Am. J. Kidney Dis.* 23, 171–175. doi: 10.1016/s0272-6386(12)80967-x

Brown, A. J., Dusso, A., and Slatopolsky, E. (1999). Vitamin D. *Am. J. Physiol.* 277, F157–F175.

Burkitt, K. I., Boyce, A. C., and Gibson, K. J. (2014). *The Developmental Programming Effects of vitamin D on Renal Nephron Endowment and Gene Expression of the Renin Angiotensin System in Weanling Male Rats*. Brisbane: Australian Physiological Society.

Caputo, C., Wood, E., and Jabbour, L. (2016). Impact of fetal alcohol exposure on body systems: a systematic review. *Birth Defects Res. C Embryo Today* 108, 174–180. doi: 10.1002/bdrc.21129

Chen, Y., Lasaitiene, D., and Friberg, P. (2004). The renin-angiotensin system in kidney development. *Acta Physiol. Scand.* 181, 529–535.

Cheng, Y., Luo, R., Wang, K., Zhang, M., Wang, Z., Dong, L., et al. (2020). Kidney disease is associated with in-hospital death of patients with COVID-19. *Kidney Int.* 97, 829–838. doi: 10.1016/j.kint.2020.03.005

Cragan, J. D., Young, B. A., and Correa, A. (2015). Renin-angiotensin system blocker fetopathy. *J. Pediatr.* 167, 792–794. doi: 10.1016/j.jpeds.2015.07.024

Delanaye, P., Radermecker, R. P., Rorive, M., Depas, G., and Krzesinski, J. M. (2005). Indexing glomerular filtration rate for body surface area in obese patients is misleading: concept and example. *Nephrol. Dial. Transplant.* 20, 2024–2028. doi: 10.1093/ndt/gfh983

Denic, A., Lieske, J. C., Chakkera, H. A., Poggio, E. D., Alexander, M. P., Singh, P., et al. (2017). The substantial loss of nephrons in healthy human kidneys with aging. *J. Am. Soc. Nephrol.* 28, 313–320. doi: 10.1681/asn.2016020154

Diehm, C. J., Lumbers, E. R., Weatherall, L., Keogh, L., Eades, S., Brown, A., et al. (2017). Assessment of fetal kidney growth and birth weight in an indigenous Australian cohort. *Front. Physiol.* 8:1129. doi: 10.3389/fphys.2017.01129

Dodic, M., May, C. N., Wintour, E. M., and Coghlan, J. P. (1998). An early prenatal exposure to excess glucocorticoid leads to hypertensive offspring in sheep. *Clin. Sci.* 94, 149–155. doi: 10.1042/cs0940149

Duffy, D. L., McDonald, S. P., Hayhurst, B., Panagiotopoulos, S., Smith, T. J., Wang, X. L., et al. (2016). Familial aggregation of albuminuria and arterial hypertension in an Aboriginal Australian community and the contribution of variants in ACE and TP53. *BMC Nephrol.* 17:183. doi: 10.1186/s12882-016-0396-2

Flynn, E. R., Alexander, B. T., Lee, J., Hutchens, Z. M., and Maric-Bilkan, C. (2013). High-fat/fructose feeding during prenatal and postnatal development in female rats increases susceptibility to renal and metabolic injury later in life. *Am. J. Physiol. Regul. Integr. Comp. Physiol.* 304, R278–R285.

Geddes, C. C., Woo, Y. M., and Brady, S. (2008). Glomerular filtration rate–what is the rationale and justification of normalizing GFR for body surface area? *Nephrol. Dial. Transplant.* 23, 4–6. doi: 10.1093/ndt/gfm662

Gezmish, O., Tare, M., Parkington, H. C., Morley, R., Porrello, E. R., Bubb, K. J., et al. (2010). Maternal vitamin D deficiency leads to cardiac hypertrophy in rat offspring. *Reprod. Sci.* 17, 168–176. doi: 10.1177/1933719109349536

Gibson, K. J., Boyce, A. C., Karime, B. M., and Lumbers, E. R. (2007). Maternal renal insufficiency alters plasma composition and renal function in the fetal sheep. *Am. J. Physiol. Regul. Integr. Comp. Physiol.* 292, R1204–R1211.

Gibson, K. J., Thomson, C. L., Boyce, A. C., Karime, B. M., and Lumbers, E. R. (2006). Effects of a reduction in maternal renal mass on pregnancy and cardiovascular and renal function of the pregnant ewe. *Am. J. Physiol. Renal Physiol.* 290, F1153–F1162.

Gilbert, S. F. (2000). *Intermediate Mesoderm*, 6th Edn. Sunderland, MA: Sinauer Associates.

Gingery, A., Soldner, E. L., Heltemes, A., Nelson, A., and Bozadjieva, N. (2009). Developmental programming of the kidney: Does sex matter? *J. Physiol.* 587(Pt 23), 5521–5522. doi: 10.1113/jphysiol.2009.179721

Glastras, S. J., Chen, H., Teh, R., McGrath, R. T., Chen, J., Pollock, C. A., et al. (2016). Mouse models of diabetes, obesity and related kidney disease. *PLoS One* 11:e0162131. doi: 10.1371/journal.pone.0162131

Gobetto, M. N., Mendes Garrido, Abregu, F., Caniffi, C., Veiras, L., Elesgaray, R., et al. (2020). Fetal and postnatal zinc restriction: sex differences in the renal renin-angiotensin system of newborn and adult Wistar rats. *J. Nutr. Biochem.* 81:108385. doi: 10.1016/j.jnutbio.2020.108385

Godron-Dubrasquet, A., Didailler, C., Harambat, J., and Llanas, B. (2017). [Solitary kidney: management and outcome]. *Arch. Pediatr.* 24, 1158–1163.

Gomez, R. A. (2017). Fate of renin cells during development and disease. *Hypertension* 69, 387–395. doi: 10.1161/hypertensionaha.116.08316

Goodyer, P., Kurpad, A., Rekha, S., Muthayya, S., Dwarkanath, P., Iyengar, A., et al. (2007). Effects of maternal vitamin A status on kidney development: a pilot study. *Pediatr. Nephrol.* 22, 209–214. doi: 10.1007/s00467-006-0213-4

Gray, S. P., Denton, K. M., Cullen-McEwen, L., Bertram, J. F., and Moritz, K. M. (2010). Prenatal exposure to alcohol reduces nephron number and raises blood pressure in progeny. *J. Am. Soc. Nephrol.* 21, 1891–1902. doi: 10.1681/asn.2010040368

Gray, S. P., Kenna, K., Bertram, J. F., Hoy, W. E., Yan, E. B., Bocking, A. D., et al. (2008). Repeated ethanol exposure during late gestation decreases nephron endowment in fetal sheep. *Am. J. Physiol. Regul. Integr. Comp. Physiol.* 295, R568–R574.

Grimson, S., Cox, A. J., Pringle, K. G., Burns, C., Lumbers, E. R., Blackwell, C. C., et al. (2016). The prevalence of unique SNPs in the renin-angiotensin system highlights the need for pharmacogenetics in Indigenous Australians. *Clin. Exp. Pharmacol. Physiol.* 43, 157–160. doi: 10.1111/1440-1681.12525

Gubhaju, L., Sutherland, M. R., Yoder, B. A., Zulli, A., Bertram, J. F., and Black, M. J. (2009). Is nephrogenesis affected by preterm birth? Studies in a non-human primate model. *Am. J. Physiol. Renal Physiol.* 297, F1668–F1677.

Hastie, R., Bergman, L., Cluver, C. A., Wikman, A., Hannan, N. J., Walker, S. P., et al. (2019). Proton pump inhibitors and preeclampsia risk among 157 720 women. *Hypertension* 73, 1097–1103. doi: 10.1161/hypertensionaha.118.12547

Helal, I., Fick-Brosnahan, G. M., Reed-Gitomer, B., and Schrier, R. W. (2012). Glomerular hyperfiltration: definitions, mechanisms and clinical implications. *Nat. Rev. Nephrol.* 8, 293–300. doi: 10.1038/nrneph.2012.19

Hinchliffe, S. A., Lynch, M. R., Sargent, P. H., Howard, C. V., and Van Velzen, D. (1992). The effect of intrauterine growth retardation on the development of renal nephrons. *Br. J. Obstet. Gynaecol.* 99, 296–301. doi: 10.1111/j.1471-0528.1992.tb13726.x

Hoy, W., and McDonald, S. P. (2004). Albuminuria: marker or target in indigenous populations. *Kidney Int. Suppl.* 66, S25–S31.

Hoy, W. E., Douglas-Denton, R. N., Hughson, M. D., Cass, A., Johnson, K., and Bertram, J. F. (2003). A stereological study of glomerular number and volume: preliminary findings in a multiracial study of kidneys at autopsy. *Kidney Int. Suppl.* 63, S31–S37.

Hoy, W. E., Hughson, M. D., Singh, G. R., Douglas-Denton, R., and Bertram, J. F. (2006). Reduced nephron number and glomerulomegaly in Australian

Aborigines: a group at high risk for renal disease and hypertension. *Kidney Int.* 70, 104–110. doi: 10.1038/sj.ki.5000397

Hoy, W. E., Mathews, J. D., McCredie, D. A., Pugsley, D. J., Hayhurst, B. G., Rees, M., et al. (1998a). The multidimensional nature of renal disease: rates and associations of albuminuria in an Australian Aboriginal community. *Kidney Int.* 54, 1296–1304. doi: 10.1046/j.1523-1755.1998.00099.x

Hoy, W. E., Mott, S. A., and McDonald, S. P. (2020). An update on chronic kidney disease in Aboriginal Australians. *Clin. Nephrol.* 93, 124–128. doi: 10.5414/cnp92s122

Hoy, W. E., Rees, M., Kile, E., Mathews, J. D., McCredie, D. A., Pugsley, D. J., et al. (1998b). Low birthweight and renal disease in Australian aborigines. *Lancet* 352, 1826–1827. doi: 10.1016/s0140-6736(05)79888-3

Hughes, J. T., Maple-Brown, L. J., Thomas, M., Lawton, P. D., Sinha, A., Cass, A., (2018). Cross-sectional associations of albuminuria among Aboriginal and Torres Strait Islander adults: the eGFR Study. *Nephrology (Carlton)* 23, 37–45. doi: 10.1111/nep.12956

Jackson, C. M., Alexander, B. T., Roach, L., Haggerty, D., Marbury, D. C., Hutchens, Z. M., et al. (2012). Exposure to maternal overnutrition and a high-fat diet during early postnatal development increases susceptibility to renal and metabolic injury later in life. *Am. J. Physiol. Renal Physiol.* 302, F774–F783.

Kabuto, H., Amakawa, M., and Shishibori, T. (2004). Exposure to bisphenol A during embryonic/fetal life and infancy increases oxidative injury and causes underdevelopment of the brain and testis in mice. *Life Sci.* 74, 2931–2940. doi: 10.1016/j.lfs.2003.07.060

Kandasamy, Y., Rudd, D., Smith, R., Lumbers, E. R., and Wright, I. M. (2018). Extra uterine development of preterm kidneys. *Pediatr. Nephrol.* 33, 1007–1012. doi: 10.1007/s00467-018-3899-1

Kandasamy, Y., Smith, R., Wright, I. M., and Lumbers, E. R. (2013). Extra-uterine renal growth in preterm infants: oligonephropathy and prematurity. *Pediatr. Nephrol.* 28, 1791–1796. doi: 10.1007/s00467-013-2462-3

Kandasamy, Y., Smith, R., Wright, I. M., and Lumbers, E. R. (2014). Reduced nephron endowment in the neonates of Indigenous Australian peoples. *J. Dev. Orig. Health Dis.* 5, 31–35. doi: 10.1017/s2040174413000494

Keijzer-Veen, M. G., Devos, A. S., Meradji, M., Dekker, F. W., Nauta, J., and van der Heijden, B. J. (2010). Reduced renal length and volume 20 years after very preterm birth. *Pediatr. Nephrol.* 25, 499–507. doi: 10.1007/s00467-009-1371-y

Keijzer-Veen, M. G., Kleinveld, H. A., Lequin, M. H., Dekker, F. W., Nauta, J., de Rijke, Y. B., et al. (2007). Renal function and size at young adult age after intrauterine growth restriction and very premature birth. *Am. J. Kidney Dis.* 50, 542–551. doi: 10.1053/j.ajkd.2007.06.015

Keller, G., Zimmer, G., Mall, G., Ritz, E., and Amann, K. (2003). Nephron number in patients with primary hypertension. *N. Engl. J. Med.* 348, 101–108. doi: 10.1056/nejmoa020549

Kleinknecht, C., Salusky, I., Broyer, M., and Gubler, M. C. (1979). Effect of various protein diets on growth, renal function, and survival of uremic rats. *Kidney Int.* 15, 534–541. doi: 10.1038/ki.1979.68

Langley-Evans, S. C., Langley-Evans, A. J., and Marchand, M. C. (2003). Nutritional programming of blood pressure and renal morphology. *Arch. Physiol. Biochem.* 111, 8–16. doi: 10.1076/apab.111.1.8.15136

Lankadeva, Y. R., Singh, R. R., Tare, M., Moritz, K. M., and Denton, K. M. (2014). Loss of a kidney during fetal life: long-term consequences and lessons learned. *Am. J. Physiol. Renal Physiol.* 306, F791–F800.

Lasaitiene, D., Chen, Y., Guron, G., Marcussen, N., Tarkowski, A., Telemo, E., et al. (2003). Perturbed medullary tubulogenesis in neonatal rat exposed to renin-angiotensin system inhibition. *Nephrol. Dial. Transplant.* 18, 2534–2541. doi: 10.1093/ndt/gfg447

Lee, Y. Q., Beckett, E. L., Sculley, D. V., Rae, K. M., Collins, C. E., and Pringle, K. G. (2019a). Relationship between maternal global nutrient restriction during pregnancy and offspring kidney structure and function: a systematic review of animal studies. *Am. J. Physiol. Renal Physiol.* 316, F1227–F1235.

Lee, Y. Q., Lumbers, E. R., Oldmeadow, C., Collins, C. E., Johnson, V., Keogh, L., et al. (2019b). The relationship between maternal adiposity during pregnancy and fetal kidney development and kidney function in infants: the Gomeroi gaaynggal study. *Physiol. Rep.* 7:e14227.

Lelievre-Pegorier, M., Vilar, J., Ferrier, M. L., Moreau, E., Freund, N., Gilbert, T., et al. (1998). Mild vitamin A deficiency leads to inborn nephron deficit in the rat. *Kidney Int.* 54, 1455–1462. doi: 10.1046/j.1523-1755.1998.00151.x

Lester, S., Heatley, S., Bardy, P., Bahnisch, J., Bannister, K., Faull, R., et al. (1999). The DD genotype of the angiotensin-converting enzyme gene occurs in very low frequency in Australian Aboriginals. *Nephrol. Dial. Transplant.* 14, 887–890. doi: 10.1093/ndt/14.4.887

Li, J., Guandalini, M., McInnes, H., Kandasamy, Y., Trnka, P., and Moritz, K. (2020). The impact of prematurity on postnatal growth of different renal compartments. *Nephrology* 25, 116–124. doi: 10.1111/nep.13623

Li, Y. C., Kong, J., Wei, M., Chen, Z. F., Liu, S. Q., and Cao, L. P. (2002). 1,25-Dihydroxyvitamin D(3) is a negative endocrine regulator of the renin-angiotensin system. *J. Clin. Invest.* 110, 229–238. doi: 10.1172/jci0215219

Lips, P. (2010). Worldwide status of vitamin D nutrition. *J. Steroid Biochem. Mol. Biol.* 121, 297–300. doi: 10.1016/j.jsbmb.2010.02.021

Lumbers, E. R., Burrell, J. H., Menzies, R. I., and Stevens, A. D. (1993). The effects of a converting enzyme inhibitor (captopril) and angiotensin II on fetal renal function. *Br. J. Pharmacol.* 110, 821–827. doi: 10.1111/j.1476-5381.1993.tb13886.x

Maka, N., Makrakis, J., Parkington, H. C., Tare, M., Morley, R., and Black, M. J. (2008). Vitamin D deficiency during pregnancy and lactation stimulates nephrogenesis in rat offspring. *Pediatr. Nephrol.* 23, 55–61. doi: 10.1007/s00467-007-0641-9

Makrakis, J., Zimanyi, M. A., and Black, M. J. (2007). Retinoic acid enhances nephron endowment in rats exposed to maternal protein restriction. *Pediatr. Nephrol.* 2, 1861–1867. doi: 10.1007/s00467-007-0572-5

Martinez-Maldonaldo, M., Benabe, J. E., and Cordova, H. R. (1992). *The Kidney: Physiology and Pathophysiology*, 2nd Edn. New York, NY: Raven Press.

Matsumoto, H., Koya, G., and Takeuchi, T. (1965). Fetal Minamata disease. A neuropathological study of two cases of intrauterine intoxication by a methyl mercury compound. *J. Neuropathol. Exp. Neurol.* 24, 563–574. doi: 10.1097/00005072-196510000-00002

Matsushita, K., Coresh, J., Sang, Y., Chalmers, J., Fox, C., Guallar, E., et al. (2015). Estimated glomerular filtration rate and albuminuria for prediction of cardiovascular outcomes: a collaborative meta-analysis of individual participant data. *Lancet Diabetes Endocrinol.* 3, 514–525. doi: 10.1016/s2213-8587(15)00040-6

Merlet-Benichou, C., Vilar, J., Lelievre-Pegorier, M., and Gilbert, T. (1999). Role of retinoids in renal development: pathophysiological implication. *Curr. Opin. Nephrol. Hypertens* 8, 39–43. doi: 10.1097/00041552-199901000-00007

Meyer, T. W., Anderson, S., and Brenner, B. M. (1983a). Dietary protein intake and progressive glomerular sclerosis: the role of capillary hypertension and hyperperfusion in the progression of renal disease. *Ann. Intern. Med.* 98(5 Pt 2), 832–838.

Meyer, T. W., Lawrence, W. E., and Brenner, B. M. (1983b). Dietary protein and the progression of renal disease. *Kidney Int.* 16, S243–S247.

Mishra, K., Datta, V., Aarushi, A., Kaur Narula, M., Iyer, R. S., and Nangia, S. (2014). The association between weight for gestational age and kidney volume: a study in newborns in India. *Iran. J. Pediatr.* 24, 93–99.

Moore, C. A., Khoury, M. J., and Liu, Y. (1997). Does light-to-moderate alcohol consumption during pregnancy increase the risk for renal anomalies among offspring? *Pediatrics* 99:E11.

Moritz, K. M., De Matteo, R., Dodic, M., Jefferies, A. J., Arena, D., Wintour, E. M., et al. (2011). Prenatal glucocorticoid exposure in the sheep alters renal development in utero: implications for adult renal function and blood pressure control. *Am. J. Physiol. Regul. Integr. Comp. Physiol.* 301, R500–R509.

Moritz, K. M., Johnson, K., Douglas-Denton, R., Wintour, E. M., and Dodic, M. (2002). Maternal glucocorticoid treatment programs alterations in the renin-angiotensin system of the ovine fetal kidney. *Endocrinology* 143, 4455–4463. doi: 10.1210/en.2002-220534

Nadeem, S., Hashmat, S., Defreitas, M. J., Westreich, K. D., Shatat, I. F., Selewski, D. T., et al. (2015). Renin angiotensin system blocker fetopathy: a midwest pediatric nephrology consortium report. *J. Pediatr.* 167, 881–885. doi: 10.1016/j.jpeds.2015.05.045

Nascimento, F. A., Ceciliano, T. C., Aguila, M. B., and Mandarim-de-Lacerda, C. A. (2012). Maternal vitamin D deficiency delays glomerular maturity in F1 and F2 offspring. *PLoS One* 7:e41740. doi: 10.1371/journal.pone.0041740

Ortiz, L. A., Quan, A., Weinberg, A., and Baum, M. (2001). Effect of prenatal dexamethasone on rat renal development. *Kidney Int.* 59, 1663–1669. doi: 10.1046/j.1523-1755.2001.0590051663.x

Ortiz, L. A., Quan, A., Zarzar, F., Weinberg, A., and Baum, M. (2003). Prenatal dexamethasone programs hypertension and renal injury in the rat. *Hypertension* 41, 328–334. doi: 10.1161/01.hyp.0000049763.51269.51

Osathanondh, V., and Potter, E. L. (1963). Development of Human Kidney as Shown by Microdissection. III. Formation and Interrelationship of Collecting Tubules and Nephrons. *Arch. Pathol.* 76, 290–302.

Painter, R. C., Roseboom, T. J., van Montfrans, G. A., Bossuyt, P. M., Krediet, R. T., Osmond, C., et al. (2005). Microalbuminuria in adults after prenatal exposure to the Dutch famine. *J. Am. Soc. Nephrol.* 16, 189–194. doi: 10.1681/asn.2004060474

Peers, A., Hantzis, V., Dodic, M., Koukoulas, I., Gibson, A., Baird, R., et al. (2001). Functional glucocorticoid receptors in the mesonephros of the ovine fetus. *Kidney Int.* 59, 425–433. doi: 10.1046/j.1523-1755.2001.059002425.x

Persson, A. E., Bianchi, G., and Boberg, U. (1985). Tubuloglomerular feedback in hypertensive rats of the Milan strain. *Acta Physiol. Scand.* 1985, 139–146. doi: 10.1111/j.1748-1716.1985.tb07570.x

Peti-Peterdi, J. (2010). High glucose and renin release: the role of succinate and GPR91. *Kidney Int.* 78, 1214–1217. doi: 10.1038/ki.2010.333

Pringle, K. G., de Meaultsart, C. C., Sykes, S. D., Weatherall, L. J., Keogh, L., Clausen, D. C., et al. (2018). Urinary angiotensinogen excretion in Australian Indigenous and non-Indigenous pregnant women. *Pregnancy Hypertens* 12, 110–117. doi: 10.1016/j.preghy.2018.04.009

Pringle, K. G., Lee, Y. Q., Weatherall, L., Keogh, L., Diehm, C., Roberts, C. T., et al. (2019). Influence of maternal adiposity, preterm birth and birth weight centiles on early childhood obesity in an Indigenous Australian pregnancy-through-to-early-childhood cohort study. *J. Dev. Orig. Health Dis.* 10, 39–47. doi: 10.1017/s2040174418000302

Queisser-Luft, A., Stolz, G., Wiesel, A., Schlaefer, K., and Spranger, J. (2002). Malformations in newborn: results based on 30,940 infants and fetuses from the Mainz congenital birth defect monitoring system (1990-1998). *Arch. Gynecol. Obstet.* 266, 163–167. doi: 10.1007/s00404-001-0265-4

Reiser, J., and Altintas, M. M. (2016). Podocytes. *F1000 Res.* 5:F1000 Faculty Rev-114.

Roberts, D., Brown, J., Medley, N., and Dalziel, S. R. (2017). Antenatal corticosteroids for accelerating fetal lung maturation for women at risk of preterm birth. *Cochrane Database Syst. Rev.* 3, CD004454.

Rogers, S. A., Droege, D., Dusso, A., and Hammerman, M. R. (2004). Incubation of metanephroi with vitamin d(3) increases numbers of glomeruli. *Organogenesis* 1, 52–54. doi: 10.4161/org.1.2.1292

Romagnani, P., Lasagni, L., and Remuzzi, G. (2013). Renal progenitors: an evolutionary conserved strategy for kidney regeneration. *Nat. Rev. Nephrol.* 9, 137–146. doi: 10.1038/nrneph.2012.290

Rosenberg, A. Z., and Kopp, J. B. (2017). Focal Segmental Glomerulosclerosis. *Clin. J. Am. Soc. Nephrol.* 12, 502–517.

Salusky, I., Kleinknecht, C., Broyer, M., and Gubler, M. C. (1981). Prolonged renal survival and stunting, with protein-deficient diets in experimental uremia. Reversal of these effects by addition of essential amino acids. *J. Lab. Clin. Med.* 97, 21–30.

Simons, J. L., Provoost, A. P., Anderson, S., Rennke, H. G., Troy, J. L., and Brenner, B. M. (1994). Modulation of glomerular hypertension defines susceptibility to progressive glomerular injury. *Kidney Int.* 46, 396–404. doi: 10.1038/ki.1994.287

Singer, M. A. (2001). Of mice and men and elephants: metabolic rate sets glomerular filtration rate. *Am. J. Kidney Dis.* 37, 164–178. doi: 10.1016/s0272-6386(01)80073-1

Singh, R. R., Denton, K. M., Bertram, J. F., Jefferies, A. J., Head, G. A., Lombardo, P., et al. (2009). Development of cardiovascular disease due to renal insufficiency in male sheep following fetal unilateral nephrectomy. *J. Hypertens.* 27, 386–396. doi: 10.1097/hjh.0b013e32831bc778

Song, R., and Yosypiv, I. V. (2011). (Pro)renin Receptor in Kidney Development and Disease. *Int. J. Nephrol.* 2011:247048.

South, A. M., Nixon, P. A., Chappell, M. C., Diz, D. I., Russell, G. B., Jensen, E. T., et al. (2019). Renal function and blood pressure are altered in adolescents born preterm. *Pediatr. Nephrol.* 34, 137–144. doi: 10.1007/s00467-018-4050-z

Sutherland, M. R., Gubhaju, L., Moore, L., Kent, A. L., Dahlstrom, J. E., Horne, R. S., et al. (2011). Accelerated maturation and abnormal morphology in the preterm neonatal kidney. *J. Am. Soc. Nephrol.* 22, 1365–1374. doi: 10.1681/asn.2010121266

Taal, H. R., Geelhoed, J. J., Steegers, E. A., Hofman, A., Moll, H. A., Lequin, M., et al. (2011). Maternal smoking during pregnancy and kidney volume in the offspring: the Generation R Study. *Pediatr. Nephrol.* 26, 1275–1283. doi: 10.1007/s00467-011-1848-3

Tare, M., Emmett, S. J., Coleman, H. A., Skordilis, C., Eyles, D. W., Morley, R., et al. (2011). Vitamin D insufficiency is associated with impaired vascular endothelial and smooth muscle function and hypertension in young rats. *J. Physiol.* 589(Pt 19), 4777–4786. doi: 10.1113/jphysiol.2011.214726

Taussig, H. B. (1962). A study of the German outbreak of phocomelia. The thalidomide syndrome. *JAMA* 180, 1106–1114.

Tomat, A. L., Costa, M. A., Girgulsky, L. C., Veiras, L., Weisstaub, A. R., Inserra, F., et al. (2007). Zinc deficiency during growth: influence on renal function and morphology. *Life Sci.* 80, 1292–1302. doi: 10.1016/j.lfs.2006.12.035

Tomat, A. L., Costa Mde, L., and Arranz, C. T. (2011). Zinc restriction during different periods of life: influence in renal and cardiovascular diseases. *Nutrition* 27, 392–398. doi: 10.1016/j.nut.2010.09.010

Tomat, A. L., Inserra, F., Veiras, L., Vallone, M. C., Balaszczuk, A. M., Costa, M. A., et al. (2008). Moderate zinc restriction during fetal and postnatal growth of rats: effects on adult arterial blood pressure and kidney. *Am. J. Physiol. Regul. Integr. Comp. Physiol.* 295, R543–R549.

Tufro-McReddie, A., Romano, L. M., Harris, J. M., Ferder, L., and Gomez, R. A. (1995). Angiotensin II regulates nephrogenesis and renal vascular development. *Am. J. Physiol.* 269(1 Pt 2), F110–F115.

Turner, A. J., Brown, R. D., Boyce, A., Gibson, K. J., and Persson, A. E. (2015). Fetal tubuloglomerular feedback in an ovine model of mild maternal renal disease. *Physiol. Rep.* 3:e12448. doi: 10.14814/phy2.12448

Turner, A. J., Brown, R. D., Brandon, A. E., Persson, A. E. G., and Gibson, K. J. (2017). Tubuloglomerular feedback responses in offspring of dexamethasone-treated ewes. *Am. J. Physiol. Renal Physiol.* 313, F864–F873.

Vallon, V. (2003). Tubuloglomerular feedback and the control of glomerular filtration rate. *News Physiol. Sci.* 18, 169–174. doi: 10.1152/nips.01442.2003

van der Ven, A. T., Vivante, A., and Hildebrandt, F. (2018). Novel insights into the pathogenesis of monogenic congenital anomalies of the kidney and urinary tract. *J. Am. Soc. Nephrol.* 29, 36–50. doi: 10.1681/asn.2017050561

Wang, N., Ning, Z., Xia, F., Chen, C., Cheng, J., Chen, Y., et al. (2018). Exposure to famine in early life and chronic kidney diseases in adulthood. *Nutr. Diabetes* 8:4.

Wilson, J. G., Roth, C. B., and Warkany, J. (1953). An analysis of the syndrome of malformations induced by maternal vitamin A deficiency. Effects of restoration of vitamin A at various times during gestation. *Am. J. Anat.* 92, 189–217. doi: 10.1002/aja.1000920202

Wintour, E. M., Moritz, K. M., Johnson, K., Ricardo, S., Samuel, C. S., and Dodic, M. (2003). Reduced nephron number in adult sheep, hypertensive as a result of prenatal glucocorticoid treatment. *J. Physiol.* 549(Pt 3), 929–935. doi: 10.1113/jphysiol.2003.042408

Woods, L. L., Ingelfinger, J. R., Nyengaard, J. R., and Rasch, R. (2001). Maternal protein restriction suppresses the newborn renin-angiotensin system and programs adult hypertension in rats. *Pediatr. Res.* 49, 460–467. doi: 10.1203/00006450-200104000-00005

Yosypiv, I. V. (2008). A new role for the renin-angiotensin system in the development of the ureteric bud and renal collecting system. *Keio J. Med.* 57, 184–189. doi: 10.2302/kjm.57.184

Yosypiv, I. V., Sequeira-Lopez, M. L. S., Song, R., and De Goes Martini, A. (2019). Stromal prorenin receptor is critical for normal kidney development. *Am. J. Physiol. Regul. Integr. Comp. Physiol.* 316, R640–R650.

Zanetti, D., Tikkanen, E., Gustafsson, S., Priest, J. R., Burgess, S., and Ingelsson, E. (2018). Birthweight, type 2 diabetes mellitus, and cardiovascular disease: addressing the barker hypothesis with mendelian randomization. *Circ. Genom. Precis. Med.* 11:e002054.

Zhang, Z., Quinlan, J., Hoy, W., Hughson, M. D., Lemire, M., Hudson, T., et al. (2008). A common RET variant is associated with reduced newborn kidney size and function. *J. Am. Soc. Nephrol.* 19, 2027–2034. doi: 10.1681/asn.2007101098

Conflict of Interest: The authors declare that the research was conducted in the absence of any commercial or financial relationships that could be construed as a potential conflict of interest.

Copyright © 2020 Lumbers, Kandasamy, Delforce, Boyce, Gibson and Pringle. This is an open-access article distributed under the terms of the Creative Commons Attribution License (CC BY). The use, distribution or reproduction in other forums is permitted, provided the original author(s) and the copyright owner(s) are credited and that the original publication in this journal is cited, in accordance with accepted academic practice. No use, distribution or reproduction is permitted which does not comply with these terms.

Advantages of publishing in Frontiers

OPEN ACCESS
Articles are free to read for greatest visibility and readership

FAST PUBLICATION
Around 90 days from submission to decision

HIGH QUALITY PEER-REVIEW
Rigorous, collaborative, and constructive peer-review

TRANSPARENT PEER-REVIEW
Editors and reviewers acknowledged by name on published articles

Frontiers
Avenue du Tribunal-Fédéral 34
1005 Lausanne | Switzerland

Visit us: www.frontiersin.org
Contact us: frontiersin.org/about/contact

REPRODUCIBILITY OF RESEARCH
Support open data and methods to enhance research reproducibility

DIGITAL PUBLISHING
Articles designed for optimal readership across devices

FOLLOW US
@frontiersin

IMPACT METRICS
Advanced article metrics track visibility across digital media

EXTENSIVE PROMOTION
Marketing and promotion of impactful research

LOOP RESEARCH NETWORK
Our network increases your article's readership